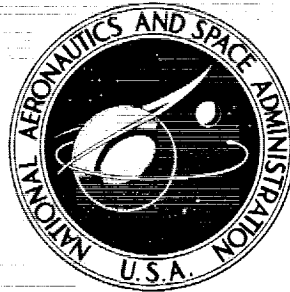


N70-31804

NASA CR-1549



**NASA CONTRACTOR  
REPORT**

NASA CR-1549

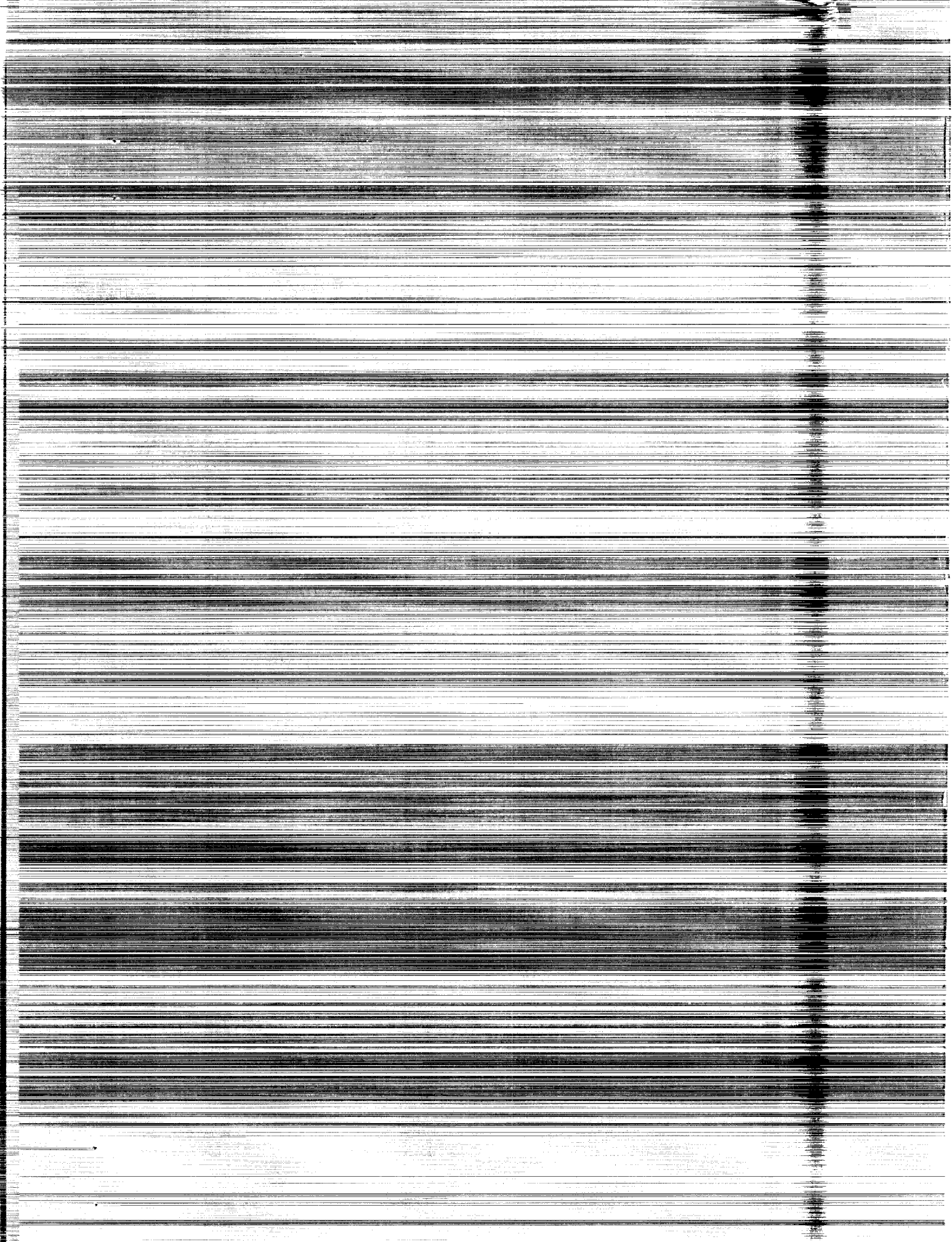
**CASE FILE  
COPY**

**TRANSIENT JOURNAL  
BEARING ANALYSIS**

*by R. Gordon Kirk and Edgar J. Gunter, Jr.*

*Prepared by*  
UNIVERSITY OF VIRGINIA  
Charlottesville, Va.  
*for Lewis Research Center*

NATIONAL AERONAUTICS AND SPACE ADMINISTRATION • WASHINGTON, D. C. • JUNE 1970



1. Report No. NASA CR-1549	2. Government Accession No.	3. Recipient's Catalog No.	
4. Title and Subtitle TRANSIENT JOURNAL BEARING ANALYSIS		5. Report Date June 1970	
		6. Performing Organization Code	
7. Author(s) R. Gordon Kirk and Edgar J. Gunter, Jr.		8. Performing Organization Report No. None	
9. Performing Organization Name and Address University of Virginia Dept. of Mechanical Engineering Charlottesville, Va.		10. Work Unit No.	
		11. Contract or Grant No. NGR-47-005-050	
12. Sponsoring Agency Name and Address National Aeronautics and Space Administration Washington, D. C. 20546		13. Type of Report and Period Covered Contractor Report	
		14. Sponsoring Agency Code	
15. Supplementary Notes			
16. Abstract The transient response of a nonlinear fluid film journal bearing is obtained by numerical methods of integration, utilizing a modern, high-speed digital computer and its component automatic plotting unit. An expression for the pressure in the fluid film of a short journal bearing is derived and the three-dimensional plots of the resulting pressure surface are presented for selected conditions. The transient orbit of the journal center is automatically plotted as a point moving in a unit clearance circle. The results show the effect of unbalance, steady loading, cyclic unidirectional and rotating loads upon the stability and performance of a short journal bearing. The results are compared to previous investigations and modified stability maps are deduced from the results obtained. The concept of whirl is examined and several plots presented of the instantaneous whirl and radius of curvature against cycles of motion (of the journal) for the various cases considered. Bearing forces are analyzed and the resulting plots of force against cycles of motion are presented for selected cases.			
17. Key Words (Suggested by Author(s)) Hydrodynamic lubrication Bearing stability		18. Distribution Statement Unclassified - unlimited	
19. Security Classif. (of this report) Unclassified	20. Security Classif. (of this page) Unclassified	21. No. of Pages 201	22. Price* \$3.00

\*For sale by the Clearinghouse for Federal Scientific and Technical Information  
Springfield, Virginia 22151



## FOREWORD

The research described herein, which was conducted at the University of Virginia, was performed under NASA Research Grant NGR-47-005-050 with Mr. William J. Anderson, Fluid System Components Division, NASA Lewis Research Center, as the Project Manager.



## TABLE OF CONTENTS

	PAGE
LIST OF FIGURES . . . . .	vii
NOMENCLATURE . . . . .	xiii
CHAPTER I. INTRODUCTION AND STATEMENT OF THE PROBLEM . . .	1
CHAPTER II. BACKGROUND AND STATE OF THE ART . . . . .	4
CHAPTER III. ANALYSIS OF THE SYSTEM . . . . .	16
3.1 Introduction . . . . .	16
3.2 Derivation of Reynolds Equation; . . . . .	19
Reduction to Short Bearing Equation	
3.3 Dynamical Equations of Motion . . . . .	33
3.4 Journal Precession Rate and Radius of Curvature . . . . .	37
3.5 Derivation and Explanation of Terms Used in Journal Bearing Studies . . . . .	41
CHAPTER IV. STABILITY ANALYSIS FOR SMALL DISPLACEMENTS . . .	47
CHAPTER V. METHOD OF SOLUTION . . . . .	53
5.1 Introduction . . . . .	53
5.2 The Fluid Film Pressure Profile . . . . .	53
5.3 Integration of the Pressure Profile . . . . .	62
5.4 Integration of the Equations of Motion . . . . .	64
5.5 Description of the Computer Program . . . . .	72

	PAGE
CHAPTER VI. PRESENTATION OF RESULTS . . . . .	77
6.1 Introduction . . . . .	77
6.2 Instability of Horizontal Balanced Journal Bearings . . . . .	78
6.3 Instability of Vertical Balanced Journal Bearings .	100
6.4 Effect of Unbalance on Journal Bearing Performance.	108
6.5 Motion of a Journal Bearing Experiencing Cyclic External Loading . . . . .	148
CHAPTER VII. SUMMARY OF BASIC ASSUMPTIONS AND RESULTS; SUGGESTIONS FOR EXTENDING THE ANALYSIS . . . . .	160
7.1 Discussion of Assumptions . . . . .	160
7.2 Discussion of Results and Conclusions . . . . .	161
7.3 Suggestions for Extending the Analysis . . . . .	165
BIBLIOGRAPHY . . . . .	168
APPENDIX A - PRESSURE PROFILE COMPUTER PROGRAM LISTING . . . . .	171
APPENDIX B - SHORT JOURNAL BEARING COMPUTER PROGRAM LISTING . . . . .	177

## LIST OF FIGURES

<u>FIGURE</u>	<u>PAGE</u>
3.1 Short Journal Bearing Configuration . . . . .	17
3.2 Unbalance Representation and a Typical Force Balance . . .	18
3.3 The Plane Slider Bearing . . . . .	20
3.4 a. Journal Bearing in Rotating Coordinates . . . . .	24
b. Journal Bearing Profile Unwrapped . . . . .	24
3.5 Journal Bearing in Fixed Cartesian Coordinates . . . . .	28
3.6 Comparison of Finite Length and Short Bearing Solutions . .	32
3.7 Typical Journal Trajectory Illustrating the Instantaneous Radius of Curvature . . . . .	38
3.8 Sommerfeld Number ( $S_g$ ) vs Eccentricity . . . . .	44
4.1 Stability for the Unloaded Short Journal Bearing (ref. Choudhury) . . . . .	49
4.2 Stability for the Unloaded Journal Bearing (Comparison of Reddi-Trumpler and Badgley-Booker Stability Maps) . . . . .	50
5.1 Pressure Profile, Pressure Surface, and Film Thickness for $X = 0.05$ , $Y = -0.02$ , $\dot{X} = \dot{Y} = 0$ . . . . .	55
5.2 Pressure Profile, Pressure Surface, and Film Thickness for $X = 0.2$ , $Y = -0.10$ , $\dot{X} = \dot{Y} = 0$ . . . . .	56
5.3 Uncavitated Pressure Profile for $X = 0.2$ , $Y = -0.10$ , $\dot{X} = \dot{Y} = 0$ . . . . .	57
5.4 Pressure Profile, Pressure Surface, and Film Thickness for $X = 0.5$ , $Y = -0.7$ , $\dot{X} = \dot{Y} = 0$ . . . . .	58
5.5 Pressure Profile, Pressure Surface, and Film Thickness for $X = 0.5$ , $Y = -0.7$ , $\dot{X} = \dot{Y} = -0.5$ . . . . .	59

FIGURE

PAGE

5.6 Pressure Profile, Pressure Surface, and Film Thickness  
for  $X = -0.9, Y = -0.05, \dot{X} = \dot{Y} = 0$  . . . . . 60

5.7 Pressure Profile, Pressure Surface, and Film Thickness  
for  $X = Y = 0, \dot{X} = -\dot{Y} = 0.5$  . . . . . 61

5.8 Euler's Integration Procedure vs Exact Solution for a  
Damped Spring-Mass System . . . . . 68

5.9 Numerical Instability with Adams Method,  $\Delta T = 0.05$  . . . . . 70

5.10 The Short Bearing Program; General Flow Chart . . . . . 73

6.1 Journal Orbit of A Balanced Horizontal Rotor  
( $N = 4000, W = 50, C = 0.005, L/D = 1/2$ ) . . . . . 79

6.2 Transmissibility and Shaft X-Y Motion vs Cycles of Motion  
( $N = 4000$ ) . . . . . 80

6.3 Radius of Curvature and Whirl vs Cycles of Motion ( $N = 4000$ ) 81

6.4 Journal Orbit of A Balanced Horizontal Rotor  
( $N = 6500, W = 50, C = 0.005, L/D = 1/2$ ) . . . . . 83

6.5 Transmissibility and Shaft X-Y Motion vs Cycles of Motion  
( $N = 6500$ ) . . . . . 84

6.6 Radius of Curvature and Whirl vs Cycles of Motion ( $N = 6500$ ) 85

6.7 a. Journal Orbit of A Balanced Horizontal Rotor for Cycles  
5 - 10 ( $N = 10,500, W = 50, C = 0.005, L/D = 1/2$ ) . . . 86  
b. Journal Orbit of A Balanced Horizontal Rotor for Cycles  
10 - 15 ( $N = 10,500, W = 50, C = 0.005, L/D = 1/2$ ) . . . 87  
c. Transmissibility and Shaft X-Y Motion vs Cycles of Motion  
for Cycles 10 - 15 ( $N = 10,500$ ). . . . . 88  
d. Radius of Curvature and Whirl vs Cycles of Motion for  
Cycles 10 - 15 ( $N = 10,500$ ) . . . . . 89

6.8 Journal Orbit of a Balanced Horizontal Rotor for 5 Cycles  
( $N = 6500, W = 200, C = 0.005, L/D = 1/2$ ) . . . . . 91

6.9 Journal Orbit of a Balanced Horizontal Rotor for Cycles  
5 - 10 ( $N = 10,500$ ) . . . . . 92

6.10 Journal Orbit of a Balanced Horizontal Rotor for 5 Cycles  
( $N = 6500, W = 1800, C = 0.005, L/D = 1/2$ ) . . . . . 93

<u>FIGURE</u>	<u>PAGE</u>
6.11 Journal Orbit of a Balanced Horizontal Rotor for Cycles 5 - 10 (N = 10,500) . . . . .	94
6.12 Journal Orbit of a Horizontal Balanced Rotor with Constant Load for 5 Cycles (N = 6500, W = 50, C = 0.005, L/D = 1/2, FOCY = -150) . . . . .	96
6.13 Journal Orbit of a Horizontal Rotor with Constant Load for Cycles 5 - 10 (N = 10,500) . . . . .	97
6.14 Stability Map for the Short Journal Bearing Considering Constant External Loading . . . . .	98
6.15 Stability Map for the Short Journal Bearing Using Modified Stability Parameters . . . . .	99
6.16 Journal Orbit of a Balanced Vertical Rotor with Zero Initial Conditions (N = 4000, W = 50, C = 0.005, L/D = 1/2 .	102
6.17 Journal Orbit of a Balanced Vertical Rotor with Small Initial Displacement for 25 Cycles (N = 4000) . . . . .	103
6.18 Radius of Curvature and Whirl vs Cycles of Motion for Cycles 20 - 25 (N = 4000) . . . . .	104
6.19 Journal Orbit of a Balanced Vertical Rotor with Small Initial Velocity for 5 Cycles (N = 6500, W = 1800, C = 0.005, L/D = 1/2) . . . . .	105
6.20 Journal Orbit of a Balanced Vertical Rotor for Cycles 5 -10 (N = 10,500, W = 1800, C = 0.005, L/D = 1/2) . . . . .	106
6.21 Journal Orbit of a Balanced Vertical Rotor with Constant Load (N = 4000, W = 50, C = 0.005, L/D = 1/2, FOCY = -50). .	107
6.22 Journal Orbit of an Unbalanced Vertical Rotor for 5 Cycles (N = 2000, W = 50, C = 0.005, L/D = 1/2, EMU = 0.2) . . . .	110
6.23 Journal Orbit of an Unbalanced Vertical Rotor for Cycles 5 - 10 (N = 2000, W = 50, C = 0.005, L/D = 1/2, EMU = 0.2) .	111
6.24 Journal Orbit of an Unbalanced Vertical Rotor for 5 Cycles (N = 4000, W = 50, C = 0.005, L/D = 1/2, EMU = 0.2) . . . .	112
6.25 Radius of Curvature and Whirl vs Cycles of Motion (N = 4000, EMU = 0.2) . . . . .	113

6.26 a. Journal Orbit of an Unbalanced Vertical Rotor for  
Cycles 5 - 10 (N = 4000, EMU = 0.2) . . . . .115

b. Analog Computer Traces of Various Combinations of  
Synchronous and Half-Frequency Whirl . . . . .116

6.27 Journal Orbit of a Slightly Unbalanced Vertical Rotor  
for 10 Cycles (N = 4000, EMU = 0.01) . . . . .117

6.28 Journal Orbit of a Slightly Unbalanced Vertical Rotor for  
10 Cycles (N = 10,500, EMU = 0.01) . . . . .118

6.29 Journal Orbit of an Unbalanced Vertical Rotor for 10 Cycles  
(N = 4000, EMU = 0.10). . . . .121

6.30 Journal Orbit of an Unbalanced Vertical Rotor for 5 Cycles  
(N = 4000, EMU = 0.14) . . . . .122

6.31 Journal Orbit of an Unbalanced Vertical Rotor for Cycles  
5 - 10 (N = 4000, EMU = 0.14) . . . . .123

6.32 Journal Orbit of an Unbalanced Vertical Rotor with the  
Critical Value of Unbalance (N = 4000, EMU = 0.16) . . . . .124

6.33 Journal Orbit of an Unbalanced Vertical Rotor for Cycles  
5 - 10 (N = 4000, EMU = 0.16) Illustrating Stable Half-  
Frequency Whirl . . . . .125

6.34 Journal Orbit of an Unbalanced Vertical Rotor for 5 Cycles  
(N = 6500, EMU = 0.2) with Damped Half-Frequency Whirl . . .126

6.35 Journal Orbit of an Unbalanced Vertical Rotor for Cycles  
5 - 10 (N = 6500, EMU = 0.2) Showing Motion Approaching  
Synchronous Precession . . . . .127

6.36 Journal Orbit of an Unbalanced Vertical Rotor Above the  
Stability Threshold for 5 Cycles (N = 10,500, EMU = 0.2) . .128

6.37 Journal Orbit of an Unbalanced Vertical Rotor for Cycles  
5 - 10 (N = 10,500, EMU = 0.2) . . . . .129

6.38 Journal Orbit of an Unbalanced Vertical Rotor for 10 Cycles  
and Showing the Limit Cycle (N = 21,000, EMU = 0.2) . . . . .130

6.39 Journal Orbit of a Highly Unbalanced Vertical Rotor  
Experiencing Synchronous Whirl Above the Stability Threshold  
for 5 Cycles (N = 18,000, W = 200, C = 0.00376, L/D = 1/2,  
EMU = 1.0) . . . . .131

FIGURE

PAGE

6.40 Journal Orbit of an Unbalanced Horizontal Rotor at the Stability Threshold for 5 Cycles (N = 6500, W = 50, C = 0.005, L/D = 1/2, EMU = 0.2) . . . . .134

6.41 Transmissibility and Shaft X-Y Motion vs Cycles of Motion (N = 6500). . . . .135

6.42 Journal Orbit (by Euler's Improved Method) of an Unbalanced Horizontal Rotor for 5 Cycles (N = 6500, W = 50, C = 0.005, L/D = 1/2, EMU = 0.2) . . . . .136

6.43 Transmissibility and Shaft X-Y Motion vs Cycles of Motion . .137

6.44 Radius of Curvature and Whirl vs Cycles of Motion (N = 6500).138

6.45 Journal Orbit of an Unbalanced Horizontal Rotor above the Stability Threshold for Cycles 5 - 10 (N = 10,500) . . . . .139

6.46 Journal Orbit of an Unbalanced Horizontal Rotor for Cycles 10 - 15 Showing the Non-Synchronous Limit Cycle (N = 10,500).140

6.47 Journal Orbit of an Unbalanced Horizontal Rotor Showing Synchronous Motion at the Stability Threshold for 5 Cycles (N = 6500, W = 50, C = 0.005, L/D = 1/2, EMU = 0.8) . . . . .141

6.48 Transmissibility and Shaft X-Y Motion vs Cycles of Motion (N = 6500). . . . .142

6.49 Radius of Curvature and Whirl vs Cycles of Motion (N = 6500).143

6.50 Unbalance-Displacement Phase Angle vs Cycles of Motion (N = 6500). . . . .144

6.51 Journal Orbit of an Unbalanced Horizontal Rotor above the Stability Threshold for Cycles 5 - 10 Showing Synchronous Limit Cycle (N = 10,500) . . . . .145

6.52 Transmissibility and Shaft X-Y Motion vs Cycles of Motion for Cycles 5 - 10 (N = 10,500) . . . . .146

6.53 Radius of Curvature and Whirl vs Cycles of Motion for Cycles 5 - 10 Illustrating Small Numerical Instability (N = 10,500).147

6.54 Journal Orbit of an Unbalanced Vertical Rotor Having a Backward Half-Frequency Rotating Load for 5 Cycles (N = 3600, W = 200, C = 0.00376, L/D = 1/2, FO = -200, EN = -0.5, EMU = 0.27) . . . . .150

FIGURE

PAGE

6.55 Journal Orbit of an Unbalanced Horizontal Rotor Having a Backward Half-Frequency Rotating Load for 5 Cycles (N = 3600, W = 200, C = 0.00376, L/D = 1/2, FO = -200, EN = -0.5, EMU = 0.27) . . . . .151

6.56 Radius of Curvature and Whirl vs Cycles of Motion for an Unbalanced Horizontal Rotor (N = 3600) . . . . .152

6.57 Journal Orbit of an Unbalanced Horizontal Rotor Having a Forward Half-Frequency Rotating Load for 5 Cycles (N = 6500, W = 50, C = 0.005, L/D = 1/2, EMU = 0.001, FO = 100, EN = -0.5) . . . . .154

6.58 Journal Orbit of an Unbalanced Horizontal Rotor Having a Backward Half-Frequency Rotating Load for 5 Cycles (N = 6500, W = 50, C = 0.005, L/D = 1/2, EMU = 0.001, FO = 100, EN = -0.5) . . . . .155

6.59 Radius of Curvature and Whirl vs Cycles of Motion (FO = 100, EN = 0.5) . . . . .156

6.60 Journal Orbit of an Unbalanced Horizontal Rotor Having Unidirectional Harmonic Loading for 5 Cycles (N = 6500, W = 50, C = 0.005, L/D = 1/2, EMU = 0.001, FHY = 100, ENY = 0.5). . . . .157

6.61 Radius of Curvature and Whirl vs Cycles of Motion (FHY = 100, ENY = 0.5) . . . . .158

NOMENCLATURE

<u>SYMBOL</u>	<u>DESCRIPTION</u>	<u>UNITS</u>
$\bar{B}$	Body forces per unit volume	lb./in. <sup>3</sup>
b	Width of slider bearing	in.
$C_{ij}$	Damping coefficients	lb.-sec./in.
C, c	Journal clearance	in.
D	Journal diameter	in.
$E_o, ES$	Eccentricity ratio calculated using the total resultant journal load for P in the Sommerfeld equation	---
$E_\mu, EMU$	Unbalance eccentricity ratio = $e_\mu/c$	---
EN	Ratio of rotating load angular speed = $\omega_{Fo}/\omega_j$	---
ENX	Ratio of oscillating horizontal load angular speed = $\omega_{FHx}/\omega_j$	---
ENY	Ratio of oscillating vertical load angular speed = $\omega_{FHy}/\omega_j$	---
ESU	Eccentricity calculated using unbalance load as loading force	---
e	Radial journal center displacement	in.
$e_\mu$	Unbalance eccentricity	in.
$\hat{e}_o, \hat{e}_r$	Unit vectors referenced from the bearing center	---
$\hat{e}_N, \hat{e}_t$	Unit vectors referenced from the instantaneous center of curvature	---
$F_o, FO$	Magnitude of rotating load	lb.
$F_x, F_y$	Force due to film in x and y coordinate directions respectively	lb.
$\bar{F}_x, \bar{F}_y$	Dimensionless forces from fluid film in x and y directions	---

<u>SYMBOL</u>	<u>DESCRIPTION</u>	<u>UNITS</u>
F	Resultant fluid film force	lb.
FHX	Magnitude of horizontal oscillating load (x-direction)	lb.
FHY	Magnitude of vertical (y-direction) oscillating load	lb.
FMAX	Maximum fluid film force developed per run	lb.
FU	Magnitude of unbalance load	lb.
FURATIO	Ratio of unbalance load to journal weight	---
FX, FY	Constant load on journal in the x and y coordinate directions respectively	lb.
g	Acceleration of gravity = 386	in./sec. <sup>2</sup>
H	Dimensionless film thickness = h/c	---
h	Film thickness	in.
h	Stepping increment of independent variable	---
$\vec{i}, \vec{j}, \vec{k}$	Unit vectors in the fixed x-y-z coordinate directions	---
$K_{ij}$	Stiffness coefficients	lb./in.
L	Length of journal	in.
l	Length of slider	in.
$M_j, m_j$	Effective mass of journal	lb <sub>m</sub> .
MU	Viscosity of fluid film	lb.-sec./in. <sup>2</sup>
N, N <sub>j</sub>	Angular speed of journal	RPM
N <sub>b</sub>	Angular speed of bearing	RPM
N', N' <sub>j</sub>	Angular speed of journal	RPS
N' <sub>b</sub>	Angular speed of bearing	RPS
n	Eccentricity ratio = $\epsilon = e/c$	---
$\vec{n}_R, \vec{n}_\theta$	Unit vector in radial and tangential direction	---

<u>SYMBOL</u>	<u>DESCRIPTION</u>	<u>UNITS</u>
$v_i$	Velocity	in./sec.
$\bar{v}_p$	Velocity of a point on the journal surface	in./sec.
$\bar{v}_Q$	Velocity of a point on the bearing surface	in./sec.
$v$	Velocity component in the y-coordinate direction	in./sec.
$W$	Effective weight of the journal	lb.
$W_i$	Velocity	in./sec.
$WS$	Speed parameter = $\sqrt{m_j c \omega_j^2 / W_T}$	---
$W_T$	Total constant load on journal	lb.
$WT$	Ratio of total constant load to journal effective weight = $W_T/W$	---
$w$	Velocity component in z-coordinate direction	in./sec.
$X$	Dimensionless displacement = $x/c$	---
$\dot{X}$	Dimensionless velocity = $\dot{x}/c\omega_j$	---
$x, x_1$	Displacement of journal in x-coordinate direction	in.
$x_2$	Displacement of bearing in x-coordinate direction	in.
$x_i$	Solution at $i^{\text{th}}$ step of independent variable	---
$Y$	Dimensionless displacement = $y/c$	---
$\dot{Y}$	Dimensionless velocity = $\dot{y}/c\omega_j$	---
$y, y_1$	Displacement of journal in y-coordinate direction	in.
$y_2$	Displacement of bearing in the y-coordinate direction	in.
$\bar{z}$	Dimensionless distance along axial or z-direction = $z/L$	---
$z$	Distance along z-coordinate	in.

<u>SYMBOL</u>	<u>DESCRIPTION</u>	<u>UNITS</u>
$\alpha$	Ratio of angular velocities = $\omega_j / (\omega_b + \omega_j)$	---
$\alpha$	Angle between velocities $R\omega_j$ and $(R + C)\omega_b$ , $\sim \frac{1}{R} \partial h / \partial \theta$	---
$\beta$	Phase angle between the journal displacement vector and the unbalance eccentricity vector	deg.
$\epsilon, \epsilon_0$	Eccentricity ratio = $e/c$	---
$\epsilon_0$	Eccentricity calculated from equation of $S_S$	---
$\eta$	Ratio of rotating load velocities = $\omega_{F0} / \omega_j$	---
$\theta'$	Angular distance from positive line of centers in rotating coordinate set	---
$\theta$	Angular distance from the positive x-axis in the fixed x-y coordinate set	---
$\dot{\theta}$	Instantaneous angular velocity about the center of curvature	sec. <sup>-1</sup>
$\lambda$	Root to the characteristic equation of journal equations of motion	sec. <sup>-1</sup>
$\mu$	Viscosity	lb.-sec./in. <sup>2</sup>
$\nu$	Kinematic viscosity, = $\mu/\rho$	in. <sup>2</sup> /sec.
$\rho$	Density	lb. <sub>m</sub> /in. <sup>3</sup>
$\rho$	Instantaneous radius of curvature	in.
$\dot{\phi}$	Whirl velocity about bearing center	sec. <sup>-1</sup>
$\phi$	Attitude angle	deg.
$\Omega, \omega_j$	Journal angular velocity	sec. <sup>-1</sup>
$\Omega_S$	Speed parameter, = $\omega_j / \sqrt{W_T / m_j c}$	---
$\omega_b$	Bearing angular velocity	sec. <sup>-1</sup>
$\omega_S$	Speed parameter, = $\omega_j / \sqrt{g/c}$	sec. <sup>-1</sup>
$\omega$	Angular speed defined as $\omega_b + \omega_j$	sec. <sup>-1</sup>

## CHAPTER I

### INTRODUCTION AND STATEMENT OF THE PROBLEM

"The study of hydrodynamic lubrication is, from a mathematical standpoint, the study of a particular form of the Navier-Stokes equations (1)\* \*\*." It was not until the 1880's that the theory of hydrodynamic lubrication came into existence. A Committee of the Institution of Mechanical Engineers had asked Beauchamp Tower to determine the proper means by which a railroad journal bearing should be lubricated. The investigation indicated that bath lubrication significantly lowered the coefficient of friction of the bearing. When a hole was drilled in the bearing to allow lubricant to be added, it was noticed that a considerable amount of oil was flowing from the hole. Tower tried to plug the hole with a wooden peg but it was soon worked out when the test was rerun. A gauge was then attached and indicated a definite pressure greater than the projected pressure of the load. Further measurements were then taken throughout the bearing and gave an indication as to the pressure profile in the bearing (2).\*\*\*

Reynolds (3) analysis, in 1886, of Towers' experiment deduced that the resultant pressure profile was due to hydrodynamic action in the fluid film and was dependent upon the viscosity of the lubricant being used. The differential equations formulated by

---

\*Number in parentheses indicate reference in Bibliography.

\*\*Reference in Bibliography, p. 1.

\*\*\*Reference in Bibliography, p. 149.

Reynolds for the determination of the hydrodynamic bearing pressure were solved by an approximate series expansion for an infinitely long bearing assuming steady state loading only.

As the speeds of the machinery using journal bearings increased after the turn of the century, the interest in the development of journal bearing theory increased considerably. The users of such machinery were reporting large vibrational amplitudes under certain conditions of loading and speed which in turn caused large forces to be transmitted to the system foundation and the system's component parts.

Newkirk (4) reported in 1924 the first recorded instance of bearing instability. He demonstrated that under certain combinations of speed and loading, the journal center did not remain fixed as predicted by the steady-state Reynolds equation, but precessed or orbited about the equilibrium position at a speed approximately equal to half the rotational speed. This phenomena was termed oil whip or whirl and is a self-excited motion.

A complete dynamical analysis of such a system requires that the hydrodynamic force terms be coupled to the dynamical equations of motion of the rotor (journal), including the external loading forces on the system and the unbalance of the journal (See Figures 3.1, 3.2 for journal bearing schematic, force balance and unbalance representation).

The resulting equations of motion for the complete system are highly nonlinear and the stability characteristics have been examined primarily from a linearized or perturbation analysis about the

equilibrium position of a balanced journal under unidirectional loading.

The bearing stability obtained from linearized theory only predicts the threshold of stability. It does not give any information as to the magnitude of the journal orbit above the whirl threshold speed. The linearized theory predicts that the journal motion will grow exponentially or become unbounded when the rotor is operated above the whirl threshold speed. In actuality, the journal motion is bounded and the motion forms limit cycles.

With the aid of the high-speed digital computer and the proper formulation of the hydrodynamic force expressions, the complete non-linear motion of the journal bearing system may be obtained through the use of numerical methods for integrating the governing equation of motion.

In addition to the determination of the journal motion under arbitrary loading above and below the stability threshold, it is equally important that the bearing forces and the bearing dynamic transmissibility characteristics be determined (see p. 45 for explanation of this term). The results of such an analysis follows a brief discussion of the earlier investigations and the state of the art (CHAPTER II).

## CHAPTER II

### BACKGROUND AND STATE OF THE ART

Under stable operating conditions the journal center will be located at some equilibrium eccentricity,  $e_o$ , and at a given constant attitude angle,  $\phi_o^*$ , as shown in Figure 3.1. This condition would be ideal for smooth operation of the machinery supported in the journal bearing. However, as mentioned earlier, numerous reports indicated that such machinery was having serious vibrational problems.

Harrison (5) in 1913 who gave fluid-film force expressions, and Newkirk (4) in 1924 were the earliest investigators of the problem of rotor stability. Working at the General Electric Laboratory, Newkirk observed and explained to some extent the phenomenon of whirl. This experimental investigation is considered by many to be the point at which the interest of the engineer and designer first centered on the fluid-film journal bearing as a contributing factor to the instability of rotating machinery (6).

Gunter (7) gives a detailed report on the findings of Newkirk (8) and discusses the work of Robertson (9) who in 1933 used the forces derived by Harrison to investigate the stability of an infinitely long, ideal  $360^\circ$  journal bearing. This analysis disagreed with experimental findings since the journal was shown to be unstable at all speeds. The discrepancy arose from the fact that Harrison, as referenced above, had included the negative pressure region of the bearing in his analysis

---

\*See footnote on page 43 for further information about the equilibrium attitude angles.

since he did not consider film cavitation or rupture. Thus the analysis by Harrison is valid only for small eccentricities or for the case where the ambient fluid pressure is greater than the maximum hydrodynamic pressure developed. In this case the uncavitated film is closely approximated.

In 1930 Cardullo's work (10) was published in which he considered the development of equations for the pressure profiles in short journal bearings. Sommerfeld (11) had earlier presented an approximate solution to Reynolds' equation in which the bearing was assumed to be infinitely long and hence the axial flow of the lubricant could be neglected. Cardullo realized this approach was in error, especially for very short bearings or bearings having circumferential grooving. He proceeded to develop a theory which accounted for only axial flow and presented curves representative of the resulting pressure profiles in short journal bearings. In a discussion to this paper, Howarth and Needs called attention to the paper of A. G. M. Michell, "The Lubrication of Plane Surfaces," published in Zeit. f. Math. u. Phys. in 1905. Michell had based his work on Reynolds' equation\*; dropping the first term on the left side of the equation. This gave the same results, without going through the long derivation and assumption, that Cardullo had presented. Due to the assumption made by Michell and Cardullo which seemed to make the pressure gradient zero in the circumferential direction, no further analysis was made of the solution until the 1950's,

---

\*Reynolds' equation is given as Eq. [3.18], p. 23.

when Ocvirk, whose work will be discussed later, presented experimental evidence of the validity of the solution and extended the analysis considerably.

In 1946 Hagg (12) reported that the upper limit of the whirling frequency was one-half the rotational frequency, the same conclusion reached by Robertson in 1933. Hagg's argument was based on the required flow for a whirling journal whereas Robertson reached his conclusion by considering the conditions necessary for a force balance of a whirling ideal journal. The stability of several types of bearing arrangements were tested experimentally and the tilting pad arrangement was found to be incapable of exciting or sustaining a vibration.

Ocvirk (13) in 1952 presented experimental data which supported the theory of Michell and Cardullo for bearings having length to diameter ratios up to about one. His complete analysis gave expressions for applied load, attitude angle, location and magnitude of peak film pressures, friction, and required oil flow rate as a function of the eccentricity ratio. The basic nondimensional expression developed, the capacity number, allowed performance curves to be drawn (capacity number vs. eccentricity ratio) and by comparison to experimental data it was concluded that reasonable agreement existed between the short bearing theory and the experimental test data.

Ocvirk's analysis clearly indicated that by dropping the first term of Reynolds' equation the circumferential pressure gradient was not zero but some finite value. The part of the circumferential flow proportional to the journal surface velocity and varying film thickness was not lost by dropping the first term of Reynolds' equation.

Burwell (14) in 1951 presented analytical solutions for journal paths under various simple types of loading (constant, square wave, sinusoidal) for a very narrow bearing. However, the regions of negative pressure were retained in the solution, which made the analysis ambiguous for other than very small eccentricities.

Poritsky (15) in 1953 stated that by neglecting the negative portion of the journal pressure profile (long bearing equation) the journal could be shown to be stable below twice the critical frequency of the rotor. However, in his analysis of the linearized equations a stiffness term was added to the radial component of motion and the negative pressure remained in the analysis. One conclusion reached by his analysis was that rotor flexibility lowered the stable range of operation. The same conclusion was reached by Hagg and Warner (16) who devised an electric analog for the flexible rotor.

DuBois and Ocvirk (17) in 1955 considered a method for estimating a maximum bearing operating temperature and discussed methods of evaluating the effects of elastic deformation and misalignment on bearing performance. A method for determining a factor of safety was also presented.

Kreisle (18) in 1955 gave experimental findings concerning the performance of short journal bearings under conditions approaching zero minimum oil-film thickness. Six different load numbers were defined and considered to be useful in predicting and analyzing the performance of short journal bearings. The results of his experimental torque measurements indicated that, as long as the minimum oil-film thickness is of the order of or exceeds the sum of the predominant peak

surface roughness of the bearing and journal in the circumferential direction, hydrodynamic film lubrication exists in the bearing.

Newkirk and Lewis (19) reported from experimental observations that short bearings, large clearances and moderate loads favored a wider range of stable operation.

Boeker and Sternlicht (20) derived the stability threshold for antiwhirl journal bearings\* and justified the stiffness term used by Poritsky as the contributing factor to predicting the region of stable operation. Hagg and Sankey (21) provide analytical and experimental results for a rotor bearing system. Linearized elastic and damping properties were incorporated in their analysis which reduced the resonant amplitude of the rotor considerably in the analytic solution and was in good agreement with the experimental amplitudes recorded.

Newkirk (22) reports experimental results obtained from two different test rigs; one rigid rotor (oil film dominant) and one more flexible (elasticity of shaft more dominant). Three general definitions were given and are repeated here:

- a. "Resonant whirl [whip]" may be defined as, "a resonant vibration of a shaft in fluid film journal bearings which occurs at speeds equal to or above twice the first critical of the rotor, and at a frequency equal approximately to a natural frequency of the rotor at the running speed."
- b. "Half-frequency whirl" is, "a vibration that may occur at any rotative speed of a shaft in fluid-film bearings and at

---

\*These have grooving on the shaft or in the bearing surface and therefore do have a radial component of force whereas the 360° full journal does not have the radial component if the negative pressures are not neglected.

a frequency approximately one half of such speed."

- c. "Fluid-criticals" are, "rotor instabilities of limited speed range due to fluid-film action in journal bearings."

Pinkus (23) reported that flexible mounting gave greater stability to rotor-bearing systems. This was in direct opposition to the findings of Poritsky (15) and Hagg and Warner (16) who stated that support flexibility will lower the stability threshold speed. (Gunter explains this apparent discrepancy in CHAPTER IV of reference (7)). High loads and high viscosities were also reported by Pinkus to increase stability, while unbalance had little or no effect on the resonant whirl.

Pinkus in his experimental investigations of bearing stability indicates that the order of bearing stability is, starting with the most stable bearing, as follows: 3-lobe, tilting pad, pressure, elliptical, 3-groove, and plain circular.

Orbeck (24) in 1958 presented an analysis of oil whip that incorporated pressure forces, viscous drag forces, and the centrifugal forces acting on the journal. A vertical shaft was used for the model and the experimental results of Kreisle were used to define the capacity number. Equations are given that determine both the amplitude and the whirling frequency for a vertical shaft arrangement. The results, as based on the experimental curves of Kreisle, show for a particular example cited that the frequency ratio varied from 0.497 at an eccentricity of 0.05 to 0.499 at an eccentricity of 0.8.

Hull (25) in 1958 demonstrated oil-whip resonance harmonics experimentally by applying a rotating load to the journal bearing test rig. The journal center traced out a different trochoid for each

ratio of exciting force frequency to running speed. Inside loops denoted a forward rotating load while outside loops denoted backward rotating loads. The formula he gave was:

$$L = \frac{N_j/N_w}{2.16} - 1$$

where:

L = number of loops (inside = +, outside = -)

$N_j$  = journal speed

$N_w$  = speed of rotating load.

These results are true only when the single rotating load is large in comparison to any other forcing function that might be acting on the journal. If unbalance is present, then the resulting orbit center traces will be altered considerably due to the synchronous unbalance force. This will be shown in the following analysis.

In 1959 Hori (26) presented the results of an investigation that allowed the inherent journal instability of previous analyses to be avoided by assuming zero pressure in place of the negative pressures in the oil film. Hori used the long bearing approximation to Reynolds' equation and applied the Hurwitz criteria to the linearized equations of motion.

Hori showed that the bearing is not unstable at all speeds as indicated by the Robertson analysis, but has a finite stability threshold which is a function of bearing clearance, transverse shaft loading, journal speed and viscosity. He presented dimensionless stability plots which show the influence of various bearing parameters on rotor stability. One important aspect of Hori's analysis is the

influence of the transverse bearing load on stability. For example Hori states that in the case of a vertical balanced rotor in which the transverse load due to gravity is zero, the journal will be unstable at all speeds. This important stability characteristic of vertical shafts has been verified by the author in this investigation. Hori also shows that if the transverse loading is sufficiently large so as to increase the operating eccentricity above 0.8 for the plain journal bearing, the system will be stable regardless of shaft flexibility.

Sternlicht (27) presents a summary of nine earlier papers that deal with both compressible and incompressible fluid film journal bearings. The concept of force transmission and its effect on the overall rotor system performance is discussed. Synchronous, half, and fractional frequency whirl, critical speeds, and resonant whip are also briefly discussed.

Reddi and Trumpler (28) in 1962 examined the stability of the 360° full journal and the 180° partial-film bearings. End leakage factors were applied to the film force expressions and the resulting equations of motion linearized and examined for stability about the equilibrium position by the Routh criteria. The complete equations of motion were programmed on a digital computer and the resulting orbits presented for the 360° journal.

Reddi also demonstrated that if bearing cavitation is not taken into consideration, the bearing will be unstable at all speeds. For example, he shows that for the case of the full film 360° infinite length bearing excluding cavitation, the journal motion will always become unstable and form limit cycles. He also shows a number of

cases in which the bearing fails for high loading and low speed operation in which the stability data of Hori and Booker indicate high stability if cavitation is included. This behavior has actually been observed in practice. Pinkus reports on stabilizing a bearing by reducing the oil inlet flow thereby changing the cavitation boundary conditions. Thus the cavitation boundary conditions of the bearing will greatly influence the stability characteristics of the system. The complete cavitation equations obtained from the Navier-Stokes equations are time transient and have not been completely investigated.\*

A stability chart was presented for the 180° film bearing which indicated regions of stable and unstable operation on a plot of Sommerfeld number versus a speed parameter. The conclusion reached was that the designer may expect large machine vibration and possible bearing failure unless the equilibrium eccentricity ratio remains  $\geq 0.76$ , i.e., a heavily loaded condition, or the speed parameter  $\Omega = \sqrt{\frac{Mc}{W}} < 0.22$ . This is equivalent to the stability parameter of the author of  $WS = 1.38$ . Badgley and Booker(30) show that the short bearing is stable for values of  $WS < 2.50$

Alford (29) in 1965 presented a completely new concept as to the possible causes of instability in turbomachinery. Forces arising from two sources were considered. These were (a) forces due to circumferential variation of static pressure acting on the cylindrical surface of the rotor (particularly within labyrinth seals) and (b) forces due to the eccentricity of the rotor causing variation of blade-tip clearances which results in variation of local efficiency and creates unbalance torques. These considerations are of extreme importance and

---

\* Cole, J.A. and Hughes, C.J., "Oil Flow and Film Extent in Complete Journal Bearings," Proc. Inst. Mech. Engrs. (London), Vol.170, No.17, 1956.

are a key factor to instabilities of high-speed axial compressors and turbines. It explains why some units run very smoothly at no load test conditions while serious stability problems arise when testing at partial or full load conditions.

Gunter (7) in 1966 after giving a complete discussion of the background and state of the art, examined the single-mass unbalanced symmetric rotor for synchronous, nonsynchronous, and zero precession and the effect of gravity. The analysis included the influence of support flexibility and damping on stability. Various stability maps were presented for the case of symmetric and unsymmetric bearing support flexibility. It was shown that foundation asymmetry alone could increase the stable region of operation considerably.\* The experimental orbits obtained by Kushul\*\* of precession above the stability threshold indicated that the precession rate was constant and equal to the rotor critical speed.

The stability of hydrodynamic bearings was also examined and confirmed the findings of Reddi (28). Whirl orbits for both linearized and nonlinear bearing characteristics obtained by analog computer simulation indicated the formation of limit cycles in the nonlinear case whereas the linearized equations gave whirl orbits that were unbounded.

Badgley (30) recently presented a nonlinear transient analysis of

---

\*This explains the conflicting reports of Pinkus versus Poritsky, Hagg and Warner, as mentioned earlier in this discussion.

\*\*Kushul, M.Y., "The Self-Induced Oscillations of Rotors," (Trans. from Russian.) Consultants Bureau, New York, 1964.

a plain journal bearing by simulating the whirl orbits on a digital computer by forward numerical integration of the equations of motion. The approximations to Reynolds equation used in that analysis were the short bearing (Ocvirk), the long bearing (Sommerfeld), and the finite length bearing using Warner's end leakage correction factor. Badgley assumed a balanced, unloaded, horizontal rotor including film cavitation. He examined the orbit behavior of the shaft for various disturbance values and showed that the stability threshold at high eccentricity is reduced by large initial velocity disturbances. Badgley did not include the influence of rotor unbalance or external loading. In the author's investigation these effects are included and it has been demonstrated that these loads can have a profound effect on journal stability.

Also of considerable importance is the magnitude of the bearing forces developed during whirl. Of the numerous papers presented on the subject of bearing instability, no mention has been made of the actual forces developed by the system. The force transmitted or the dynamic transmissibility coefficient developed by a bearing is an important factor in the design of a bearing which has been ignored in the past.

The most recent contribution to the analysis of nonlinear whirl motion of a journal bearing was the paper presented by Tolle (30) at the ASME 1968 Vibrations Conference. In this analysis the author attempts to calculate the pressure profile by means of a series expansion. The equations of motion are expressed in rotating coordinates and are integrated on a digital computer using the fourth-order Runge-Kutta procedure. Since Tolle has considered a noncavitating film the journal motion is unstable at all speeds, forming limit cycles.

This analysis, similar to Badgley's work is also limited in its scope and does not consider the influence of external loads on the system.

These authors have contributed greatly to the understanding of journal bearing lubrication problems, however, at present there has been little data published on the transient nonlinear motion and forces transmitted in a journal bearing.

The following analysis will combine the nonlinear hydrodynamic fluid-film forces to the dynamical equation of motion, which may then be numerically integrated to obtain the transient behavior of the journal. Horizontal, vertical, and unbalanced journals will be considered as well as the transient response to loading, both constant and cyclic (rotating and unidirectional). The instantaneous whirl and forces transmitted to the bearing are easily obtained as a result of the method of solution.

CHAPTER III  
ANALYSIS OF THE SYSTEM

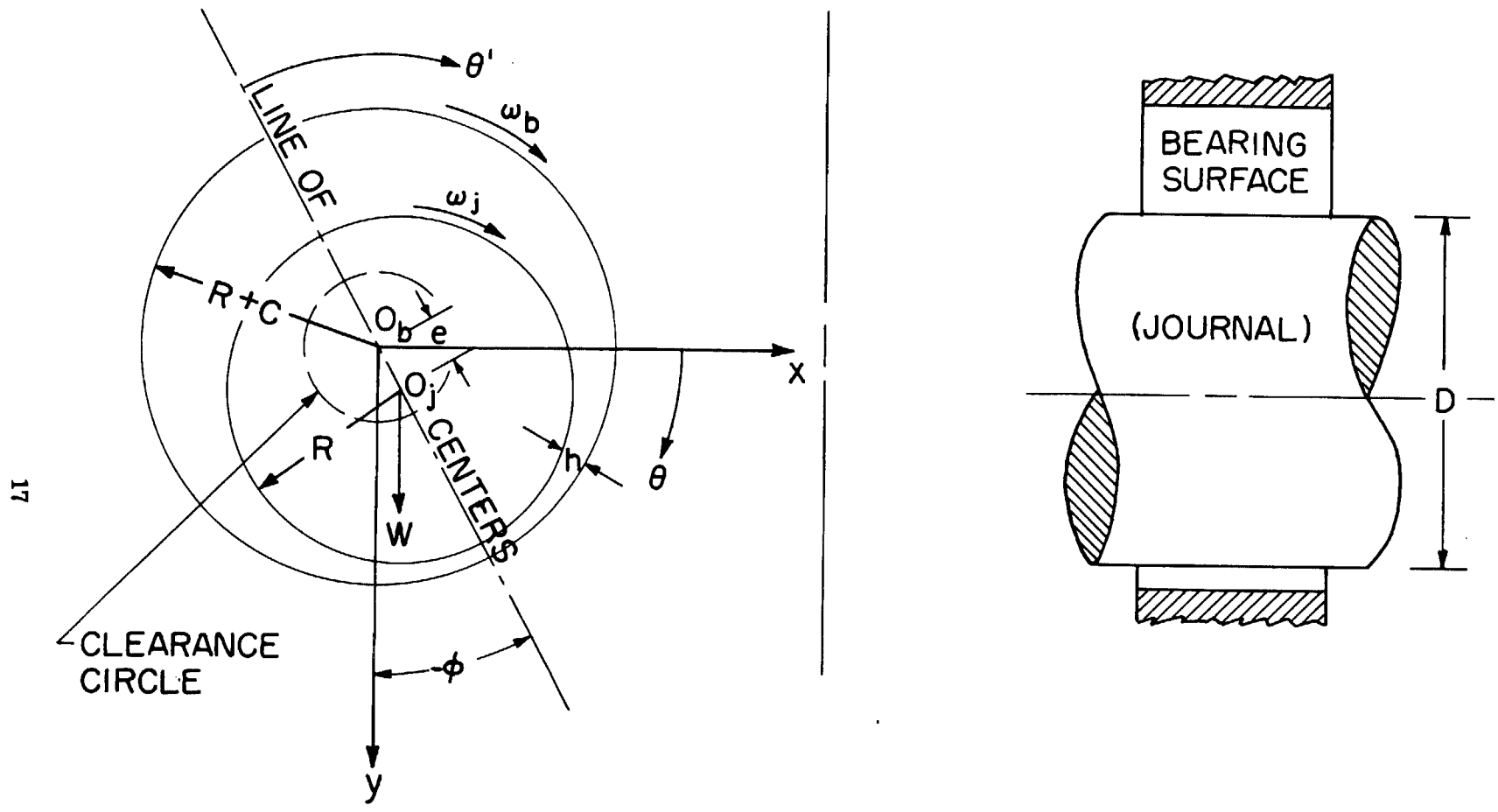
3.1 Introduction

This chapter contains the derivation of the equations of motion for the journal bearing. Figure 3.1 gives a schematic of a typical journal bearing. The clearance between the journal and bearing has been greatly exaggerated to clarify the representation of the bearing parameters. The journal center,  $o_j$ , is free to move about in the imaginary clearance circle depicted by the dashed circle in Figure 3.1. The radial displacement of the journal center,  $o_j$ , from the bearing center,  $o_b$ , is denoted as the eccentricity,  $e$ , of the journal, and when divided by the clearance,  $c$ , the eccentricity ratio,  $\epsilon$ , may then take on values only from zero to unity.\* It is therefore possible to represent the journal motion by a point moving about in a unit clearance circle, where all displacements are made dimensionless by dividing them by the clearance. This representation will be used extensively throughout the following analysis.

Reynolds' equation for the plane slider bearing is derived from the Navier-Stokes equation for incompressible fluids. This equation is then further modified for journal bearings for both rotating and fixed coordinates. The short bearing assumption is discussed and compared to a finite width bearing solution. With an expression for

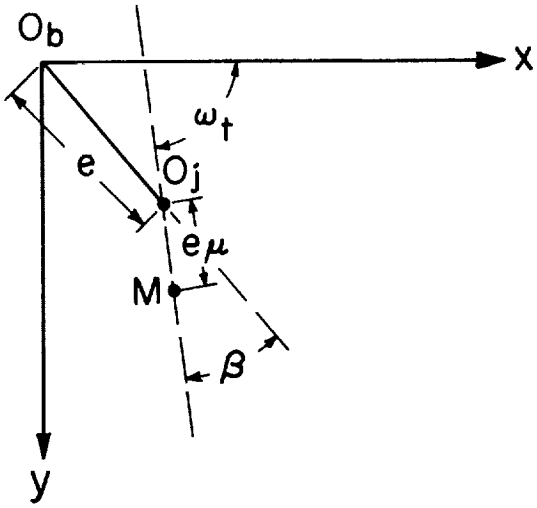
---

\*Unity represents bearing failure, while a value of zero has the journal perfectly centered in the bearing. See Figure 3.2 for a typical force balance.

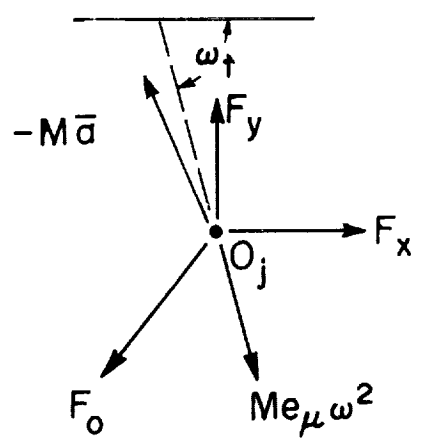


17

3.1 Short Journal Bearing Configuration



UNBALANCE REPRESENTATION



TYPICAL FORCE BALANCE

3.2 Unbalance Representation and a Typical Force Balance

the fluid film forces, the equations of motion of the journal are easily obtained in the fixed coordinate set. A derivation of the instantaneous whirl and radius of curvature is presented and finally some import parameters used for bearing analysis are presented to clarify the terminology of the chapters that follow.

### 3.2 Derivation of Reynolds' Equation;

#### Reduction to the Short Bearing Equation

The Navier-Stokes equations can be expressed in vector notation as:

$$\rho \frac{D\bar{u}}{Dt} = -\bar{\nabla}P + \bar{B} + \mu \cdot \left[ \frac{1}{3} \bar{\nabla}(\bar{\nabla} \cdot \bar{u}) + \nabla^2 \bar{u} \right] \quad [3.1]$$

For the purpose of this particular derivation, the incompressible fluid film between two flat plates of length  $l$  and width  $b$ , separated by some small distance,  $h = f(x, z)$  will be examined.\*\* If in addition the body forces are neglected, Eq. [3.1] may be expressed as follows:\*\*\*

$$\rho \frac{D\bar{u}}{Dt} = -\bar{\nabla}P + \mu \nabla^2 \bar{u} \quad [3.2]$$

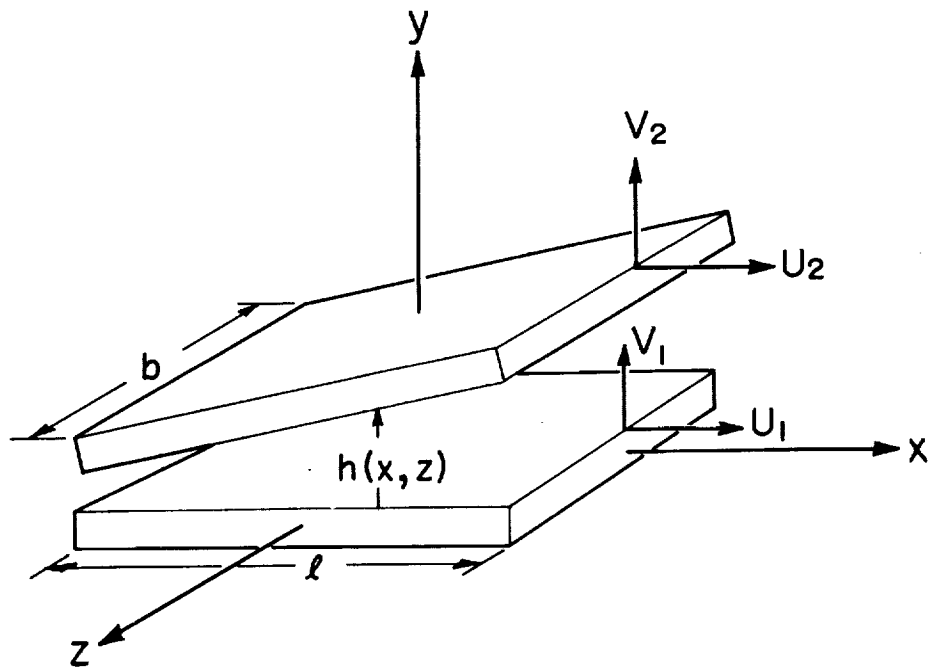
Furthermore, if the ratio of  $h/l$  is restricted to be much less than unity, i.e.  $h/l \ll 1$ , it may be concluded that the reduced Reynolds Number, <sup>(\*)</sup>  $Re^*$ , is much much less than unity and it is hence possible to neglect the inertia force terms on the left of Eq. [3.2].

---

(\*)Discussion of this quantity may be found in Section 5, page 4].

\*\* See Figure 3.3.

\*\*\*This equation can also be applied in journal bearing analysis for the case of a compressible fluid due to the order of magnitude of the term  $\bar{\nabla}(\bar{\nabla} \cdot \bar{u})$ .



### 3.3 The Plane Slider Bearing

Then Eq. [3.2] may be expressed as

$$0 = -\frac{\partial P}{\partial x} + \mu \frac{\partial^2 u}{\partial y^2} \quad [3.3]$$

$$0 = -\frac{\partial P}{\partial y} + \mu \frac{\partial^2 v}{\partial y^2} \quad [3.4]$$

$$0 = -\frac{\partial P}{\partial z} + \mu \frac{\partial^2 w}{\partial y^2} \quad [3.5]$$

where the terms  $\frac{\partial^2}{\partial x^2}$ ,  $\frac{\partial^2}{\partial z^2}$  have been neglected, since they are higher order terms. By restricting the pressure to be constant across the film, i.e.  $\partial p / \partial y = 0$ , it is now possible to integrate Eqs. [3.3] and [3.5] to obtain expressions for the velocity profiles in the x and z coordinate directions.

$$\int \left[ \frac{\partial^2 u}{\partial y^2} = \frac{1}{\mu} \frac{\partial P}{\partial x} \right] dy$$

$$\text{or} \quad \frac{\partial u}{\partial y} = \frac{1}{\mu} \frac{\partial P}{\partial x} y + c_1$$

$$\text{and} \quad u(y) = \frac{1}{2\mu} \frac{\partial P}{\partial x} y^2 + c_1 y + c_2 \quad [3.6]$$

The next step is to impose the following boundary conditions:

$$\text{At } y = 0, u = U_1 \quad [3.7]$$

$$y = h, u = U_2 \quad [3.8]$$

Therefore,

$$c_2 = U_1, \text{ and}$$

$$U_2 = u(h) = \frac{1}{2\mu} \frac{\partial P}{\partial x} h^2 + c_1 h + c_2$$

$$\text{or, } c_1 = \frac{U_2 - U_1}{h} - \frac{1}{2\mu} \frac{\partial P}{\partial x} h$$

Substituting these values of  $c_1$  and  $c_2$  into Eq. [3.6] results in:

$$u(y) = \frac{1}{2\mu} \frac{\partial P}{\partial x} y(y-h) + \frac{h-y}{h} u_1 + \frac{y}{h} u_2 \quad [3.9]$$

In a similar derivation, it can be shown that

$$w(y) = \frac{1}{2\mu} \frac{\partial P}{\partial z} y(y-h) + \frac{h-y}{h} w_1 + \frac{y}{h} w_2 \quad [3.10]$$

where  $w = w_1$  at  $y = 0$

$w = w_2$  at  $y = h$

The remainder of the derivation consists of integrating the continuity equation across the film. Continuity is expressed as:

$$\frac{\partial \rho}{\partial t} + \nabla \cdot (\rho \vec{u}) = 0 \quad [3.11]$$

Integrating this expression from  $y = 0$  to  $y = h$ ,

$$\int_{y=0}^h \left\{ \frac{\partial(\rho v)}{\partial y} = - \left[ \frac{\partial \rho}{\partial t} + \frac{\partial(\rho u)}{\partial x} + \frac{\partial(\rho w)}{\partial z} \right] \right\} dy \quad [3.12]$$

where Eqs. [3.9] and [3.10] are used for  $u$  and  $w$  in this equation.

Doing the indicated integrations yields the following equations:

$$\int_0^h \frac{\partial(\rho v)}{\partial y} dy = \rho v \Big|_0^h = \rho(v_2 - v_1), \text{ where } \rho = f(y) \quad [3.13]$$

$$\int_0^h \frac{\partial \rho}{\partial t} dy = \frac{\partial \rho}{\partial t} y \Big|_0^h = \frac{\partial \rho}{\partial t} h, \text{ } \rho = f(y) \quad [3.14]$$

$$\begin{aligned} \int_0^h \frac{\partial(\rho u)}{\partial x} dy &= \frac{\partial}{\partial x} \int_0^h \rho u dy - \rho u_2 \frac{\partial h}{\partial x} \\ &= -\frac{\partial}{\partial x} \left[ \frac{\rho}{12\mu} \frac{\partial P}{\partial x} h^3 \right] + \frac{\partial}{\partial x} \left[ \frac{1}{2} \rho h (u_1 + u_2) \right] - \rho u_2 \frac{\partial h}{\partial x} \end{aligned} \quad [3.15]$$

Likewise,

$$\int_0^h \frac{\partial(\rho\omega)}{\partial z} dy = -\frac{\partial}{\partial z} \left[ \frac{\rho}{12} \mu \frac{\partial P}{\partial z} h^3 \right] + \frac{\partial}{\partial z} \left[ \frac{1}{2} \rho h (w_1 + w_2) \right] - \rho w_2 \frac{\partial h}{\partial z} \quad [3.16]$$

Combining Eqs. [3.13] through [3.16] and multiplying by 12 results in the following equation:

$$\begin{aligned} \frac{\partial}{\partial x} \left[ \frac{\rho}{\mu} \frac{\partial P}{\partial x} h^3 \right] + \frac{\partial}{\partial z} \left[ \frac{\rho}{\mu} \frac{\partial P}{\partial z} h^3 \right] &= 12\rho(v_2 - v_1) + 12h \frac{\partial \rho}{\partial t} \\ + 6 \frac{\partial}{\partial x} [\rho h (u_1 + u_2)] + 6 \frac{\partial}{\partial z} [\rho h (w_1 + w_2)] &- 12\rho \left[ u_2 \frac{\partial h}{\partial x} + w_2 \frac{\partial h}{\partial z} \right] \end{aligned} \quad [3.17]$$

Inserting the conditions of:

$$\rho = \text{constant}$$

$$w_1 = w_2 = 0$$

$$\partial h / \partial z = 0,$$

the following form of Reynolds' equation may be obtained:

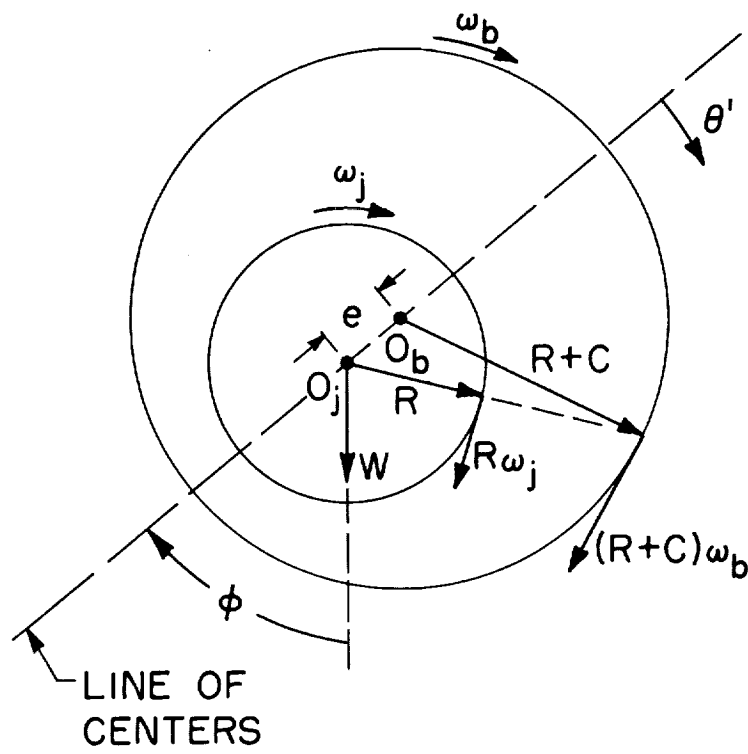
$$\frac{\partial}{\partial x} \left[ \frac{h^3}{\mu} \frac{\partial P}{\partial x} \right] + \frac{\partial}{\partial z} \left[ \frac{h^3}{\mu} \frac{\partial P}{\partial z} \right] = \underbrace{12(v_2 - v_1)}_{\text{"Squeeze"}} + \underbrace{6(u_1 - u_2) \frac{\partial h}{\partial x}}_{\text{"Wedge"}} + \underbrace{6h \frac{\partial}{\partial x} (u_1 + u_2)}_{\text{"Stretch"}} \quad [3.18]$$

It is now desired to relate this solution to the geometry of the journal bearing. The first approach considers rotating coordinates, in which the film thickness\* may be expressed as (see Fig. 3.4):

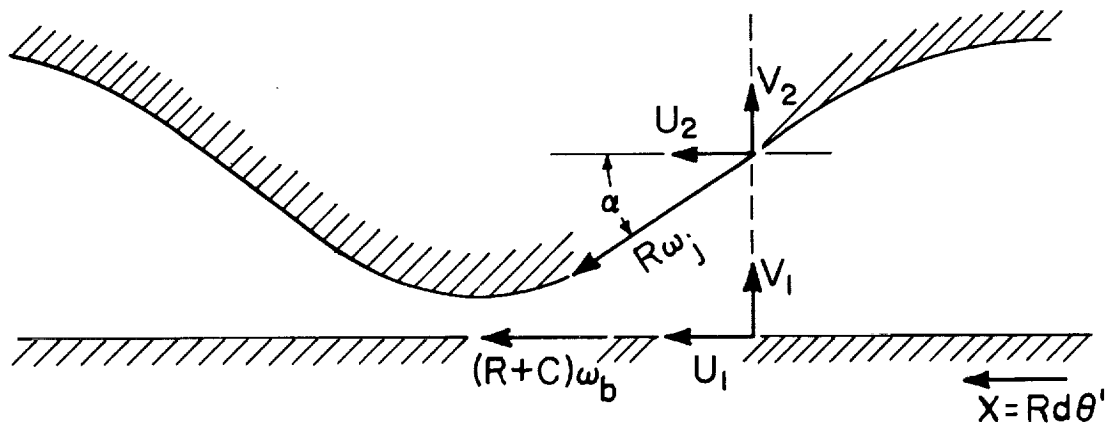
$$h(\theta) = c(1 + \epsilon \cos \theta) \quad [3.19]$$

---

\*For derivation see Reference (32), p. 104.



(a)



(b)

- 3.4 a. Journal Bearing in Rotating Coordinates  
 b. Journal Bearing Profile Unwrapped

Linear combinations of the following components of motion will be considered.

- a. Rotation of journal about  $o_j$ , at  $\omega_j$ .
- b. Rotation of bearing about  $o_b$ , at  $\omega_b$ .
- c. Radial motion of  $o_j$  along the line of centers.
- d. Precession of  $o_j$  about  $o_b$  with angular velocity,  $\omega_p = \dot{\phi}$ .

If the film thickness is "unwrapped" the velocities due to "a" and "b", above may be expressed by the following components:

$$U_1 = (R + C)\omega_b \approx R\omega_b$$

$$U_2 = R\omega_j \cos \alpha \sim R\omega_j$$

$$V_1 = 0$$

$$V_2 = R\omega_j \sin \alpha \approx \alpha R\omega_j = \omega_j \frac{\partial h}{\partial \theta'}$$

Since,

$$\tan(\alpha) = \frac{dh}{dx} = \frac{1}{R} \frac{dh}{d\theta'}$$

and for  $\alpha \ll 1$ ,

$$\alpha \approx \frac{1}{R} \frac{dh}{d\theta'}$$

By neglecting the stretch effect in Eq. [3.18], the contributions due to rotation  $\omega_b$  and  $\omega_j$  are given by:

$$\left[ \frac{1}{6} \bar{\nabla} \cdot \left( \frac{h^3}{\mu} \bar{\nabla} P \right) \right]_{a,b} = (R\omega_b - R\omega_j) \frac{1}{R} \frac{\partial h}{\partial \theta'} + 2\omega_j \frac{\partial h}{\partial \theta'}$$

$$\left[ \frac{1}{6} \bar{\nabla} \cdot \left( \frac{h^3}{\mu} \bar{\nabla} P \right) \right]_{a,b} = (\omega_b + \omega_j) \frac{\partial h}{\partial \theta'} \quad [3.20]$$

For the radial motion along the line of centers it can be shown that:

$$U_2 = \dot{e} \sin \theta'$$

$$V_2 = \dot{e} \cos \theta'$$

$$U_1 = V_1 = 0.$$

Therefore,

$$\left[ \frac{1}{6} \bar{v} \cdot \left( \frac{h^3}{\mu} \bar{v} P \right) \right]_c = (-\dot{e} \sin \theta') \frac{1}{R} \frac{\partial h}{\partial \theta'} + 2 \dot{e} \cos \theta'$$

but by differentiating Eq. [3.19],

$$\frac{\partial h}{\partial \theta'} = \frac{\partial}{\partial \theta'} [C (1 + e \cos \theta')]$$

or

$$\frac{\partial h}{\partial \theta'} = -e \sin \theta'$$

and,

$$\frac{\partial h}{\partial t} = \dot{e} \cos \theta'$$

Hence,

$$\begin{aligned} \left[ \frac{1}{6} \bar{v} \cdot \left( \frac{h^3}{\mu} \bar{v} P \right) \right]_c &= \dot{e} \left[ \sin^2 \theta' \frac{e}{R} + 2 \cos \theta' \right] \\ &= 2 \frac{\partial h}{\partial t} \end{aligned} \quad [3.21]$$

For precession, it is known that every point in the journal has velocity  $e\dot{\phi}$  and is directed normal to the line of centers. Therefore the following velocity components are due to precession:

$$U_2 = -e\dot{\phi} \cos \theta'$$

$$V_2 = e\dot{\phi} \sin \theta'$$

$$U_1 = V_1 = 0$$

Substituting these expressions into Eq. [3.18] yields:

$$\begin{aligned} \frac{1}{6} \left[ \bar{v} \cdot \left( \frac{h^3}{\mu} \bar{v} P \right) \right]_d &= \frac{e}{R} \dot{\phi} \cos \theta' \frac{\partial h}{\partial \theta'} + 2 e \dot{\phi} \sin \theta' \\ &= -2 \dot{\phi} \frac{\partial h}{\partial \theta'} \end{aligned} \quad [3.22]$$

Combining Eqs. [3.20], [3.21] and [3.22] results in:

$$\frac{1}{6} \left[ \bar{v} \cdot \left( \frac{h^3}{\mu} \bar{v} P \right) \right] = (\omega_b + \omega_j - 2\dot{\phi}) \frac{\partial h}{\partial \theta'} + 2 \frac{\partial h}{\partial t} \quad [3.23a]$$

or:

$$\frac{1}{6} \left[ \frac{1}{R^2} \frac{\partial}{\partial \theta} \left( \frac{h^3}{\mu} \frac{\partial P}{\partial \theta} \right) + \frac{\partial}{\partial z} \left( \frac{h^3}{\mu} \frac{\partial P}{\partial z} \right) \right] = (\omega_b + \omega_j - 2\dot{\phi}) \frac{\partial h}{\partial \theta} + 2 \frac{\partial h}{\partial t} \quad [3.23b]$$

This expression, i.e. Eq. [3.23], is the Reynolds equation for a plain journal bearing using rotating coordinates, where  $\theta$  is the angle measured from the line of centers in the positive coordinate direction. This form of Reynolds equation is the expression that most of the work in this field is based on. However, for the purpose of this investigation, the use of Eq. [3.23] was considered to be unnecessarily complicated due to the choice of coordinates. To avoid the complexity of coordinate transformations, the following derivation in fixed cartesian coordinates is presented.

The following unit vectors will be used to express the derived velocity components (see Figure 3.5):

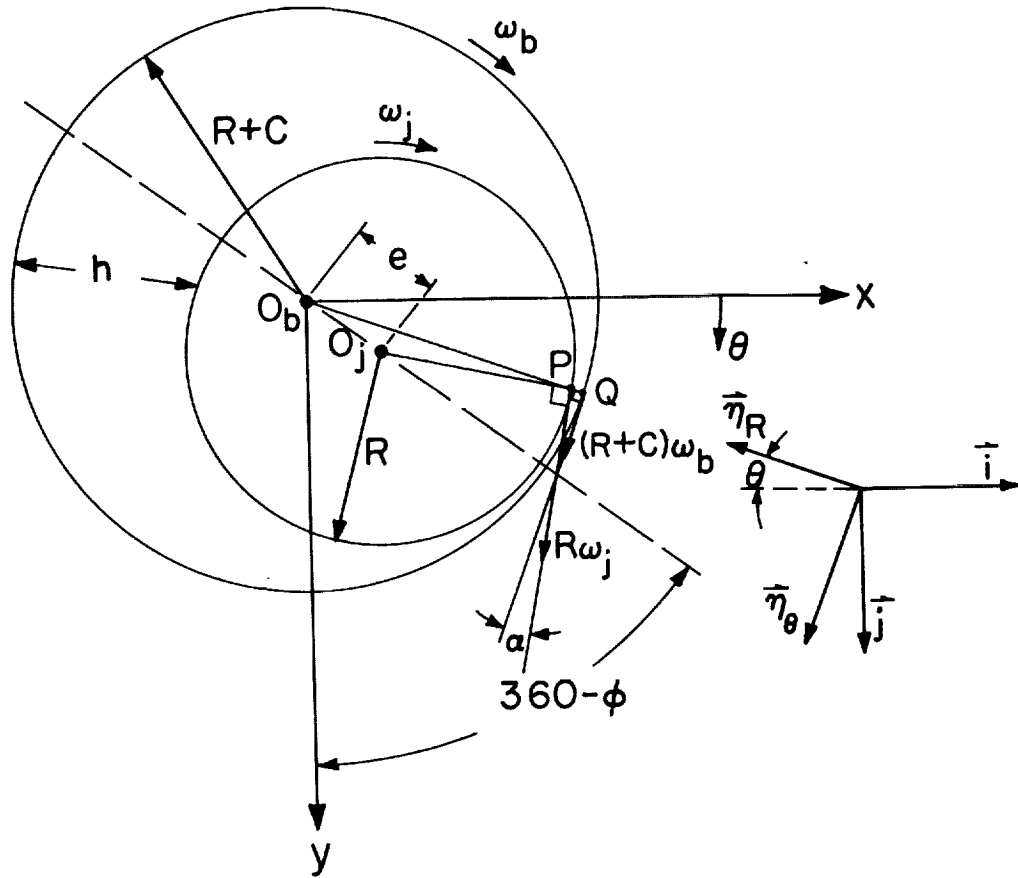
$$\begin{aligned} \vec{i} &= -\cos \theta \mathbf{m}_R - \sin \theta \mathbf{m}_\theta \\ \vec{j} &= -\sin \theta \mathbf{m}_R + \cos \theta \mathbf{m}_\theta \\ \mathbf{m}_R &= -\cos \theta \vec{i} - \sin \theta \vec{j} \\ \mathbf{m}_\theta &= -\sin \theta \vec{i} + \cos \theta \vec{j} \end{aligned} \quad [3.24]$$

The velocities of the bearing and journal centers are as follows:

$$\begin{aligned} V_{ob} &= \dot{x}_1 \vec{i} + \dot{y}_1 \vec{j} \\ V_{oj} &= \dot{x}_2 \vec{i} + \dot{y}_2 \vec{j} \end{aligned}$$

The velocity of point "Q" is:

$$\begin{aligned} \vec{V}_Q &= \vec{V}_{ob} + \vec{\omega}_b \times \vec{R} \\ &= \dot{x}_1 \vec{i} + \dot{y}_1 \vec{j} + R \omega_b \mathbf{m}_\theta \end{aligned}$$



### 3.5 Journal Bearing in Fixed Cartesian Coordinates

and also:

$$\vec{V}_Q = V_1 \mathbf{i}_R + u_1 \mathbf{i}_\theta$$

or

$$V_1 = \vec{V}_Q \cdot \mathbf{i}_R = -\dot{x}_1 \cos \theta - \dot{y}_1 \sin \theta \quad [3.25]$$

and

$$u_1 = \vec{V}_Q \cdot \mathbf{i}_\theta = \omega_b R - \dot{x}_1 \sin \theta + \dot{y}_1 \cos \theta \quad [3.26]$$

For point "P", it is necessary to relate the velocities to

$V_2$  and  $U_2$ .

The  $R\omega_j$  component is not in line with the  $R\omega_b$  component; they differ by the angle  $\alpha$ . For small displacements these are related small angles and it is thus possible to approximate  $\alpha$  as follows:

$$\tan \alpha \approx \alpha = \frac{\Delta h}{\Delta x} \sim \frac{\partial h}{\partial x} = \frac{1}{R} \frac{\partial h}{\partial \theta}$$

Also,

$$\tan \alpha \approx \sin \alpha \approx \alpha$$

For the theta direction:

$$Vel_\theta = R\omega_j \cos \alpha \approx R\omega_j$$

and for the radial direction:

$$Vel_r = R\omega_j \sin \alpha \approx \omega_j \frac{\partial h}{\partial \theta}$$

So, it is now possible to express the velocity of point "P" as:

$$\vec{V}_P = \dot{x}_2 \vec{i} + \dot{y}_2 \vec{j} + R\omega_j \mathbf{i}_\theta + \omega_j \frac{\partial h}{\partial \theta} \mathbf{i}_R$$

Therefore,

$$u_2 = \vec{V}_P \cdot \mathbf{i}_\theta = -\dot{x}_2 \sin \theta + \dot{y}_2 \cos \theta + R\omega_j \quad [3.27]$$

and:

$$V_2 = \vec{V}_P \cdot \mathbf{i}_R = -\dot{x}_2 \cos \theta - \dot{y}_2 \sin \theta + \omega_j \frac{\partial h}{\partial \theta} \quad [3.28]$$

By neglecting the stretch effect of Eq. [3.18], i.e.  $h \frac{\partial}{\partial x} [U_1 + U_2]$ , substitution of the appropriate velocities into that equation gives:

$$\begin{aligned} \frac{1}{6} \left[ \bar{\nabla} \cdot \left( \frac{h^3}{\mu} \bar{\nabla} P \right) \right] &= \frac{1}{R} (u_1 - u_2) \frac{\partial h}{\partial \theta} + 2(v_2 - v_1) \\ &= (\omega_b + \omega_j) \frac{\partial h}{\partial \theta} + (\dot{x}_2 - \dot{x}_1) \left( -2 \cos \theta + \frac{1}{R} \frac{\partial h}{\partial \theta} \sin \theta \right) \\ &\quad - (\dot{y}_2 - \dot{y}_1) \left( 2 \sin \theta + \frac{1}{R} \frac{\partial h}{\partial \theta} \cos \theta \right) \end{aligned}$$

In addition, by neglecting the  $\frac{1}{R} \frac{\partial h}{\partial \theta}$  terms,

$$\frac{1}{6} \left[ \bar{\nabla} \cdot \left( \frac{h^3}{\mu} \bar{\nabla} P \right) \right] = (\omega_b + \omega_j) \frac{\partial h}{\partial \theta} + (\dot{x}_2 - \dot{x}_1) (-2 \cos \theta) - (\dot{y}_2 - \dot{y}_1) (2 \sin \theta) \quad [3.29]$$

But for small deflection, the film thickness,  $h$ , is given as (see Fig. 3.5):

$$h = C - (x_2 - x_1) \cos \theta - (y_2 - y_1) \sin \theta \quad [3.30]$$

since from Eq. [3.19] we can write:

$$\begin{aligned} h(\theta) &= C - e \cos (\theta - (90 - \phi)) \\ &= C - e \cos \theta \sin \phi - e \sin \theta \cos \phi \end{aligned}$$

where:

$$e \sin \phi = x_2 - x_1, \quad e \cos \phi = y_2 - y_1$$

It is now possible to rewrite Eq. [3.29] as follows:

$$\begin{aligned} \frac{1}{6} \left[ \frac{1}{R^2} \frac{\partial}{\partial \theta} \left( \frac{h^3}{\mu} \frac{\partial P}{\partial \theta} \right) + \frac{\partial}{\partial \theta} \left( \frac{h^3}{\mu} \frac{\partial P}{\partial \theta} \right) \right] &= (\omega_b + \omega_j) \frac{\partial h}{\partial \theta} + 2 \frac{\partial h}{\partial t} \\ &= (\omega_b + \omega_j) [(x_2 - x_1) \sin \theta - (y_2 - y_1) \cos \theta] - (\dot{x}_2 - \dot{x}_1) (2 \cos \theta) - (\dot{y}_2 - \dot{y}_1) (2 \sin \theta) \end{aligned} \quad [3.31]$$

It must be remembered that in this equation the " $\theta$ " is measured from the fixed x-axis and should not be confused with the rotating coordinate set where the " $\theta'$ " is measured from the line of

centers.

Two basic approaches to the solution of Eq. [3.31] have been reported in the Literature. If it is assumed that the journal bearing is very long, then it is possible to neglect the fluid flow and pressure gradients along the z-axis and hence reduce Eq. [3.31] to:

$$\frac{1}{6R^2} \frac{\partial}{\partial \theta} \left( \frac{h^3}{\mu} \frac{\partial P}{\partial \theta} \right) = (\omega_b + \omega_j) \frac{\partial h}{\partial \theta} + 2 \frac{\partial h}{\partial t} \quad [3.32]$$

This solution is known as the Long Bearing Solution and was first solved by Sommerfeld who used an adroite substitution and succeeded in integrating the equation (1).\*

On the other hand, if it is assumed that the bearing is relatively short, the appropriate approach is to neglect the flow in the radial direction due to pressure gradients and arrive at:

$$\frac{1}{6} \frac{\partial}{\partial z} \left( \frac{h^3}{\mu} \frac{\partial P}{\partial z} \right) = (\omega_b + \omega_j) \frac{\partial h}{\partial \theta} + 2 \frac{\partial h}{\partial t} \quad [3.33]$$

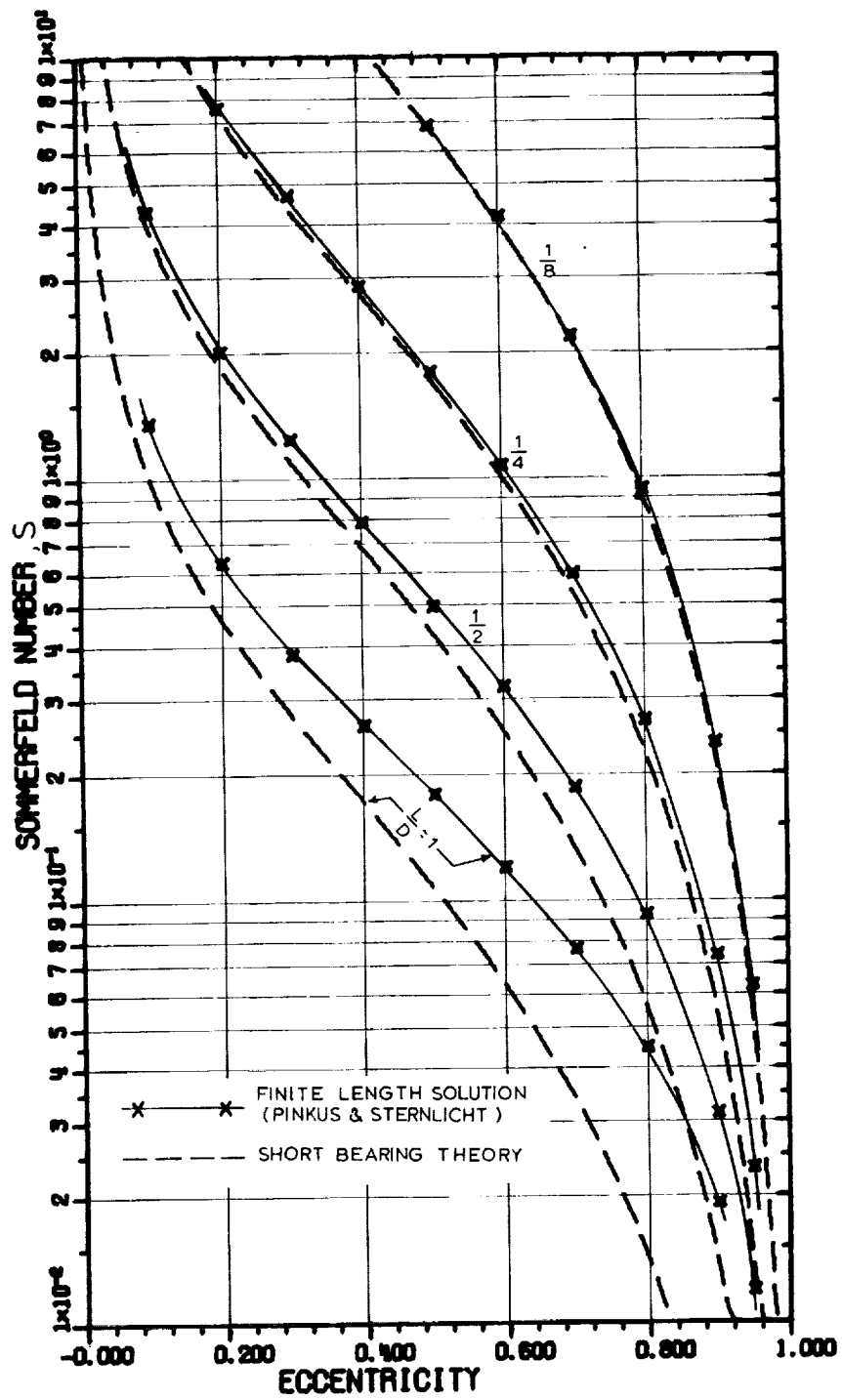
which is known as the governing equation for the Short Bearing Solution. This approach to Reynolds' equation is the basis for the computer program and resulting analysis to be presented in the following sections.

To have a better understanding of when the above assumption is a valid one, the solid curves in Figure 3.6 were drawn from data for a finite full journal bearing.\*\* That data was reported to have come from digital computer solutions of the general Reynolds equation. In

---

\*Reference in Bibliography, p. 42.

\*\*From Reference (1), pp. 86-88.



3.6 Comparison of Finite Length and Short Bearing Solutions

addition, the corresponding Sommerfeld Number\*\* obtained from the short bearing solution is plotted for the same length to diameter ratios. It is easy to see that the assumption is very good for L/D ratios of 1/2 or less, or for  $L/R \leq 1$ . It is also apparent that more deviation exists at larger eccentricity values for  $L/R \geq 1$ , whereas for smaller values the agreement is very good indeed.

The reason for the deviation in the short bearing solution has been explained by Ocvirk (13) to arise from the higher pressures predicted due to neglecting the radial pressure flow in the journal. However, by realizing the limitations of the solution there should be no confusion about the results and conclusions obtained from the given theory.

### 3.3 Dynamical Equations of Motion

The Reynolds equation has been derived in the previous section for the plane slider and by proper substitution and assumptions, it has been reduced to the following equation which is valid for a "short" journal bearing:

$$\frac{\partial}{\partial z} \left( \frac{h^3}{6\mu} \frac{\partial p}{\partial z} \right) = (\omega_b + \omega_j) \frac{\partial h}{\partial \theta} + 2 \frac{\partial h}{\partial t} \quad [3.34]$$

In fixed coordinates, the film thickness, h, is given by:

$$h = c - x \cos \theta - y \sin \theta \quad [3.35]$$

---

\*\*See Section 3.5, p. 42 for explanation of Sommerfeld Number.

This equation is valid for a journal bearing that has no axial misalignment and was derived by considering small motions in the x and y directions to be linearly related. In addition, by limiting the motion of the bearing to rotation,  $\omega_b$ , all displacements will be relative to the bearing center,  $o_b$ .

Equation [3.34] can be integrated directly and by applying the boundary conditions:

$$P(\theta, 0) = P(\theta, L) = 0 \quad [3.36]$$

to evaluate the two constants of integration, the following equation results:

$$P(\theta, z) = \frac{3\mu z(z-L)}{h^3} [(\omega_b + \omega_j) \frac{\partial h}{\partial \theta} + 2 \frac{\partial h}{\partial t}] \quad [3.37]$$

From [3.35],

$$\frac{\partial h}{\partial \theta} = x \sin \theta - y \cos \theta \quad [3.38]$$

and:

$$\frac{\partial h}{\partial t} = -\dot{x} \cos \theta - \dot{y} \sin \theta \quad [3.39]$$

The increment of force on the journal is given as:

$$\Delta \vec{F} = P(\theta, z) R d\theta dz n_R$$

where:

$$n_R = -\cos \theta \hat{i} - \sin \theta \hat{j}$$

Therefore,

$$\Delta \vec{F}_x = (\Delta \vec{F} \cdot \hat{i}) \hat{i} = -[P(\theta, z) R d\theta dz \cos \theta] \hat{i} \quad [3.40]$$

and:

$$\Delta \vec{F}_y = (\Delta \vec{F} \cdot \hat{j}) \hat{j} = -[P(\theta, z) R d\theta dz \sin \theta] \hat{j} \quad [3.41]$$

where the total force component is:

$$F_x = -\iint P(\theta, z) R \cos \theta d\theta dz$$

and:

$$F_y = -\iint P(\theta, z) R \sin \theta d\theta dz$$

The result of integrating over the length of the bearing and substituting Eqs. [3.38] and [3.39] leads to the following equations:

$$\begin{Bmatrix} F_x \\ F_y \end{Bmatrix} = \frac{\mu R L^3}{2} \int_0^{2\pi} \frac{(\omega_j + \omega_b)(x \sin \theta - y \cos \theta) - 2(\dot{x} \cos \theta + \dot{y} \sin \theta)}{(c - x \cos \theta - y \sin \theta)^3} \begin{Bmatrix} \cos \theta \\ \sin \theta \end{Bmatrix} d\theta \quad [3.42]$$

The integral of Eq. [3.42] must be integrated very carefully since a subambient pressure will not be permitted to exist in the fluid film. This follows from reports on experimental test rigs as discussed by Reference (1), page 435. The approach to this particular integral is discussed in more detail in Chapter 5, page 53.

It is possible to put Eq. [3.42] into dimensionless form if the following representation is used:

$$X = \frac{x}{c}, Y = \frac{y}{c}, \omega = \omega_b + \omega_j, \dot{X} = \frac{\dot{x}}{c\omega_j}, \dot{Y} = \frac{\dot{y}}{c\omega_j}, \alpha = \frac{\omega_j}{\omega}$$

then [3.42] becomes:

$$\begin{Bmatrix} F_x \\ F_y \end{Bmatrix} = \frac{\mu L^3 R \omega}{2c^2} \int_0^{2\pi} \frac{(X - 2\dot{Y}\alpha) \sin \theta - (Y + 2\dot{X}\alpha) \cos \theta}{(1 - X \cos \theta - Y \sin \theta)^3} \begin{Bmatrix} \cos \theta \\ \sin \theta \end{Bmatrix} d\theta \quad [3.43]$$

The equations of motion of the journal can be derived by considering Newton's second law.

$$(\Sigma F)_{x,y} = m_j a_{j,x,y}$$

A position vector to the center of mass of the journal is:

$$\mathbf{P}_m = (x + e_\mu \cos \omega_j t) \vec{i} + (y + e_\mu \sin \omega_j t) \vec{j}$$

where the mass center is located a radial distance of  $e_\mu$  from the geometric center of the journal. Then the acceleration is given by:

$$\mathbf{a}_m = (\ddot{x} - e_\mu \omega_j^2 \cos \omega_j t) \vec{i} + (\ddot{y} - e_\mu \omega_j^2 \sin \omega_j t) \vec{j}$$

therefore:

$$m_j (\ddot{x} - e_\mu \omega_j^2 \cos \omega_j t) = (\Sigma F)_x$$

$$m_j (\ddot{y} - e_\mu \omega_j^2 \sin \omega_j t) = (\Sigma F)_y \quad [3.44]$$

where the right hand side of the above equations represents all loading on the journal, including the forces given by Eq. [3.42] that are developed in the fluid film. By letting:

$$\omega_j = \Omega, \quad \Omega t = \tau, \quad \frac{e_\mu}{C} = E_\mu$$

and dividing through by  $m_j c \Omega^2$ , the equations become:

$$\frac{d^2 x}{d\tau^2} = E_\mu \cos \tau + \frac{F_o}{m_j c \Omega^2} \cos(\eta \tau) + \frac{\mu R L^3 \omega}{2 m c^3 \Omega^2} \bar{F}_x(x, y, \dot{x}, \dot{y}) + \frac{F_x}{m c \Omega^2} + \dots \quad [3.45]$$

$$\frac{d^2 y}{d\tau^2} = E_\mu \sin \tau + \frac{F_o}{m_j c \Omega^2} \sin(\eta \tau) + \frac{\mu R L^3 \omega}{2 m c^3 \Omega^2} \bar{F}_y(x, y, \dot{x}, \dot{y}) + \frac{F_y}{m c \Omega^2} + \dots \quad [3.46]$$

where:

$F_o$  = Rotating load at some multiple of the journal frequency

$F_x, F_y$  = Constant loading in x and y direction respectively

Also, other loading can be added as noted by + ...

The above equations are for a vertical journal bearing since we have not included the gravity loading in the equations of motion.

If it is assumed that gravity is acting in the negative y-coordinate direction, then the term  $(-g/c\Omega^2)$  must be added to [3.46] to account for this affect.

The solution of Eqs. [3.45] and [3.46] will give the journal orbit as a function of dimensionless time, T. Numerical methods will be used to integrate these equations of motion forward in time. The method of solution will be discussed in detail in CHAPTER V.

### 3.4 Journal Precession Rate and Radius of Curvature

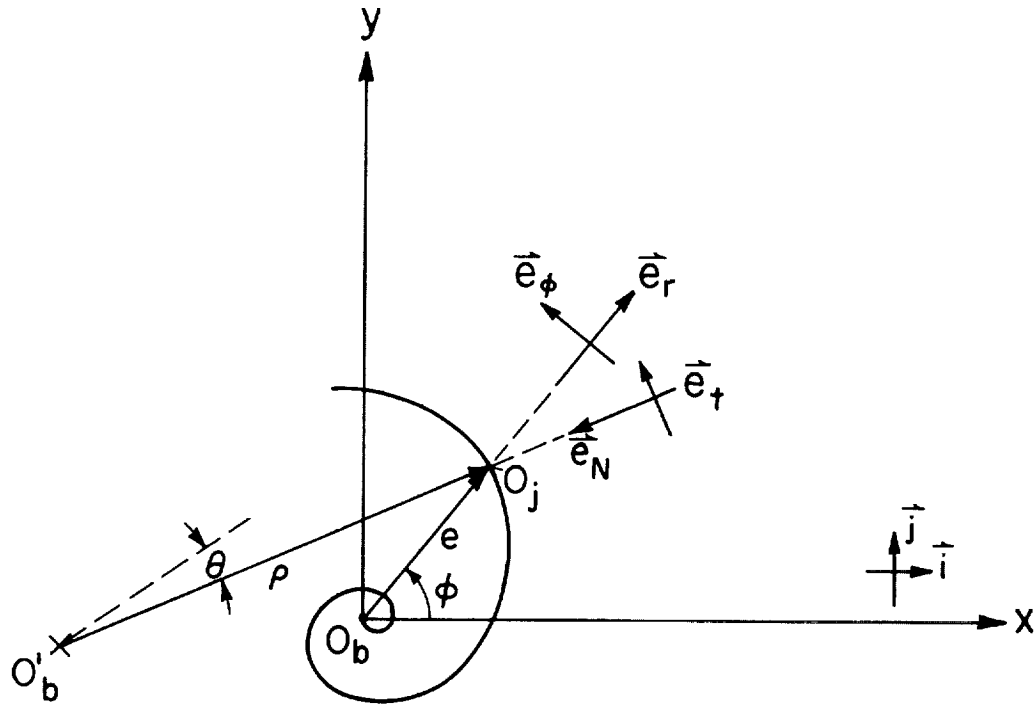
When a journal bearing is acted upon by some unbalance force or other cyclic forcing function the journal tends to move in an orbit due to the forces acting upon it. If the orbit encloses the center of the journal then it is possible to think of the distance from the bearing center to the journal center as the radius of the path and the angular velocity with respect to the bearing center as the whirl frequency. Referring to Figure 3.7, these quantities would be radius, e, and angular velocity  $\dot{\phi}$ .

These values may be expressed in terms of the displacements and velocities, x, y,  $\dot{x}$ ,  $\dot{y}$  by the following procedure. The velocity of the journal center may be expressed as

$$\begin{aligned}\vec{V}_j &= \dot{x} \vec{i} + \dot{y} \vec{j} \\ &= \dot{e} \hat{e}_r + e\dot{\phi} \hat{e}_\phi\end{aligned}$$

The relation among the unit vectors is as follows:

$$\begin{aligned}\hat{e}_r &= \cos\phi \vec{i} + \sin\phi \vec{j} \\ \hat{e}_\phi &= -\sin\phi \vec{i} + \cos\phi \vec{j} \\ x &= e\cos\phi, \quad y = e\sin\phi\end{aligned}$$



3.7 Typical Journal Trajectory Illustrating the Instantaneous Radius of Curvature

So,

$$\vec{V}_j \cdot \hat{e}_\phi = e \dot{\phi} = \dot{x} \vec{i} \cdot \hat{e}_\phi + \dot{y} \vec{j} \cdot \hat{e}_\phi = -\sin\phi \dot{x} + \cos\phi \dot{y}$$

Therefore,

$$\dot{\phi} = \frac{e}{e} \frac{(\cos\phi \dot{y} - \sin\phi \dot{x})}{e} = \frac{x\dot{y} - y\dot{x}}{e^2}$$

or, since  $e^2 = x^2 + y^2$

then,

$$\dot{\phi} = \frac{x\dot{y} - y\dot{x}}{x^2 + y^2}$$

In dimensionless form:

$$\frac{\dot{\phi}}{\Omega} = \frac{X\dot{Y} - Y\dot{X}}{X^2 + Y^2} \quad [3.47]$$

where

$$X = x/c, \quad Y = y/c$$

and

$$\dot{X} = x/c \Omega, \quad \dot{Y} = y/c \Omega, \quad \text{with } \Omega = \omega_j \text{ as before.}$$

The radius,  $e$ , is given by:

$$e = c \times \sqrt{x^2 + y^2} \quad [3.48]$$

However, it is obvious that [3.47] has little meaning if the journal orbit does not enclose the bearing center, "o<sub>b</sub>".

The equations for the instantaneous radius of curvature,  $\rho$ , and angular velocity  $\dot{\theta}$  will now be developed.

The velocity can be expressed for this purpose as:

$$\vec{V}_j = v \hat{e}_t = \rho \dot{\theta} \hat{e}_t$$

where:

$\rho$  = instantaneous radius of curvature

$\dot{\theta}$  = instantaneous angular velocity about o<sub>b</sub>'

The acceleration is expressed as:

$$\begin{aligned}\vec{a}_j &= \frac{d}{dt} (v \hat{e}_t) = \dot{v} \hat{e}_t + v \frac{d\hat{e}_t}{dt} \\ &= a_t \hat{e}_t + \frac{v^2}{\rho} \hat{e}_N\end{aligned}$$

But since:

$$\vec{a}_j = \ddot{x} \vec{i} + \ddot{y} \vec{j}$$

and:

$$\vec{a}_j \cdot \hat{e}_N = \frac{v^2}{\rho} = \ddot{x} \vec{i} \cdot \hat{e}_N + \ddot{y} \vec{j} \cdot \hat{e}_N \quad [3.49]$$

The new unit vectors are determined as follows:

$$\vec{v} = v \hat{e}_t = \dot{x} \vec{i} + \dot{y} \vec{j}$$

therefore,

$$\hat{e}_t = \frac{1}{v} [\dot{x} \vec{i} + \dot{y} \vec{j}]$$

and:

$$\hat{e}_n = \vec{k} \times \hat{e}_t = \frac{1}{v} [\dot{x} \vec{j} - \dot{y} \vec{i}]$$

Hence,

$$\vec{i} \cdot \hat{e}_n = -\dot{y}/v$$

and:

$$\vec{j} \cdot \hat{e}_n = \dot{x}/v$$

So, from Eq. [3.49],

$$v^2/\rho = \frac{\ddot{y} \dot{x} - \ddot{x} \dot{y}}{v}$$

Solving for  $\rho$  and  $\dot{\theta} = v/\rho$  results in:

$$\rho = v^3 / (\dot{y} \ddot{x} - \ddot{x} \dot{y}) \quad [3.50]$$

and

$$\dot{\theta} = \frac{\ddot{y} \dot{x} - \ddot{x} \dot{y}}{\dot{x}^2 + \dot{y}^2} \quad [3.51]$$

since,

$$v^2 = \dot{x}^2 + \dot{y}^2$$

In dimensionless form, the instantaneous whirl ratio is given by:

$$\frac{\dot{\theta}}{\Omega} = \frac{\ddot{Y}\dot{X} - \dot{Y}\ddot{X}}{\dot{X}^2 + \dot{Y}^2} \quad [3.52]$$

This expression is meaningful for any orbit path the journal might traverse and will be easily calculated since it involves quantities readily available in the method of solution of the journal orbit.

### 3.5 Derivation and Explanation of Terms Used in Journal Bearing Studies

As the theory of lubrication has developed several important equations and groupings of terms have evolved that are used frequently in this field. One of the basic assumptions that has been used in the derivation of the Reynolds equation arose from considering the ratio of inertia to viscous forces in the incompressible Navier-Stokes equation.

$$\rho \frac{D\bar{u}}{Dt} = -\nabla P + \mu \nabla^2 u$$

Considering the x-direction, the result is

$$Re^* = \frac{\text{Inertia}}{\text{Viscous}} = \rho \frac{U^2}{L} / \mu \frac{U}{h^2} = \frac{UL}{\nu} \left(\frac{h}{L}\right)^2 \quad [3.53]$$

where

Re\* = modified (reduced) Reynolds Number

U = velocity

L = characteristic length

h = film thickness

$\nu$  = kinematic viscosity

The distinction has been made to call this expression a modified Reynolds number since the expression frequently used as the Reynolds Number in fluid mechanics work is given as:  $Re = UL/\nu$ .

From this relation it is seen that:

$$Re^* = Re \times \left( \frac{h}{L} \right)^2. \quad [3.54]$$

Another much used expression known as Sommerfeld's Number resulted from the work of Sommerfeld in 1904 when he presented the exact solution to the long bearing assumption form of Reynolds' equation. The result of this work was an expression for the loading of an idealized full journal bearing. The result can be expressed as<sup>(\*)</sup>:

$$\left( \frac{r}{C} \right)^2 \frac{\mu N'}{P} = \frac{(2+n^2) \sqrt{1-n^2}}{12 \pi^2 n} \quad [3.55]$$

where

$N'$  = journal speed (RPS)

$n$  = eccentricity =  $e/c = \epsilon$

$r$  = journal radius =  $R$

$P$  = load per area of the projected area of journal

=  $W/(L \times D)$ ,  $D = 2R$

The expression,

$$\frac{\mu N'}{P} \left( \frac{R}{C} \right)^2$$

is known as Sommerfeld's Number (S).

An equivalent expression can be derived for the short-bearing assumption form of Reynolds' equation. Using polar coordinates and making use of certain integral formulae due to Sommerfeld, it is

---

(\*)See Reference (32), p. 122.

possible to successfully integrate Reynolds' equation to obtain the load capacity. This result can be expressed (1)\* by

$$S_s = \frac{\mu N'}{P} \left(\frac{L}{2c}\right)^2 = S \left(\frac{L}{D}\right)^2 = \frac{(1-\epsilon^2)^2}{\pi \epsilon [\pi^2(1-\epsilon^2) + 16\epsilon^2]^{1/2}} \quad [3.56]$$

The same expression has been derived by Ocvirk (13) and is referred to as the "capacity number" for the bearing in that report (see Figure 3.8).

The attitude  $\phi$  (see Figure 3.1) can be found by forming the ratio of the tangential and radial load components, the result of which is given by (1)\*\*

$$\tan \phi = \frac{\pi}{4} \frac{(1-\epsilon^2)^{1/2}}{\epsilon} \quad [3.57]$$

The value of P, the projected load is usually considered as the effective journal weight divided by the product of length and diameter of the bearing. When considering unbalance loading effects it may be helpful to form the Sommerfeld Number based on the rotating load. In doing this, P becomes the quantity  $m e_{\mu} \omega_j^2$ , the magnitude of the unbalance loading. The resulting expression is:

$$S_U = \frac{\mu N'}{P_U} \left(\frac{R}{C}\right)^2 \quad [3.58]$$

where

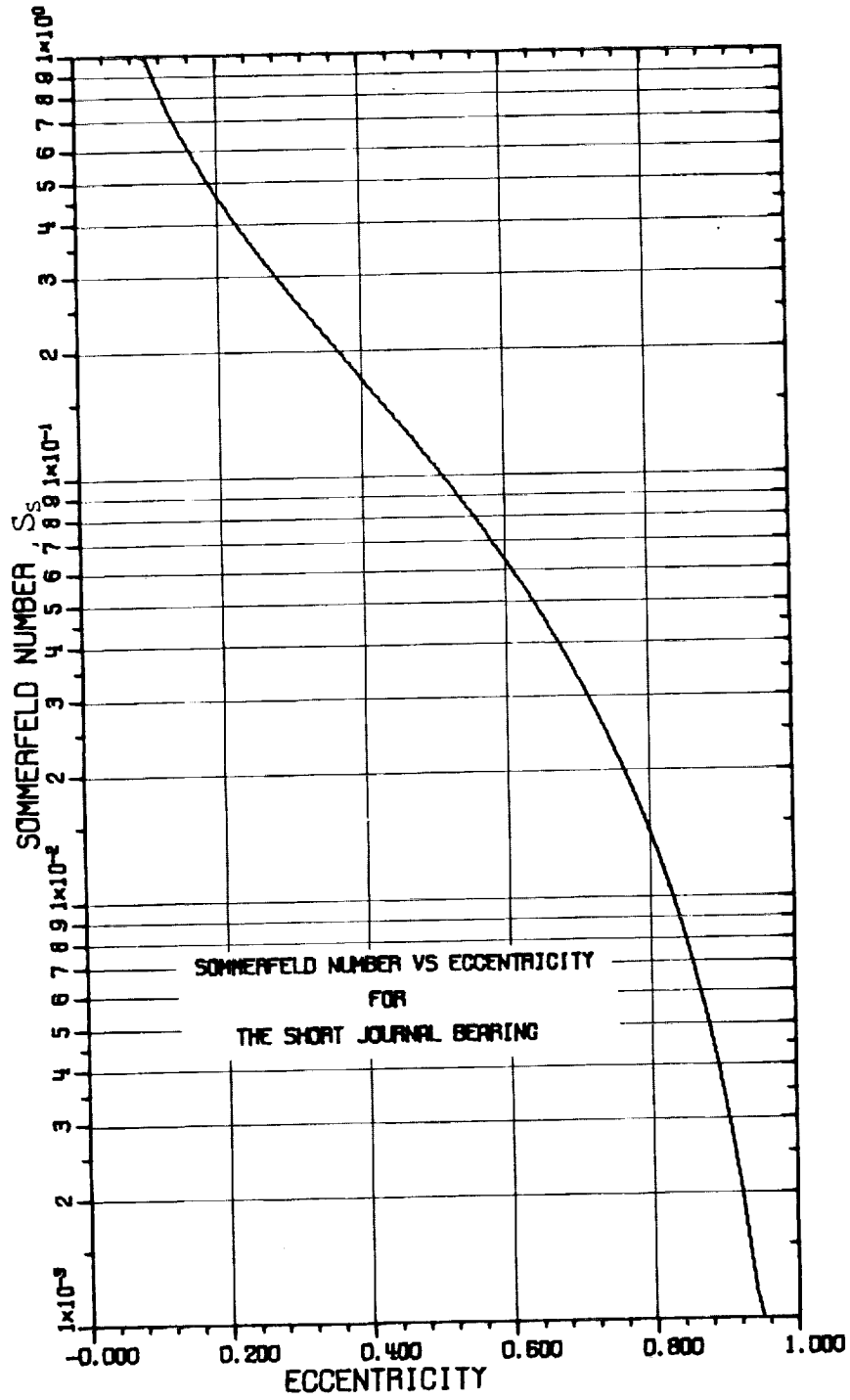
$$P_U = (m e_{\mu} \omega_j^2) / (L \times D)$$

$S_U$  = Sommerfeld Number for unbalance loading

---

\*Reference in Bibliography, p. 49

\*\*Reference in Bibliography, p. 92 has polar plots of eccentricity for various L/D values.



3.8 Sommerfeld Number ( $S_s$ ) vs Eccentricity

The stability\* plots for journal bearings that appear in the literature are usually plotted with a dimensionless speed parameter as ordinate and eccentricity ratio,  $e$ , as abscissa. The speed parameter may be thought of as the square root of the ratio of the unbalance force (with  $e_\mu = c$ ) to the journal weight. That is:

$$\omega_s = \sqrt{\frac{mC\omega_j^2}{mg}} \quad [3.59a]$$

or,

$$\omega_s = \omega_j / \sqrt{\frac{g}{c}} \quad [3.59b]$$

where  $\sqrt{g/c}$  has units of  $\text{sec.}^{-1}$  and, as stated previously, makes the speed parameter dimensionless.

An important consideration when designing bearings is the magnitude of the actual forces transmitted to the bearing surface.

This quantity can be calculated from Eq. [3.43] and could be represented as:

$$\hat{F} = \sqrt{F_x^2 + F_y^2}$$

where  $F_x, F_y$  = magnitude of fluid-film forces in the x and y coordinate directions respectively.

It is possible now to form two dimensionless force parameters, to be denoted as static and dynamic transmissibility, given by:

$$TR_S = \hat{F}/W \quad [3.60]$$

and,

$$TR_D = \hat{F}/(m e_\mu \omega_j^2) \quad [3.61]$$

---

\*See CHAPTER IV for discussion of stability.

These ratios give an indication of the isolation of the journal from the support system. A value of 1 is equivalent to a system on rigid ball bearing supports, whereas for  $TR < 1$ , there is an improvement of performance due to lower forces transmitted. If  $TR > 1$ , then the journal bearings are actually developing higher forces than if the system was mounted in rigid ball bearings. This latter mode of operation is not desirable and should be avoided by the designer. If this is not possible, the transmissibility should be reduced to the lowest value attainable.

## CHAPTER IV

### STABILITY ANALYSIS FOR SMALL DISPLACEMENTS

The equation for the fluid-film force components has been derived for the short bearing model and is given by Eq. [3.43]. It is now possible to obtain from this equation the stiffness and damping coefficients which are given as:

$$K_{ij} = -\frac{\partial F_i}{\partial x_j} \quad ; \quad i = 1, 2 \quad ; \quad j = 1, 2 \quad [4.1]$$

$$C_{ij} = -\frac{\partial F_i}{\partial \dot{x}_j} \quad ; \quad i = 1, 2 \quad ; \quad j = 1, 2 \quad [4.2]$$

These coefficients can now be inserted into the equation of motion of the journal and a stability analysis performed. The equation to be examined is given as follows:

$$\ddot{x}_i + \bar{C}_{ij} \dot{x}_j + \bar{K}_{ij} x_j = 0 \quad [4.3]$$

$$\text{where } \bar{M}_j = \frac{m c \omega_j^2}{W}, \quad \bar{K}_{ij} = \frac{C K_{ij}}{\bar{M}_j W}, \quad \bar{C}_{ij} = \frac{\omega C C_{ij}}{\bar{M}_j W}$$

The assumed solution is of the form:

$$x_1 = A e^{\lambda t}, \quad x_2 = B e^{\lambda t}$$

Making these substitutions results in the following equations:

$$\begin{bmatrix} \lambda^2 + \bar{C}_{11} \lambda + \bar{K}_{11} & \bar{C}_{12} \lambda + \bar{K}_{12} \\ \bar{C}_{21} \lambda + \bar{K}_{21} & \lambda^2 + \bar{C}_{22} \lambda + \bar{K}_{22} \end{bmatrix} \begin{bmatrix} A \\ B \end{bmatrix} = \begin{bmatrix} 0 \\ 0 \end{bmatrix} \quad [4.4]$$

By expanding the determinant of coefficients the following fourth order equation is obtained:

$$\lambda^4 + (\bar{C}_{11} + \bar{C}_{22})\lambda^3 + (\bar{K}_{11} + \bar{K}_{22} + \bar{C}_{11} C_{22} - \bar{C}_{12} \bar{C}_{21})\lambda^2 + (\bar{K}_{11} \bar{C}_{22} + \bar{K}_{22} C_{11} - \bar{K}_{12} \bar{C}_{21} - \bar{K}_{21} \bar{C}_{12})\lambda + (\bar{K}_{22} \bar{K}_{11} - \bar{K}_{12} \bar{K}_{21}) = 0 \quad [4.5]$$

In general terms the characteristic equation can be expressed as:

$$\sum_{I=0}^N A_{N-I} \lambda^I = 0 \quad [4.6]$$

For  $N = 4$ ,

$$A_4 + A_3 \lambda + A_2 \lambda^2 + A_1 \lambda^3 + A_0 \lambda^4 = 0$$

The stability condition is given by (7)\*

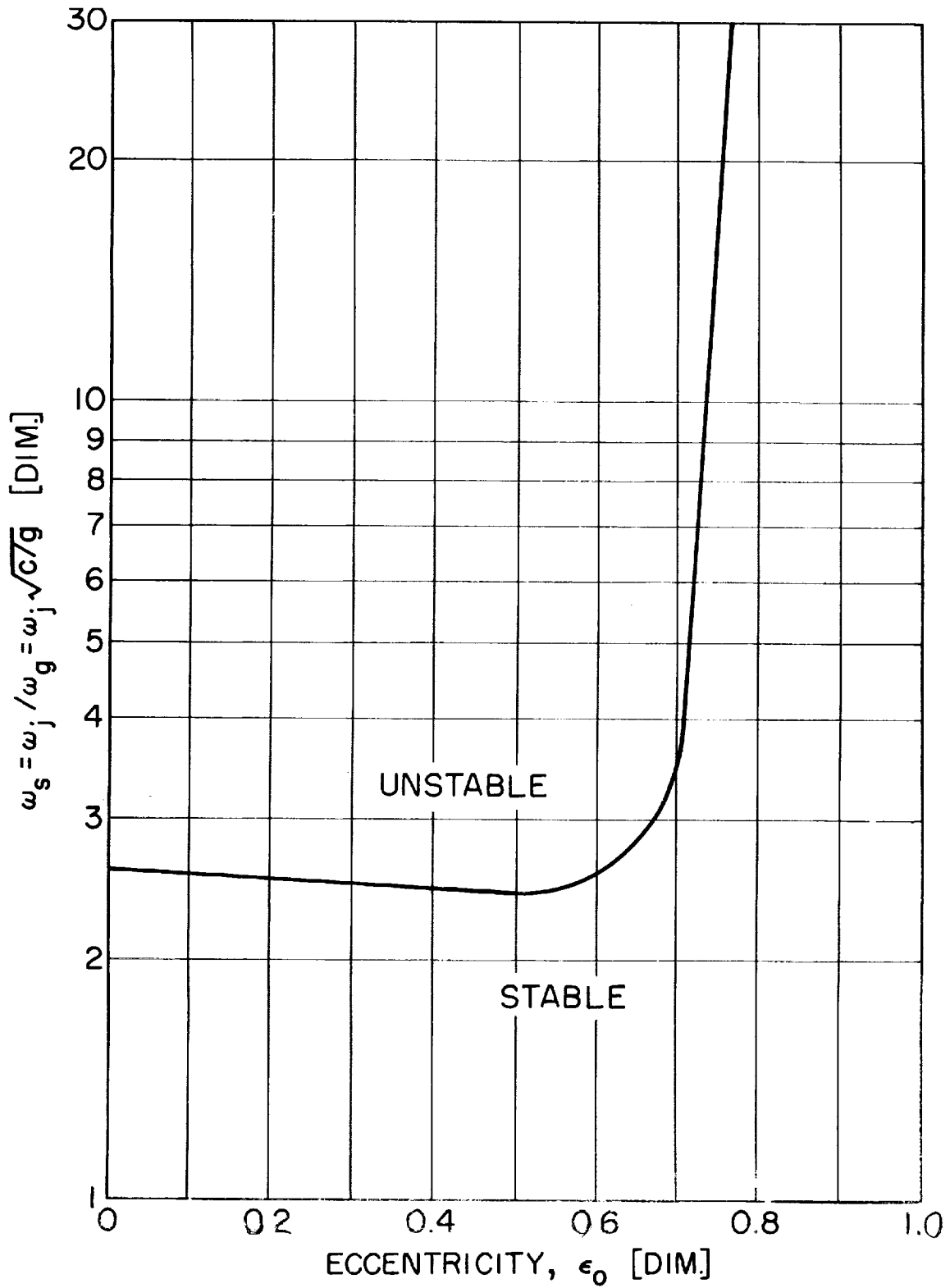
$$A_1 A_2 A_3 > A_4 A_1^2 + A_0 A_3^2 \quad [4.7]$$

A stability analysis has been performed by the approach just described by Mr. Pranabesh De Choudhury.\*\* His analysis considered stability about the equilibrium eccentricity and attitude angle considering the journal center to be initially at rest. The stability map resulting from his work is shown in Figure 4.1 and is comparable to that of Badgley and Booker (30) who examined orbital plots for the journal center to determine whether or not the system was stable (see Figure 4.2).

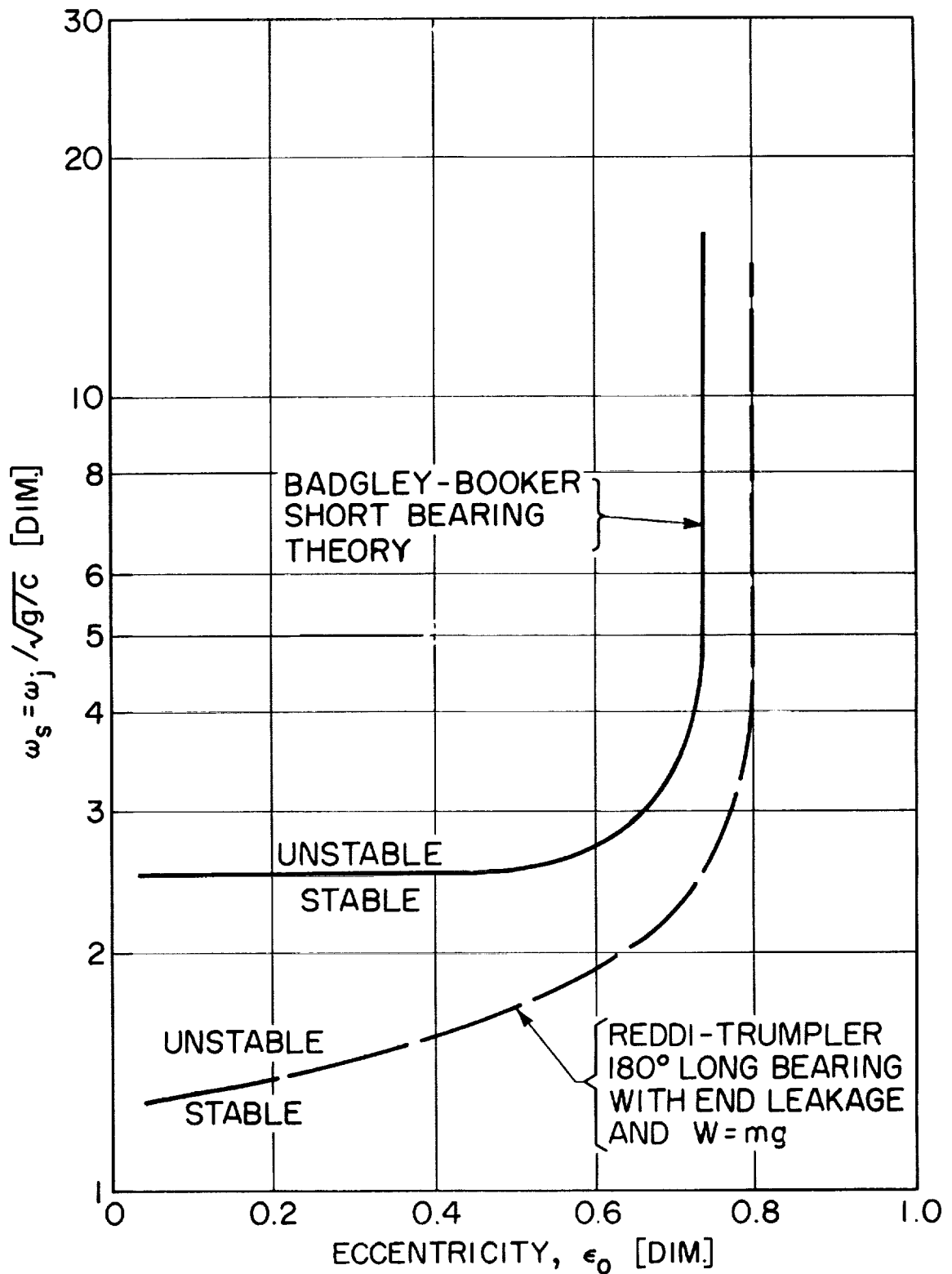
---

\*Reference in Bibliography, p. 124.

\*\*Doctoral candidate, Mechanical Engineering, University of Virginia, doing research in stability of rotor systems.



4.1 Stability for the Unloaded Short Journal Bearing  
(ref. Choudhury)



4.2 Stability for the Unloaded Journal Bearing  
 (Comparison of Reddi-Trumpler and Badgley-Booker.  
 Stability Maps)

The criteria for instability that they used was an increasing radius arm as the orbit tracked out the journal center path.

These approaches to the problem of stability have only considered the horizontal, unloaded journal. A loaded journal will be shown\* to exhibit a greater area of stability on the stability map, while an unloaded vertical journal will be unstable over the entire range of the map. These are important facts that are not obvious from a plot such as Figure 4.1, or the similar plots of Badgley and Booker, Figure 4.2.

The analysis presented by Reddi (28) for the  $180^\circ$  long bearing, with end leakage considered, has given a lower threshold speed than the stability analysis using the short bearing equations. The threshold curve resulting from their analysis has been converted into the parameter used by Badgley and Booker for the special case that the loading is due to the weight of the journal (rotor) only. The Reddi-Trumpler threshold speed is less than that of Badgley-Booker but the limit of eccentricity at which the journal is completely stable is very nearly the same. This value is in agreement with Hori who gave 0.8 as the upper limit of eccentricity past which the journal is always stable.

In all of the various analyses of stability, only the threshold speed of unstable motion is predicted. In an actual bearing operated above the stability threshold speed, the journal does not fail but forms a finite limit cycle which increases with speed.

In this analysis, the motion of the journal and forces

---

\*See CHAPTER VII, page 95 , and Figure 6.14.

produced when operating above the stability threshold will be examined.

CHAPTER V  
METHOD OF SOLUTION

5.1 Introduction

The analysis presented in CHAPTER III resulted in the equations of motion for the journal bearing in the fixed cartesian coordinate set. The present chapter presents computer drawn three-dimensional plots of the pressure profile resulting from the Short Bearing Solution derived in CHAPTER III. To obtain the fluid film forces the expression for the pressure must be integrated over the bearing surface. A brief discussion of numerical integration is presented to clarify the manner in which the forces just mentioned are obtained.

The equations of motion for the journal are two coupled, non-linear differential equations. A discussion of numerical methods for the step-wise integration of this type of differential equation (initial value problem) is followed by a description of the computer program that has been developed to solve the journal bearing equations of motion.

5.2 The Fluid Film Pressure Profile

The pressure in the fluid film was given in fixed coordinates by Eq. [3.37]. Substituting Eqs. [3.38], [3.39] into Eq. [3.37] and expressing the result in dimensionless form gives:\*

$$\bar{P} = \frac{P(\theta, \bar{z})}{\mu(N_b' + N_j')} \left(\frac{C}{L}\right)^2 = 6\pi \bar{z}(1-\bar{z}) \alpha \left[ \frac{-X \sin \theta + Y \cos \theta + 2\alpha (\dot{X} \cos \theta + \dot{Y} \sin \theta)}{(1 - X \cos \theta - Y \sin \theta)^3} \right]$$

where:

$$\bar{z} = \frac{z}{L}, \quad \alpha = \frac{\omega_j}{\omega_b + \omega_j}, \quad X = \frac{x}{C}, \quad \dot{X} = \frac{1}{C\omega_j} \frac{dx}{dt} \quad [5.1]$$

\*Note similarity of dimensionless group to 1/S, the inverse of the Sommerfeld Number.

If no values of negative pressure are allowed to exist in the fluid film, then all  $\bar{P}$ 's less than zero are equated to zero. The above equation was programmed on the digital computer and the results plotted via a Calcomp Plotter unit. Various cases were considered and are presented as Figures 5.1 - 5.7.

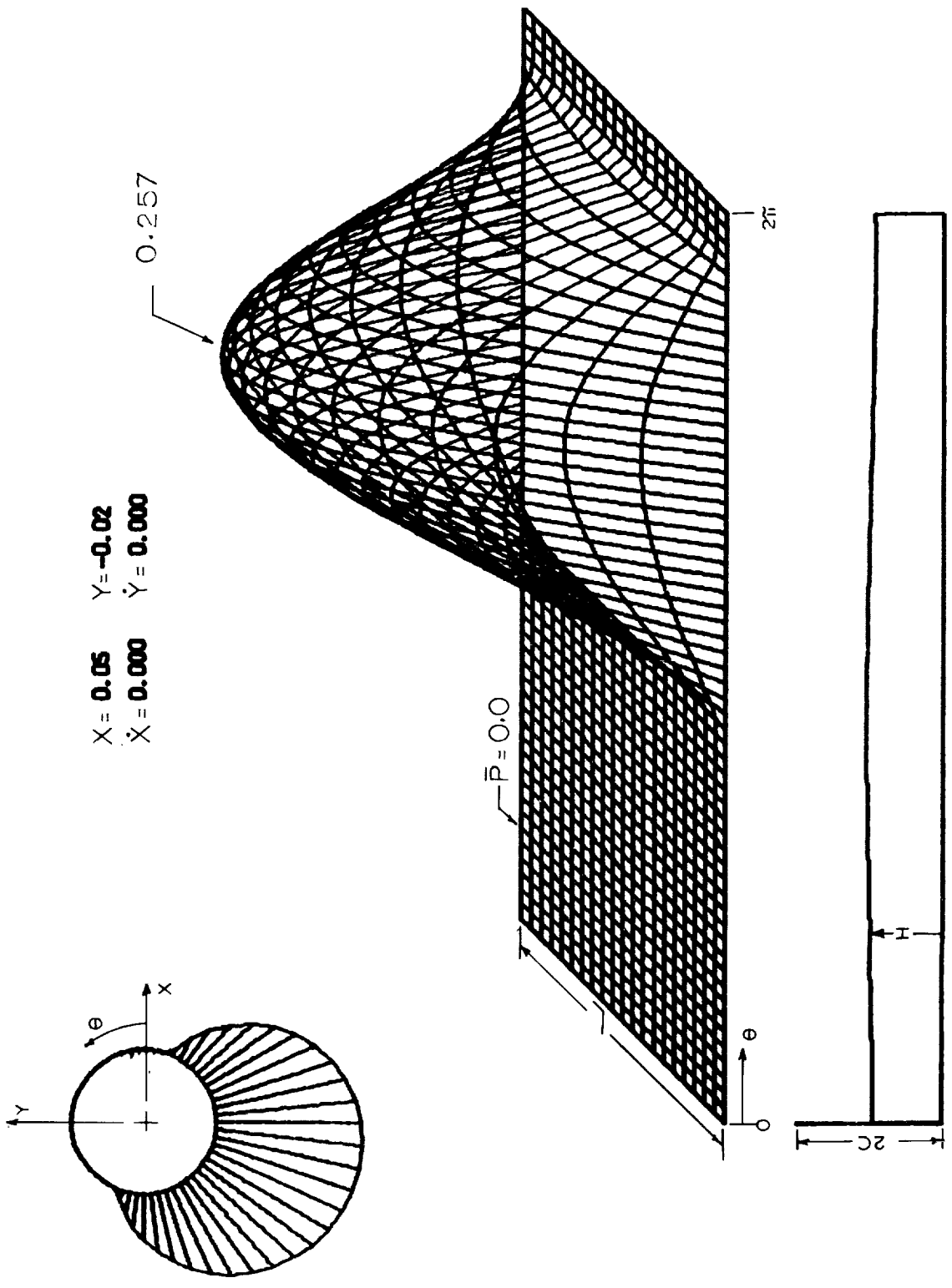
The values of the dimensionless displacements and velocities are given at the top of the figures. An end view of the section at the bearing midspan is given in the upper left corner with the pressure profile represented as radial lines. The center figure is a 3-dimensional plot of the "unwrapped" pressure profile. At the bottom of the figure is the film thickness,  $H$ , plotted versus angular distance,  $\theta$ .

The maximum dimensionless pressure increases as the journal moves from near the center (Figure 5.1) out to  $X = 0.2$ ,  $Y = -0.10$  (Figure 5.2). Figure 5.3 shows the uncavitated pressure surface for the case of Figure 5.2. The negative pressures cannot be sustained in the fluid film and therefore cavitates (for discussion, see page 62). A prominent pressure peak is noticed as the journal moves out to  $X = 0.5$ ,  $Y = -0.7$  (Figure 5.4). In Figure 5.5 the case of Figure 5.4 is given a small velocity which results in a slight increase of peak pressure.

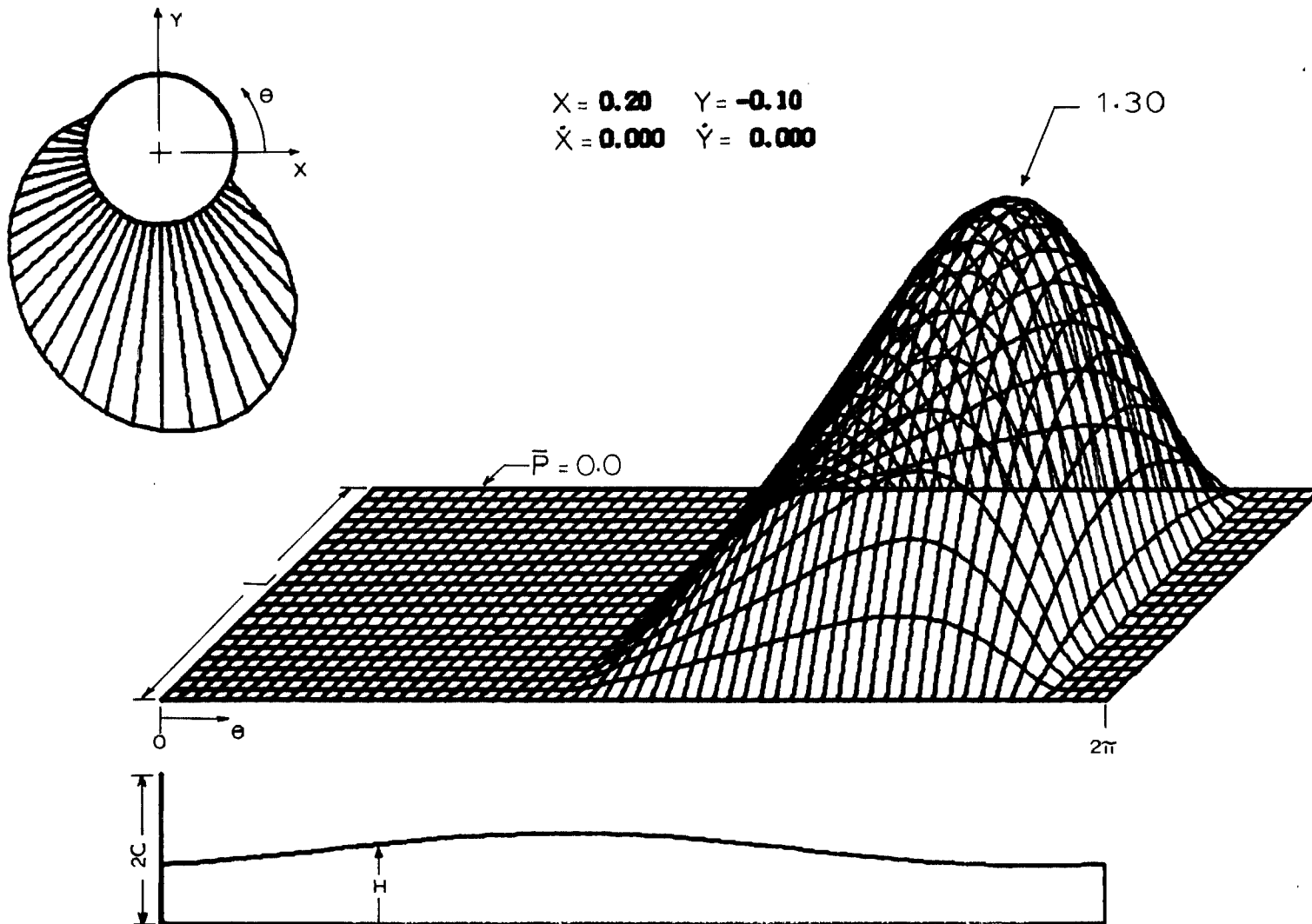
In Figure 5.6 the journal has been shifted to  $X = -0.9$ ,  $Y = -0.05$  and is accompanied by a shift in the pressure profile. Figure 5.7 has been given the condition of synchronous whirl\* at an eccentricity of 0.5. All cases plotted were for  $\alpha = 1$ , i.e.  $\omega_b = 0$ .

---

\*The journal center is precessing in the bearing at the journal rotational angular velocity.

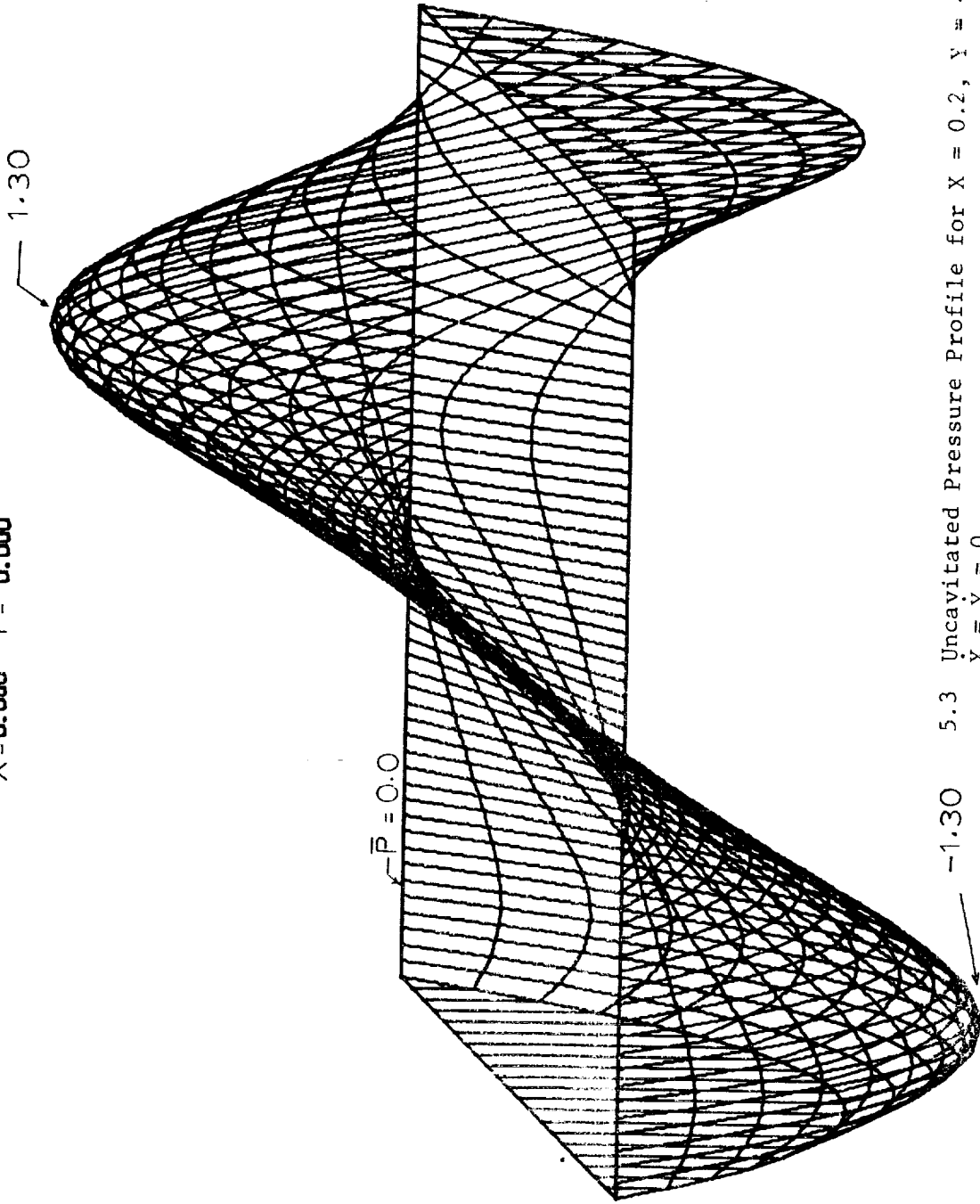


5.1 Pressure Profile, Pressure Surface, and Film Thickness for  $X = 0.05$ ,  $Y = -0.02$ ,  $\dot{X} = \dot{Y} = 0$

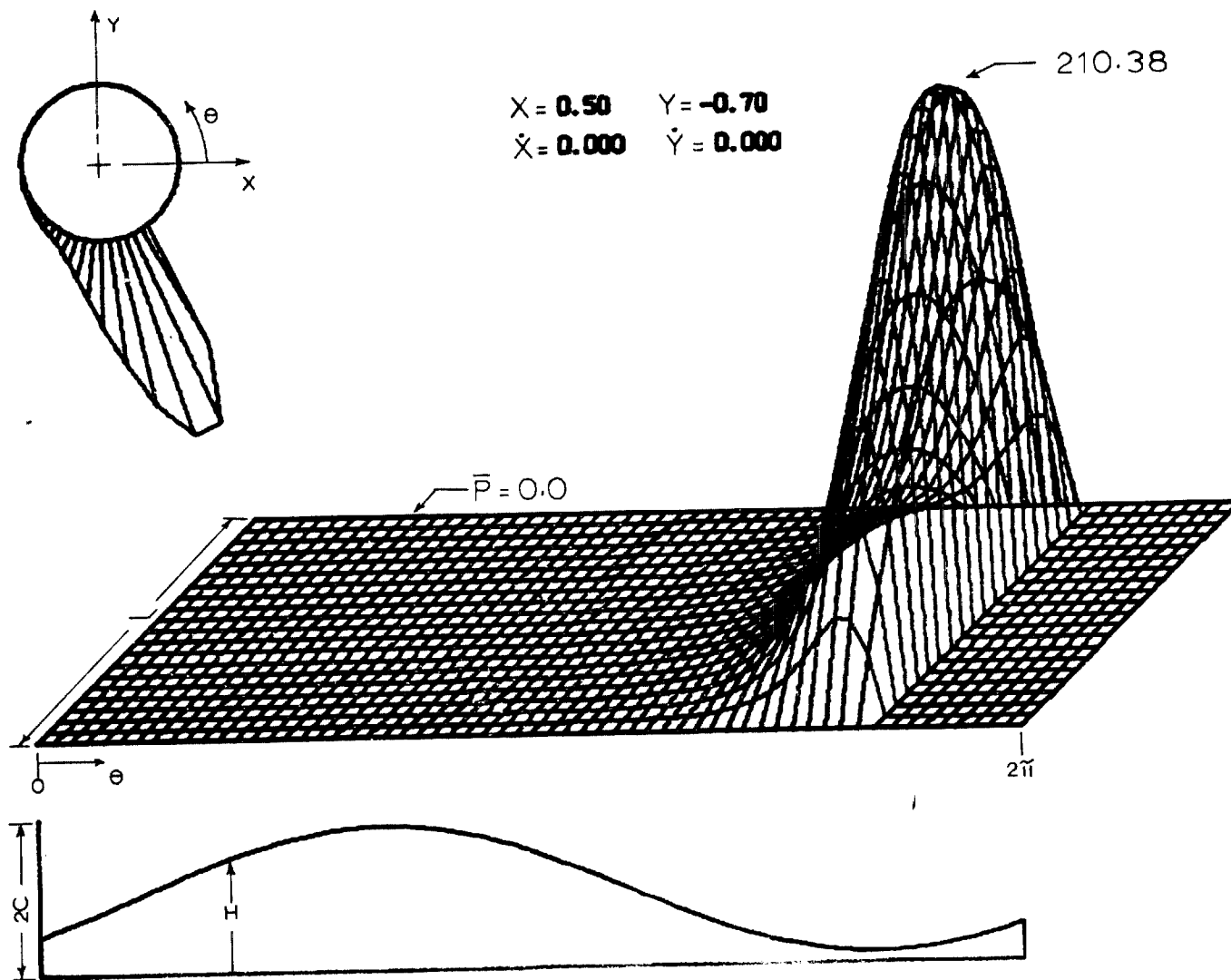


5.2 Pressure Profile, Pressure Surface, and Film Thickness for  $X = 0.2$ ,  $Y = -0.10$ ,  $\dot{X} = \dot{Y} = 0$

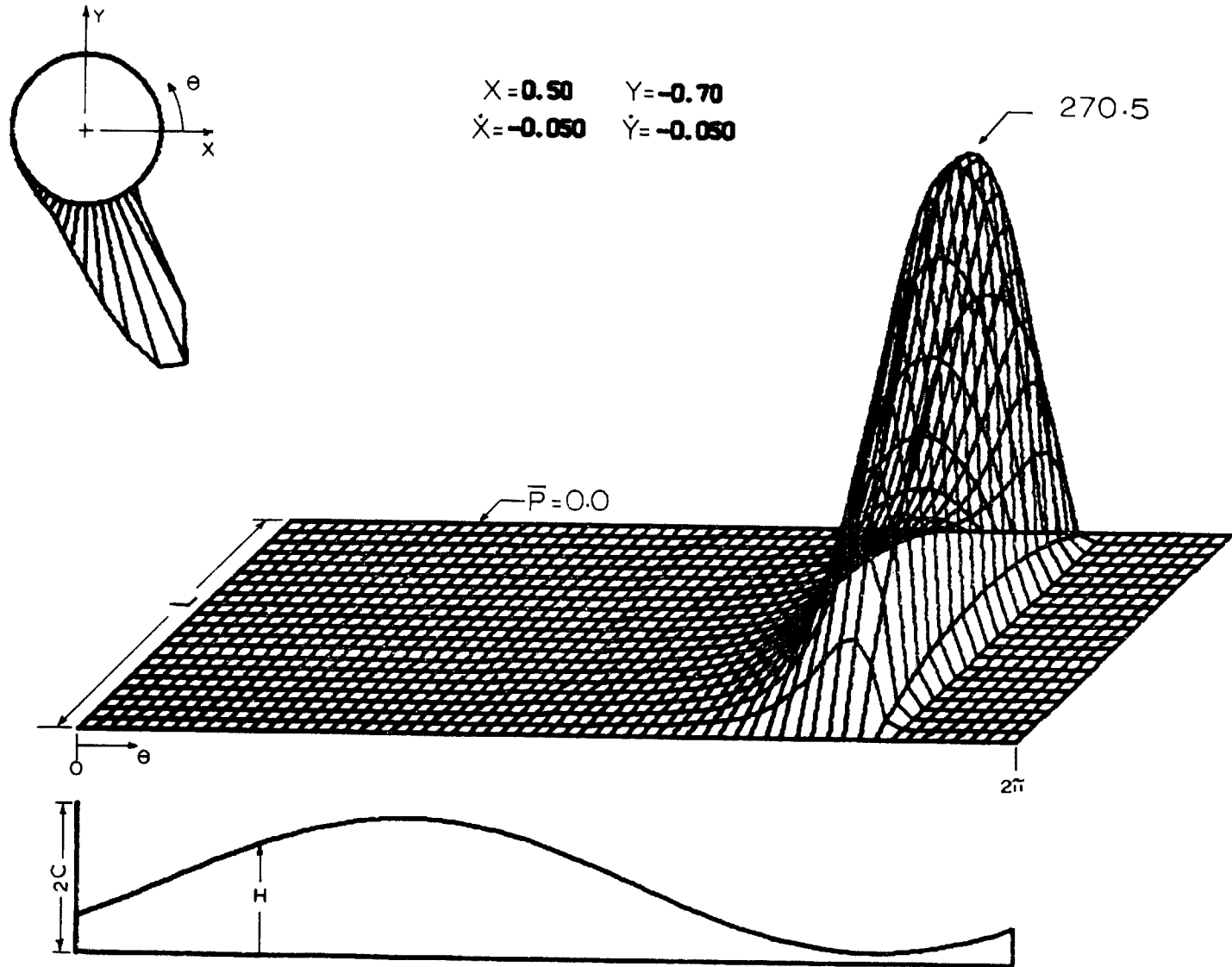
$X = 0.20$     $Y = -0.10$   
 $\dot{X} = 0.000$     $\dot{Y} = 0.000$



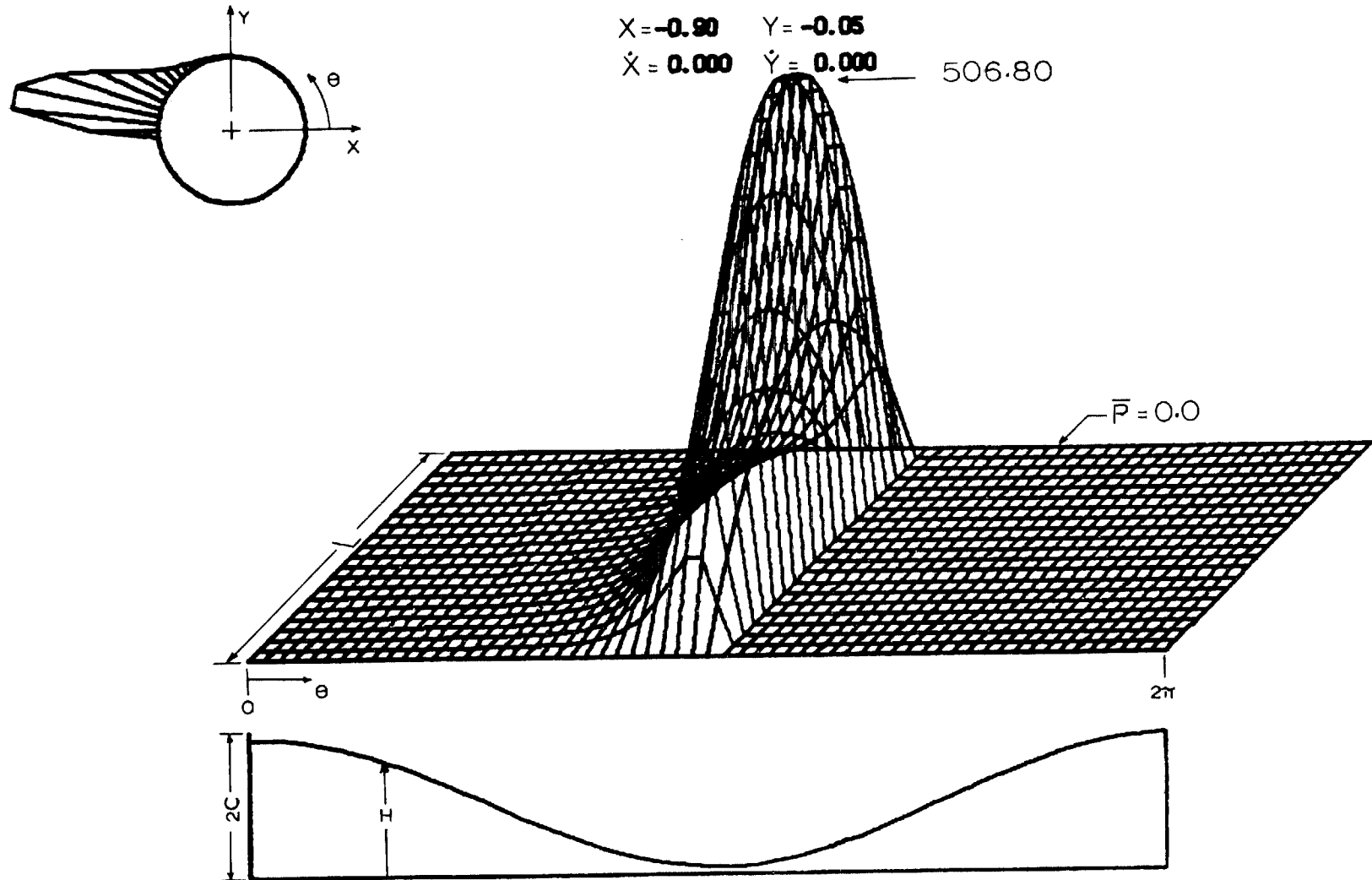
5.3   Uncavitated Pressure Profile for  $X = 0.2$ ,  $Y = -0.10$ ,  
 $\dot{X} = \dot{Y} = 0$



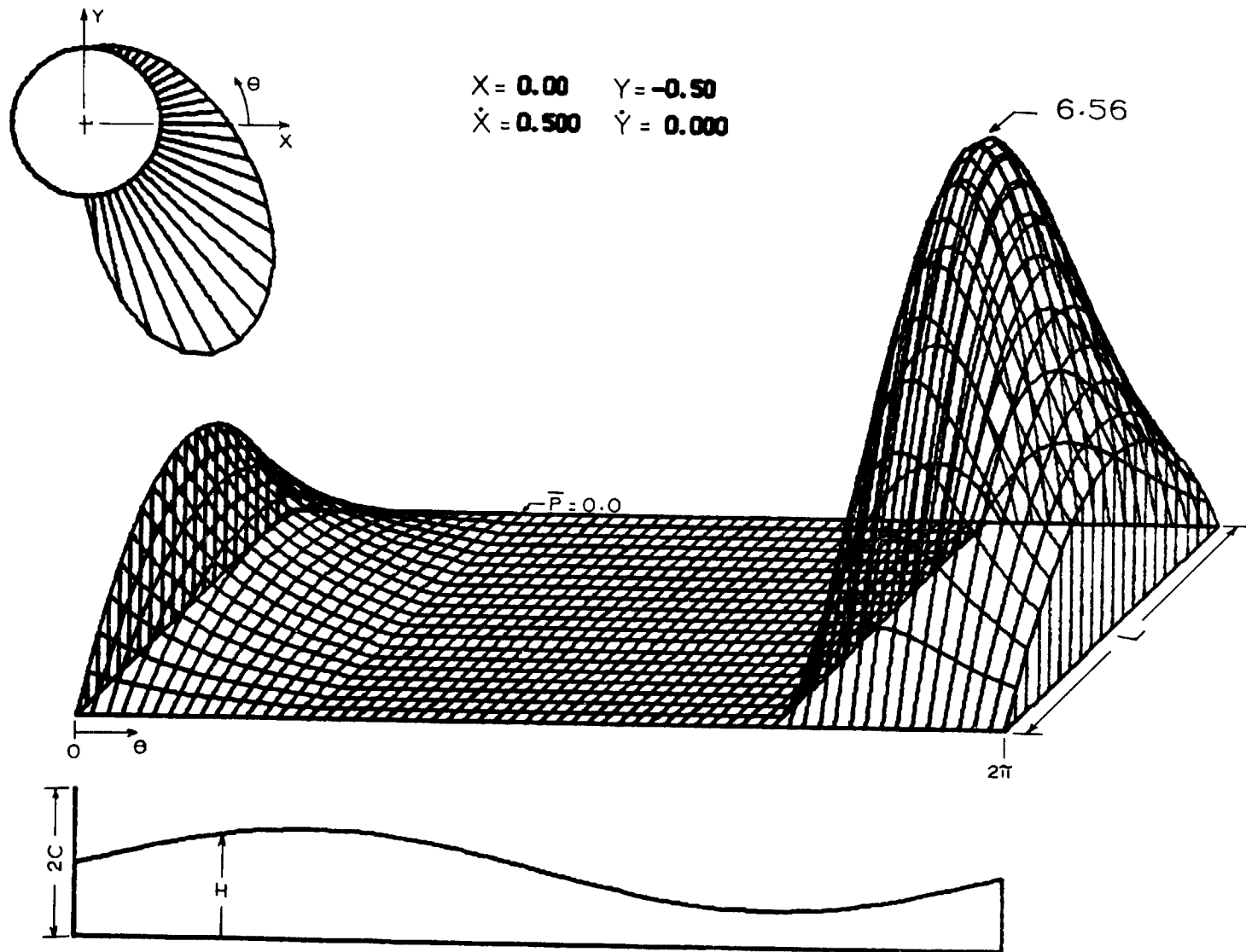
5.4 Pressure Profile, Pressure Surface, and Film Thickness for  $X = 0.5$ ,  $Y = -0.7$ ,  $\dot{X} = \dot{Y} = 0$



5.5 Pressure Profile, Pressure Surface, and Film Thickness for  $X = 0.5$ ,  $Y = -0.7$ ,  $\dot{X} = \dot{Y} = -0.5$



5.6 Pressure Profile, Pressure Surface, and Film Thickness for  $X = -0.9$ ,  $Y = -0.05$ ,  $\dot{X} = \dot{Y} = 0$



5.7 Pressure Profile, Pressure Surface, and Film Thickness for  $X = Y = 0, \dot{X} = -\dot{Y} = 0.5$

### 5.3 Integration of the Pressure Profile

The forces arising in the fluid film have been expressed as an integral over the circumference of the journal. The forces are given by Eq. [3.43] and are given below in the following form:

$$\begin{Bmatrix} F_x \\ F_y \end{Bmatrix} = - \frac{\mu L^3 R \omega}{2 C^2} \int_0^{2\pi} \frac{(2\dot{Y}\alpha - X) \sin\theta + (Y + 2\dot{X}\alpha) \cos\theta}{(1 - X \cos\theta - Y \sin\theta)^3} \begin{Bmatrix} \cos\theta \\ \sin\theta \end{Bmatrix} d\theta \quad [5.2]$$

The expression under the integral is now representative of the pressure in the film and hence will be equated to zero when its value is less than zero. This is equivalent to keeping only those pressures that are greater than ambient (i.e. larger than zero, since the pressures at the bearing ends are assumed to be atmospheric and hence it is gauge pressures that will be used in the calculations). This will avoid the subambient pressure contributions that appear in closed-form solutions and the need to calculate the extent of the positive pressure region.

The exact region of film cavitation and the resulting pressure therein are by no means well understood or well defined in the literature. Reddi-Trumpler (28) states that cavitation occurs at or near the vapor pressure of the fluid film if  $L/D \gg 1$ , while reference has previously been made to Pinkus and Sternlicht (1) who reference test data where the film cavitates at 0.13 psi below atmospheric (or the pressure at the journal ends). The results of the work reported herein are based on the latter argument. However, the nature of the method of solution makes the task of dictating cavitation pressure as simple as changing one card from the computer program deck. Ocvirk (13)

argued that in the absence of high datum pressures, the effect of any negative pressure (not exceeding atmospheric) could be neglected as being negligible in comparison to the positive pressure region.

It is possible to use numerical methods of integration to solve for the film forces from the above integral. It is only necessary to choose an appropriate method from the various ones listed in numerical analysis texts (34, 36). The most basic approach is the well-known trapezoidal rule, which can be expressed as follows:

$$\int_{x_0}^L f(x) dx = \sum_{i=0}^{N-1} \left[ \left( \frac{f(x_{i+1}) + f(x_i)}{2} \right) (x_{i+1} - x_i) \right]$$

where: N = number of subdivisions

$$x_n = L$$

By choosing a constant increment of X, it is possible to express the trapezoidal rule as:

$$\int_{x_0}^{x_n} f(x) dx = \Delta x \left[ \frac{f(x_0)}{2} + f(x_1) + f(x_2) + \dots + \frac{f(x_n)}{2} \right]$$

The error of the above formula is of course directly related to the increment,  $\Delta X$  and hence the number of points chosen to evaluate, as well as the order of curve that is being integrated.

Various other more accurate formulae exist, such as Simpson's and Weddle's Rules which are two of the series of Newton-Cotes formulae.\* Less known is the method of Romberg (34)\*\* which uses the Trapezoidal Rule and an extrapolation process to improve the accuracy of the

---

\*See Reference (36), p. 137 and (38), p. 110.

\*\*Reference in Bibliography, p. 130.

calculation.

For the purpose of integrating the pressure profile, a form of the following Newton-Cotes quadrature formula was chosen:

$$\int_{\theta_0}^{\theta_6} f(\theta) d\theta = \frac{h}{140} (41 f_0 + 216 f_1 + 27 f_2 + 272 f_3 + 27 f_4 + 216 f_5 + 41 f_6) \quad [5.3]$$

The basic restriction to this formula is that the number of intervals taken around the bearing must be a multiple of six. However, this restriction is easily satisfied on the digital computer and presents no problem for this application.

The above formula can be very closely approximated by (36).\*

$$\int_{\theta_0}^{\theta_6} f(\theta) d\theta = \frac{3h}{10} (f_0 + 5f_1 + f_2 + 6f_3 + f_4 + 5f_5 + f_6) \quad [5.4]$$

and can be applied in hand calculations more readily than can the Newton-Cotes formula. This simplified version is known as Weddle's Rule, and by inspection it can be seen that this form has four less multiplications per six intervals than the Newton-Cotes formula. Each multiplication that can be omitted at no cost in desired accuracy must be taken advantage of in this type of solution.

#### 5.4 Integration of the Equations of Motion

With the ability to calculate the film force at any instant of time the only remaining task is integrating the equations of motion of

---

\*Reference in Bibliography, p. 138.

the journal. The equations of interest are of the form:

$$\frac{d^2x}{dt^2} = f_x(x, y, \dot{x}, \dot{y}) \quad [5.5]$$

$$\frac{d^2y}{dt^2} = f_y(x, y, \dot{x}, \dot{y}) \quad [5.6]$$

Many methods of integrating first order differential equations are reported in numerical analysis texts (34), (35), (36). Since any second order differential equation can be expressed as two first order equations, there will be four first order equations to integrate forward in time. These equations are:

$$\frac{du}{dt} = f_x(x, y, \dot{x}, \dot{y}) \quad [5.7]$$

$$\frac{dx}{dt} = u \quad [5.8]$$

$$\frac{dv}{dt} = f_y(x, y, \dot{x}, \dot{y}) \quad [5.9]$$

$$\frac{dy}{dt} = v \quad [5.10]$$

where the variables  $u$  and  $v$  have been introduced to represent the velocities in the  $x$  and  $y$  directions, respectively and the expression for  $f_x$ ,  $f_y$  are as given in Eqs. [3.45], [3.46].

The methods of solution may be either (a) self-starting and require only that the initial values of each dependent variable at time  $t = t_0$  be known, or (b) may require two or more initial values of each

dependent variable at their respective times. It is obvious that the type (b) methods must be supplemented by a type (a) method for obtaining the number of starting values necessary to begin the solution process.

The most basic self-starting method is simply a Taylor Series Expansion truncated after some arbitrary number of terms, that is:

$$f(t+\Delta t) = f(t) + \Delta t f'(t) + \frac{\Delta t^2}{2!} f''(t) + \dots + \frac{\Delta t^n}{n!} f^{(n)}(t) + \mathcal{R}$$

where

$$\mathcal{R} = \frac{\Delta t^{n+1}}{(n+1)!} f^{(n+1)}(\xi), \quad t \leq \xi \leq t + \Delta t \quad [5.11]$$

By truncating the series after only two terms,

$$f(t+\Delta t) = f(t) + \Delta t f'(t) \quad [5.12]$$

which is known as Euler's Method. Since in dynamics problems the higher derivatives are not usually easily obtained in closed form, this method gives easily calculated results which have accuracy  $O(h^2)$ .

For any second order equation that may be expressed as:

$$\frac{d^2 y}{dt^2} = f(y, \dot{y}, t)$$

two first order equations may be written as:

$$\frac{dv}{dt} = f(y, \dot{y}, t)$$

$$\frac{dy}{dt} = v.$$

Euler's method can be written as:

$$f_{n+1} = f_n + hf'_n$$

therefore,

$$v_{n+1} = v_n + \Delta t \cdot f(y_n, \dot{y}_n, t_n) \dots \quad [5.13]$$

likewise,

$$y_{n+1} = y_n + \Delta t(v_n)$$

But the value of  $v$  at the  $(n+1)^{\text{th}}$  step is known, therefore a better guess for  $y_{n+1}$  might be:

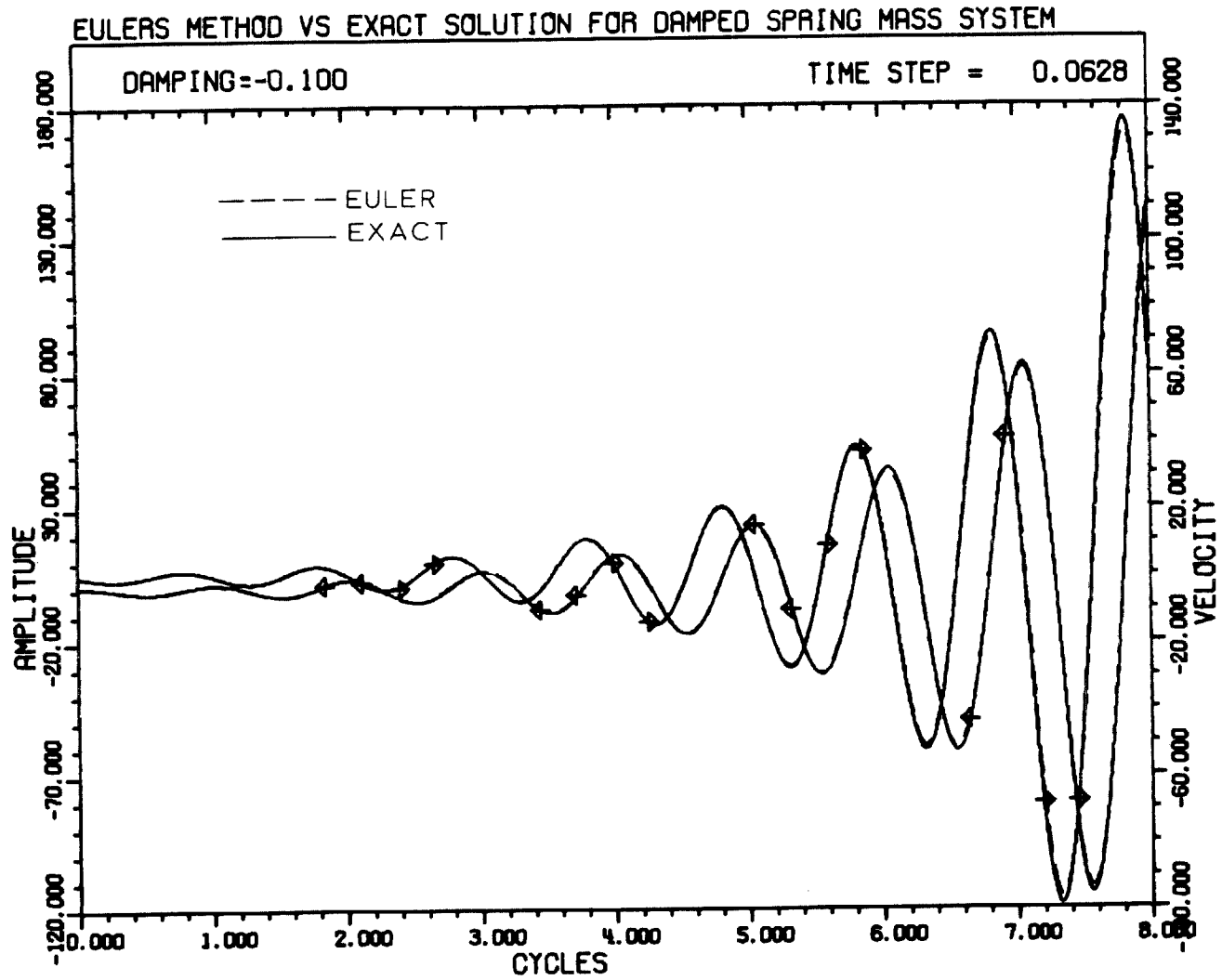
$$y_{n+1} = y_n + \Delta t(v_{n+1}) \dots \quad [5.13a]$$

(See Figure 5.8 for an indication of the capabilities of this method. The Euler's method solution is so close to the actual solution that it is hard to distinguish the prediction from the exact solution.)

More elaborate equations can be developed by using finite-difference methods. Other self-starting equations are second-order Runge-Kutta, fourth-order Runge-Kutta, and sixth-order Runge-Kutta. Of course the more elaborate the equations, the more time is required for each solution and this is what must be kept to a minimum to make the approach worthwhile.

The type (b) methods of solution usually are applied in pairs (predictor-corrector). The predictor and corrector equations are applied in an iterative manner until they agree to within desired limits at some time  $t_n$ , then the same approach is repeated for the next increment,  $t_{n+1} = t_n + \Delta t$ .

This type of solution is obviously going to be very time consuming if it is allowed to iterate at each increment. In addition, solutions of this type have shown great numerical instability in several test cases and must be applied with due caution (See Figure 5.9



5.8 Euler's Integration Procedure vs Exact Solution for a Damped Spring-Mass System

for example of instability of Adams Method with  $\Delta T = 0.05$ ).

The Milne (39) predictor-corrector pair and the Hammings(40) method have each proven to be highly unstable for the problem under discussion. The Adams-Bashforth predictor equation can be expressed in finite difference notation as (34)\*

$$X_{n+1} = X_n + h \left( m_n + \frac{1}{2} \Delta m_{n-1} + \frac{5}{12} \Delta^2 m_{n-2} + \frac{3}{8} \Delta^3 m_{n-3} + \frac{251}{720} \Delta^4 m_{n-4} \right) \quad [5.14]$$

where

$$m_n = \left. \frac{df}{dt} \right|_{t_n}$$

and,

$$\Delta m_{n-1} = m_n - m_{n-1}$$

$$\Delta^k m_{n-1} = \Delta^{k-1} m_n - \Delta^{k-1} m_{n-1}$$

Expanding this equation,

$$X_{n+1} = X_n + \frac{h}{720} [1901 m_n - 2774 m_{n-1} + 2616 m_{n-2} - 1274 m_{n-3} + 251 m_{n-4}] \quad [5.15]$$

which is the fifth-order equation. Keeping only terms through  $\Delta^3$  gives:

$$X_{n+1} = X_n + \frac{h}{24} [55 m_n - 59 m_{n-1} + 37 m_{n-2} - 9 m_{n-3}] \quad [5.16]$$

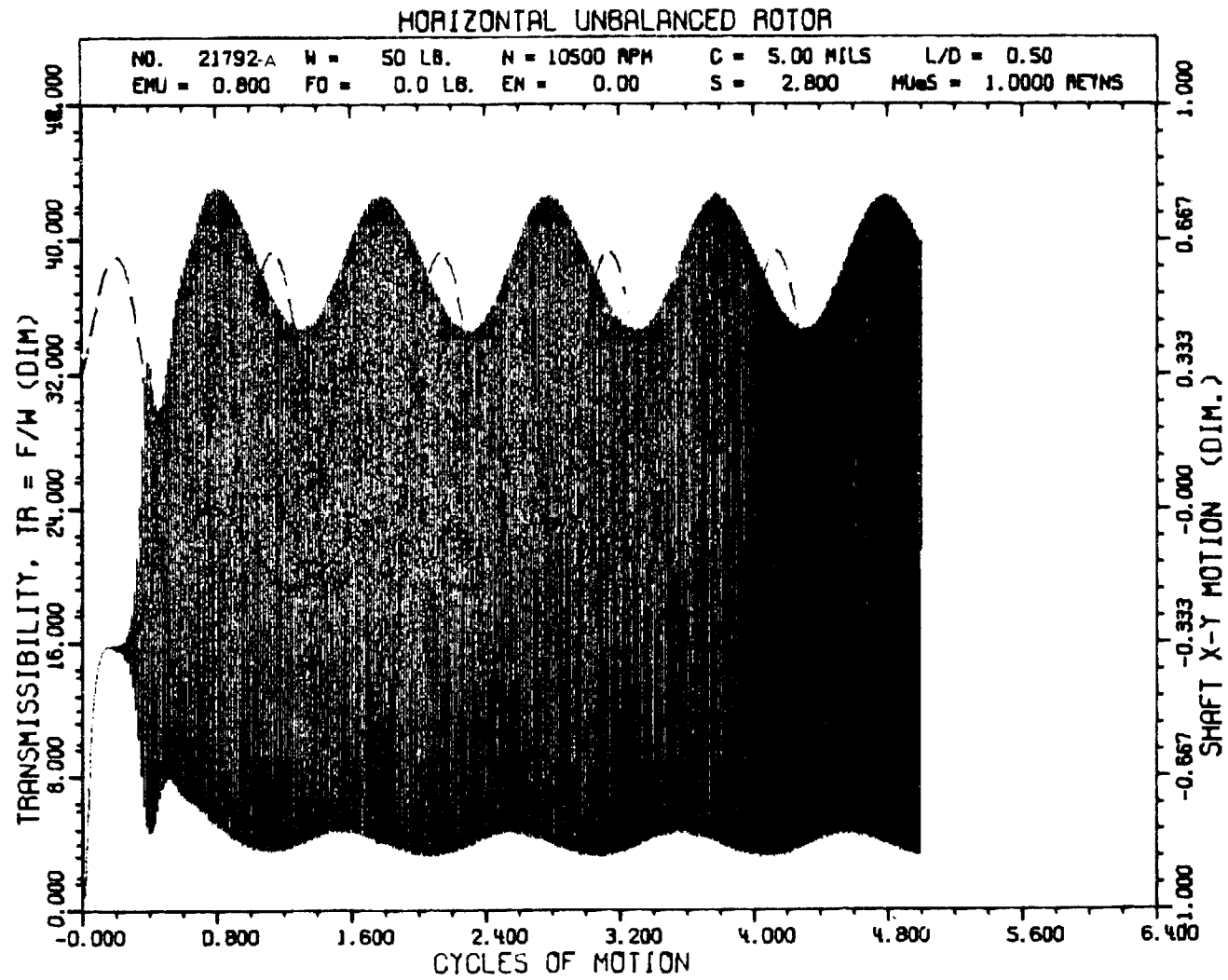
The Adams-Moulton corrector equation can be expressed as (34)\*:

$$X_n = X_{n-1} + h \left( m_n - \frac{1}{2} \Delta m_{n-1} - \frac{1}{12} \Delta^2 m_{n-2} - \frac{1}{24} \Delta^3 m_{n-3} - \frac{19}{720} \Delta^4 m_{n-4} \right) \quad [5.17]$$

---

\*Reference in Bibliography, p. 226.

\*\*Reference in Bibliography, p. 235.



5.9 Numerical Instability with Adams Method,  $\Delta T = 0.05$

Expanding this results in:

$$X_{n+1} = X_n + \frac{h}{720} [251 m_{n+1} + 646 m_n - 264 m_{n-1} + 106 m_{n-2} - 19 m_{n-3}] \quad [5.18]$$

or, keeping terms through  $\Delta^3$  gives:

$$X_{n+1} = X_n + \frac{h}{24} [9 m_{n+1} + 19 m_n - 5 m_{n-1} + m_{n-2}] \quad [5.19]$$

The above equations are typical of the predictor-corrector type formulations, some being less complex while others are much more elaborate and lengthy. The proper choice of the method of solution is very difficult and has proven to be dependent upon the particular problem being solved. As an example, while testing several of the methods of integration on a simple sine wave, the Milne equations gave excellent results. However, upon applying the same method to the journal bearing equation, violent oscillations occurred indicating numerical instability, whereas the simple Euler equations gave very smooth response predictions. Figure 5.9 gives an indication of the instability which may be encountered when too large a stepping increment is used.

The computer program that has been developed has several options as to the method of solution desired and will be explained in the following section.

## 5.5 Explanation of Computer Program

A listing of the actual computer program developed from the theory discussed in the earlier chapters is given as Appendix B. The program was written in ALGOL programming language and all runs have been made on the Burroughs B-5500 machine at the Computer-Science Center of the University of Virginia. The most important feature of the program is the fact that the results are automatically plotted by the Calcomp Plotter unit from the magnetic tape output of the computer program. The plotted data is also written out on the line printer along with other information that is not plotted.

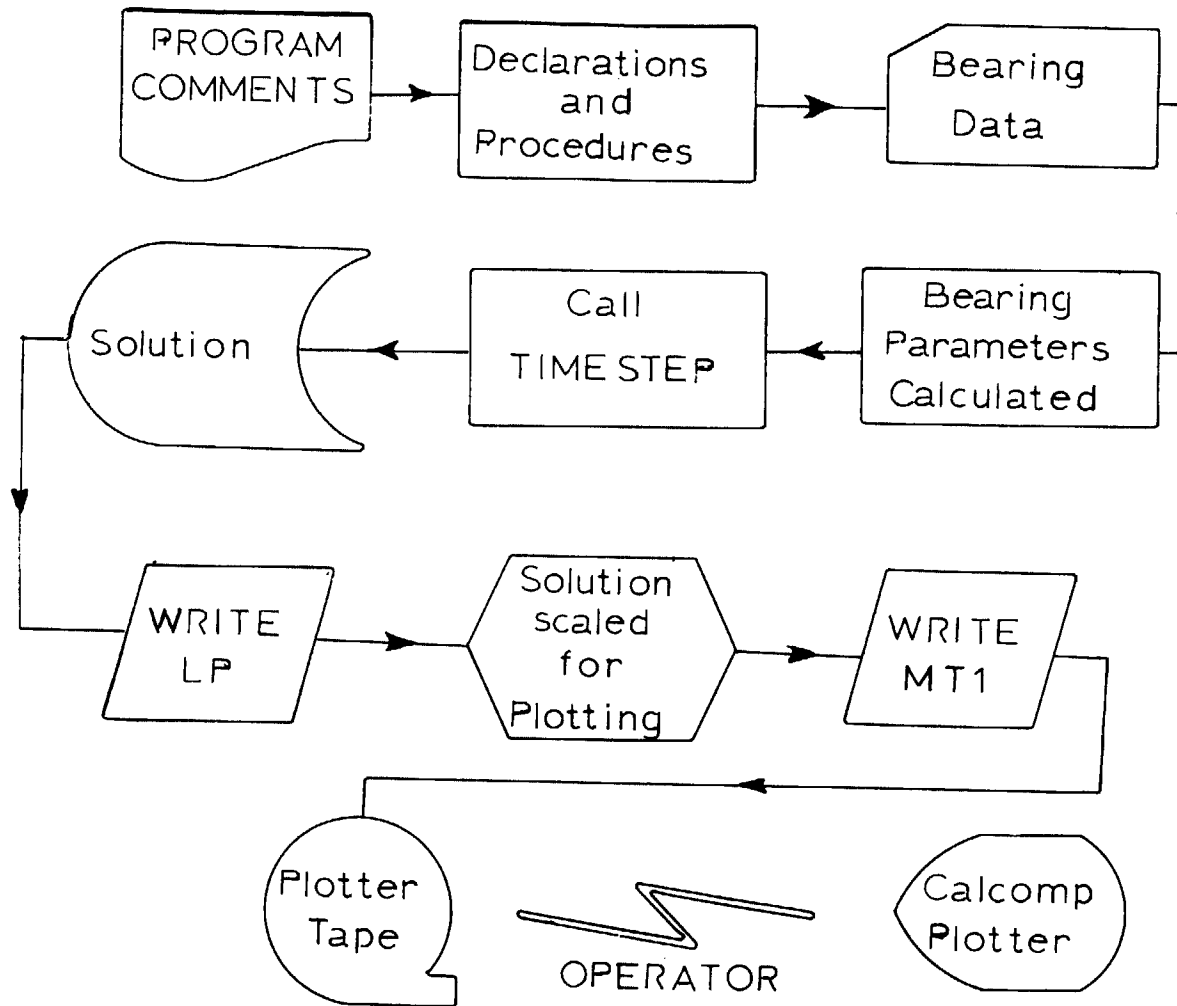
The major divisions of the program are as follows (See Figure 5.10 for Flow Chart):

1. Card Input of Specifications
2. Integration of Dynamical Equations of Motion
  - a. Integration of Pressure Profile
3. Line printer listing of results
4. Plotter Routine to Make Tapes for the Calcomp Plotter Unit.

A detailed explanation of the card input is included as a comment at the beginning of the program (See Appendix B). Card 12 gives the option as to the method of solution of the equations. Three methods are available in the program at present and additional changes in the method of solution can easily be made by any proficient programmer. The three methods included in the program are:

1. Sixth-order (self-starting) Runge-Kutta (41)
2. Adams - Moulton - Adams - Bashforth (Predictor-Corrector)
3. Modified Euler's Method

# THE SHORT BEARING PROGRAM



73

5.10 The Short Bearing Program; General Flow Chart

For the purpose of integrating the pressure profile the Weddle's Rule formula was chosen over the Romberg Method due to the anticipated future additional feature of having circumferential grooving specified over certain angles of the bearing surface. This addition will require very little change to the program as a result of the "fixed nature" of the Weddle's Rule formula.

The line printer output of the program gives the following information (see example following computer program listing, Appendix B):

- A. Case number (corresponds to number on plotter output)
- B. Bearing input data listed
- C. Bearing information calculated in program (Sommerfeld number, unbalance information, etc.)
- D. Additional forcing functions on journal listed as given on input cards
- E. Journal retainer specifications (stiffness and damping terms)
- F. Continuous listing at each time increment of the following information:
  - 1. Dimensionless time ( $\omega t$ ), [RAD.]
  - 2. Displacement in x-direction ( $x/c$ ), [DIM.]
  - 3. Velocity in x-direction ( $\dot{x}/\omega c$ ), [DIM.]
  - 4. Displacement in y-direction ( $y/c$ ), [DIM.]
  - 5. Velocity in y-direction ( $\dot{y}/c\omega$ ), [DIM.]
  - 6. Fluid film force, [lb.]
  - 7. Static transmissibility, [DIM.]
  - 8. Radius of curvature, [DIM.]

9. Instantaneous whirl ratio, [DIM.]
10. Whirl ratio about bearing center, [DIM.]
11. Phase angle between unbalance and journal center displacement vector, [DEG.]

The Calcomp Plotter gives four plots for each case submitted (see Figures 6.47 - 6.50 for examples). These are as follows:

(a) Journal Transient Orbit - (see Figure 6.47)

A list of important journal specifications appears at the top of the plot as well as a case number corresponding to the one on the line printer output. A six inch diameter circle representative of the clearance circle appears below the specifications. The journal center path is traced out as a continuous curve. The small circles on the orbit path are timing marks that represent one revolution of the journal in real time with the initial input time as base reference. In addition, the computer tracks the forces in the fluid film and places an asterisk at the point of maximum force (magnitude printed as FMAX in specification list above orbit).

(b) Transmissibility and Journal X-Y Motion

This plot has the transmissibility scaled on the left vertical axis while the journal X-Y motion is scaled on the right vertical axis. Each quantity is plotted versus cycles of motion of the journal. Arrows indicate which scale is to be used in addition to labeling the dashed X and Y motion curves.

A selected group of specifications appears at the top of each plot for easy reference (see Figure 6.48).

(c) Radius of Curvature and Whirl Ratio

The same general setup is used for this plot as was explained for the second plot (see Figure 6.49). The quantities plotted are the instantaneous radius of curvature (solid line) and the instantaneous whirl ratio (dashed line).

(d) Phase Angle VS Cycles of Motion

This plot gives the phase relation between the journal center displacement vector and the journal unbalance vector as a function of cycles of motion (see Figure 6.50).

The program was developed to allow the user to input bearing specifications and program control cards with a minimum of effort. Data card number eight gives the option of having the data printed on the line printer without having it plotted. If plots are desired, then data card number nine gives the option as to which plots will be produced (exception: orbit plot is made regardless of the value of PLOT1 if "plotter control" = 1).

CHAPTER VI  
PRESENTATION OF RESULTS

6.1 Introduction

The methods of solution incorporated in the computer program described in the preceding chapter were chosen to give the program the best overall features. The investigator has been given the choice of:

- (a) Rapid solution and reasonable accuracy (Improved Euler's method).
- (b) Reasonable speed of solution and improved accuracy (Modified Adam's method), but with the problem of numerical instability greatly increased over (a) above.
- (c) Excellent accuracy and less instability than (b) but very time consuming (sixth-order Runge-Kutta method).

Many runs have been made with the program and an extensive file of different operating conditions has been compiled. The following chapter will be given four major divisions to help classify the material being presented in a systematic manner. The basic journal bearing under consideration has the following specifications:

Journal Weight - 50 lb.

Clearance - 0.005 in.

Diameter - 2.0 in.

Length - 1.0 in.

Viscosity of Lubricant -  $1 \times 10^{-5}$  lb-sec/in.<sup>2</sup>

Unbalance - Variable

Loading - Variable

Journal Speed - Variable

Modified specifications are used to help clarify the different concepts being discussed and also to demonstrate the flexibility of the developed program.

The stability of a horizontal balanced journal is considered initially and results in a modification of the stability map discussed previously in CHAPTER IV. The next section deals with axially vertical journal bearings. The last two sections will take into consideration the effect of unbalance and other cyclic external loading functions on the overall journal bearing performance.

## 6.2 Instability of Horizontal Balanced Journal Bearings

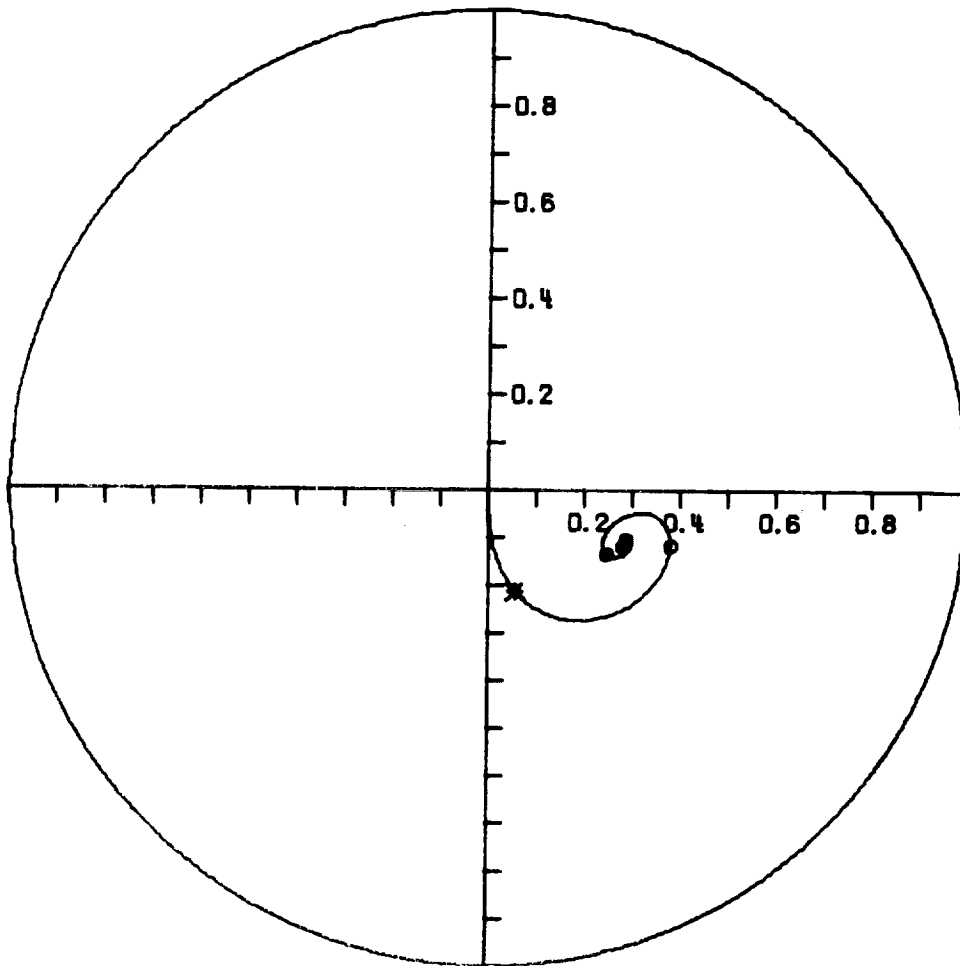
For the purpose of this discussion, a horizontal bearing is one having the journal effective weight acting at right angles to the axial coordinate of the journal. Figure 6.1 shows the orbit of the 50 pound journal as it is started at the bearing center while operating at a speed of 4,000 rpm. Five cycles of motion are shown in the figure and it is obvious that the journal has settled to the equilibrium eccentricity of 0.306 as computed from the bearing capacity number and indicated as ES on the figure. The maximum force transmitted to the bearing is indicated by FMAX and is recorded as 58.7 pounds and occurs 0.29 cycles after the journal was released. By checking the speed parameter, WS, and the eccentricity on the stability map (Fig. 4.2), it is apparent that the system is operating in a stable region as predicted by the stability map.

# HORIZONTAL BALANCED ROTOR

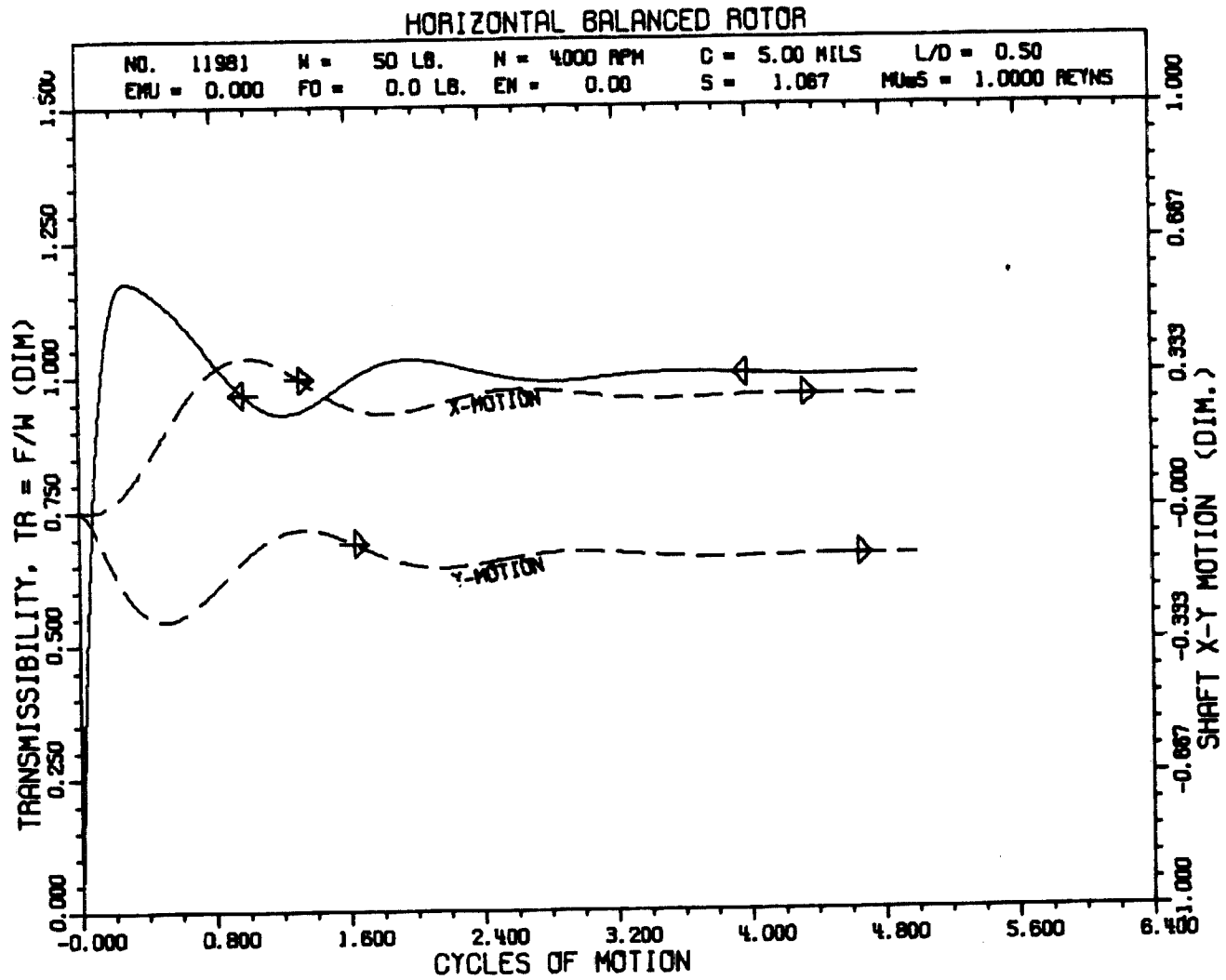
NO. 11981

N = 4000 RPM  
R = 1.00 IN.  
L = 1.00 IN.  
C = 5.00 MILS  
TASMAX = 1.17  
S = 1.067  
SS = 0.267

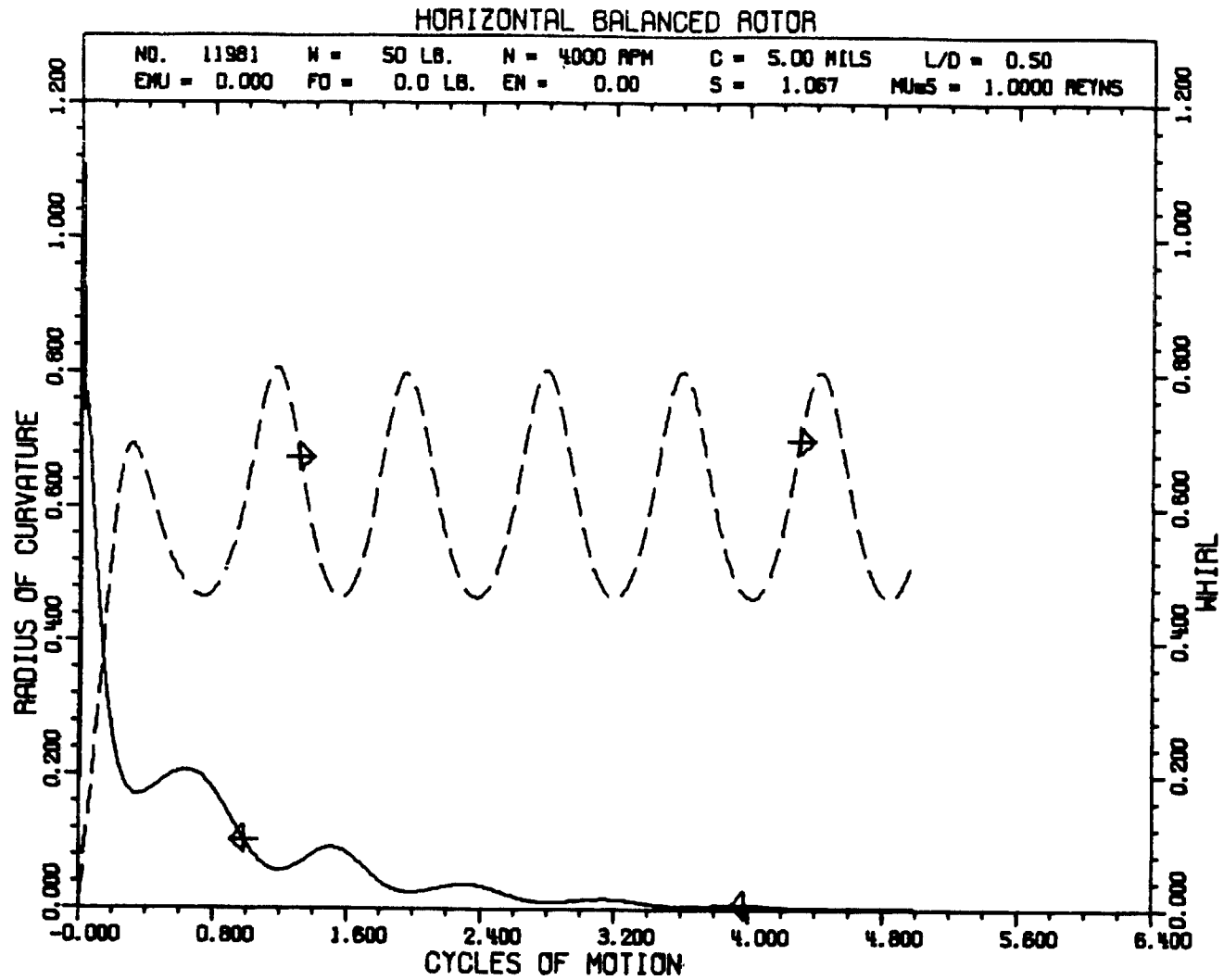
WT = 1.00  
W = 50 LB.  
MUS = 1.000 REYNS  
FMAX = 58.7 LB. AND  
OCCURS AT 0.29 CYCLE  
WS = 1.51  
ES = 0.306



6.1 Journal Orbit of A Balanced Horizontal Rotor  
(N = 4000, W = 50, C = 0.005, L/D = 1/2)



6.2 Transmissibility and Shaft X-Y Motion vs Cycles of Motion  
(N = 4000)



6.3 Radius of Curvature and Whirl vs Cycles of Motion (N = 4000)

The transmissibility, TR, is plotted for this case in Figure 6.2 (the solid line). Notice that the TR factor levels off to a value of 1 after about three cycles of motion. The dashed lines on this plot give the X and Y motion versus cycles of journal motion as indicated. Figure 6.3 shows the instantaneous whirl and radius of curvature for this case. The radius reduces to zero as it should while the whirl is oscillating in a very regular manner. Constant whirl ratios have been reported to exist in test rigs but it will be apparent from the following discussion and figures that this is a misnomer for the horizontal bearing.

The next series of plots (Figures 6.4, 6.5, 6.6) represents the previous case with the speed increased to 6500 rpm. A different behavior is immediately noticed and by checking the stability map (Fig. 4.2), it is apparent that the system is operating on the threshold of instability by the values given for WS and ES. The maximum force has increased to 64.4 pounds and Figure 6.5 indicates that the force variations are more pronounced than in the previous force plot (Figure 6.2). From Figure 6.6, the whirl is varying from a value of 0.44 up to a value about 0.64. The timing circles on the orbit of Figure 6.4 are indicative of an average whirl of approximately one-half.

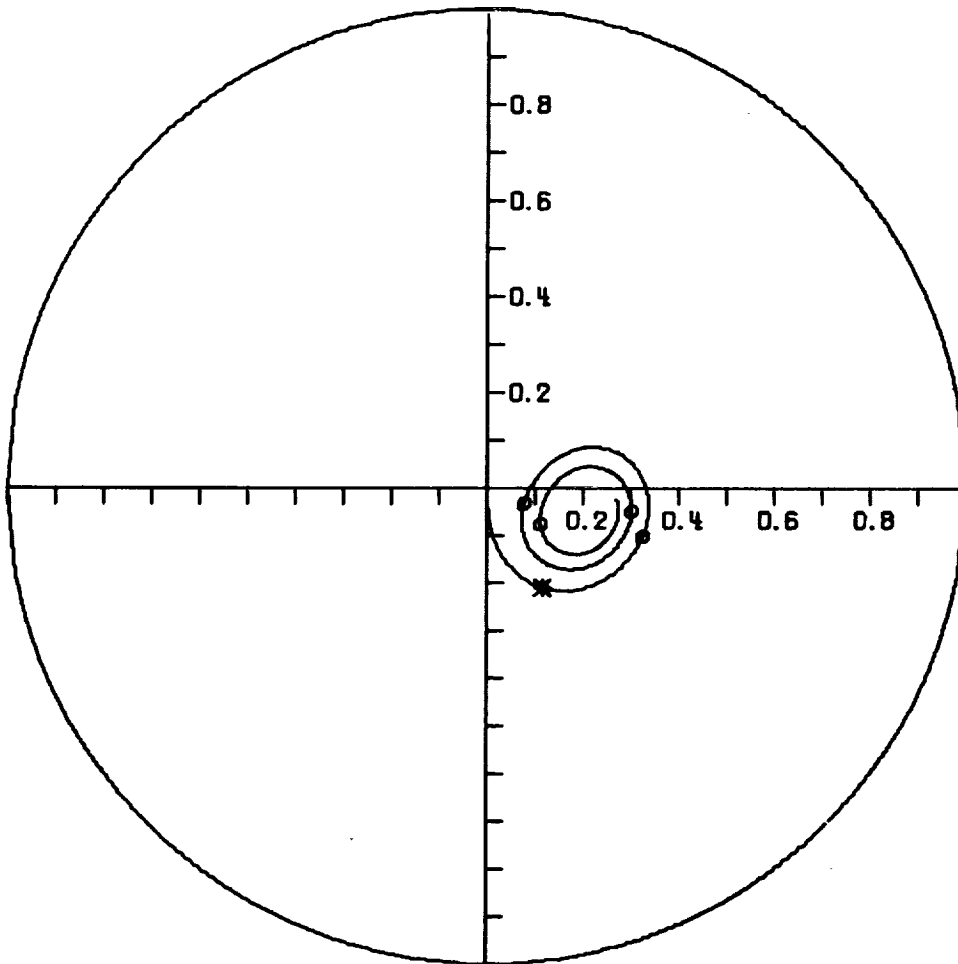
If the journal speed were now increased to 10,500 rpm the speed parameter, WS, would be 3.96 and well into the region of instability as predicted by Figure 4.2. Figure 6.7a shows this condition with the final position in Figure 6.4 as the initial condition for this plot. The spiral is evidence of the instability of the system and if

# HORIZONTAL BALANCED ROTOR

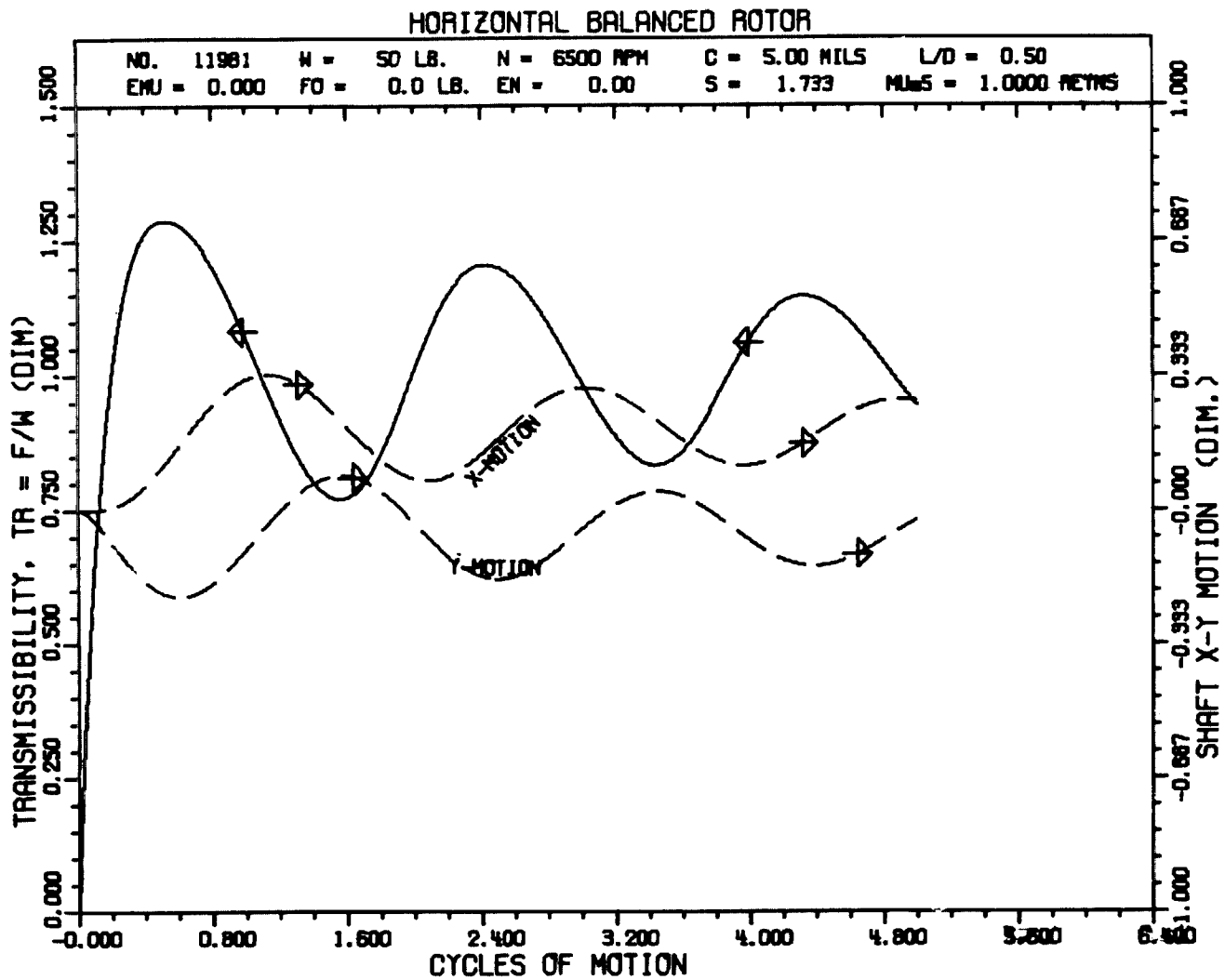
NO. 11981

N = 6500 RPM  
R = 1.00 IN.  
L = 1.00 IN.  
C = 5.00 MILS  
TRSMAX = 1.29  
S = 1.733  
SS = 0.433

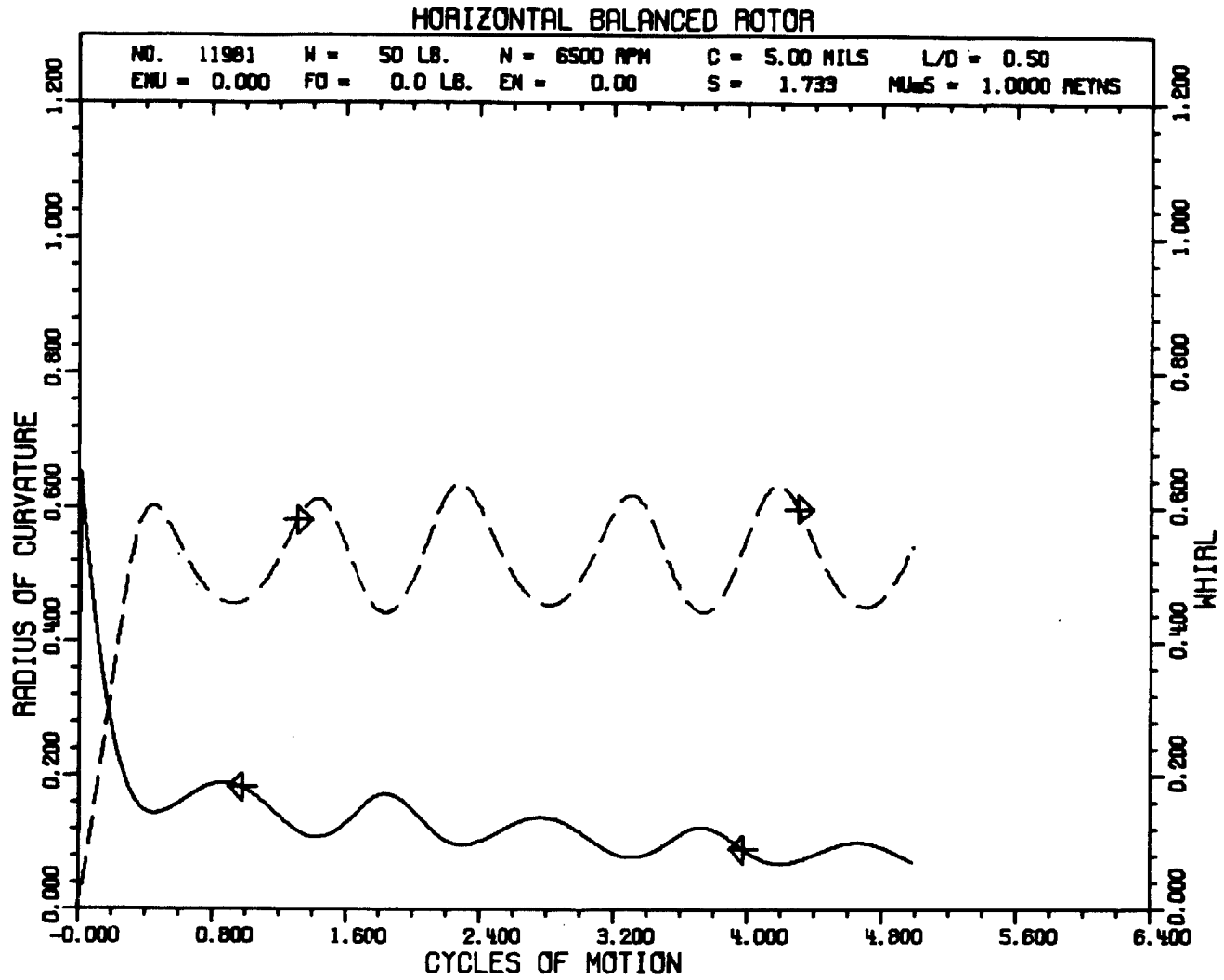
WT = 1.00  
W = 50 LB.  
MUS = 1.000 REYNS  
FMAX = 64.4 LB. AND  
OCCURS AT 0.53 CYCLE  
WS = 2.45  
ES = 0.211



6.4 Journal Orbit of A Balanced Horizontal Rotor  
(N = 6500, W = 50, C = 0.005, L/D = 1/2)



6.5 Transmissibility and Shaft X-Y Motion vs Cycles of Motion  
(N = 6500)



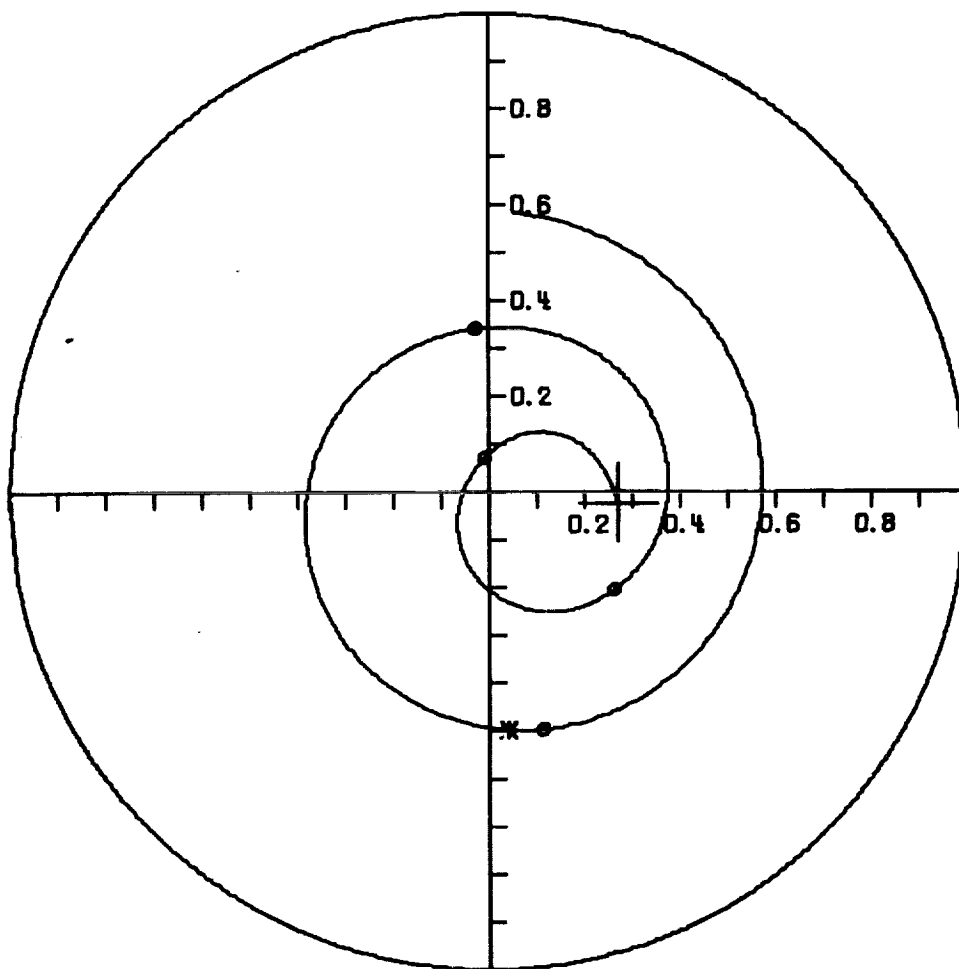
6.6 Radius of Curvature and Whirl vs Cycles of Motion (N = 6500)

# HORIZONTAL BALANCED ROTOR

NO. 11981

N = 10500 RPM  
R = 1.00 IN.  
L = 1.00 IN.  
C = 5.00 MILS  
TRSMAX = 2.91  
S = 2.800  
SS = 0.700

WT = 1.00  
W = 50 LB.  
MUM5 = 1.000 REYNS  
FMAX = 145.6 LB. AND  
OCCURS AT 8.96 CYCLE  
WS = 3.96  
ES = 0.139



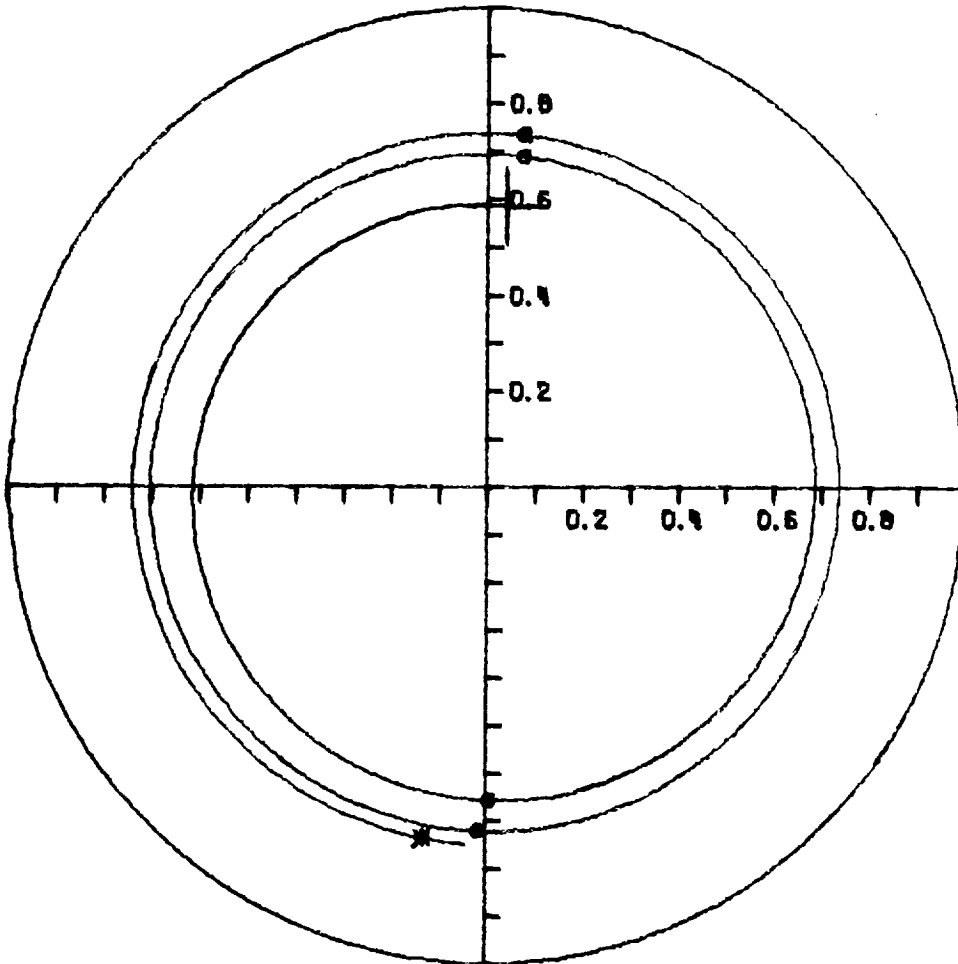
6.7 a. Journal Orbit of A Balanced Horizontal Rotor for Cycles 5 - 10 (N = 10,500, W = 50, C = 0.005, L/D = 1/2)

# HORIZONTAL BALANCED ROTOR

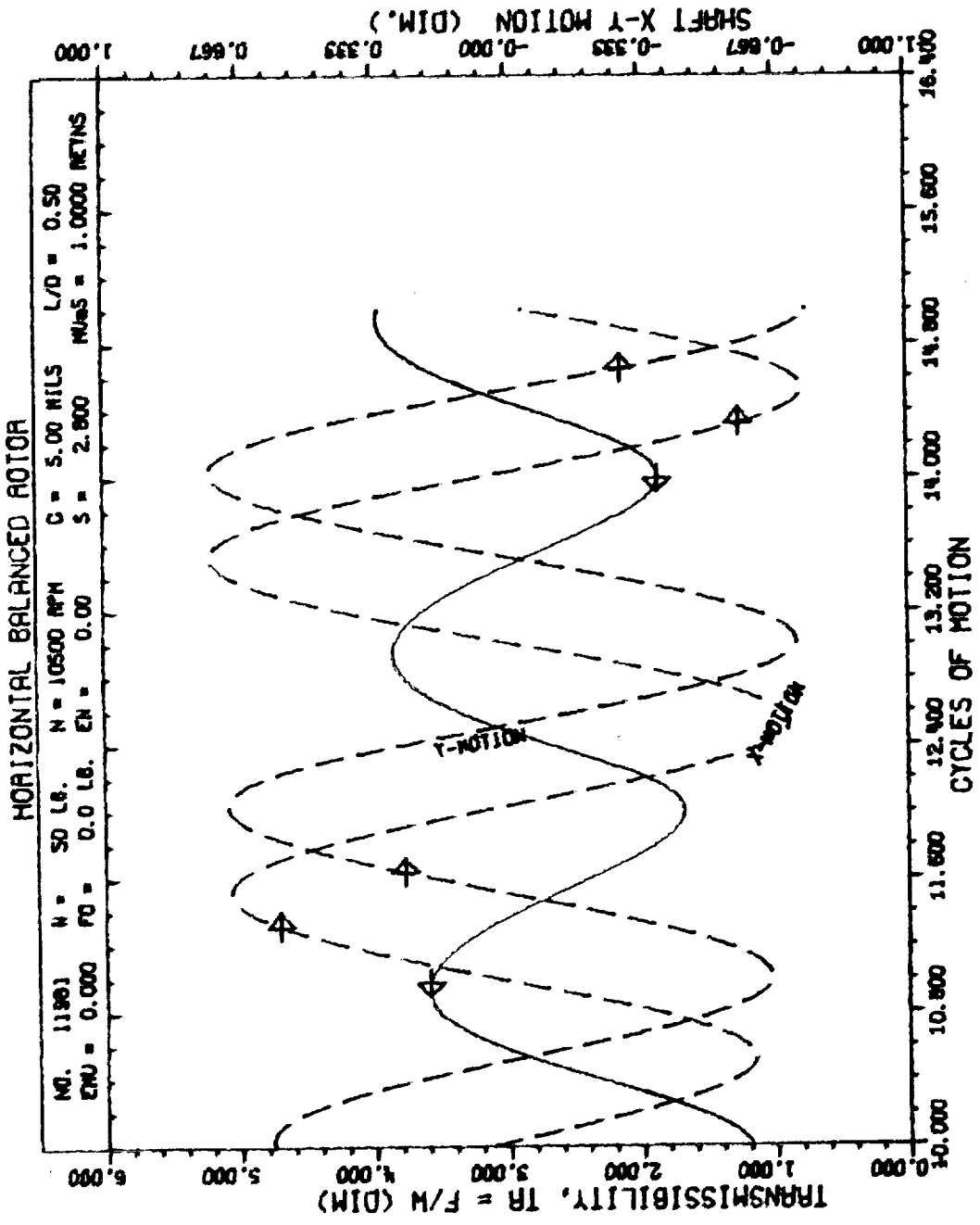
NO. 11901

N = 10500 RPM  
R = 1.00 IN.  
L = 1.00 IN.  
C = 5.00 MILS  
TASMAX = 3.96  
S = 2.800  
SS = 0.700

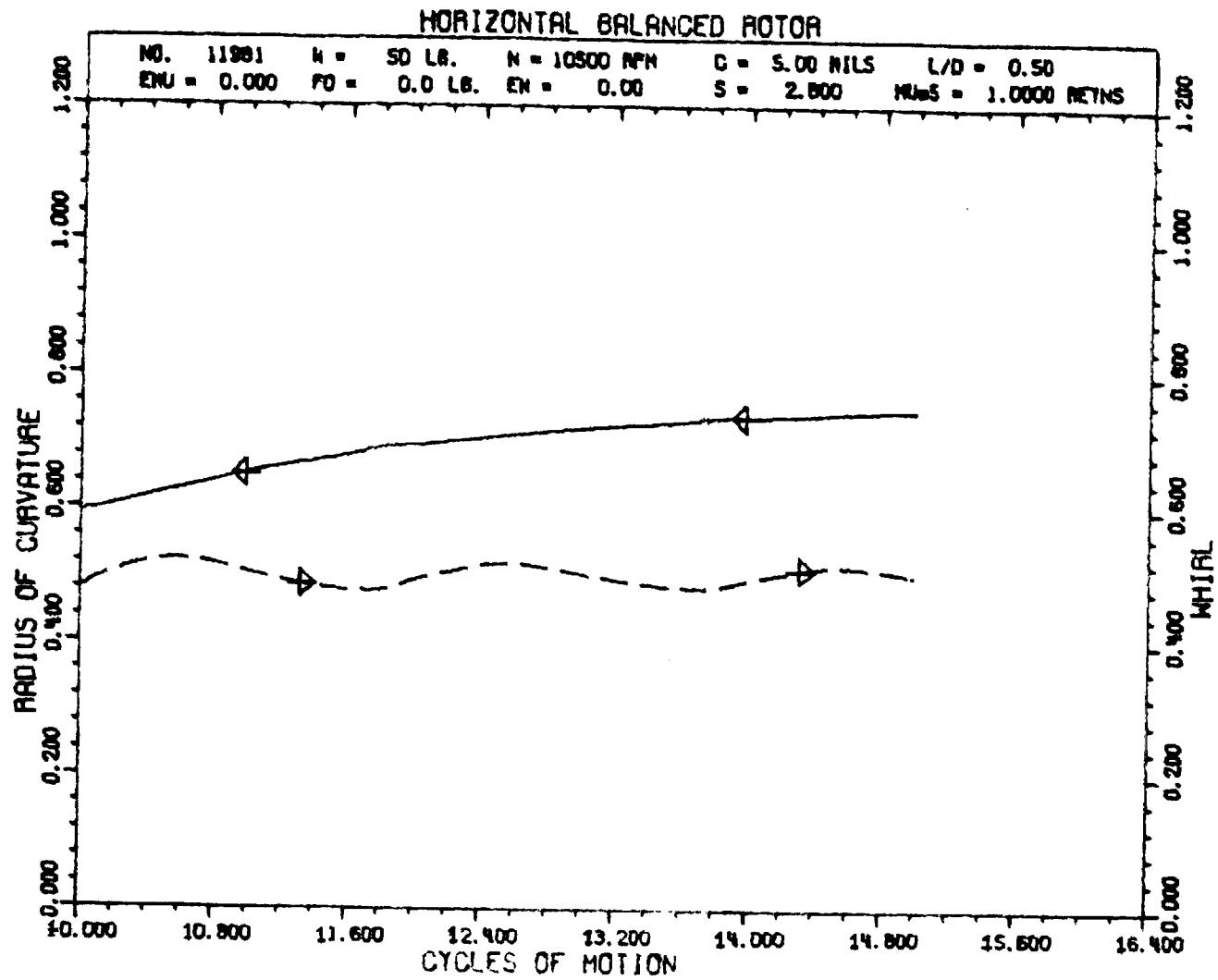
WT = 1.00  
W = 50 LB.  
MUS = 1.000 REYNS  
FMAX = 197.9 LB. AND  
OCCLAS AT 14.96 CYCLE  
WS = 3.96  
ES = 0.139



6.7 b. Journal Orbit of A Balanced Horizontal Rotor for Cycles 10 - 15 (N = 10,500, W = 50, C = 0.005, L/D = 1/2)



6.7 c. Transmissibility and Shaft X-Y Motion vs Cycles of Motion for Cycles 10 - 15 (N = 10,500)



6.7 d. Radius of Curvature and Whirl vs Cycles of Motion for Cycles 10 - 15 (N = 10,500)

more cycles were run the orbit would reach a limit cycle\* and continue the violent whirling motion. Also notice the fact that the maximum force has increased to 145.6 pounds (as compared to 58.7 pounds for the stable condition, i.e. Figure 6.1. The orbit of Figure 6.7a is continued for five additional cycles in Figure 6.7b. It is apparent that the rate of growth of the orbit has reduced and a limit cycle would eventually be formed. The maximum force has increased to a value of 197.9 pounds. Figure 6.7c show the cyclic nature of the resultant forces on the bearing surface. The whirl ratio is oscillating around approximately 0.5, as shown in Figure 6.7d.

Figure 6.8 depicts the initial transient orbit for a heavier journal with an effective weight of 200 pounds and operating at 6500 rpm. This case is still at the threshold of stability although the equilibrium eccentricity has increased to 0.497. An increase of journal speed to 10,500 rpm raises the stability speed parameter to 3.96 and the system exhibits the predicted instability as shown in Figure 6.9. The maximum force is indicated to be 826.8 pounds, or 4.13 times the weight of the journal.

The stability map predicts that for systems with an equilibrium eccentricity above approximately 0.73, there should exist stable conditions at any speed. With the journal weight increased to 1800 pounds, Figures 6.10 and 6.11 indicate that the system is tending toward the stable equilibrium position, even when the speed is increased to 10,500 rpm. The stability map of Figure 4.2 has predicted all the

---

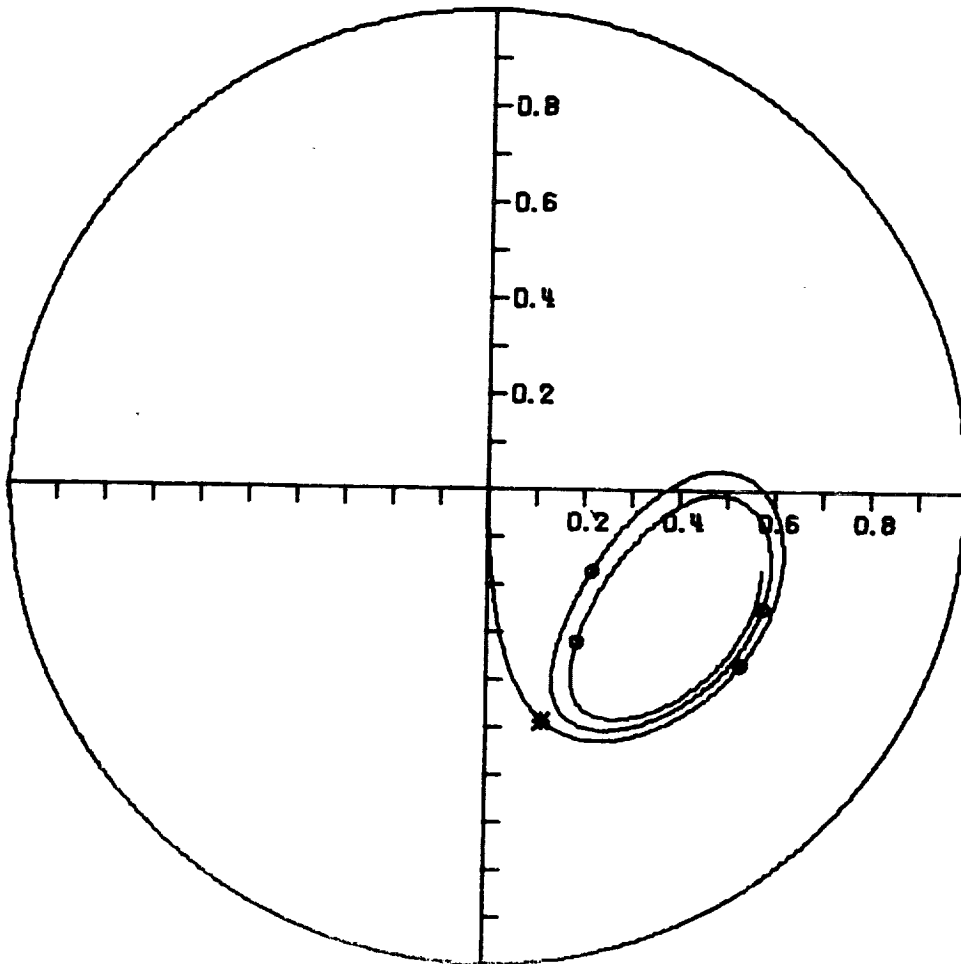
\*See Figure 6.17 for example of a limit cycle.

# HORIZONTAL BALANCED ROTOR

NO.111181

N = 6500 RPM  
R = 1.00 IN.  
L = 1.00 IN.  
C = 5.00 MILS  
TRSMAX = 1.80  
S = 0.433  
SS = 0.108

WT = 1.00  
W = 200 LB.  
MU<sub>5</sub> = 1.000 REYNS  
FMAX = 359.9 LB. AND  
OCCURS AT 0.54 CYCLE  
WS = 2.45  
ES = 0.497



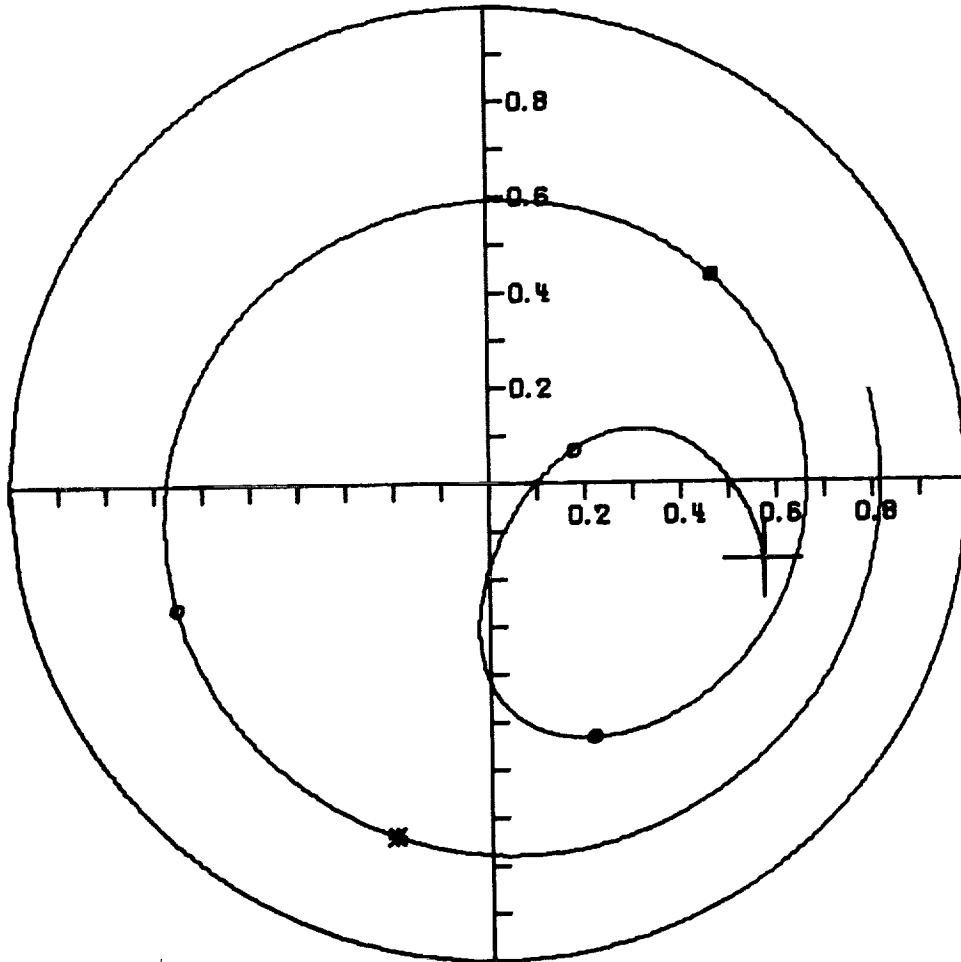
6.8 Journal Orbit of a Balanced Horizontal Rotor for 5 Cycles  
(N = 6500, W = 200, C = 0.005, L/D = 1/2)

# HORIZONTAL BALANCED ROTOR

NO.111181

N = 10500 RPM  
R = 1.00 IN.  
L = 1.00 IN.  
C = 5.00 MILS  
TRSMAX = 4.13  
S = 0.700  
SS = 0.175

WT = 1.00  
W = 200 LB.  
MUS = 1.000 REYNS  
FMAX = 826.8 LB. AND  
OCCURS AT 9.30 CYCLE  
WS = 3.96  
ES = 0.395



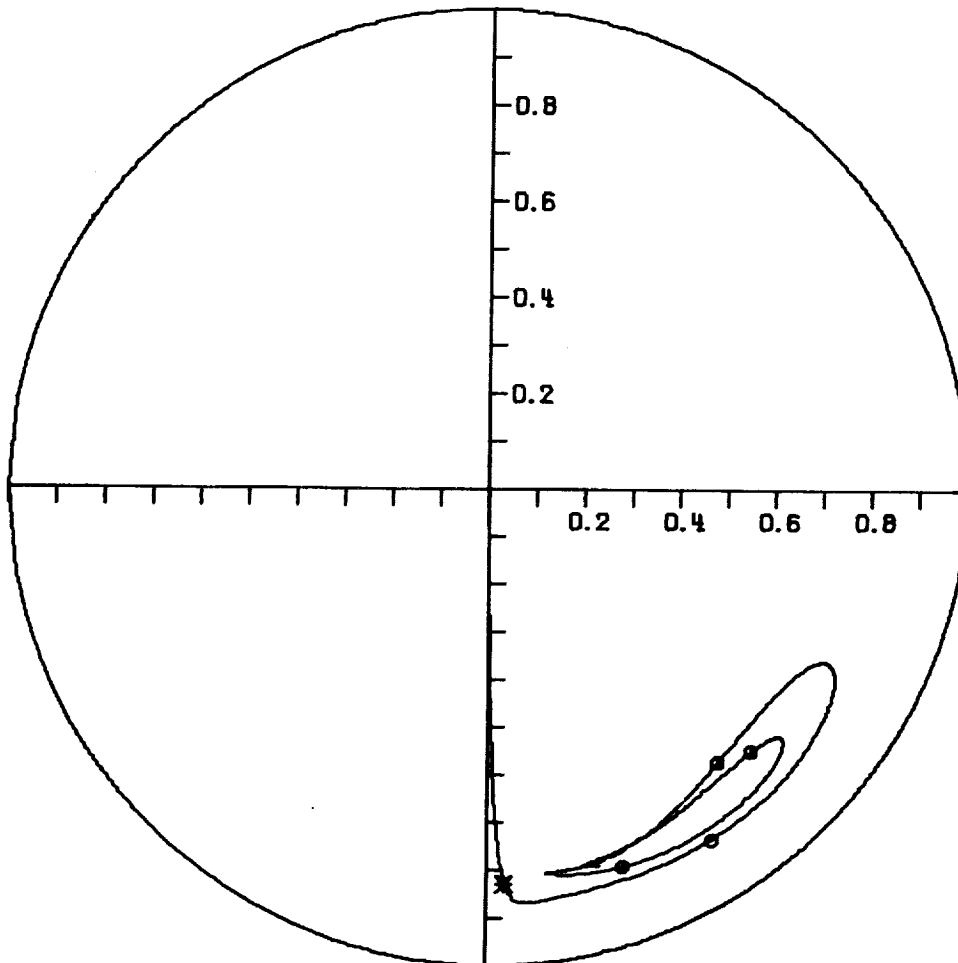
6.9 Journal Orbit of a Balanced Horizontal Rotor for Cycles 5 - 10 (N = 10,500)

# HORIZONTAL BALANCED ROTOR

NO.111182

N = 6500 RPM  
R = 1.00 IN.  
L = 1.00 IN.  
C = 5.00 MILS  
TRSMAX = 4.77  
S = 0.048  
SS = 0.012

WT = 1.00  
W = 1800 LB.  
MU<sub>5</sub> = 1.000 REYNS  
FMAX = 8588.7 LB. AND  
OCCURS AT 0.56 CYCLE  
WS = 2.45  
ES = 0.814



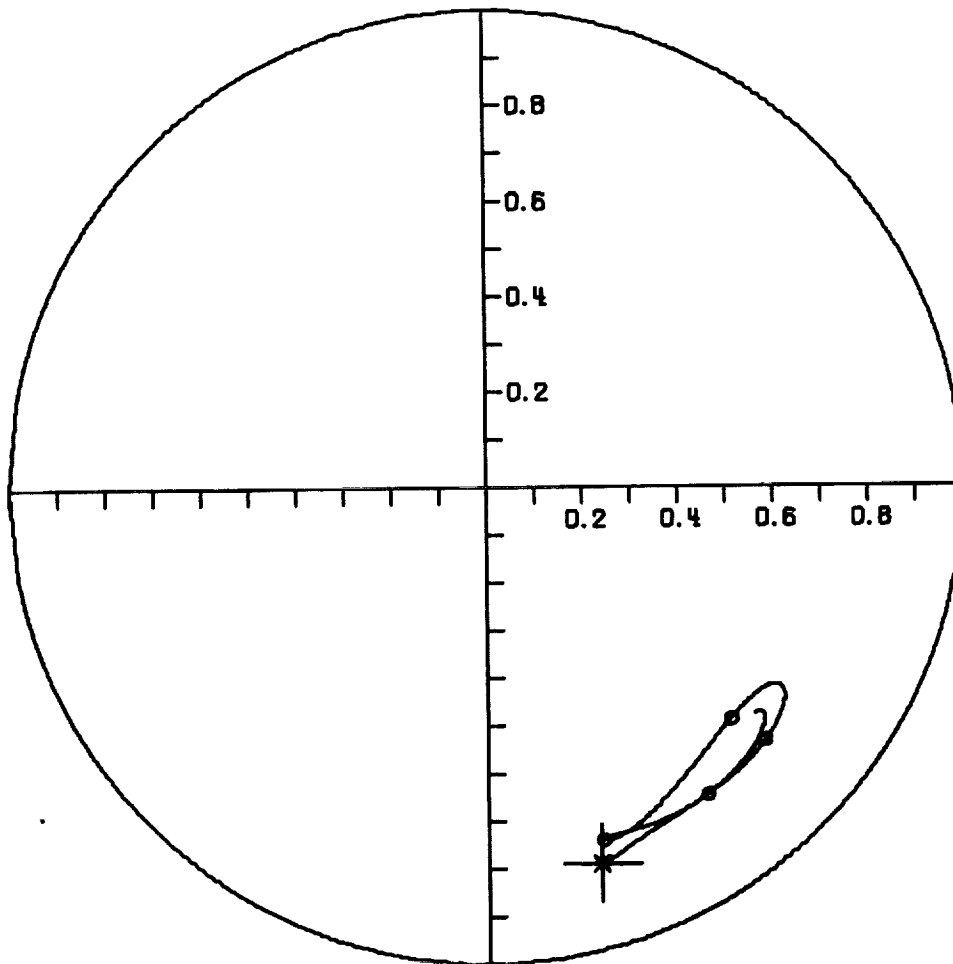
6.10 Journal Orbit of a Balanced Horizontal Rotor for 5 Cycles  
(N = 6500, W = 1800, C = 0.005, L/D = 1/2)

# HORIZONTAL BALANCED ROTOR

NO.111182

N = 10500 RPM  
R = 1.00 IN.  
L = 1.00 IN.  
C = 5.00 MILS  
TRSMAX = 1.79  
S = 0.078  
SS = 0.019

WT = 1.00  
W = 1800 LB.  
MU<sub>5</sub> = 1.000 REYNS  
FMAX = 3221.1 LB. AND  
OCCURS AT 5.01 CYCLE  
WS = 3.96  
ES = 0.766



6.11 Journal Orbit of a Balanced Horizontal Rotor for Cycles  
5 - 10 (N = 10,500)

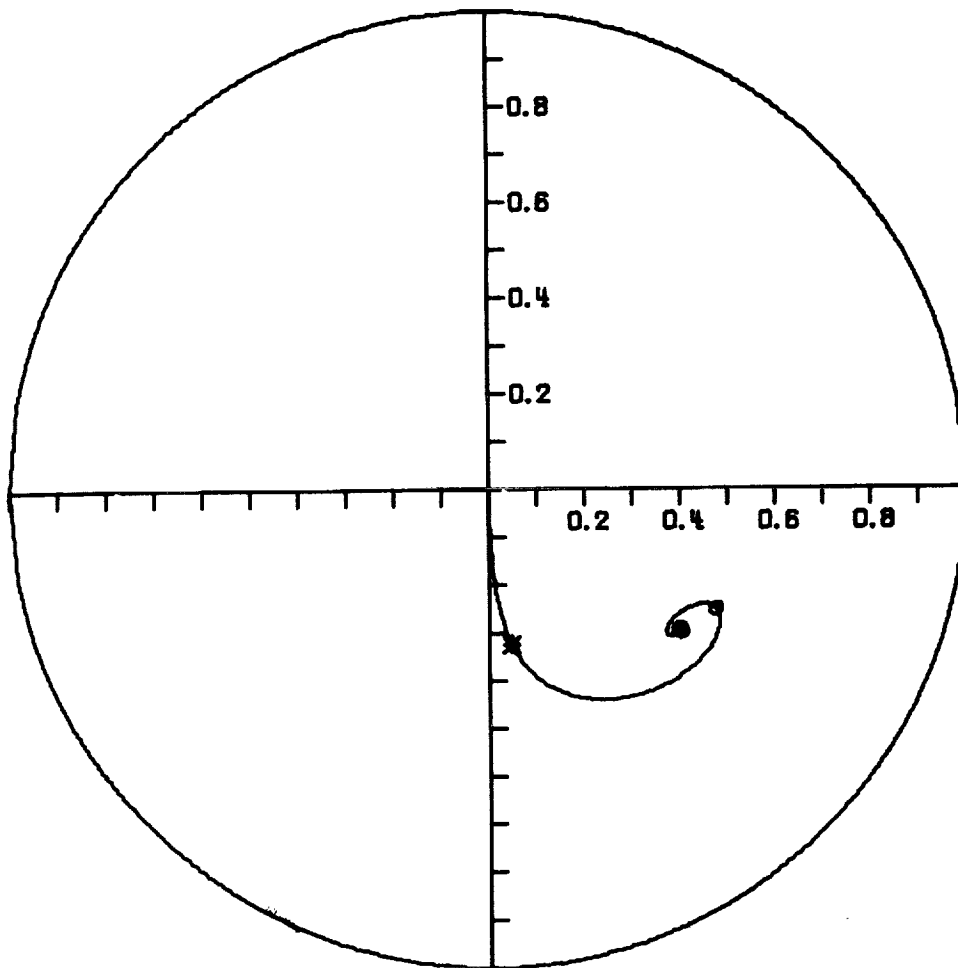
results obtained thus far in this analysis. However, no indication can be obtained from such a stability map of the behavior of a system that has external loading. To examine this condition, a constant force of 150 pounds was applied vertically downward (i.e. negative y-direction) to the 50 pound journal to see if the conditions of the 200 pound journal were repeated. Figure 6.12 gives the interesting results of that loading. The journal has settled very smoothly into its equilibrium eccentricity of 0.497. The speed parameter corresponding to Figure 4.2 is still 2.45 and indicates that the system should be at its threshold speed. An increase of journal speed to 10,500 rpm should produce violent whirling if Figure 4.2 is valid. It is readily apparent from Figure 6.13 that the system is stable at 10,500 rpm and has settled very nicely into the new equilibrium eccentricity of 0.395. In response to these results, Figure 4.2 has been modified to indicate the stability of a journal bearing with constant external loading. Figure 6.14 presents the stability map that was formulated after the results of the previous test case were examined. The quantity WT is an indication of the magnitude of all constant forces acting on the system. For a horizontal unloaded journal, the value for WT is unity whereas for the case of the 150 pound loading on the 50 pound journal the value of WT is four. The old speed parameter,  $\omega_s$ , for 10,500 rpm and clearance of 5 mils resulted in a value of 3.96 and a value of eccentricity of 0.139, which has obviously changed. However, going into the modified stability map of Figure 6.14 with those values for  $\omega_s$  and  $\epsilon_o$ , plus the value of WT = 4, it is apparent that the journal is stable as verified by the highly damped transient rotor orbit

# HORIZONTAL BALANCED ROTOR

NO. 11982

N = 6500 RPM  
R = 1.00 IN.  
L = 1.00 IN.  
C = 5.00 MILS  
TRSMAX = 5.33  
S = 0.433  
SS = 0.108  
FOCY = -150 LB.

WT = 4.00  
W = 50 LB.  
MUS = 1.000 REYNS  
FMAX = 266.4 LB. AND  
OCCURS AT 0.24 CYCLE  
WS = 1.22  
ES = 0.497



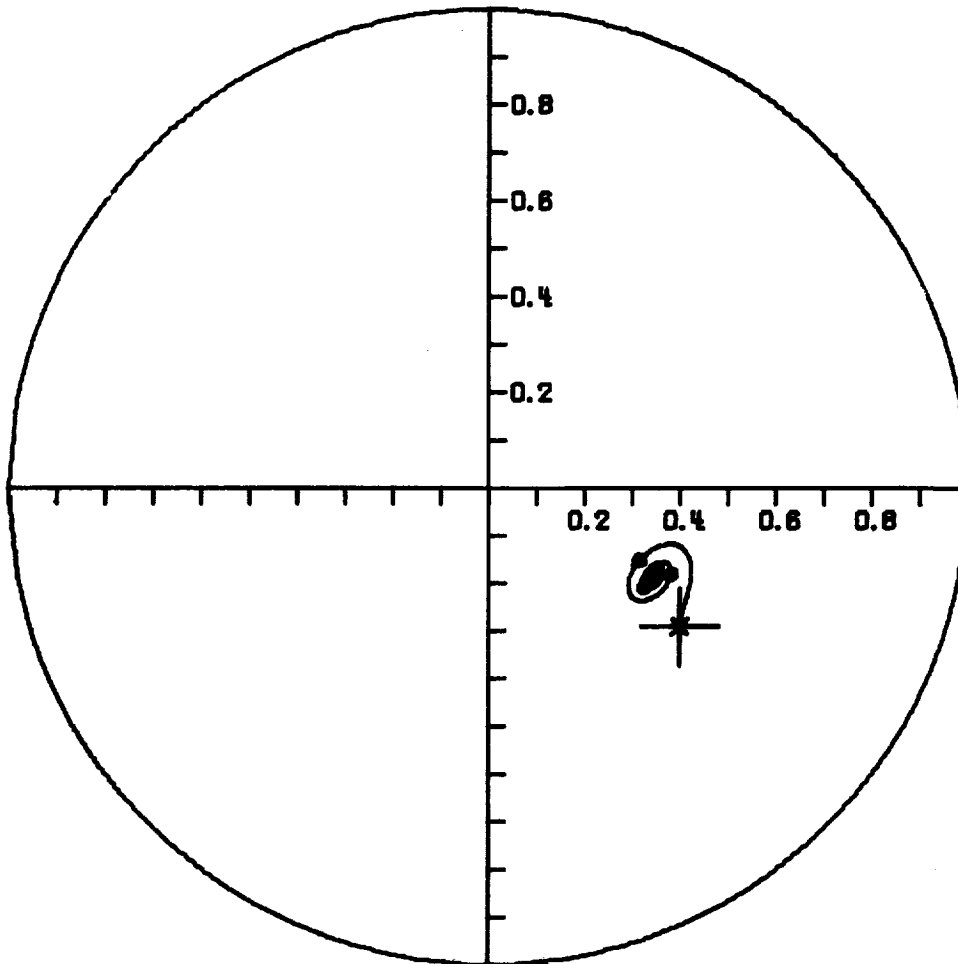
6.12 Journal Orbit of a Horizontal Balanced Rotor with Constant Load for 5 Cycles (N = 6500, W = 50, C = 0.005, L/D = 1/2, FOCY = -150)

# HORIZONTAL BALANCED ROTOR

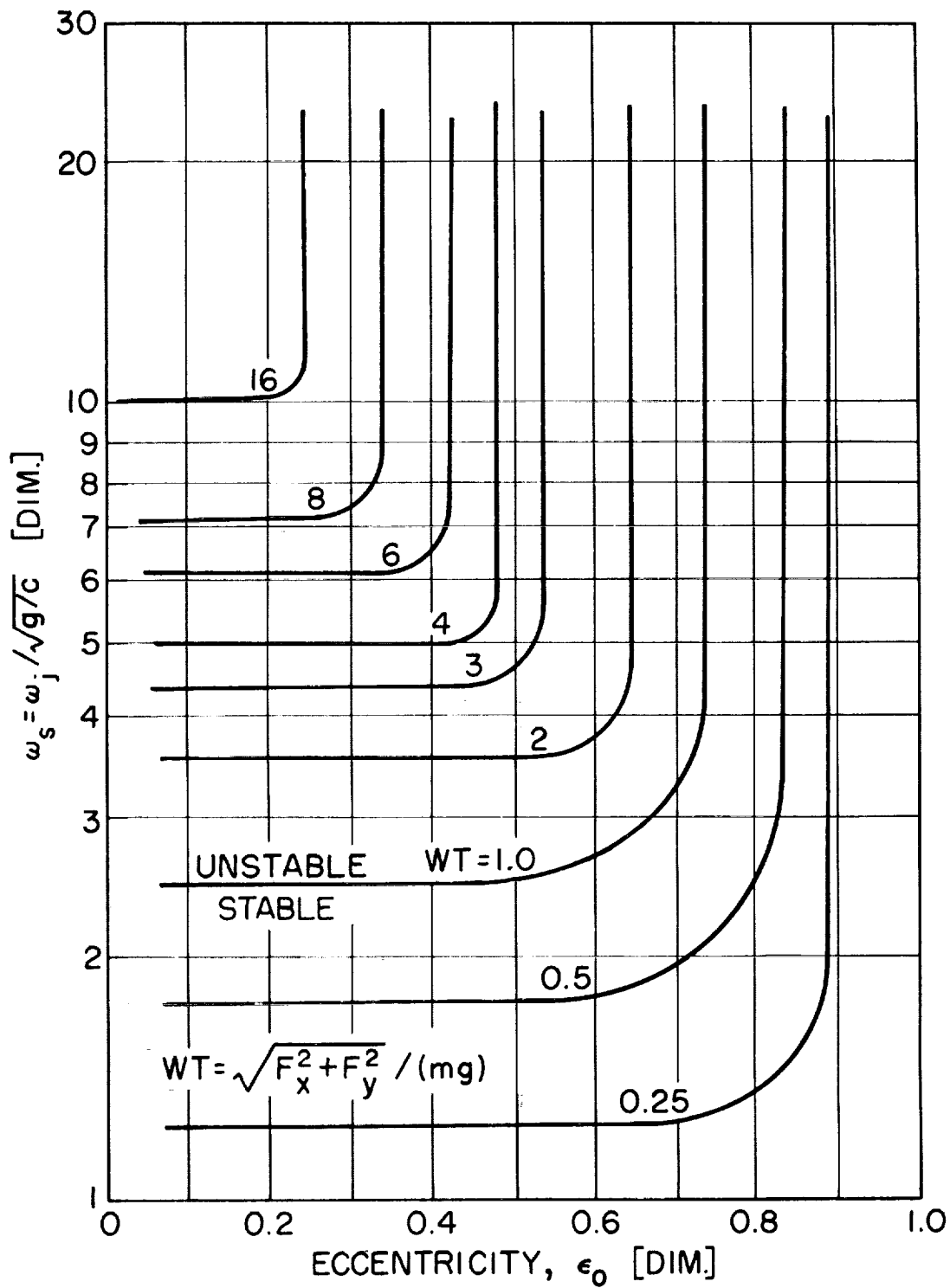
NO. 11982

N = 10500 RPM  
R = 1.00 IN.  
L = 1.00 IN.  
C = 5.00 MILS  
TASMAX = 6.46  
S = 0.700  
SS = 0.175  
FOCY = -150 LB.

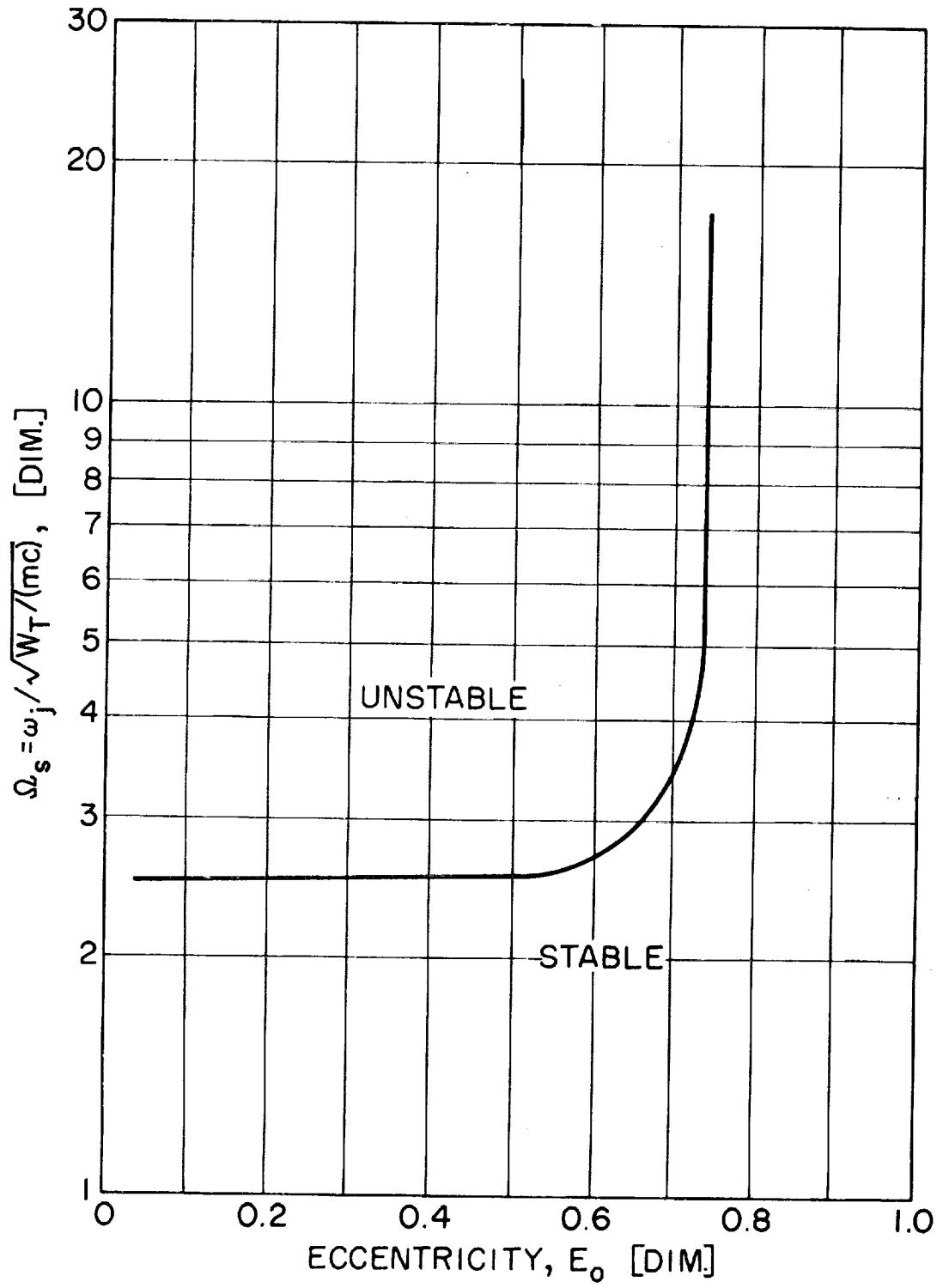
WT = 4.00  
W = 50 LB.  
MU<sub>5</sub> = 1.000 REYNS  
FMAX = 323.1 LB. AND  
OCCURS AT 5.01 CYCLE  
WS = 1.98  
ES = 0.395



6.13 Journal Orbit of a Horizontal Rotor with Constant Load for Cycles 5 - 10 (N = 10,500)



6.14 Stability Map for the Short Journal Bearing Considering Constant External Loading



6.15 Stability Map for the Short Journal Bearing Using Modified Stability Parameters

shown in Figure 6.13.

If a new speed parameter\* is defined as:

$$\Omega_s = \omega_j / \sqrt{W_T / m_j c}$$

where,

$$W_T = \text{total loading} \neq WT$$

and,

$E_o$  = eccentricity of journal calculated by using  $W_T$  instead of  $W$  in the projected load,  $P$ , of the Sommerfeld equation ( $S_s$ )

then the stability map of Figure 6.15 may be obtained. By redefining the speed parameter and using the actual value of equilibrium eccentricity, then and only then can the curve of Figure 4.1 or 4.2 be considered as correct for other than unloaded bearings.

For a vertical journal the equilibrium eccentricity,  $E_o$ , approaches 0 as can be seen from Figure 3.8, while the speed parameter,  $\Omega_s$ , approaches  $\infty$ . Therefore, from Figure 6.15, it is apparent that the vertical journal is unstable regardless of the speed of operation. The same conclusion was reported by Hori (26) but it cannot be shown from the stability map as presented by Badgley (Fig. 4.2).

### 6.3 Instability of Vertical Balanced Journal Bearings

The stability map of Figure 6.15 in the previous section indicates that the vertical unloaded journal bearing is unstable for the entire operating speed range. To verify this condition several cases were

---

\*This is the same parameter used by Reddi and Trumpler (28) in their linearized approach to the stability problem.

examined, some of which will be presented here for discussion.

The same 50 pound journal is considered in Figure 6.16. The initial conditions were all zero and as the plot indicates, no orbit was obtained for the five cycles the program was allowed to run. The forces on the bearing are zero, as they should be. By inspection of the equations of motion it is readily apparent that the origin is an equilibrium point for the unloaded vertical journal bearing. To investigate the stability of this point, the system is given a small displacement from the origin and released. If the system is in stable equilibrium then the journal would return to the origin, otherwise the configuration is an unstable equilibrium point (saddle point) and the solution will continue to grow as time increases until it eventually forms a limit cycle due to the bearing nonlinearity.

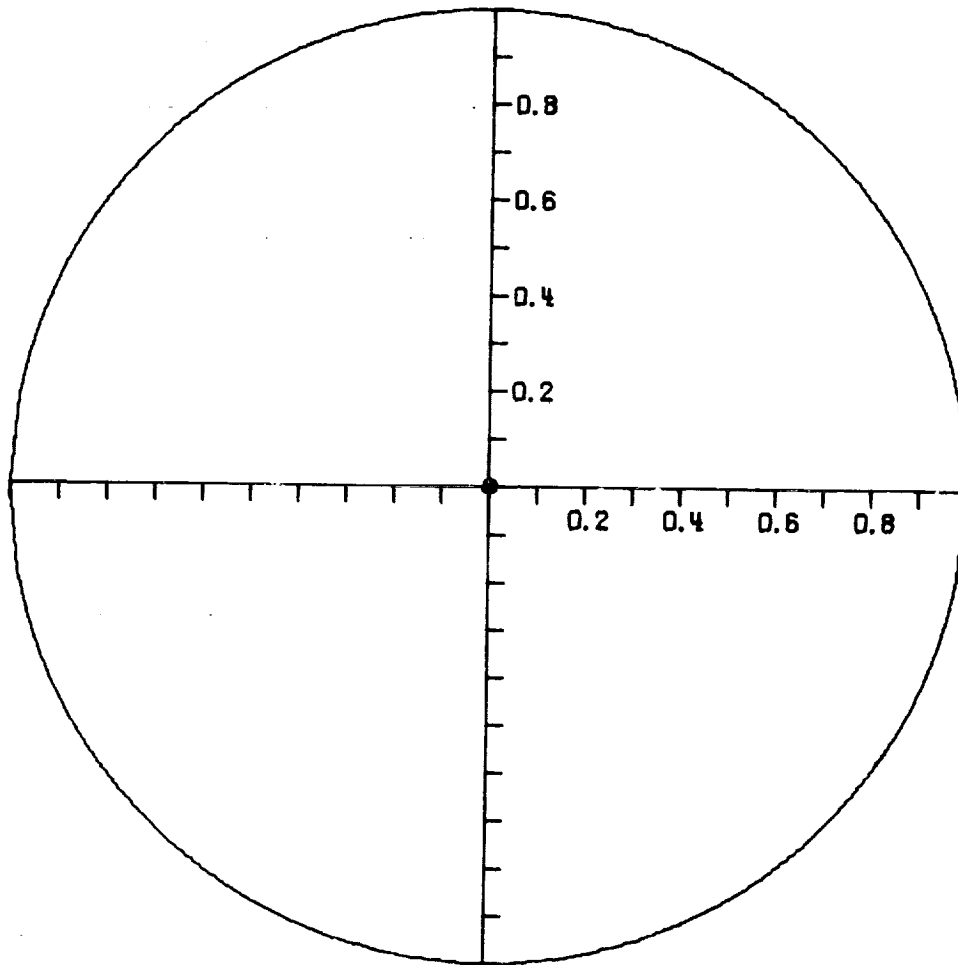
Figure 6.17 represents twenty-five cycles of motion of the journal with the initial conditions all zero except for a displacement of 0.01 (dimensionless, i.e.  $x = 0.01 \times c$ ) in the positive x-coordinate direction. The initial exponential growth is readily apparent. The figure is an excellent example of a limit cycle, which arises from the nonlinear nature of the fluid-film force expression derived in CHAPTER III. The whirl for this particular case is constant and has a value very near one-half, as indicated by Figure 6.18. The vertical rotor is the only configuration that has produced a constant value for the whirl ratio. It was shown in the previous section that a horizontal rotor does not have a constant whirl ratio, but one which varies in a cyclic manner due to gravitational loading. Because the system being considered has gone into the half-frequency whirl, the

# VERTICAL BALANCED ROTOR

NO. 41591

N = 4000 RPM  
R = 1.00 IN.  
L = 1.00 IN.  
C = 5.00 MILS  
TRSMAX = 0.00  
S = 1.067  
SS = 0.267

WT = 0.00  
W = 50 LB.  
MU<sub>5</sub> = 1.000 REYNS  
FMAX = 0.0 LB. AND  
OCCURS AT 0.00 CYCLE  
WS = 1.51  
ES = 0.306



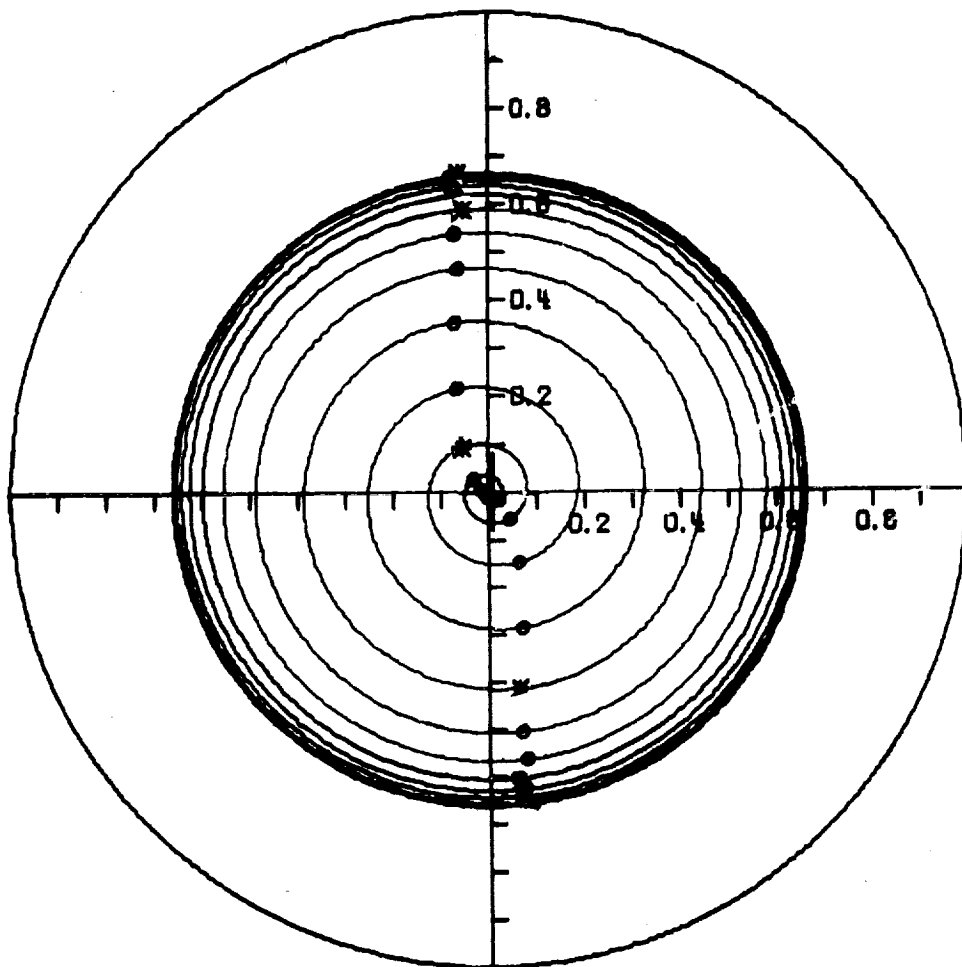
6.16 Journal Orbit of a Balanced Vertical Rotor with Zero Initial Conditions (N = 4000, W = 50, C = 0.005, L/D = 1/2)

# VERTICAL BALANCED ROTOR

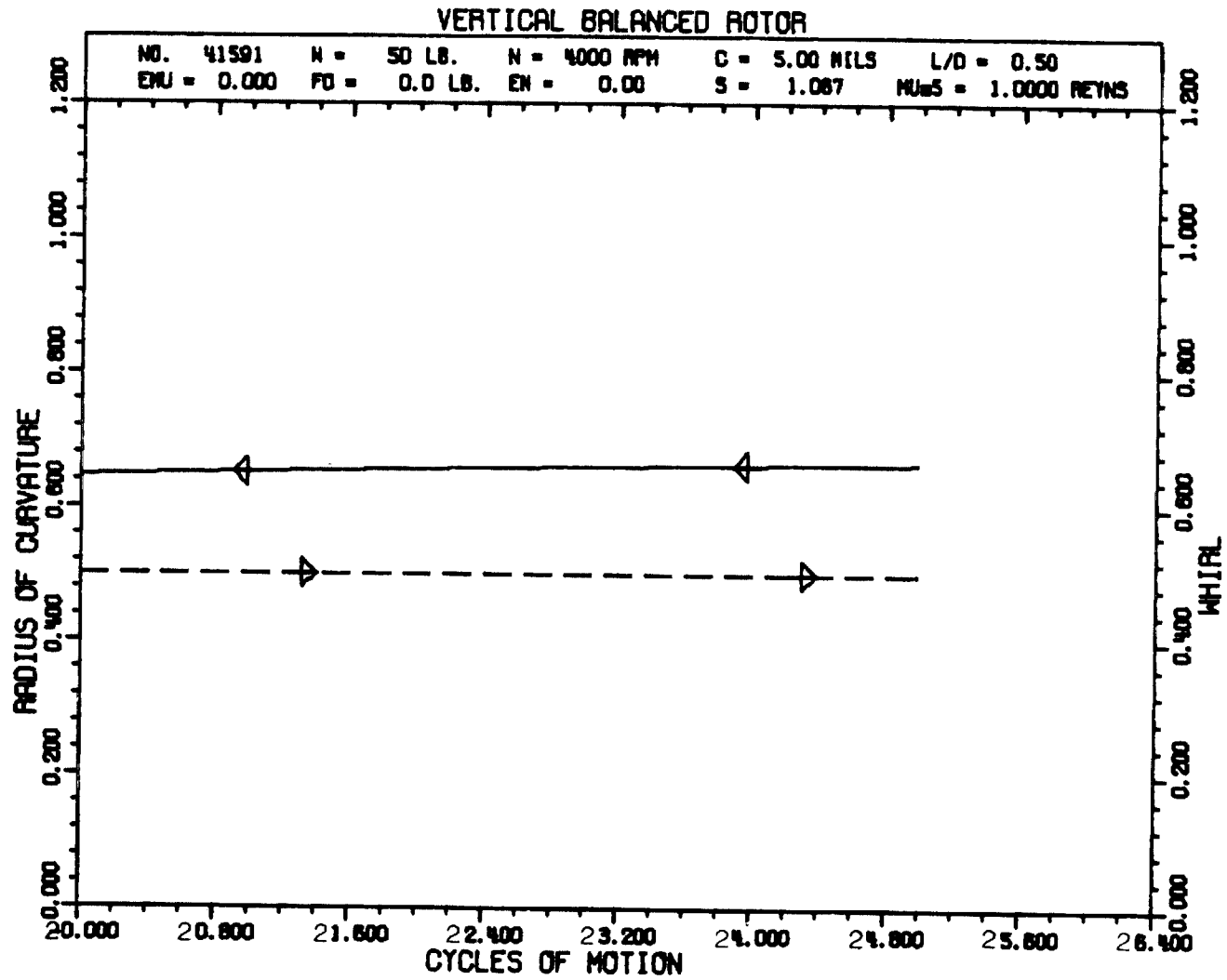
NO. 41591

N = 4000 RPM  
R = 1.00 IN.  
L = 1.00 IN.  
C = 5.00 MILS  
TRSMAX = 0.38  
S = 1.067  
SS = 0.267  
X(T=0)=0.01

WT = 0.00  
W = 50 LB.  
MU<sub>5</sub> = 1.000 REYNS  
FMAX = 18.9 LB. AND  
OCCURS AT 25.00 CYCLE  
WS = 1.51  
ES = 0.306



6.17 Journal Orbit of a Balanced Vertical Rotor with Small Initial Displacement for 25 Cycles (N = 4000)



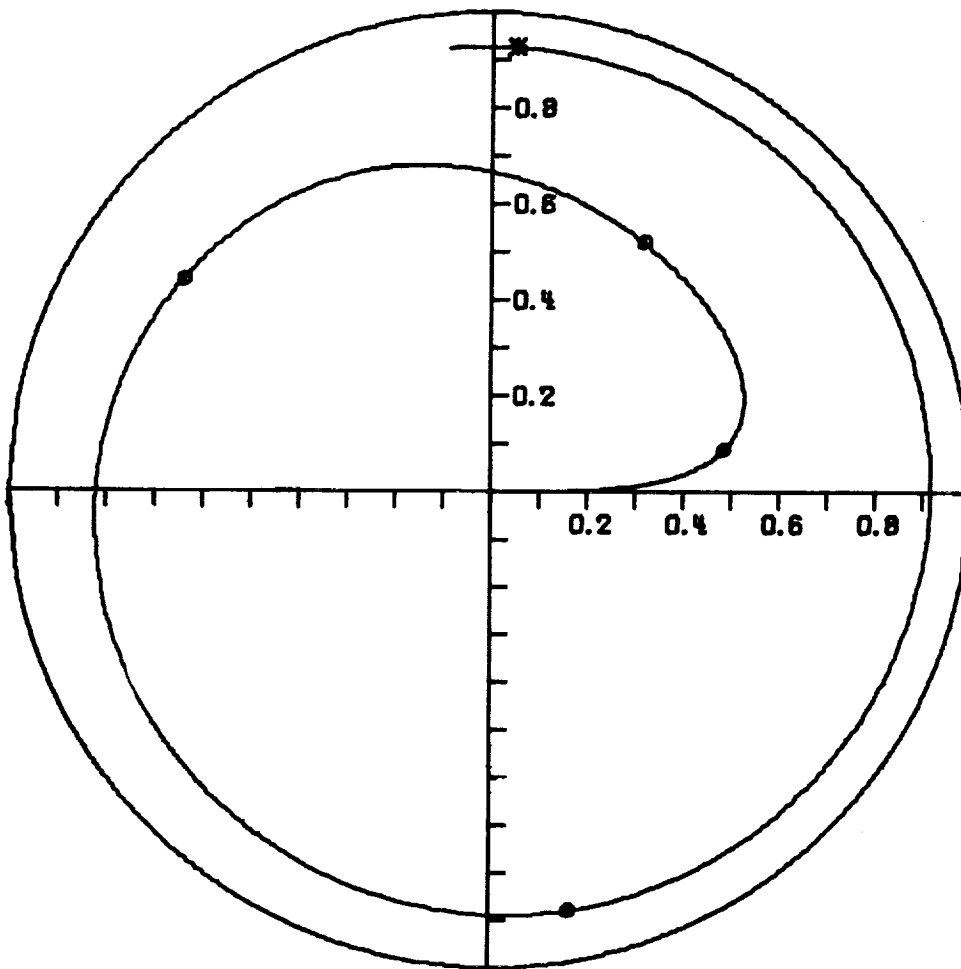
6.18 Radius of Curvature and Whirl vs Cycles of Motion for Cycles 20 - 25 (N = 4000)

# VERTICAL BALANCED ROTOR

NO.111189

N = 6500 RPM  
R = 1.00 IN.  
L = 1.00 IN.  
C = 5.00 MILS  
TRSMAX = 1.39  
S = 0.048  
SS = 0.012  
 $\dot{X}(T=0) = 0.1$

WT = 0.00  
W = 1800 LB.  
MU<sub>5</sub> = 1.000 REYNS  
FMAX = 2493.0 LB. AND  
OCCURS AT 4.96 CYCLE  
WS = 2.45  
ES = 0.814



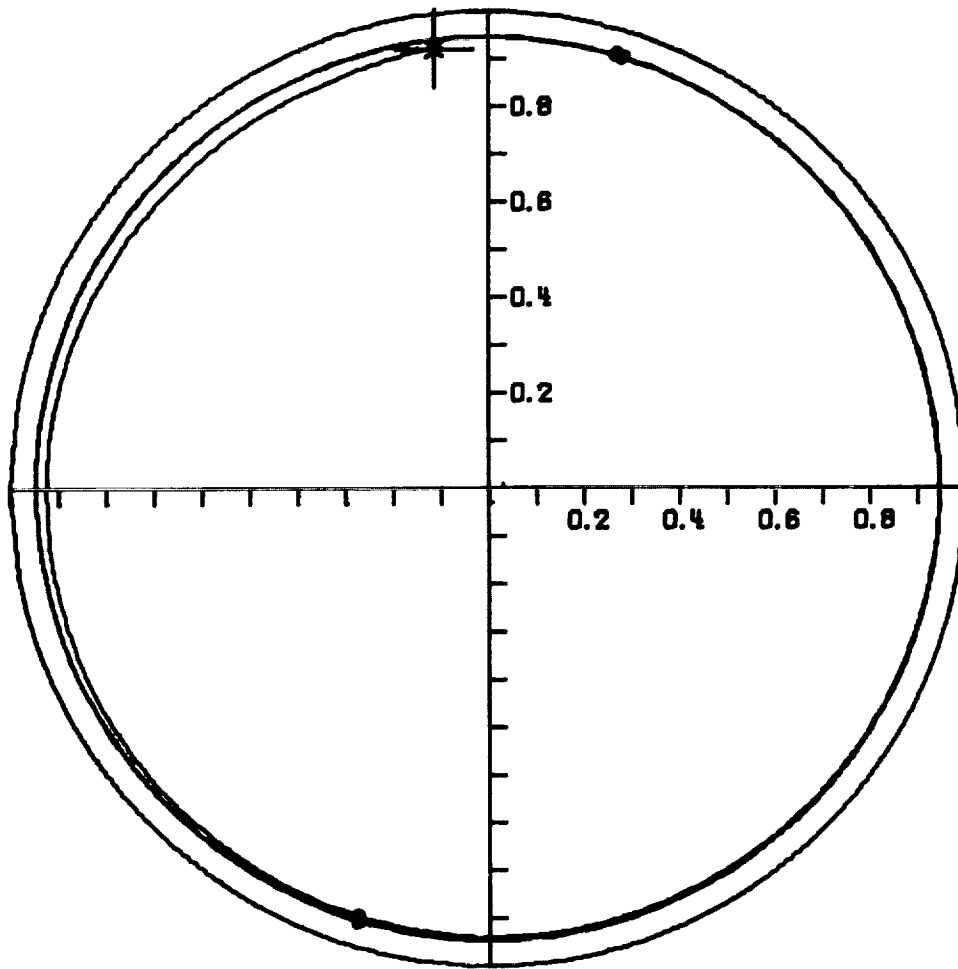
6.19 Journal Orbit of a Balanced Vertical Rotor with Small Initial Velocity for 5 Cycles (N = 6500, W = 1800, C = 0.005, L/D = 1/2)

# VERTICAL BALANCED ROTOR

NO.111183

N = 10500 RPM  
A = 1.00 IN.  
L = 1.00 IN.  
C = 5.00 MILS  
TASMAX = 5.33  
S = 0.078  
SS = 0.019

WT = 0.00  
W = ~~1800~~ LB.  
MU<sub>5</sub> = 1.000 REYNS  
FMAX = 9598.1 LB. AND  
OCCURS AT 5.01 CYCLE  
WS = 3.96  
ES = 0.766



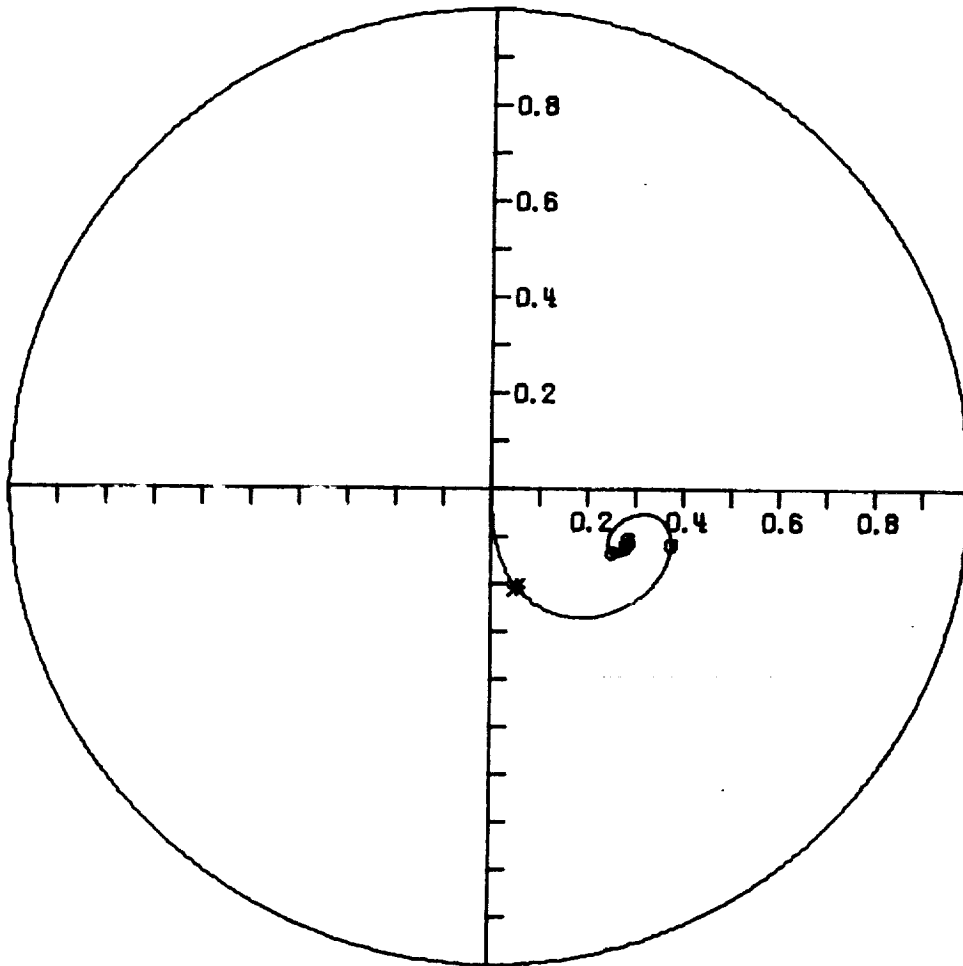
6.20 Journal Orbit of a Balanced Vertical Rotor for Cycles 5 -10  
(N = 10,500, W = 1800, C = 0.005, L/D = 1/2)

# VERTICAL BALANCED ROTOR

NO. 41592

N = 4000 RPM  
R = 1.00 IN.  
L = 1.00 IN.  
C = 5.00 MILS  
TRSMAX = 1.18  
S = 1.067  
SS = 0.267  
FOCY = -50 LB.

WT = 1.00  
W = 50 LB.  
MU<sub>5</sub> = 1.000 REYNS  
FMAX = 58.9 LB. AND  
OCCURS AT 0.28 CYCLE  
WS = 1.51  
ES = 0.306



6.21 Journal Orbit of a Balanced Vertical Rotor with Constant Load (N = 4000, W = 50, C = 0.005, L/D = 1/2, FOCY = -50)

bearing surfaces are being loaded as a result of the journal whirling. The value of TR had leveled off at a constant value of 0.38 as indicated by the plot of that quantity (not included in this report).

The next two plots (Figures 6.19 and 6.20) are for the 1800 pound journal that was found to be stable in the horizontal position. As indicated by these present plots for the vertical journal, the violent half-frequency whirl has developed a static transmissibility, TRS, equal to 5.33, (i.e. FMAX = 9598.1 pounds). The whirling was initiated by an initial velocity as indicated by Figure 6.19.

The stability plot given by Figure 6.14 indicates that the vertical journal can be stabilized by adding an external force. With the addition of a 50 pound force directed along the negative y-direction (perpendicular to axial coordinate), Figure 6.21 indicates that the system is very stable and furthermore, the resulting transient orbit is identical to an unloaded 50 pound horizontal rotor operating at the same speed (See Figure 6.1 for comparison).

The sample cases presented in this section have supported the stability maps as presented in Figures 6.14 and 6.15. This concludes the discussion of balanced journals and any future reference to stability will refer to the plot of Figure 6.14 or 6.15 as being the appropriate stability boundaries.

#### 6.4 Effect of Unbalance on Journal Bearing Performance

##### 6.4.1 The Vertical Journal Bearing

The discussion thus far has been restricted to balanced journals. This section is devoted entirely to the effect of unbalance as indicated

by the section heading. In view of the fact that all journals or rotor systems have some residual unbalance, the effect of unbalance on bearing performance is of great importance to the manufacturers of such units. This is especially true when the company must guarantee the reliability of the units to the buyers and give compensation for lost production due to "downtime" when the unit does not function as specified in the guarantee.

The following journal orbits should help clarify the effect that unbalance has on a vertical system. Figure 6.22 shows the initial transient motion of the 50 pound vertical journal with an effective unbalance of 0.20 (i.e.  $EMU = e_{\mu} = 0.2 \times c$ ) or an unbalance load of 5.68 pounds at the given shaft speed of 2000 rpm. Notice there is a small half frequency whirl component present which appears to diminish in time. The speed parameter for the vertical rotors is calculated as  $\omega_s$  and not as  $\Omega_s$ . The value of the unbalance Sommerfeld number,  $S_{\mu}$ , gives an eccentricity of 0.085 and indicates that the steady-state orbit radius, based on the rotating load value of  $F_u = 5.68$  pounds, should be 0.085. Figure 6.23 gives the journal motion for five more shaft revolutions. The inner loop continues to increase in size as the outer loop reduces indicating that the nonsynchronous component is damping out. Notice that the orbit is approaching the calculated steady-state orbit radius.

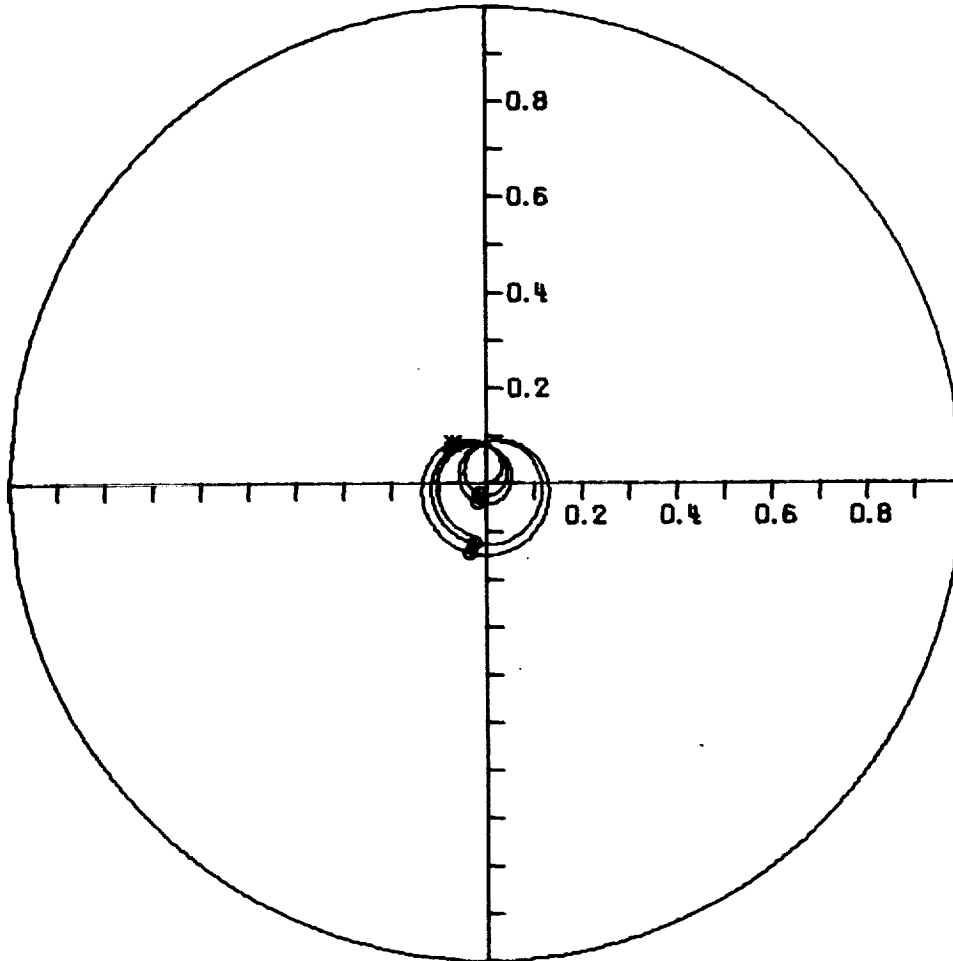
An increase of journal speed to 4000 rpm results in the larger transient motion of Figure 6.24. The same behavior of the inner and outer loops converging is also observed in this figure. Figure 6.25 confirms that the instantaneous radius of curvature is converging

# VERTICAL UNBALANCED ROTOR

NO. 41593

N = 2000 RPM  
R = 1.00 IN.  
L = 1.00 IN.  
C = 5.00 MILS  
TRSMAX = 0.12  
S = 0.533  
SS = 0.133  
EMU = 0.20  
SU = 4.698  
TRDMAX = 1.08

WT = 0.00  
W = 50 LB.  
MUS = 1.000 REYNS  
FMAX = 6.1 LB. AND  
OCCURS AT 0.53 CYCLE  
WS = 0.75  
ES = 0.453  
FU = 5.68 LB.  
FURATIO = 0.11  
ESU = 0.085



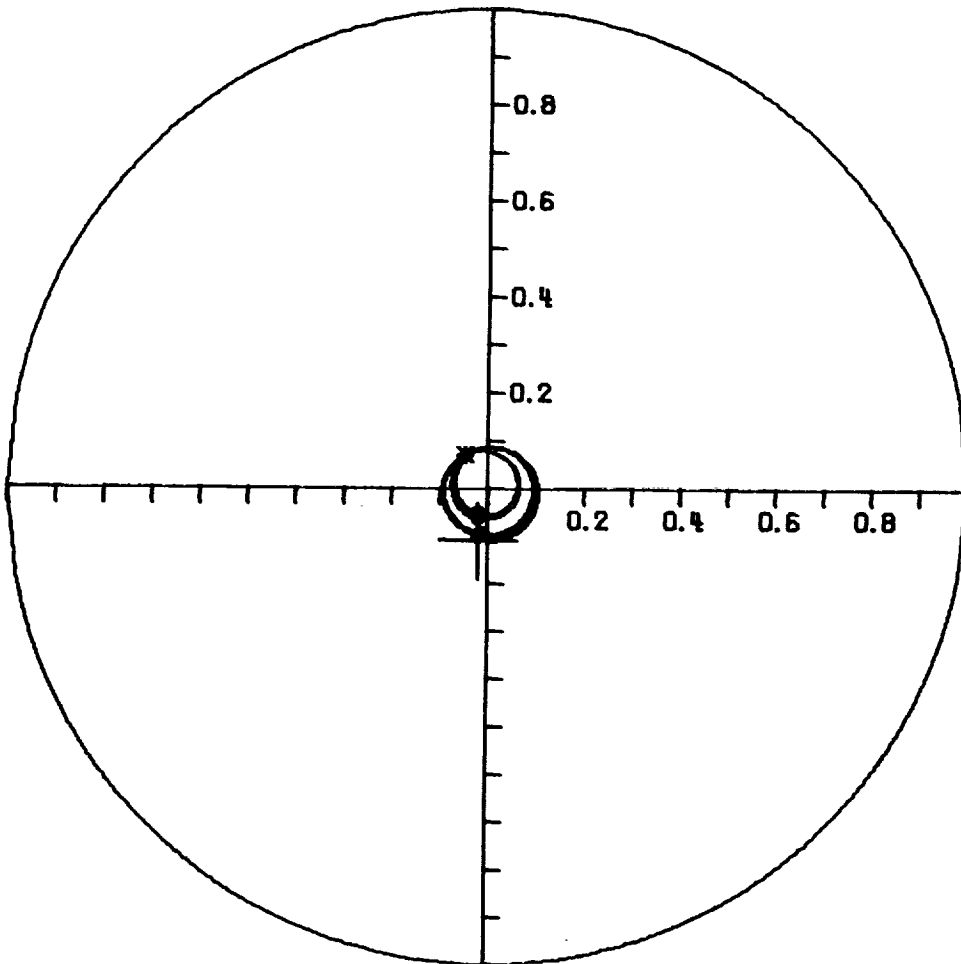
6.22 Journal Orbit of an Unbalanced Vertical Rotor for 5 Cycles  
(N = 2000, W = 50, C = 0.005, L/D = 1/2, EMU = 0.2)

# VERTICAL UNBALANCED ROTOR

NO. 41593

N = 2000 RPM  
R = 1.00 IN.  
L = 1.00 IN.  
C = 5.00 MILS  
TRSMAX = 0.11  
S = 0.533  
SS = 0.133  
EMU = 0.20  
SU = 4.698  
TRDMAX = 1.01

WT = 0.00  
W = 50 LB.  
MUS = 1.000 REYNS  
FMAX = 5.7 LB. AND  
OCCURS AT 6.59 CYCLE  
WS = 0.75  
ES = 0.453  
FU = 5.68 LB.  
FURATIO = 0.11  
ESU = 0.085



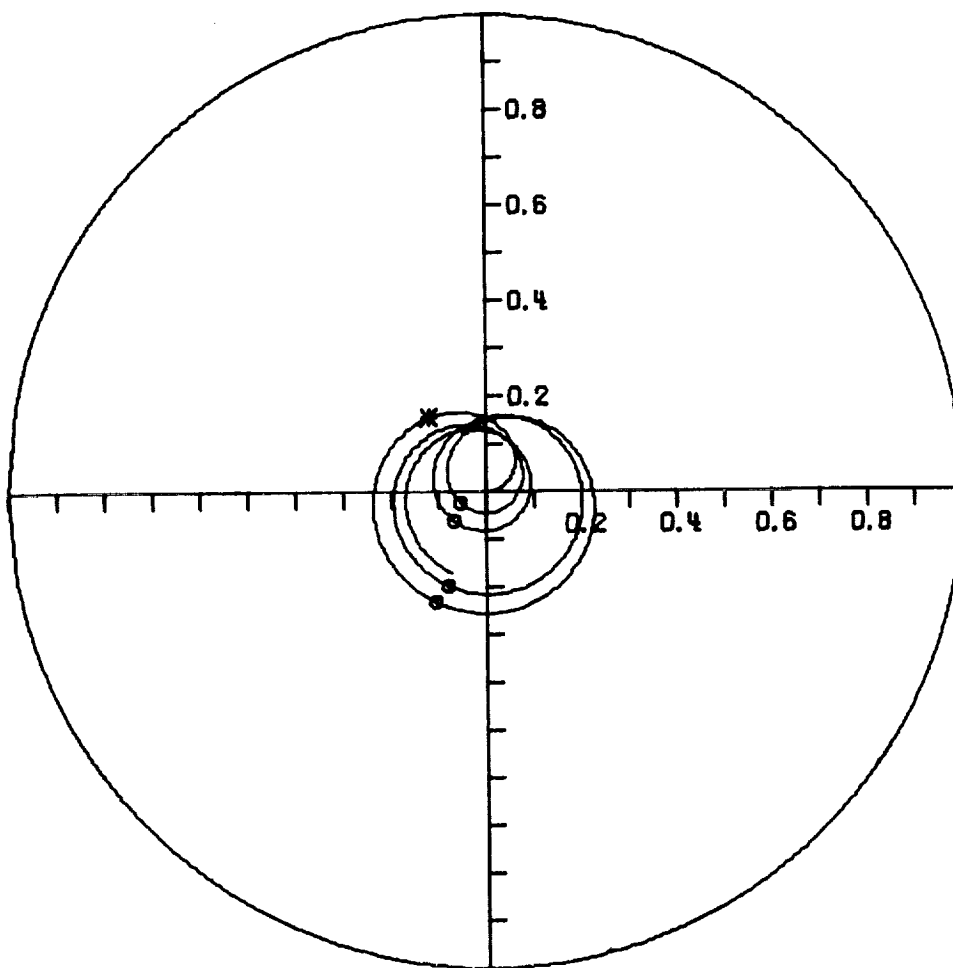
6.23 Journal Orbit of an Unbalanced Vertical Rotor for Cycles  
5 - 10 (N = 2000, W = 50, C = 0.005, L/D = 1/2, EMU = 0.2)

# VERTICAL UNBALANCED ROTOR

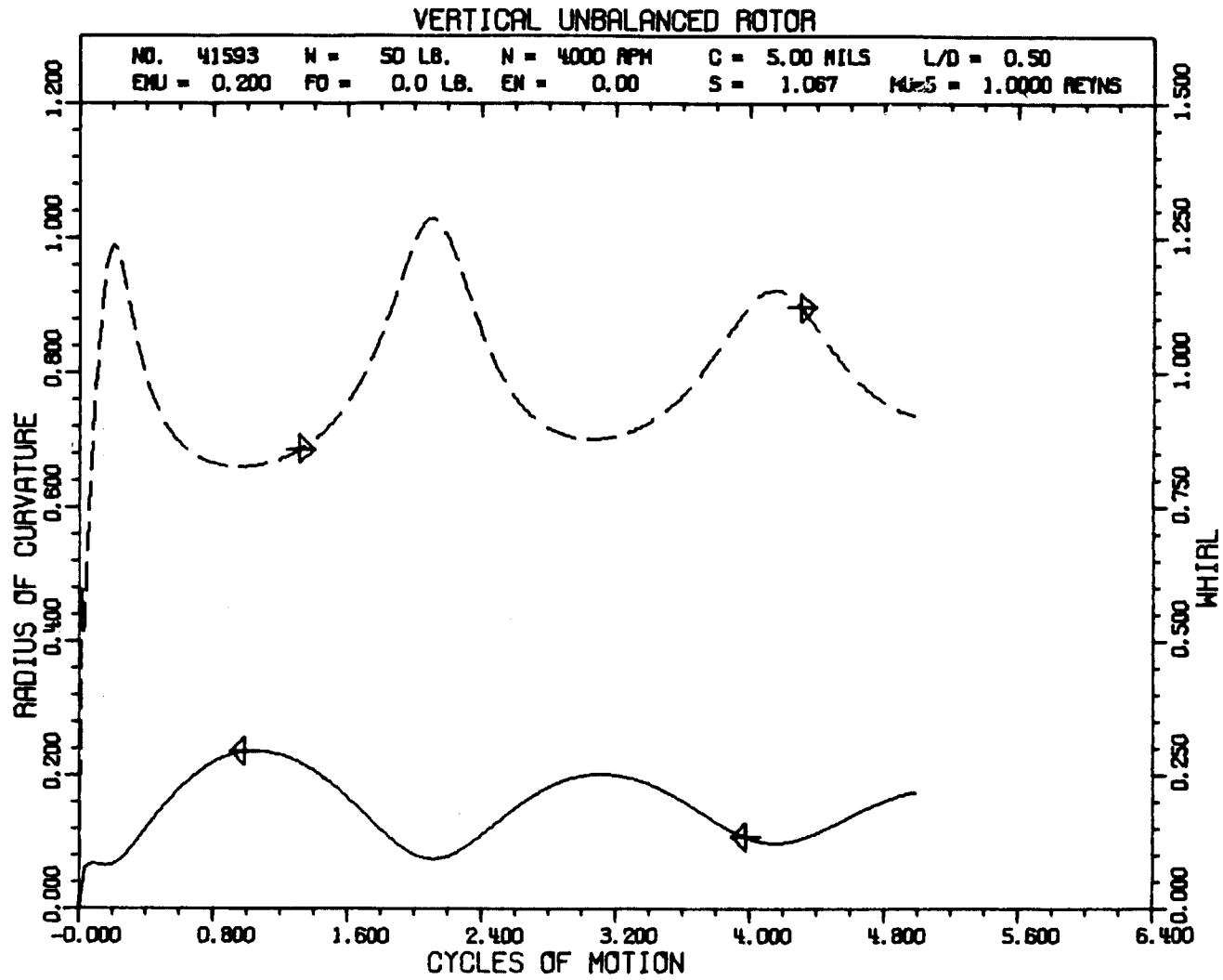
NO. 41593

N = 4000 RPM  
R = 1.00 IN.  
L = 1.00 IN.  
C = 5.00 MILS  
TRSMAX = 0.50  
S = 1.067  
SS = 0.267  
EMU = 0.20  
SU = 2.349  
TRDMAX = 1.10

WT = 0.00  
W = 50 LB.  
MU<sub>5</sub> = 1.000 REYNS  
FMAX = 25.1 LB. AND  
OCCURS AT 0.56 CYCLE  
WS = 1.51  
ES = 0.306  
FU = 22.70 LB.  
FURATIO = 0.45  
ESU = 0.163



6.24 Journal Orbit of an Unbalanced Vertical Rotor for 5 Cycles  
(N = 4000, W = 50, C = 0.005, L/D = 1/2, EMU = 0.2)



6.25 Radius of Curvature and Whirl vs Cycles of Motion  
(N = 4000, EMU = 0.2)

toward the calculated value of  $ESU = 0.163$  as given in Figure 6.24. The whirl is oscillating about the value of one, with the oscillation becoming smaller as the motion continues. Figure 6.26a shows five more cycles of motion, the initial conditions corresponding to the final values of Figure 6.24. The value of  $TRD_{MAX}$  is 0.94 which indicates that the bearing force is less than the unbalance loading, a very desirable mode of operation.

Gunter (7)\* explained that an orbit such as Figure 6.24 is composed of a synchronous and a nonsynchronous component and as the inner loop approaches the outer one the nonsynchronous component is reducing and approaches zero as the orbits coincide. In the same discussion, Gunter notes that the expression "half-frequency whirl" has been given to this type orbit since two vectors, one rotating at  $\omega$ , the other at  $\frac{1}{2}\omega$  and placed head to tail will trace out the pattern as indicated in the orbit of Figure 6.22 or 6.24. This effect is shown for different magnitudes of the two vectors in Figure 6.26b.

It might seem reasonable to assume that the amount of unbalance in the journal could be made very small and produce a very small synchronous limit cycle. Figure 6.27 indicates that this assumption is false. The resulting journal center orbit is growing and should reach the same limit cycle as the perfectly balanced journal (See Fig. 6.17). Figure 6.28 shows the increased rate of growth with the same unbalance of 0.01 but at the higher speed of 10,500 rpm. The high value of  $TRD_{MAX} = 19$  in this orbit and the previous value of 10

---

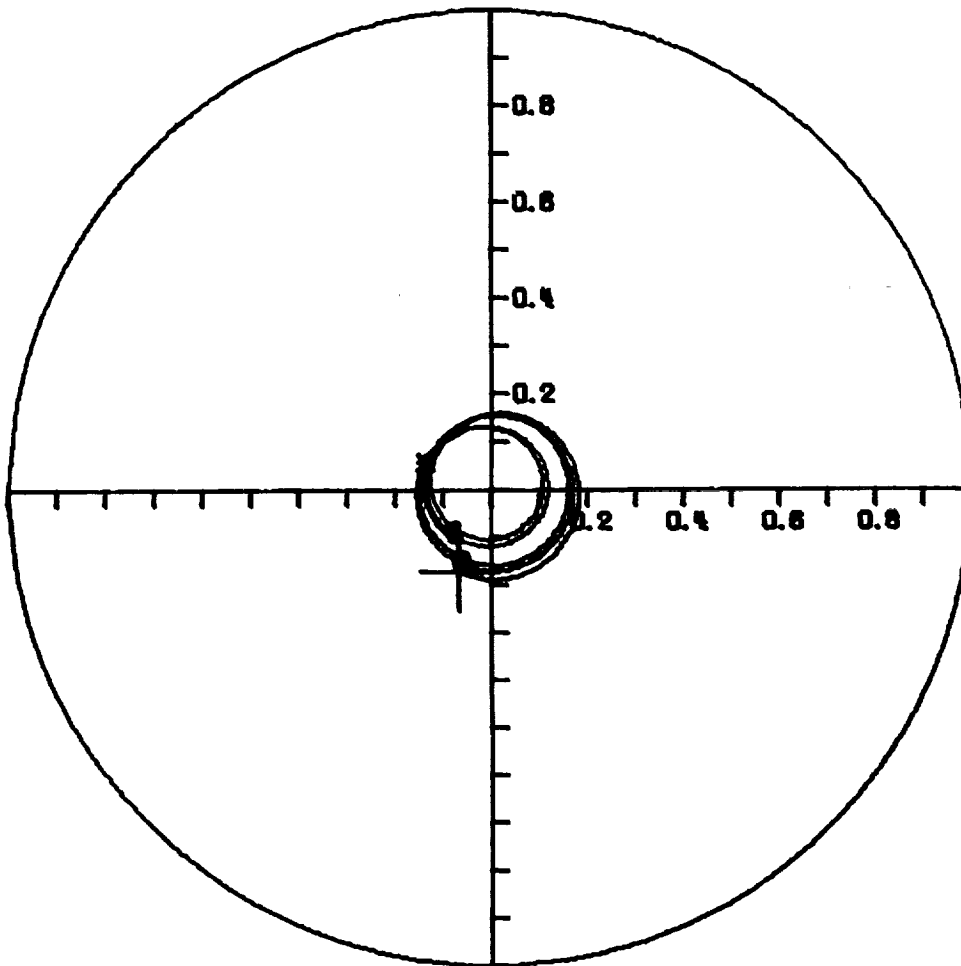
\*Reference in Bibliography, pp. 133-140.

# VERTICAL UNBALANCED ROTOR

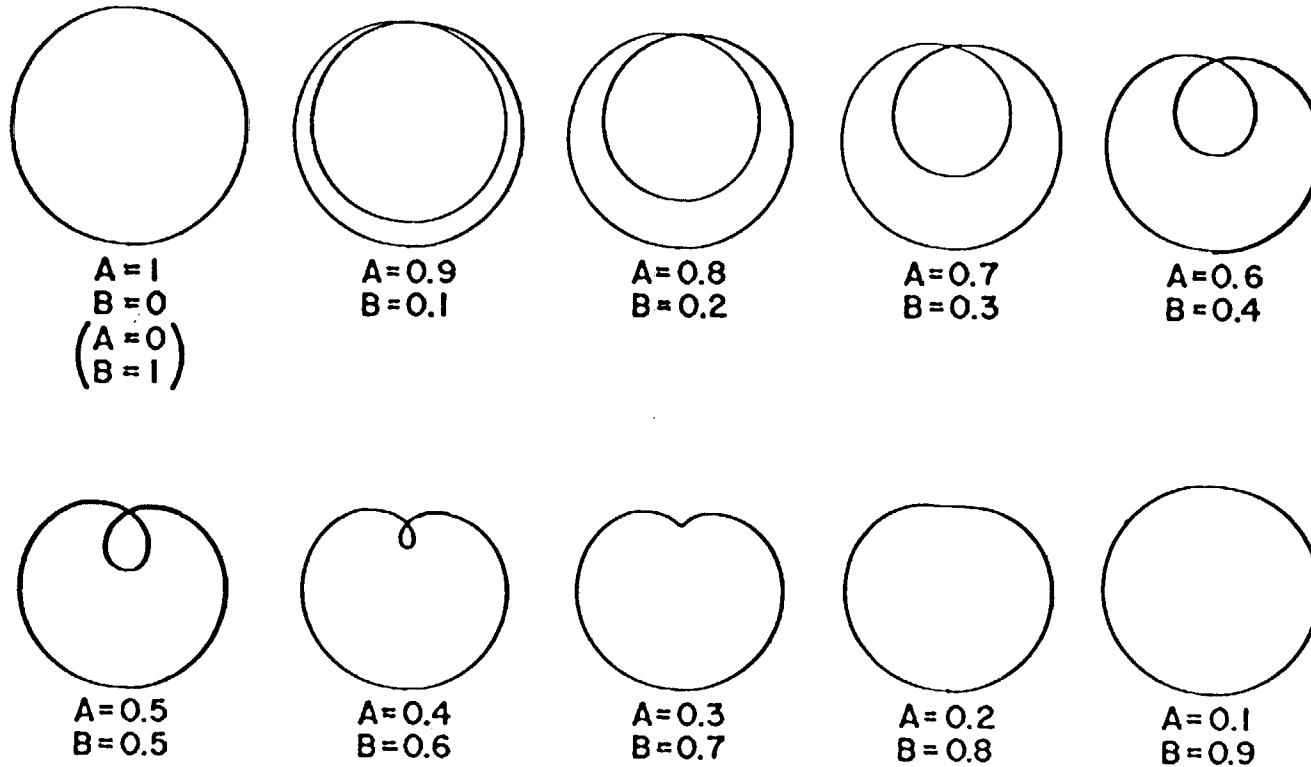
NO. 41983

N = 4000 RPM  
R = 1.00 IN.  
L = 1.00 IN.  
C = 5.00 MILS  
TRSMAX = 0.43  
S = 1.067  
SS = 0.267  
EMU = 0.20  
SU = 2.349  
TRDMAX = 0.94

WT = 0.00  
W = 50 LB.  
MUS = 1.000 REYNS  
FMAX = 21.4 LB. AND  
OCCURS AT 6.74 CYCLE  
WS = 1.51  
ES = 0.306  
FU = 22.70 LB.  
FURATIO = 0.45  
ESU = 0.163

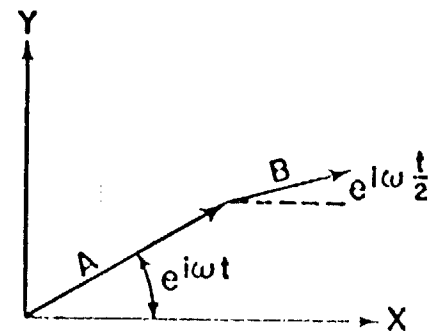


6.26 a. Journal Orbit of an Unbalanced Vertical Rotor for Cycles 5 - 10 (N = 4000, EMU = 0.2)



A = MAGNITUDE OF SYNCHRONOUS WHIRL COMPONENT

B = MAGNITUDE OF HALF-FREQUENCY WHIRL COMPONENT



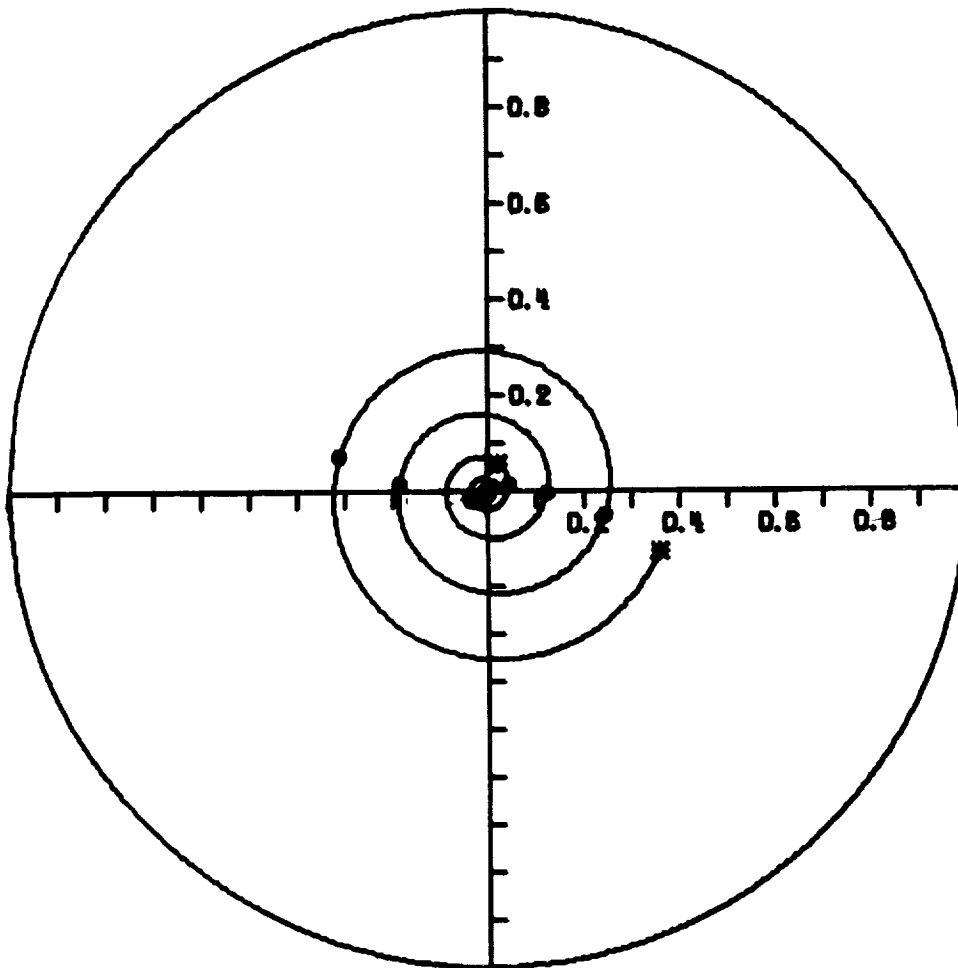
6.26 b. Analog Computer Traces of Various Combinations of Synchronous and Half-Frequency Whirl

# VERTICAL UNBALANCED ROTOR

NO. 5291

N = 4000 RPM  
R = 1.00 IN.  
L = 1.00 IN.  
C = 5.00 MILS  
TRSMAX = 0.24  
S = 1.067  
SS = 0.267  
EMU = 0.01  
SU = 46.981  
TADMAX = 10.38

WT = 0.00  
W = 50 LB.  
MU<sub>5</sub> = 1.000 REYNS  
FMAX = 11.8 LB. AND  
OCCURS AT 10.00 CYCLE  
WS = 1.51  
ES = 0.306  
FU = 1.14 LB.  
FURATIO = 0.02  
ESU = 0.009



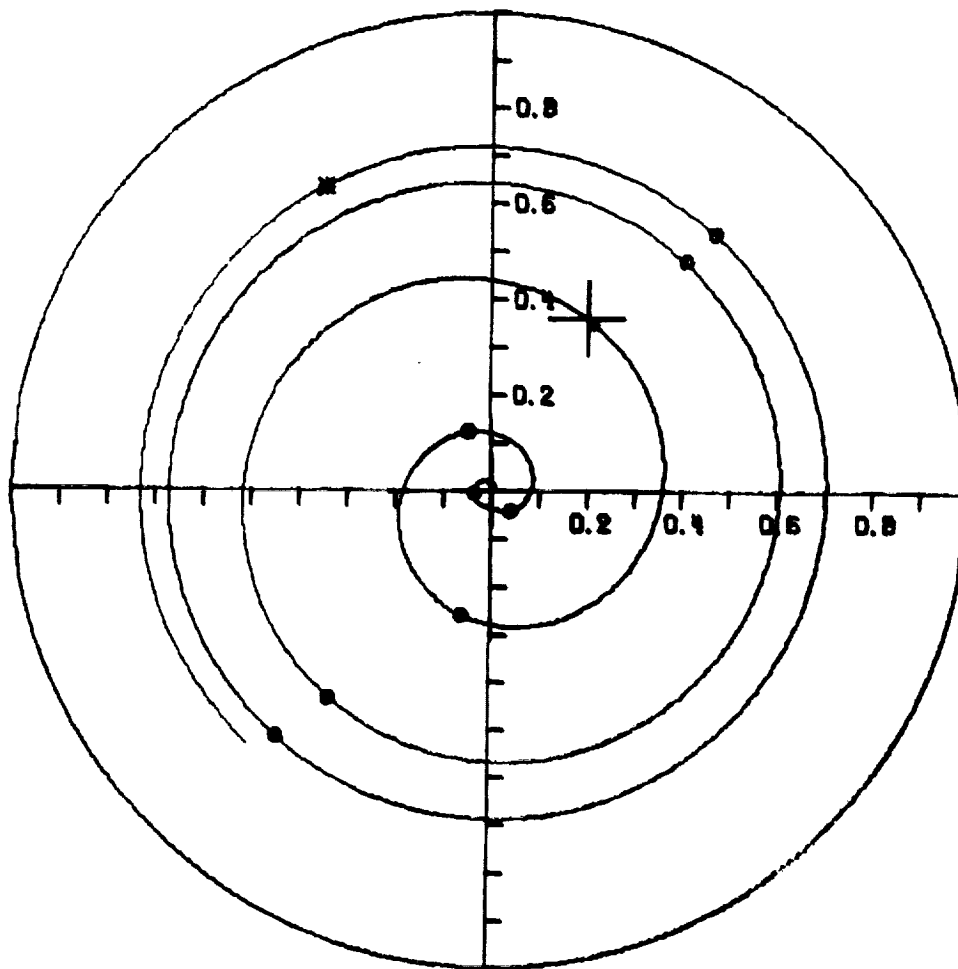
6.27 Journal Orbit of a Slightly Unbalanced Vertical Rotor  
for 10 Cycles (N = 4000, EMU = 0.01)

# VERTICAL UNBALANCED ROTOR

NO. 5291

N = 10500 RPM  
R = 1.00 IN.  
L = 1.00 IN.  
C = 5.00 MILS  
TRSMAX = 2.98  
S = 2.800  
SS = 0.700  
EMU = 0.01  
SU = 17.897  
TADMAL = 19.02

WT = 0.00  
W = 50 LB.  
MUS = 1.000 REYNS  
FMAX = 148.8 LB. AND  
OCCURS AT 9.40 CYCLE  
WS = 3.96  
ES = 0.139  
FU = 7.82 LB.  
FURATIO = 0.16  
ESU = 0.023



6.28 Journal Orbit of a Slightly Unbalanced Vertical Rotor for 10 Cycles (N = 10,500, EMU = 0.01)

indicate that this is a very undesirable mode of operation.

The stability speed parameter of Figure 6.15 for a horizontal rotor under constant loading is given by the following relation:

$$\Omega_s = \omega_j \sqrt{\frac{mc}{W_T}} \quad [6.1]$$

This parameter may be used to approximate the stability characteristics of the vertical rotor with unbalance by assuming that the constant load  $W_T$  may be replaced by the rotating load component:

$$W_T = m e_{\mu} \omega_j^2 \quad [6.2]$$

Therefore, an approximate stability parameter for the unbalance vertical rotor is:

$$\Omega_s = \sqrt{c/e_{\mu}} = \sqrt{\frac{1}{(EMU)}} < 2.5 \quad [6.3]$$

for stability.

The above appears to be a necessary but not sufficient condition for complete stability. For example in Figure 6.24  $EMU = 0.2$  and the speed parameter from Eq. 6.3 is 2.236 which lies in the stable region of Figure 6.15. In Figure 6.27  $EMU = 0.01$  for which the speed parameter is 10.0 and well into the unstable region of the stability map. For  $EMU = 0.1$  the speed parameter is 3.16 which is just above the threshold. In Figure 6.29 where  $EMU = 0.1$ , 10 cycles of the initial transient motion are shown which confirms the predicted instability. The threshold speed has a value of 2.5, therefore the critical unbalance value is given as:

$$EMU_{CR} = \frac{1}{(2.5)^2} = 0.16 \quad [6.4]$$

Figure 6.30 shows the initial transient orbit of the 50 pound journal with EMU equal to 0.14, just past the threshold or just below the critical value of unbalance. Figure 6.31 verifies that the system is in the unstable region since the orbit is increasing in size and the value of TRDMAX has increased to 1.13.

Figures 6.32 and 6.33 are for the critical value of unbalance, EMU = 0.16. The orbit is decreasing in size and the value of TRDMAX has reduced from 1.09 in Figure 6.32 to 1.03 in Figure 6.33.

The behavior of the journal according to the level of unbalance can be predicted from the stability map (Figure 6.15), but it is obvious that as the speed increases, the size of the resulting limit cycle will increase. Figures 6.34 - 6.39 demonstrate the effect of increasing the speed for a given unbalance level of 0.2. Figure 6.34 gives the initial transient at the speed of 6500 rpm. The size of the initial orbit has increased and the predicted steady-state orbit would have a radius (dim.) of 0.244. The inner loops are precessing counter-clockwise as have all the orbits having EMU > 0.16. Gunter (7)\* indicates that this is caused by the nonsynchronous component of motion having a frequency of less than one-half running speed. Figure 6.35 is a continuation of the orbit of Figure 6.34 and has the TRDMAX reduced to 0.91.

For a journal speed of 10,500 rpm as shown in Figure 6.36, the resulting transient orbit is similar to the case of Figure 6.29 for which the orbit was unstable. The orbit is getting larger and the

---

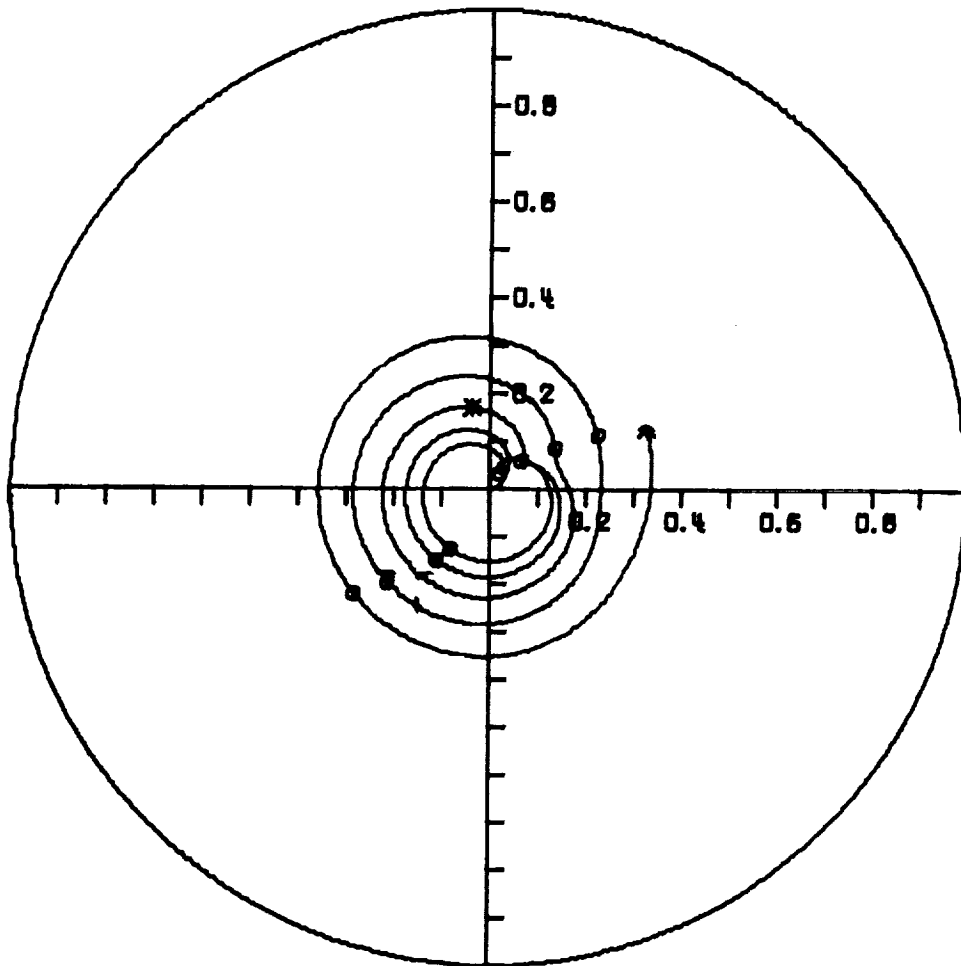
\*Reference in Bibliography, p. 134.

# VERTICAL UNBALANCED ROTOR

NO. 41593

N = 4000 RPM  
R = 1.00 IN.  
L = 1.00 IN.  
C = 5.00 MILS  
TRSMAX = 0.29  
S = 1.067  
SS = 0.267  
EMU = 0.10  
SU = 4.698  
TRDMAX = 1.29

WT = 0.00  
W = 50 LB.  
MUS = 1.000 REYNS  
FMAX = 19.7 LB. AND  
OCCURS AT 10.08 CYCLE  
WS = 1.51  
ES = 0.306  
FU = 11.35 LB.  
FURATIO = 0.23  
ESU = 0.085



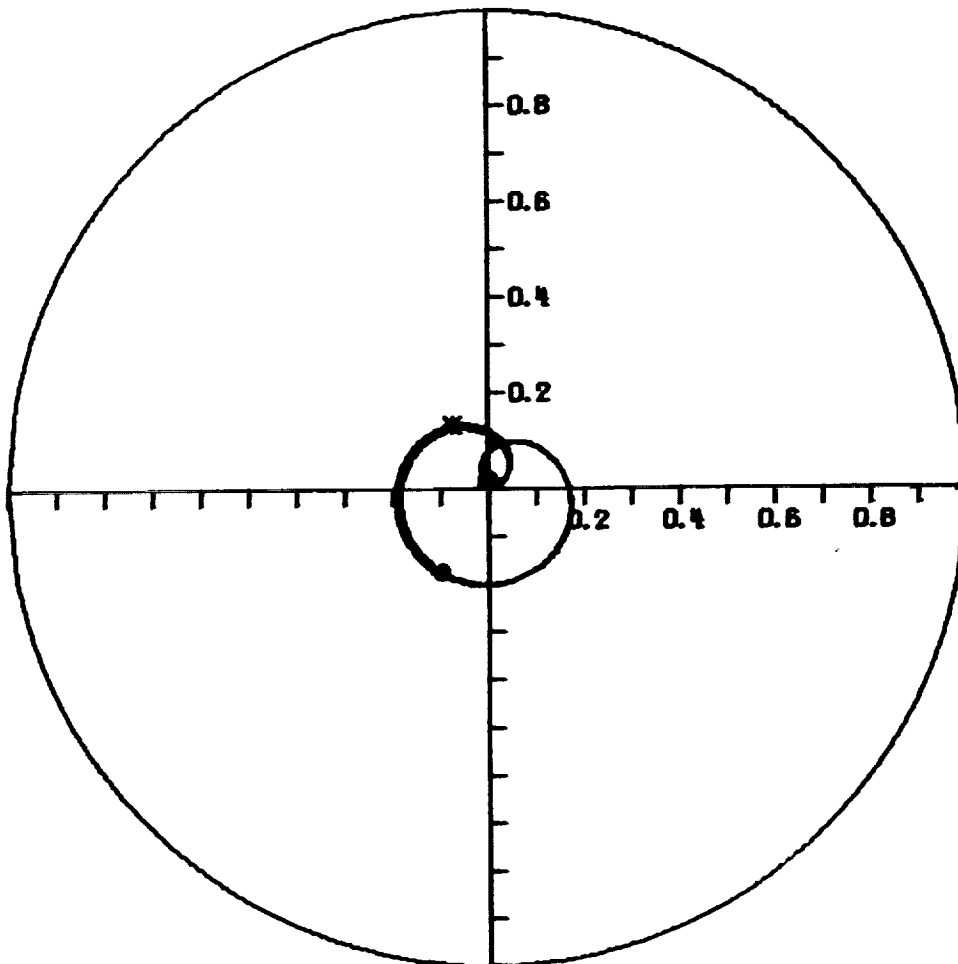
6.29 Journal Orbit of an Unbalanced Vertical Rotor for 10 Cycles  
(N = 4000, EMU = 0.10)

# VERTICAL UNBALANCED ROTOR

NO. 41583

N = 4000 RPM  
R = 1.00 IN.  
L = 1.00 IN.  
C = 5.00 MILS  
TRSMAX = 0.35  
S = 1.067  
SS = 0.267  
EMU = 0.14  
SU = 3.356  
TRDMAX = 1.10

WT = 0.00  
W = 50 LB.  
MUS = 1.000 REYNS  
FMAX = 17.5 LB. AND  
OCCURS AT 4.53 CYCLE  
WS = 1.51  
ES = 0.306  
FU = 15.89 LB.  
FURATIO = 0.32  
ESU = 0.117



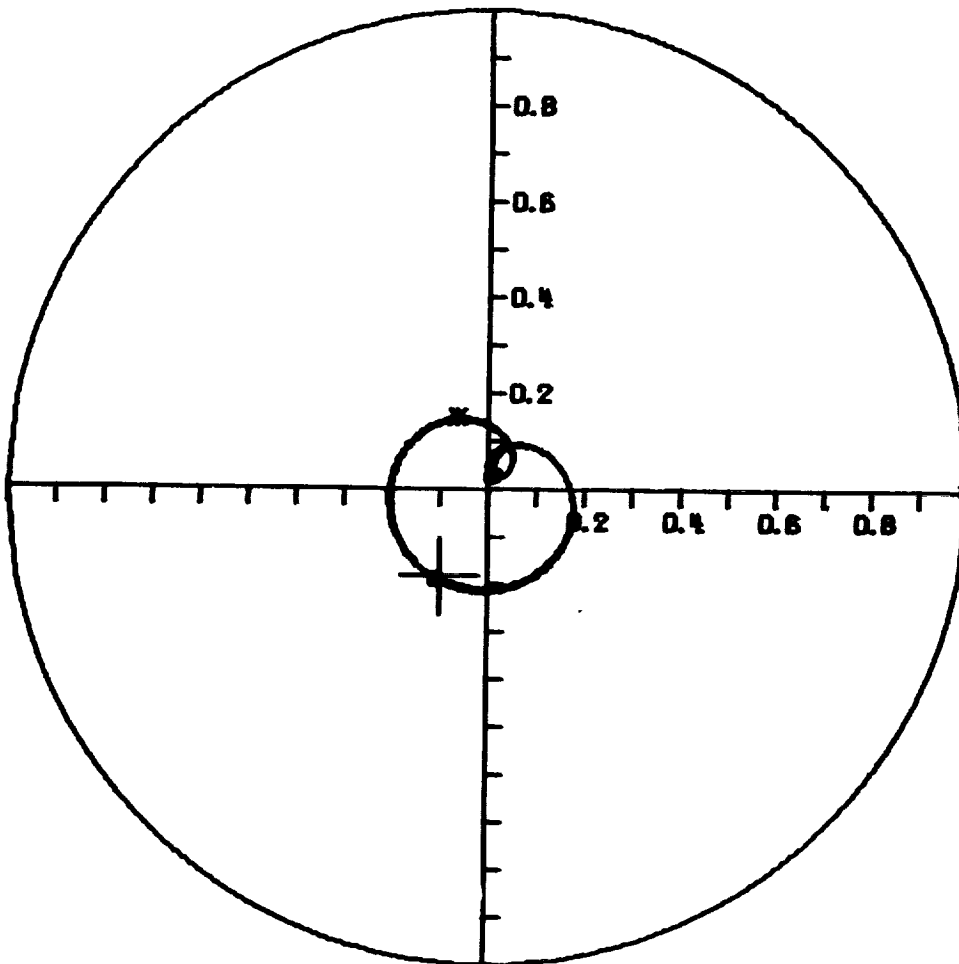
6.30 Journal Orbit of an Unbalanced Vertical Rotor for 5 Cycles  
(N = 4000, EMU = 0.14)

# VERTICAL UNBALANCED ROTOR

NO. 41589

N = 4000 RPM  
R = 1.00 IN.  
L = 1.00 IN.  
C = 5.00 MILS  
TRSMAX = 0.36  
S = 1.067  
SS = 0.267  
EMU = 0.14  
SU = 3.356  
TRDMAX = 1.13

WT = 0.00  
W = 50 LB.  
MU5 = 1.000 REYNS  
FMAX = 17.9 LB. AND  
OCCURS AT 8.50 CYCLE  
WS = 1.51  
ES = 0.306  
FU = 15.89 LB.  
FURATIO = 0.32  
ESU = 0.117



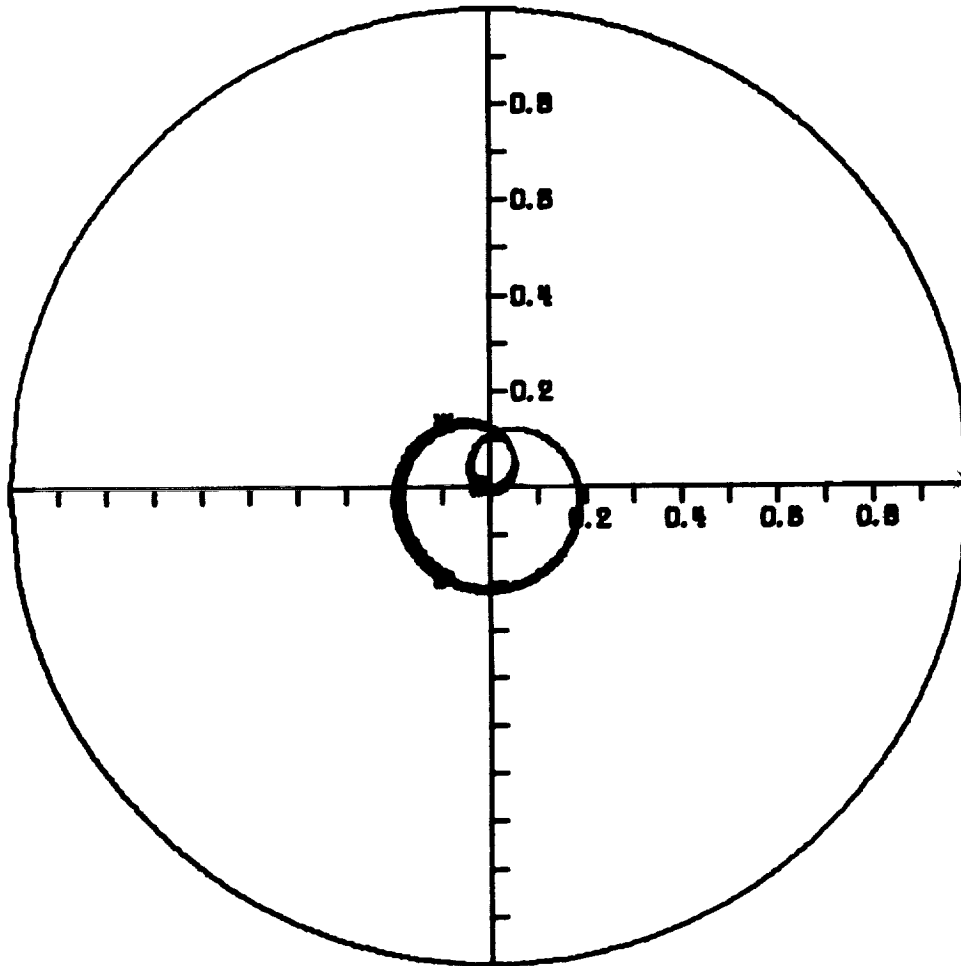
6.31 Journal Orbit of an Unbalanced Vertical Rotor for Cycles  
5 - 10 (N = 4000, EMU = 0.14)

# VERTICAL UNBALANCED ROTOR

NO. 41989

N = 4000 RPM  
R = 1.00 IN.  
L = 1.00 IN.  
C = 5.00 MILS  
TASMAX = 0.39  
S = 1.067  
SS = 0.267  
EMU = 0.16  
SU = 2.936  
TRDMAX = 1.09

WT = 0.00  
W = 50 LB.  
MUS = 1.000 REYNS  
FMAX = 19.7 LB. AND  
OCCURS AT 0.56 CYCLE  
WS = 1.51  
ES = 0.306  
FU = 18.16 LB.  
FURATIO = 0.36  
ESU = 0.133



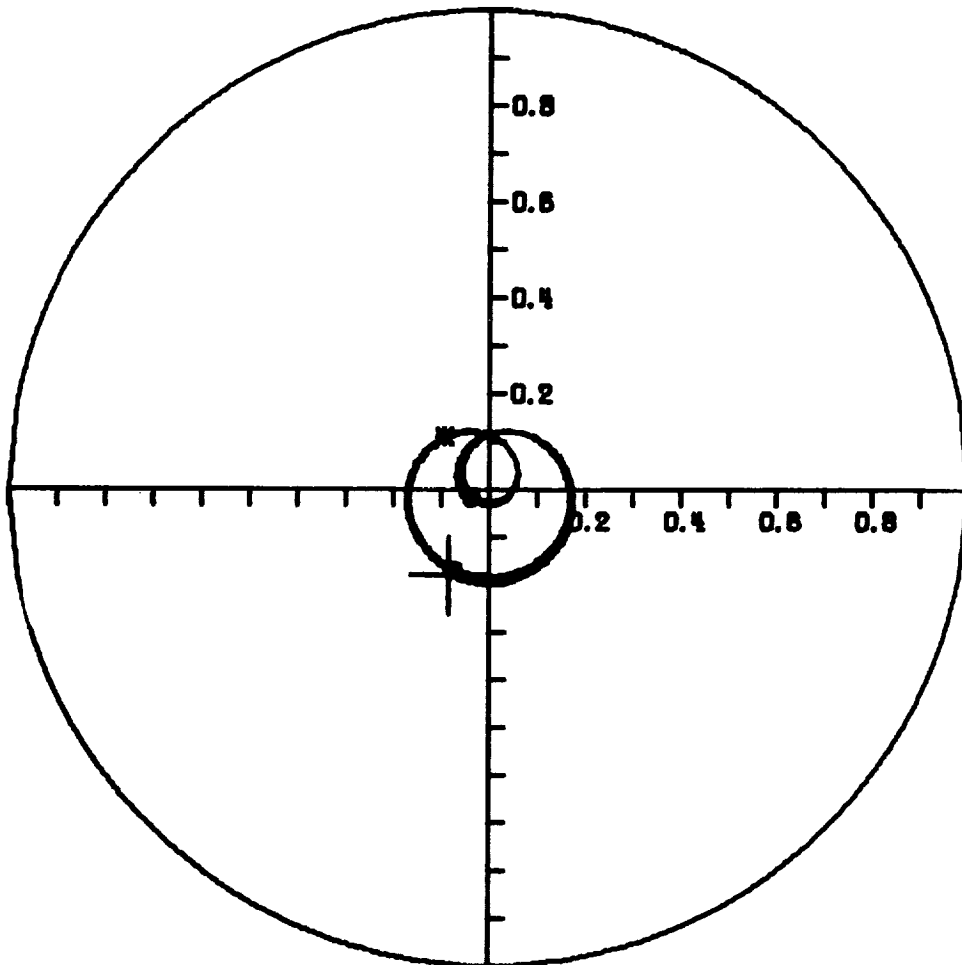
6.32 Journal Orbit of an Unbalanced Vertical Rotor with the Critical Value of Unbalance (N = 4000, EMU = 0.16)

# VERTICAL UNBALANCED ROTOR

NO. 41593

N = 4000 RPM  
R = 1.00 IN.  
L = 1.00 IN.  
C = 5.08 MILS  
TRSMAX = 0.37  
S = 1.067  
SS = 0.267  
EMU = 0.16  
SU = 2.936  
TRDMAX = 1.02

WT = 0.00  
W = 50 LB.  
MUS = 1.000 REYNS  
FMAX = 18.6 LB. AND  
OCCURS AT 6.60 CYCLE  
WS = 1.51  
ES = 0.306  
FU = 18.16 LB.  
FURATIO = 0.36  
ESU = 0.133



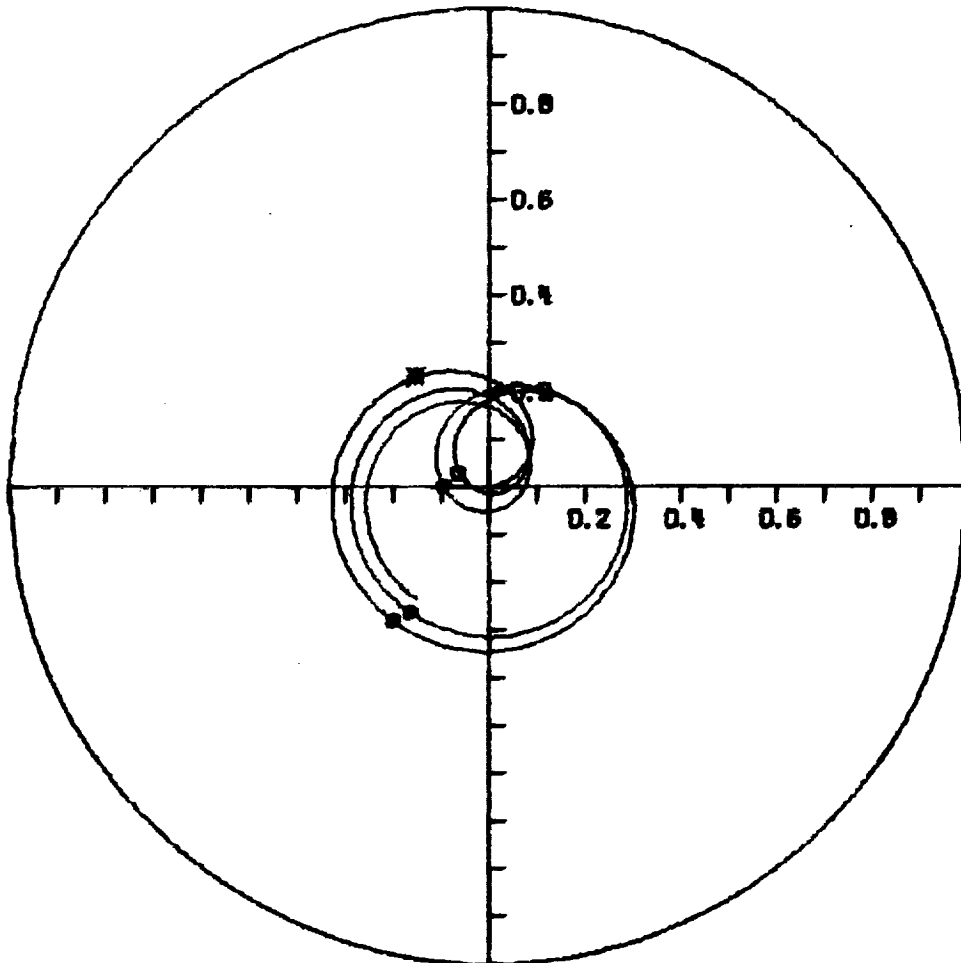
6.33 Journal Orbit of an Unbalanced Vertical Rotor for Cycles 5 - 10 (N = 4000, EMU = 0.16) Illustrating Stable Half-Frequency Whirl

# VERTICAL UNBALANCED ROTOR

NO. 41583

N = 6500 RPM  
R = 1.00 IN.  
L = 1.00 IN.  
C = 5.00 MILS  
TRSMAX = 1.31  
S = 1.733  
SS = 0.433  
EMU = 0.20  
SU = 1.446  
TADMAX = 1.10

WT = 0.00  
W = 50 LB.  
MU<sub>5</sub> = 1.000 REYNS  
FMAX = 65.7 LB. AND  
OCCURS AT 0.58 CYCLE  
WS = 2.45  
ES = 0.211  
FU = 59.95 LB.  
FURATIO = 1.20  
ESU = 0.244



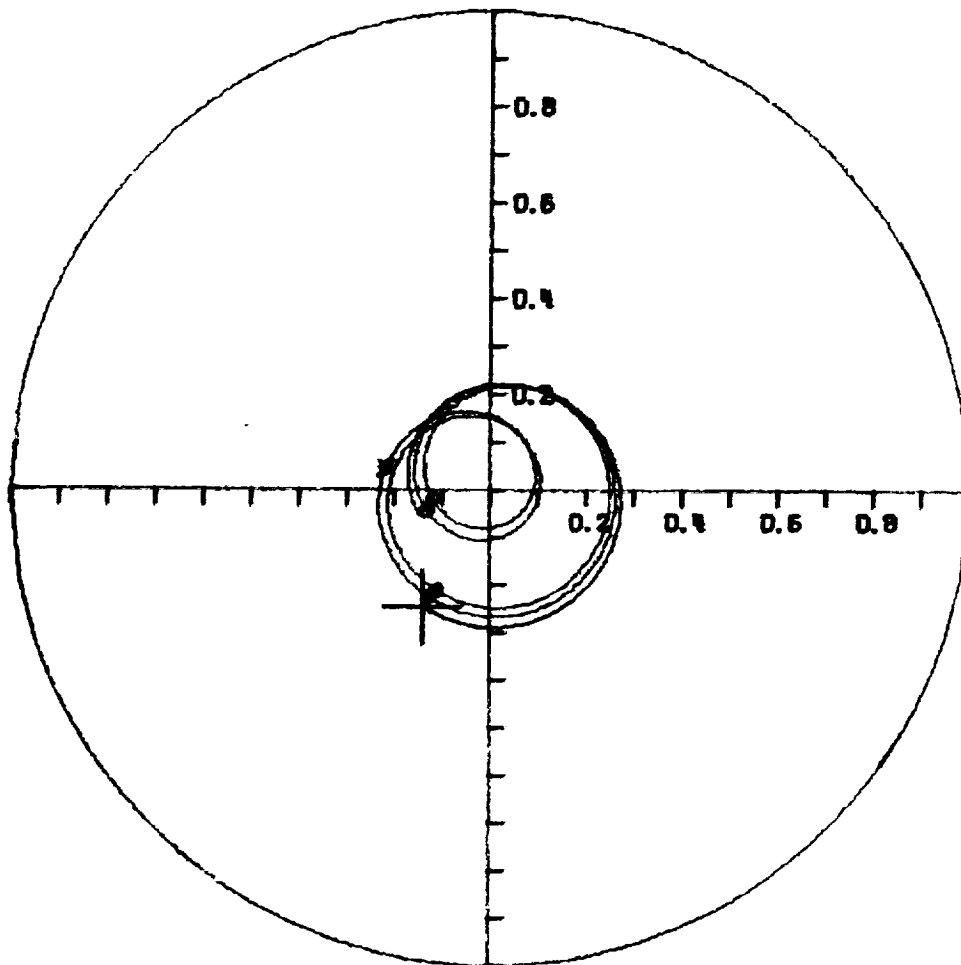
6.34 Journal Orbit of an Unbalanced Vertical Rotor for 5 Cycles  
(N = 6500, EMU = 0.2) with Damped Half-Frequency Whirl

# VERTICAL UNBALANCED ROTOR

NO. 41593

N = 6500 RPM  
R = 1.00 IN.  
L = 1.00 IN.  
C = 5.00 MILS  
TASMAX = 1.09  
S = 1.733  
SS = 0.433  
EMU = 0.20  
SU = 1.446  
TROMAX = 0.91

WT = 0.00  
W = 50 LB.  
MUS = 1.000 REYNS  
FMAX = 54.6 LB. AND  
OCCURS AT 6.76 CYCLE  
WS = 2.45  
ES = 0.211  
FU = 59.95 LB.  
FURATIO = 1.20  
ESU = 0.244



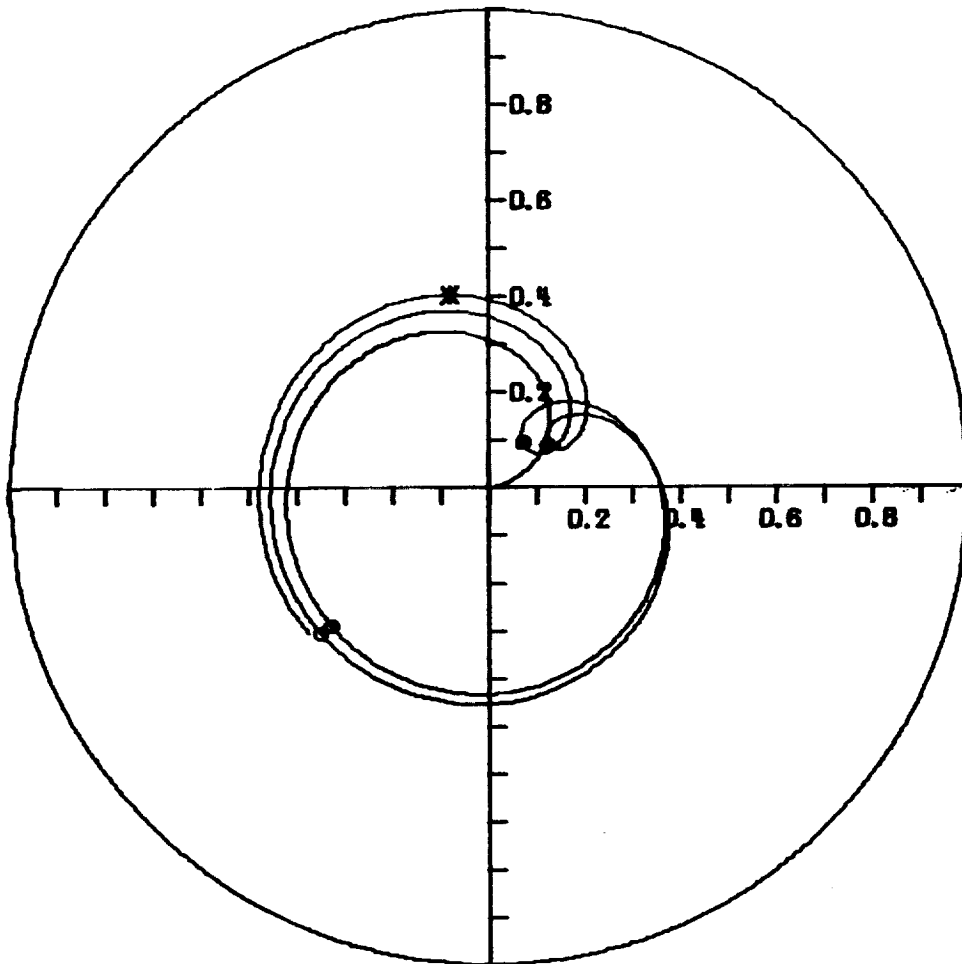
6.35 Journal Orbit of an Unbalanced Vertical Rotor for Cycles 5 - 10 (N = 6500, EMU = 0.2) Showing Motion Approaching Synchronous Precession

# VERTICAL UNBALANCED ROTOR

NO. 41593

N = 10500 RPM  
R = 1.00 IN.  
L = 1.00 IN.  
C = 5.00 MILS  
TRSMAX = 3.76  
S = 2.800  
SS = 0.700  
EMU = 0.20  
SU = 0.895  
TRDMAX = 1.20

WT = 0.00  
W = 50 LB.  
MUS = 1.000 REYNS  
FMAX = 188.1 LB. AND  
OCCURS AT 4.53 CYCLE  
WS = 3.96  
ES = 0.139  
FU = 156.45 LB.  
FURATIO = 3.13  
ESU = 0.342



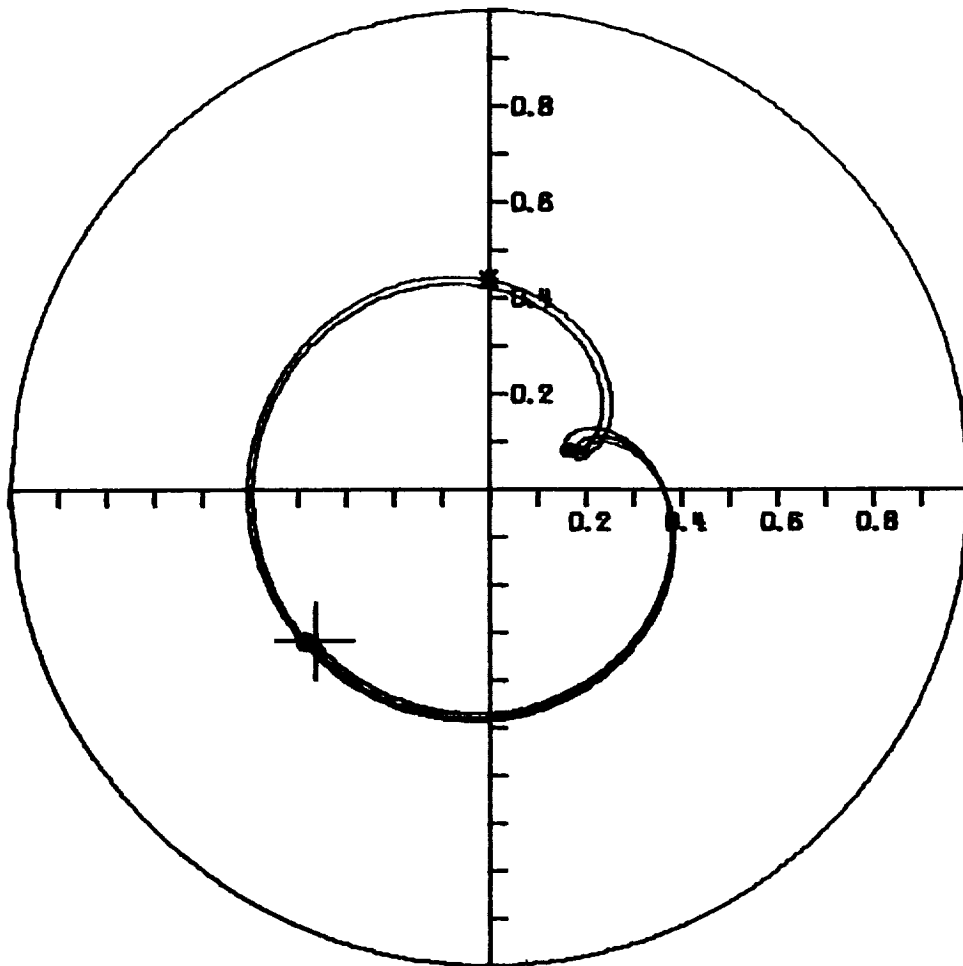
6.36 Journal Orbit of an Unbalanced Vertical Rotor Above the Stability Threshold for 5 Cycles (N = 10,500, EMU = 0.2)

# VERTICAL UNBALANCED ROTOR

NO. 41583

N = 10500 RPM  
R = 1.00 IN.  
L = 1.00 IN.  
C = 5.00 MILS  
TASMAX = 4.02  
S = 2.800  
SS = 0.700  
EMU = 0.20  
SU = 0.895  
TRDMAX = 1.28

WT = 0.00  
W = 50 LB.  
MUS = 1.000 REYNS  
FMAX = 201.0 LB. AND  
OCCURS AT 8.49 CYCLE  
WS = 3.96  
ES = 0.139  
FU = 156.45 LB.  
FURATIO = 3.13  
ESU = 0.342



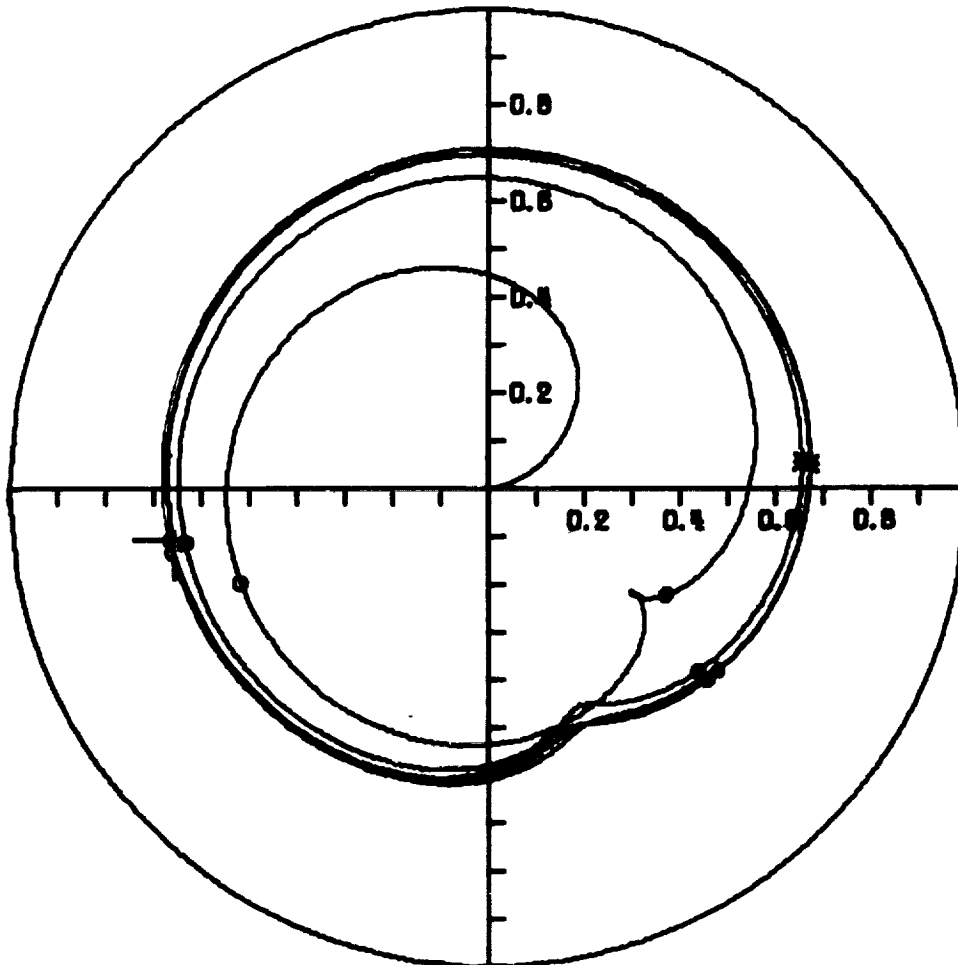
6.37 Journal Orbit of an Unbalanced Vertical Rotor for Cycles 5 - 10 (N = 10,500, EMU = 0.2)

# VERTICAL UNBALANCED ROTOR

NO. 41585

N = 21000 RPM  
R = 1.00 IN.  
L = 1.00 IN.  
C = 5.00 MILS  
TRSMAX = 21.34  
S = 5.600  
SS = 1.400  
EMU = 0.20  
SU = 0.447  
TRDMAX = 1.71

WT = 0.00  
W = 50 LB.  
MU<sub>5</sub> = 1.000 REYNS  
FMAX = 1067.0 LB. AND  
OCCURS AT 8.22 CYCLE  
WS = 7.91  
ES = 0.072  
FU = 625.79 LB.  
FURATIO = 12.52  
ESU = 0.491



6.38 Journal Orbit of an Unbalanced Vertical Rotor for 10 Cycles and Showing the Limit Cycle (N = 21,000, EMU = 0.2)

# UNBALANCED ROTOR

N = 18000 RPM

NO. 82782

R = 1.00 IN.

W = 200 LB.

L = 1.00 IN.

MU<sub>S</sub> = 1.000 REYNS

C = 3.76 MILS

FMAX = 15475.2 LB. AND

TASMAX = 77.38

OCCURS AT 0.22 CYCLE

S = 2.122

WS = 5.88

SS = 0.531

ES = 0.178

EMU = 1.00

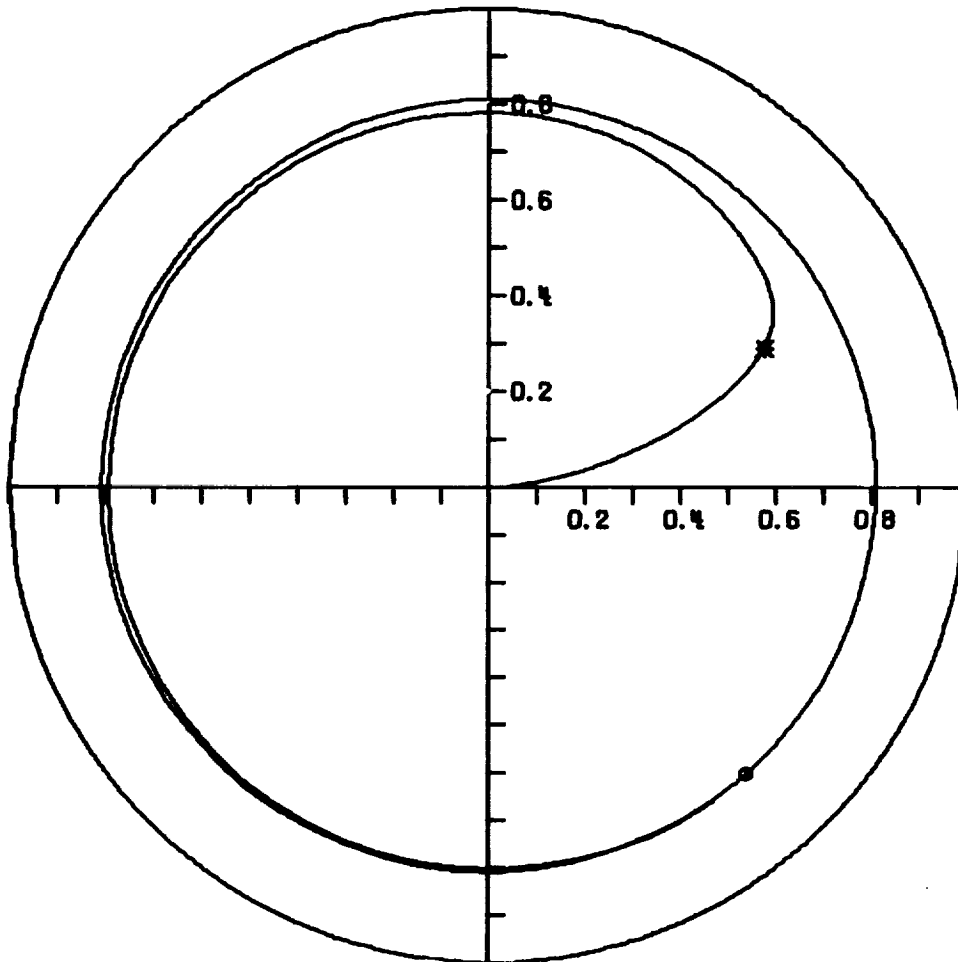
FU = 6914.85 LB.

SU = 0.061

FURATIO = 34.57

TADMAX = 2.24

ESU = 0.791



EULER'S METHOD W-60 H = 0.10  
VERTICAL ROTOR

6.39 Journal Orbit of a Highly Unbalanced Vertical Rotor  
 Experiencing Synchronous Whirl Above the Stability Threshold  
 for 5 Cycles (N = 18,000, W = 200, C = 0.00376, L/D = 1/2,  
 EMU = 1.0)

inner loop is precessing clockwise and becoming smaller, indicating a predominant nonsynchronous component of motion. The orbit is continued in Figure 6.37 where the TRDMAX has increased from 1.20 to 1.28.

With the journal speed increased to 21,000 rpm, the transient orbit of Figure 6.38 shows the limit cycle is well above the predicted unbalance radius of 0.491 and is predominated by the nonsynchronous component of motion. From these figures there is a strong indication that if the value of journal speed is above  $2.5 \times \sqrt{g/c}$  (i.e.  $\omega_s > 2.5$ ), the vertical rotor with  $EMU > 0.16$  will be unstable. In addition, the stability map indicates that if the predicted bearing eccentricity (ESU) due to unbalance is larger than 0.73, then the system should have synchronous motion only. Figure 6.39 represents five cycles of a 200 pound rotor with large unbalance ( $EMU = 1.0$ ), a speed of 18,000 rpm, and a speed parameter of  $\omega_s = 5.88$ . The predicted unbalance eccentricity ESU was 0.791 and the motion is completely synchronous as indicated by the timing marks. The orbit has a radius of 0.81 which is slightly above the predicted value. This mode of operation is obviously undesirable even though the nonsynchronous component of motion is not present, as predicted. The TRDMAX is 2.24 which indicates that the bearing is subjected to a load of over 7 tons.

The results of the discussion on the unbalanced vertical rotor give strong indications that a stability criteria can be developed for this system. The results of this section have shown that the level of unbalance and the speed of the journal are both factors that must be considered when trying to determine the stability of the vertical journal.

The results of this limited study on the stability of the vertical rotor shows that:

1. The balanced unloaded rotor is always unstable.
2. Unidirectional loads can stabilize the bearing according to Figure 6.15.
3. For light values of unbalance  $EMU \leq 0.16$  the system will exhibit nonsynchronous motion for all speeds.
4. The necessary and sufficient conditions for complete stability (synchronous precessive motion only) is that the unbalance EMU must be greater than 0.16 and the speed parameter  $\omega_s$  must be less than 2.5.
5. For large values of rotor unbalance where  $ESU > 0.73$ , then the resulting orbit will be synchronous even for values of the speed parameter  $\omega_s$  above 2.5. Stabilizing the rotor by the addition of large unbalance values is highly undesirable due to the large bearing forces transmitted.

#### 6.4.2 The Horizontal Journal

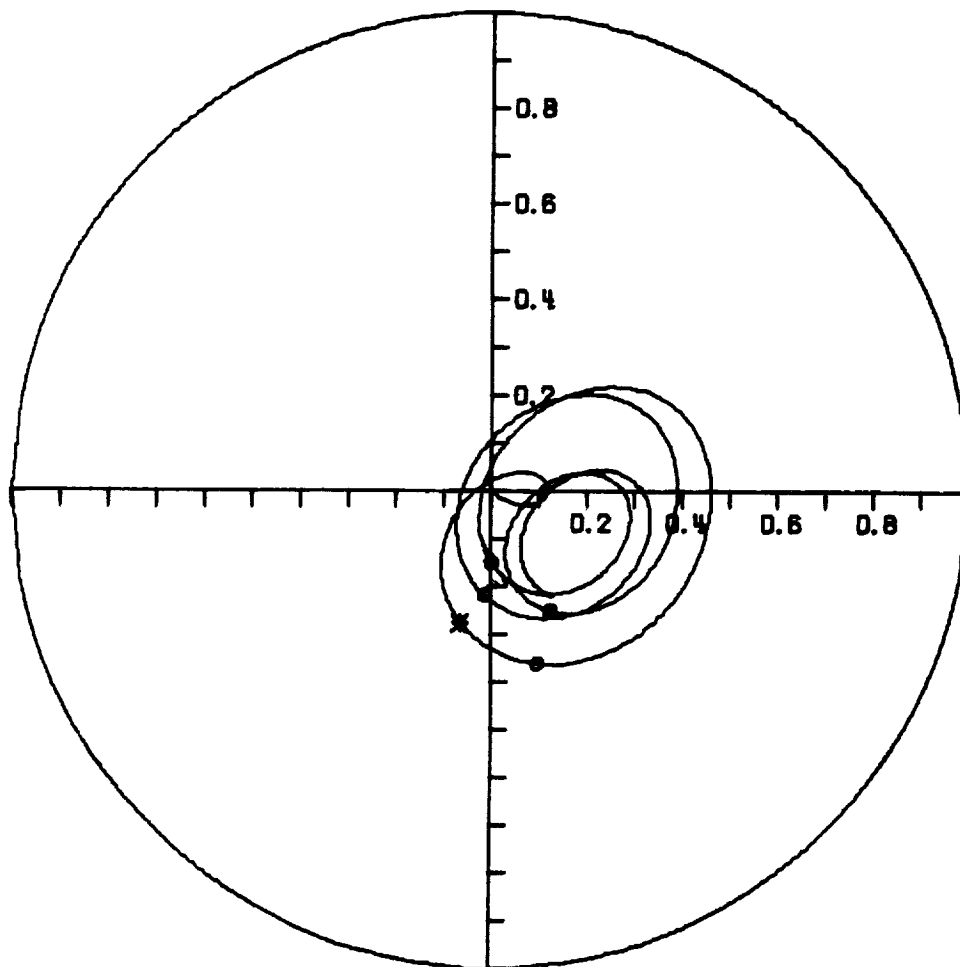
Figure 6.40 represents the behavior of a horizontal 50 pound journal operating at 6500 rpm. Due to the gravity loading, the orbit is displaced by the steady-state eccentricity  $ES = 0.21$  (see Figure 6.34 for the vertical case). The nonsynchronous component is less than one-half due to the inner loop precessing in a counterclockwise direction. The unbalance load is 59.95 pounds as indicated by FU. The TR factor (Figure 6.41) is observed to be oscillating between a value of almost zero and up to a maximum of about 2.3. This is approximately

# HORIZONTAL UNBALANCED ROTOR

NO. 21791-A

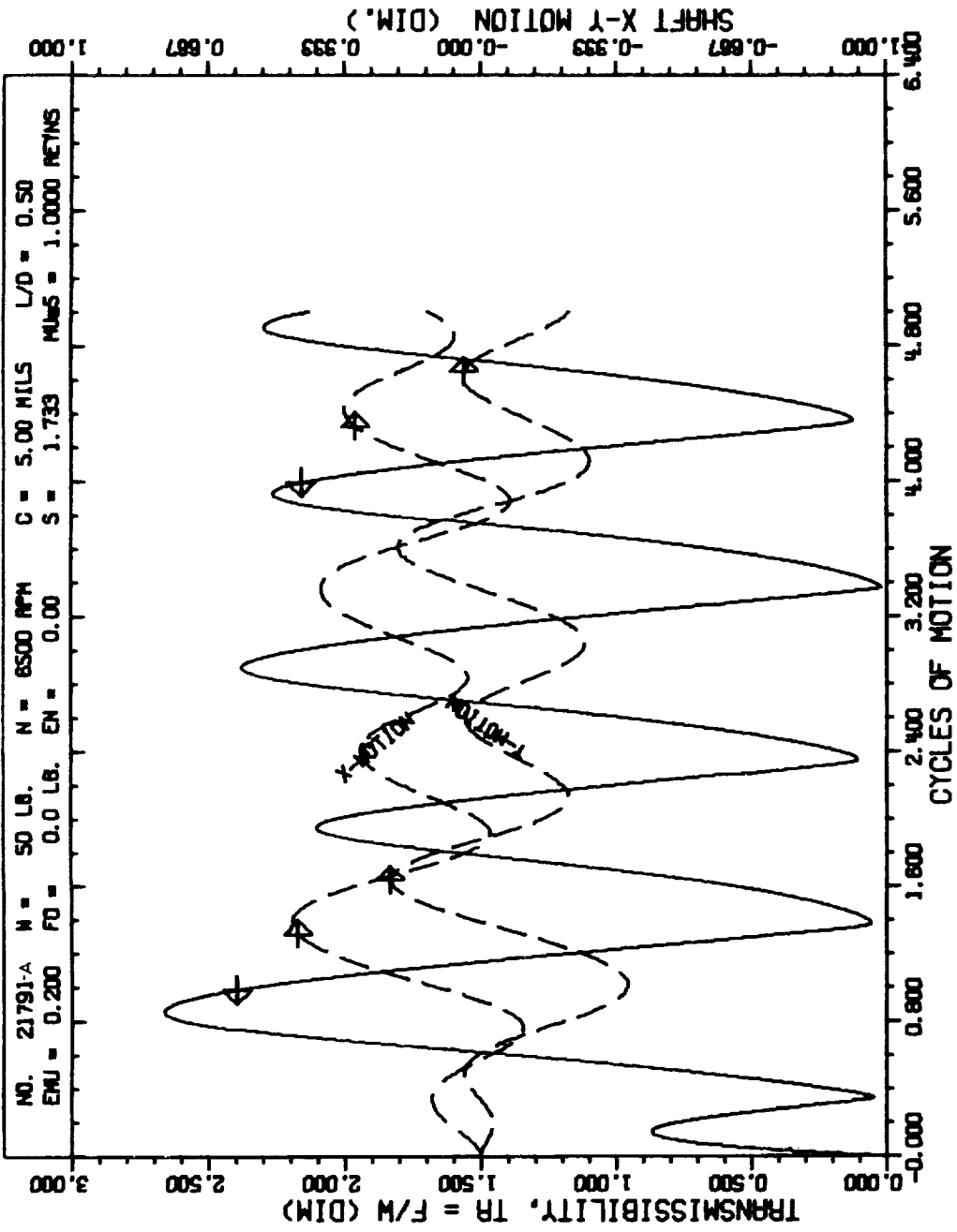
N = 6500 RPM  
R = 1.00 IN.  
L = 1.00 IN.  
C = 5.00 MILS  
TRSMAX = 2.66  
S = 1.733  
SS = 0.433  
EMU = 0.20  
SU = 1.446  
TRDMAX = 2.22

WT = 1.00  
W = 50 LB.  
MU<sub>5</sub> = 1.000 REYNS  
FMAX = 133.0 LB. AND  
OCCURS AT 0.86 CYCLE  
WS = 2.45  
ES = 0.211  
FU = 59.95 LB.  
FURATIO = 1.20  
ESU = 0.244



6.40 Journal Orbit of an Unbalanced Horizontal Rotor at the Stability Threshold for 5 Cycles (N = 6500, W = 50, C = 0.005, L/D = 1/2, EMU = 0.2)

HORIZONTAL UNBALANCED ROTOR



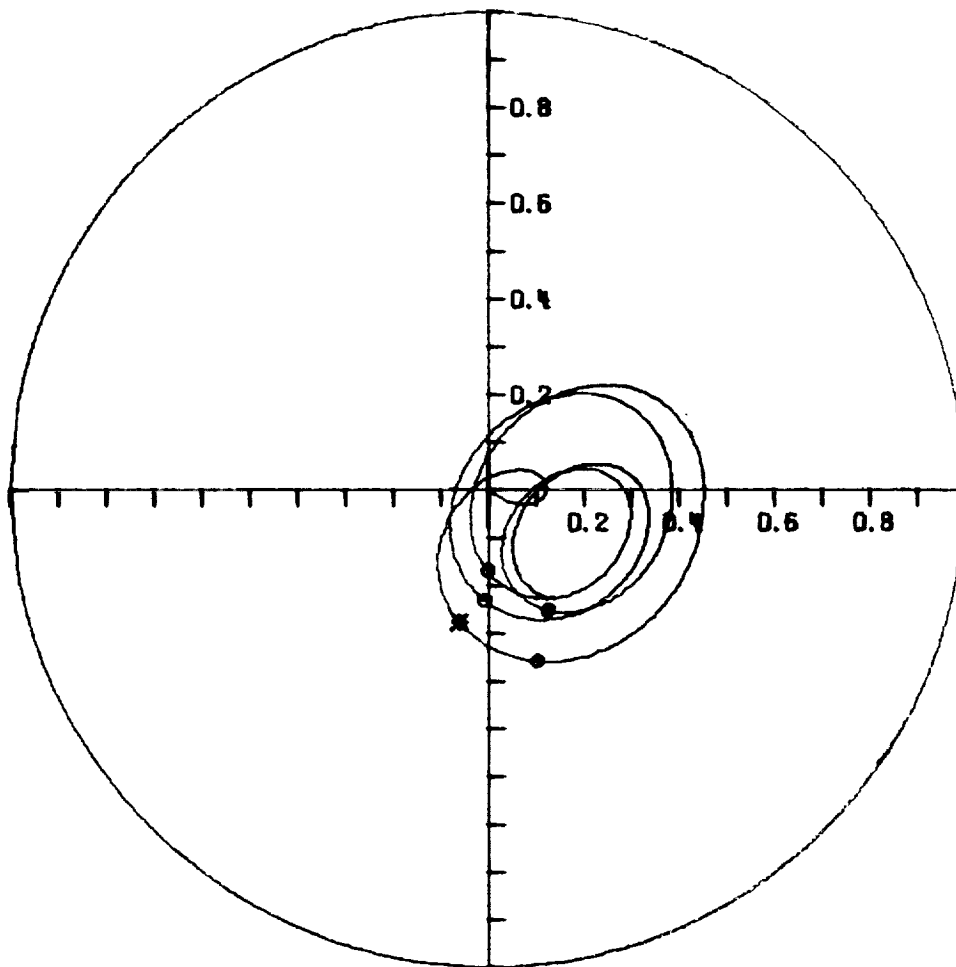
6.41 Transmissibility and Shaft X-Y Motion vs Cycles of Motion  
 (N = 6500)

# HORIZONTAL UNBALANCED ROTOR

NO. 21791-E

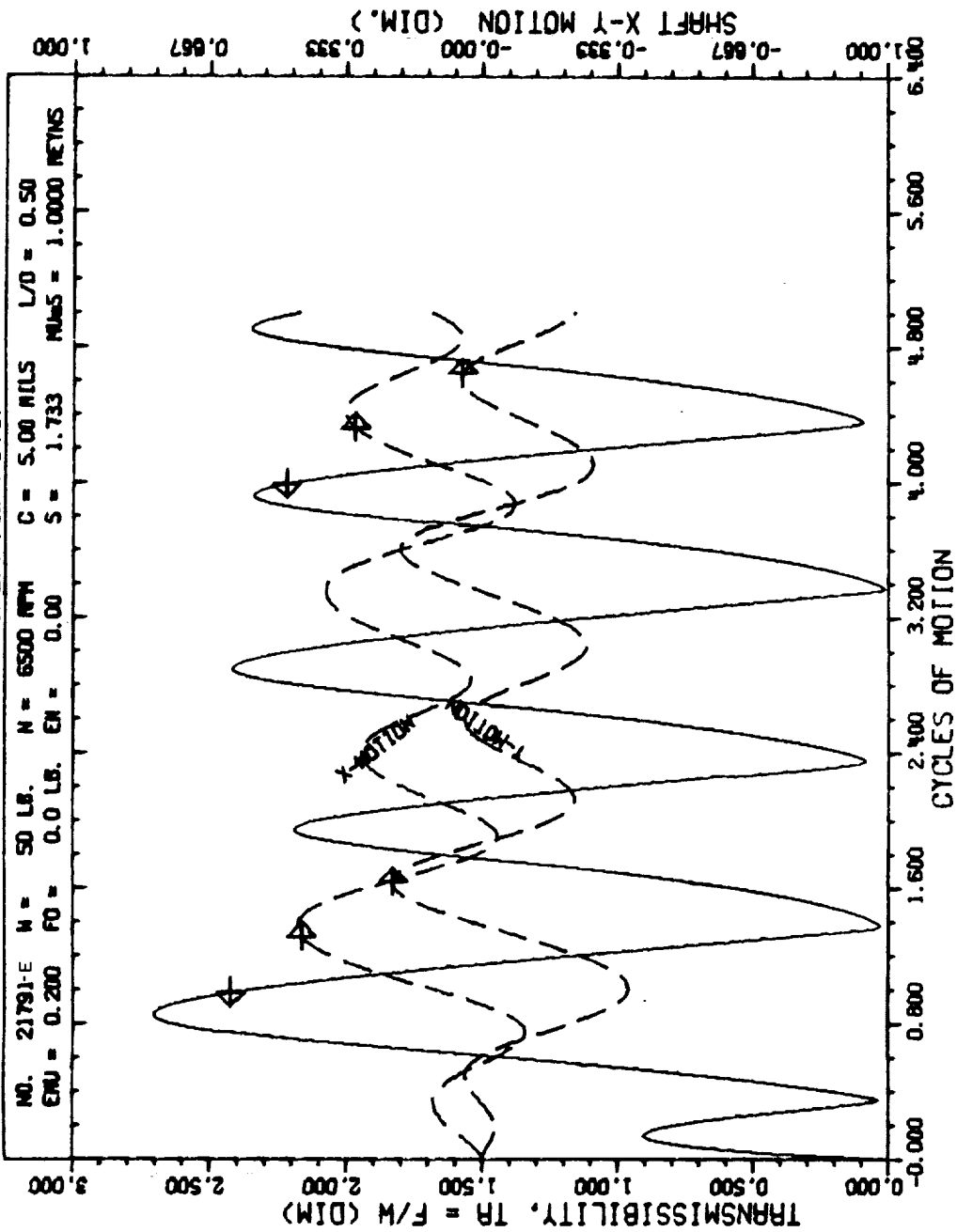
N = 6500 RPM  
R = 1.00 IN.  
L = 1.00 IN.  
C = 5.00 MILS  
TRSMAX = 2.70  
S = 1.733  
SS = 0.433  
EMU = 0.20  
SU = 1.446  
TROMAX = 2.26

WT = 1.00  
W = 50 LB.  
MU<sub>5</sub> = 1.000 REYNS  
FMAX = 135.2 LB. AND  
OCCURS AT 0.86 CYCLE  
WS = 2.45  
ES = 0.211  
FU = 59.95 LB.  
FURATIO = 1.20  
ESU = 0.244

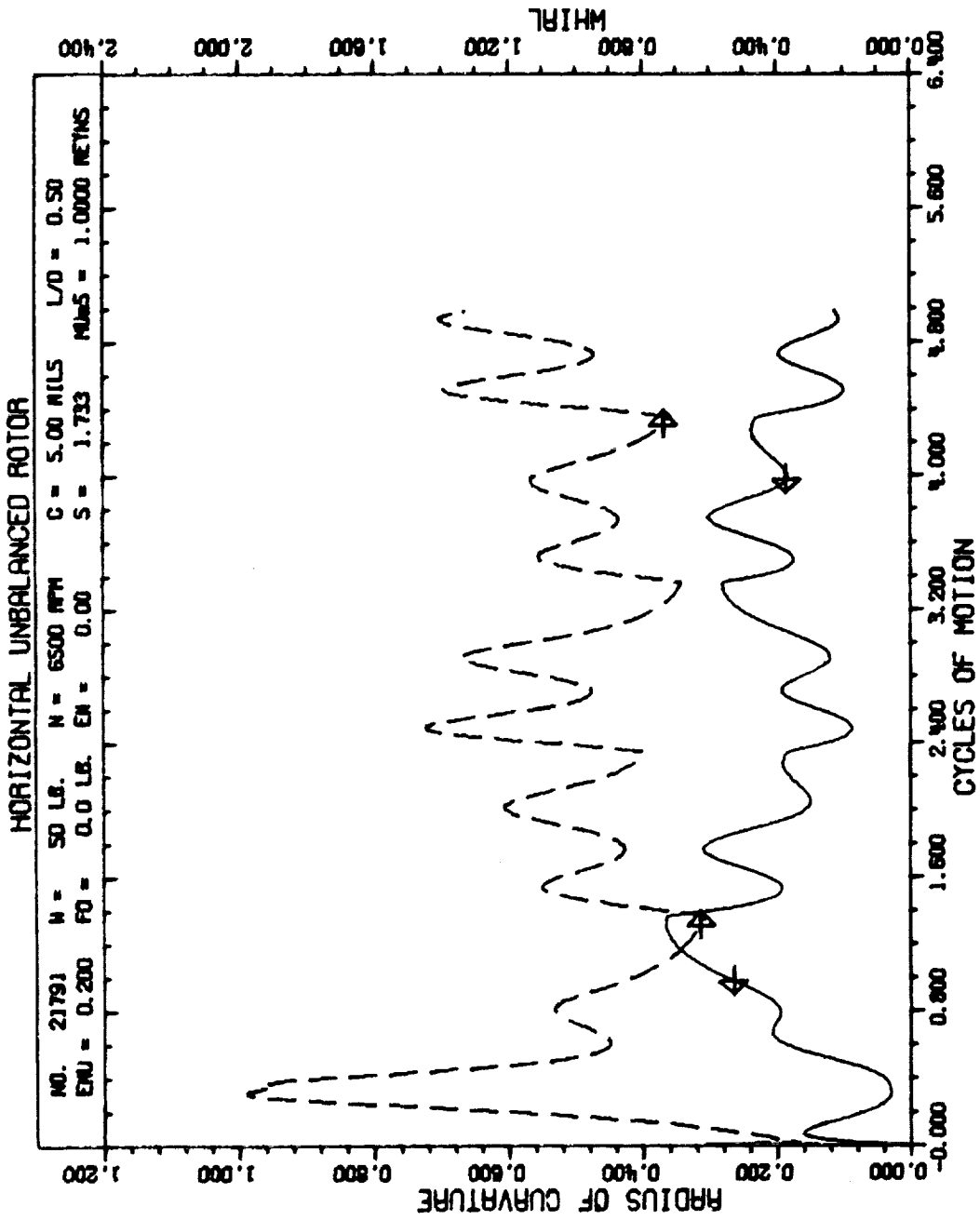


6.42 Journal Orbit (by Euler's Improved Method) of an Unbalanced Horizontal Rotor for 5 Cycles ( $N = 6500$ ,  $W = 50$ ,  $C = 0.005$ ,  $L/D = 1/2$ ,  $EMU = 0.2$ )

HORIZONTAL UNBALANCED ROTOR



6.43 Transmissibility and Shaft X-Y Motion vs Cycles of Motion



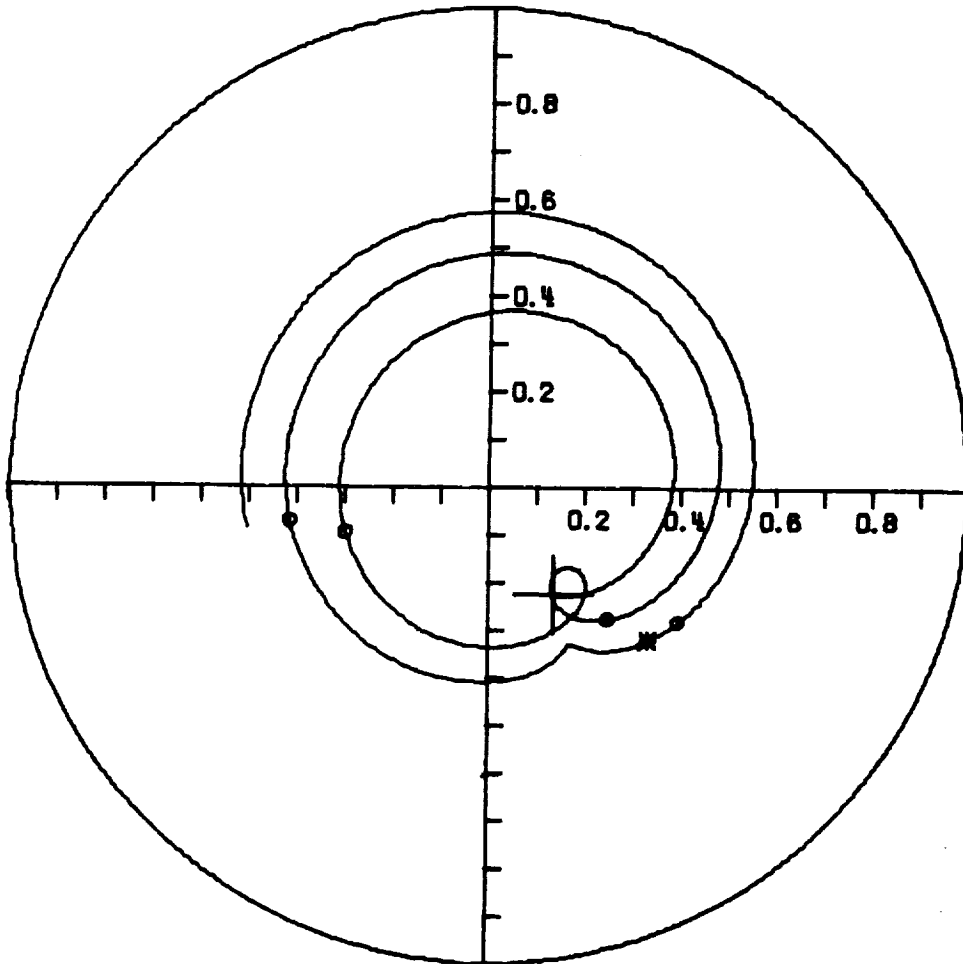
6.44 Radius of Curvature and Whirl vs Cycles of Motion (N = 6500)

# HORIZONTAL UNBALANCED ROTOR

NO. 21791

N = 10500 RPM  
R = 1.00 IN.  
L = 1.00 IN.  
C = 5.00 MILS  
TRSMAX = 4.97  
S = 2.800  
SS = 0.700  
EMU = 0.20  
SU = 0.895  
TRDMAX = 1.59

WT = 1.00  
W = 50 LB.  
MU<sub>5</sub> = 1.000 REYNS  
FMAX = 248.7 LB. AND  
OCCURS AT 8.95 CYCLE  
WS = 3.96  
ES = 0.139  
FU = 156.45 LB.  
FURATIO = 3.13  
ESU = 0.342



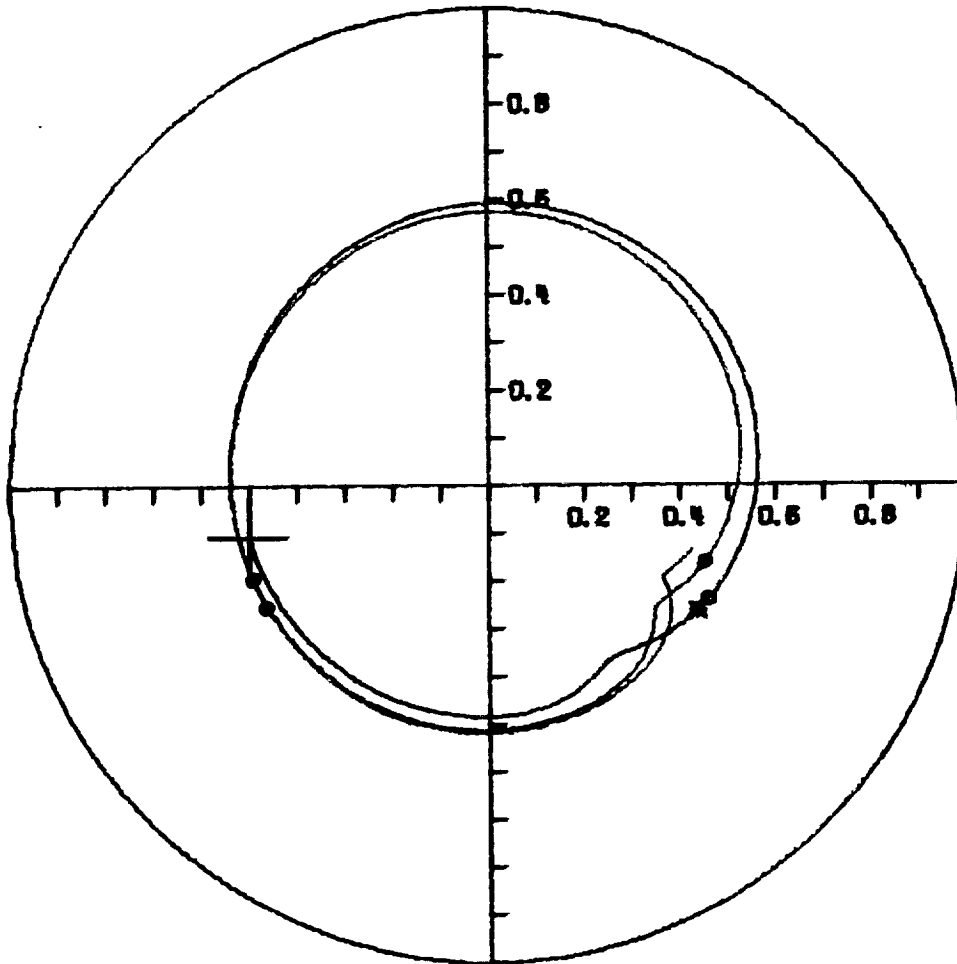
6.45 Journal Orbit of an Unbalanced Horizontal Rotor above the Stability Threshold for Cycles 5 - 10 (N = 10,500)

# HORIZONTAL UNBALANCED ROTOR

NO. 21791

N = 10500 RPM  
R = 1.00 IN.  
L = 1.00 IN.  
C = 5.00 MILS  
TASMAX = 5.11  
S = 2.800  
SS = 0.700  
EMU = 0.20  
SU = 0.895  
TROMAX = 1.63

WT = 1.00  
W = 50 LB.  
MUS = 1.000 REYNS  
FMAX = 255.4 LB. AND  
OCCURS AT 10.97 CYCLE  
WS = 3.96  
ES = 0.139  
FU = 156.45 LB.  
FURATIO = 3.13  
ESU = 0.342



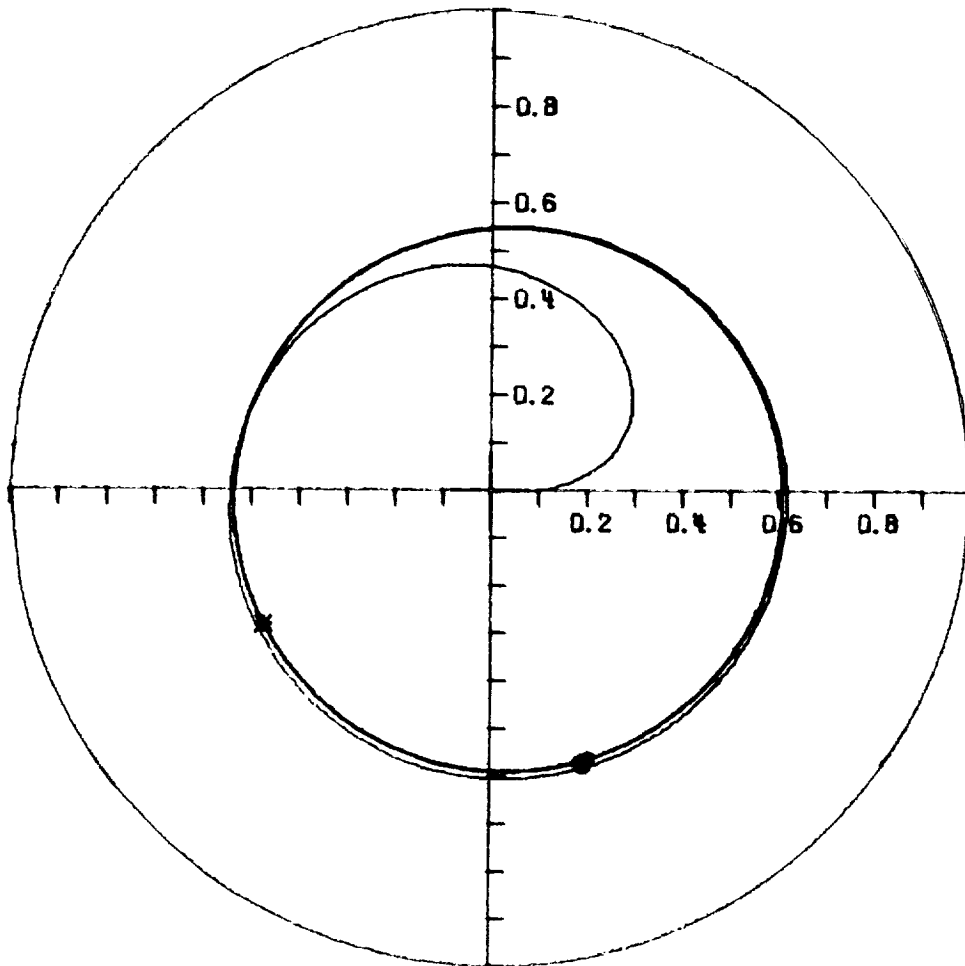
6.46 Journal Orbit of an Unbalanced Horizontal Rotor for Cycles 10 - 15 Showing the Non-Synchronous Limit Cycle (N = 10,500)

# HORIZONTAL UNBALANCED ROTOR

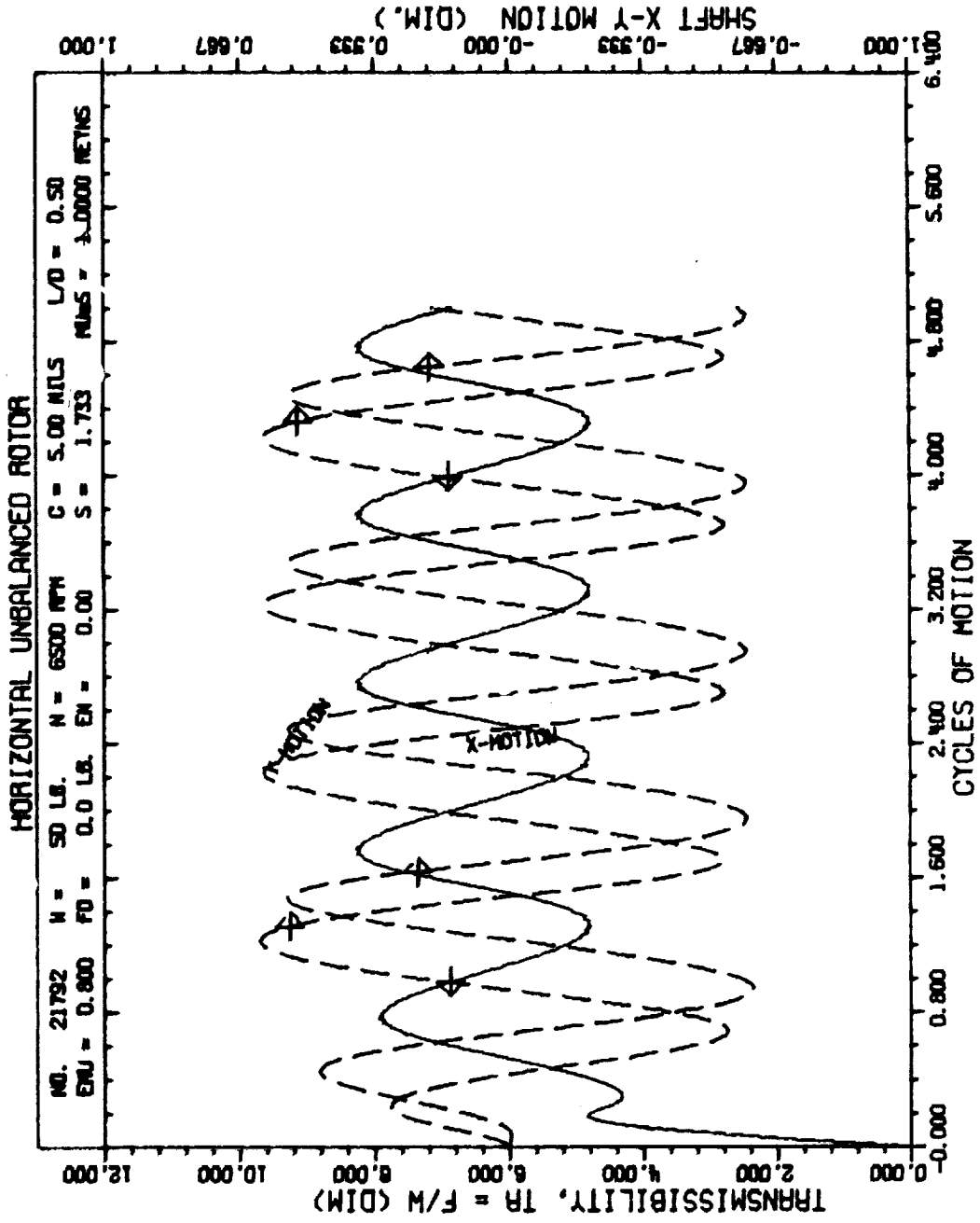
NO. 21792

N = 6500 RPM  
R = 1.00 IN.  
L = 1.00 IN.  
C = 5.00 MILS  
TRSMAX = 8.27  
S = 1.733  
SS = 0.433  
EMU = 0.80  
SU = 0.361  
TRDMAX = 1.72

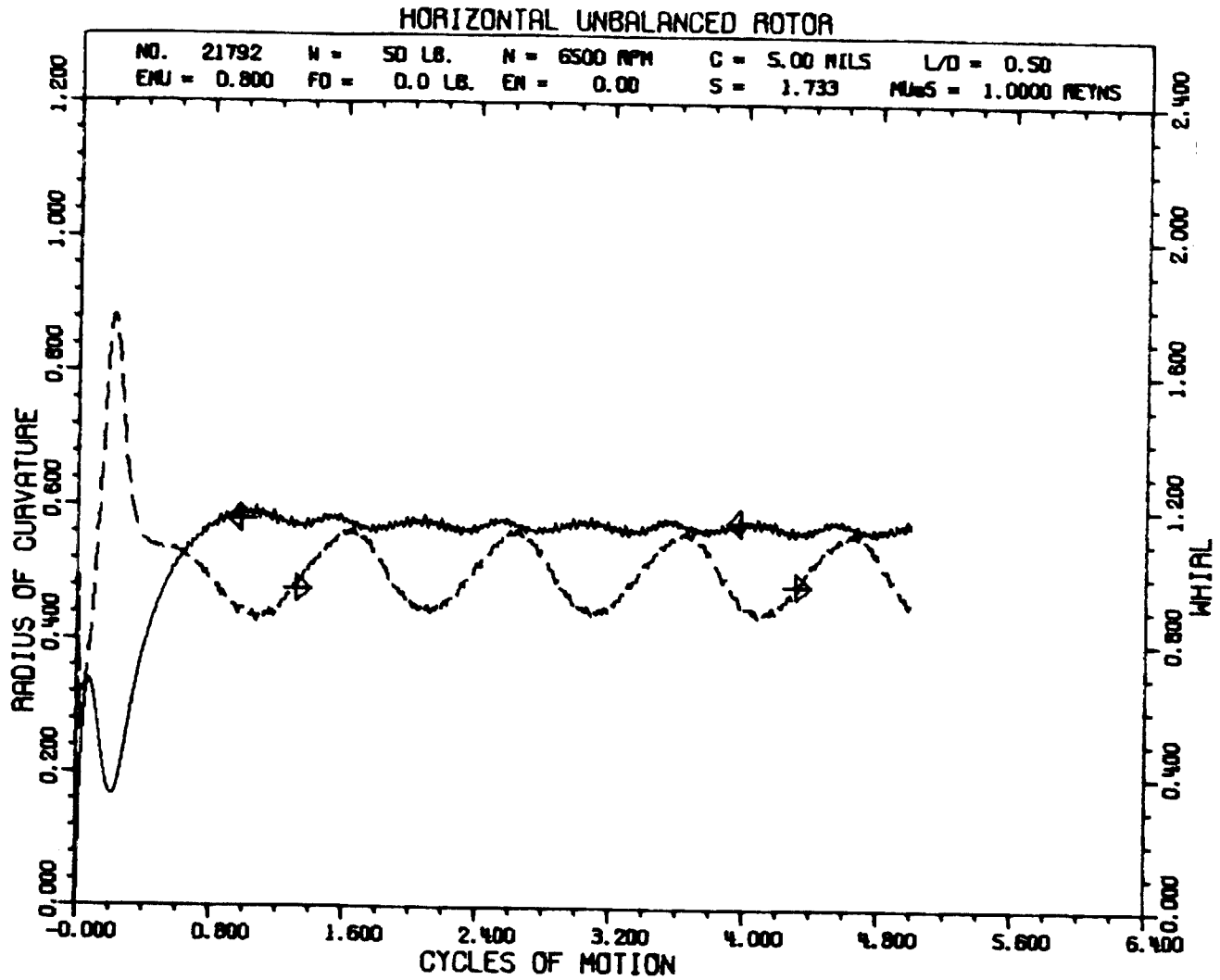
WT = 1.00  
W = 50 LB.  
MUS = 1.000 REYNS  
FMAX = 413.5 LB. AND  
OCCURS AT 1.78 CYCLE  
WS = 2.45  
ES = 0.211  
FU = 239.82 LB.  
FURATIO = 4.80  
ESU = 0.533



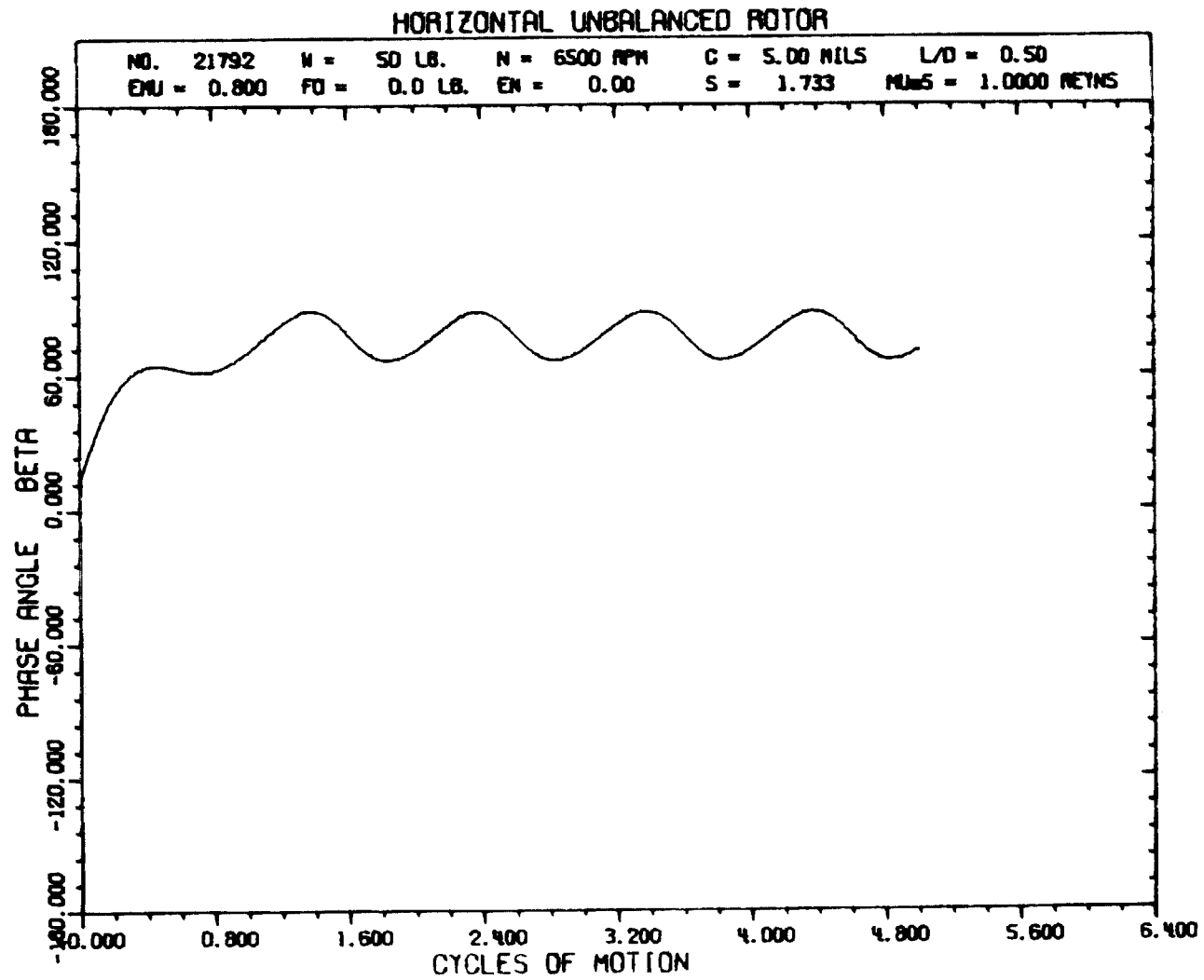
6.47 Journal Orbit of an Unbalanced Horizontal Rotor Showing Synchronous Motion at the Stability Threshold for 5 Cycles (N = 6500, W = 50, C = 0.005, L/D = 1/2, EMU = 0.8)



6.48 Transmissibility and Shaft X-Y Motion vs Cycles of Motion  
(N = 6500)



6.49 Radius of Curvature and Whirl vs Cycles of Motion (N = 6500)



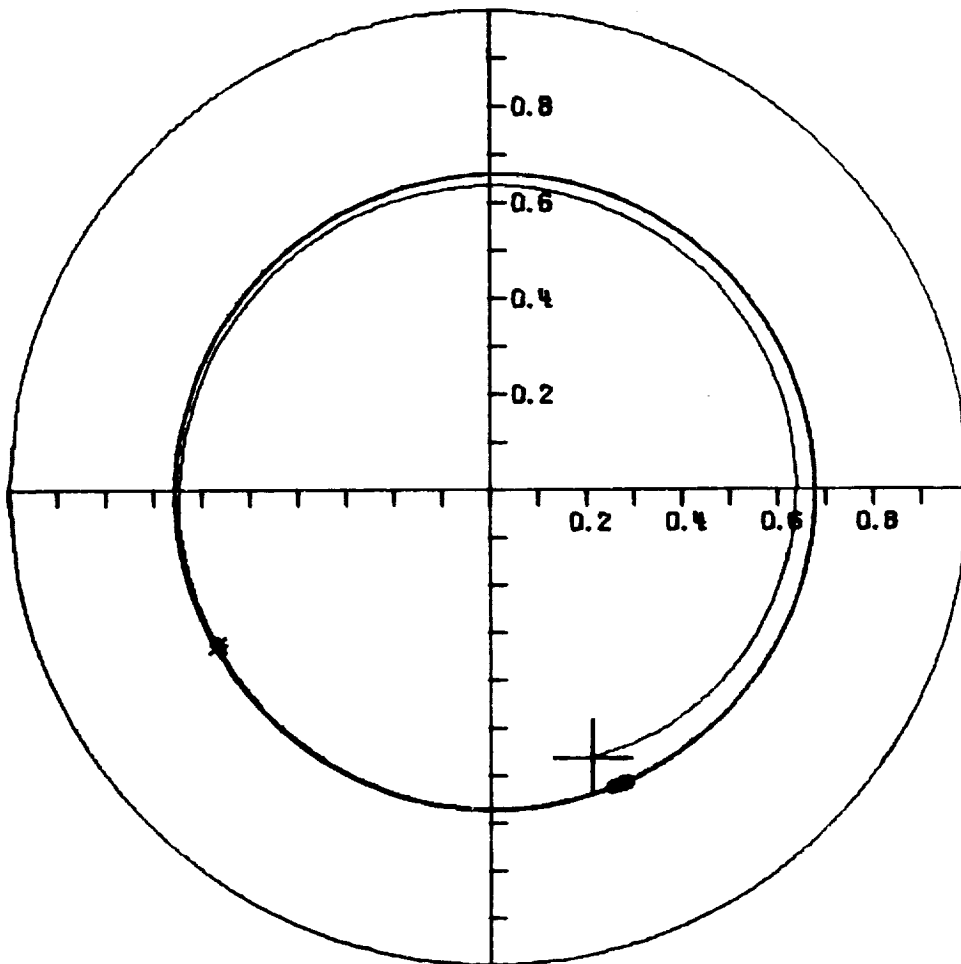
6.50 Unbalance-Displacement Phase Angle vs Cycles of Motion  
(N = 6500)

# HORIZONTAL UNBALANCED ROTOR

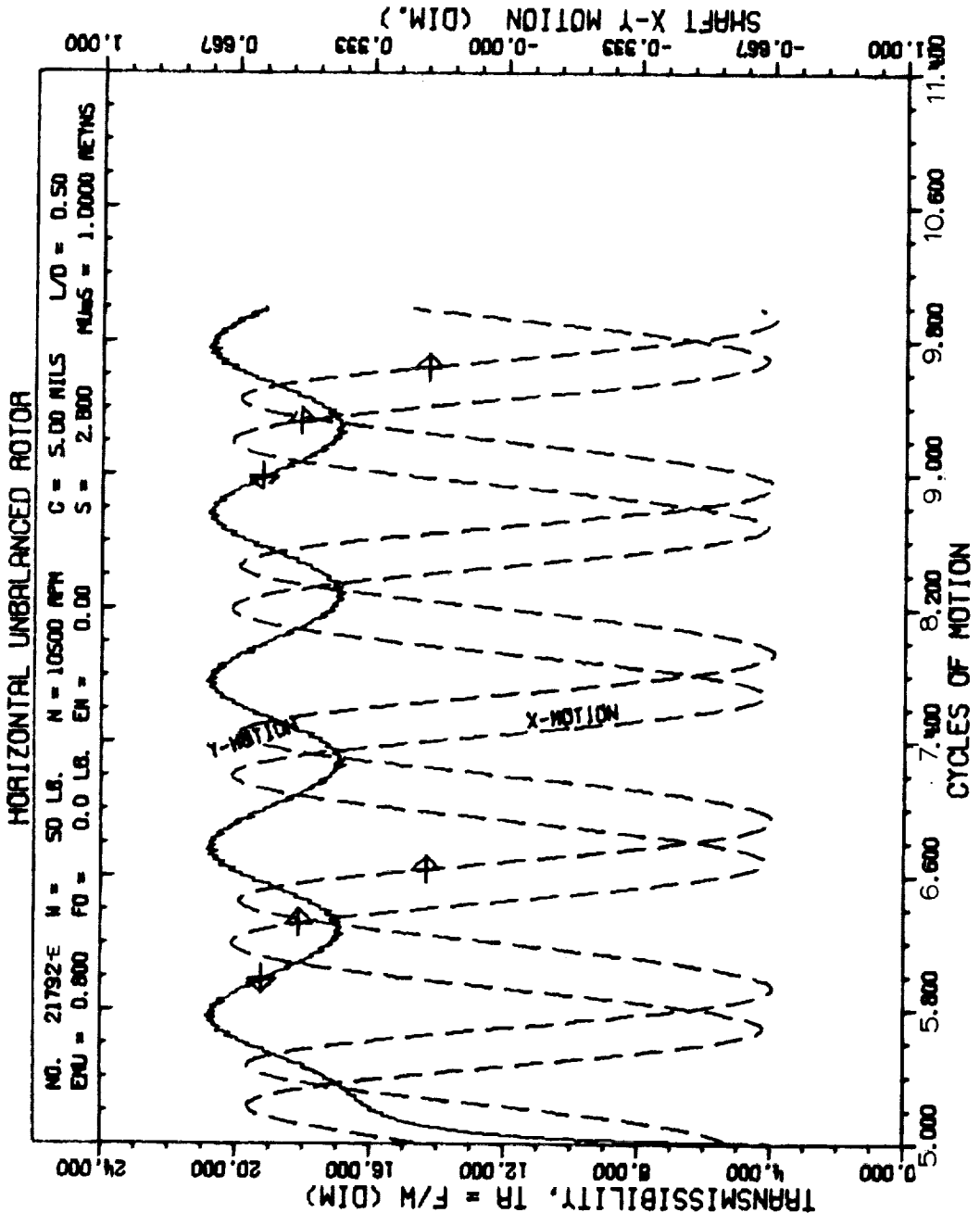
NO. 21792-E

N = 10500 RPM  
R = 1.00 IN.  
L = 1.00 IN.  
C = 5.00 MILS  
TRSMAX = 20.89  
S = 2.800  
SS = 0.700  
EMU = 0.80  
SU = 0.224  
TROMAX = 1.67

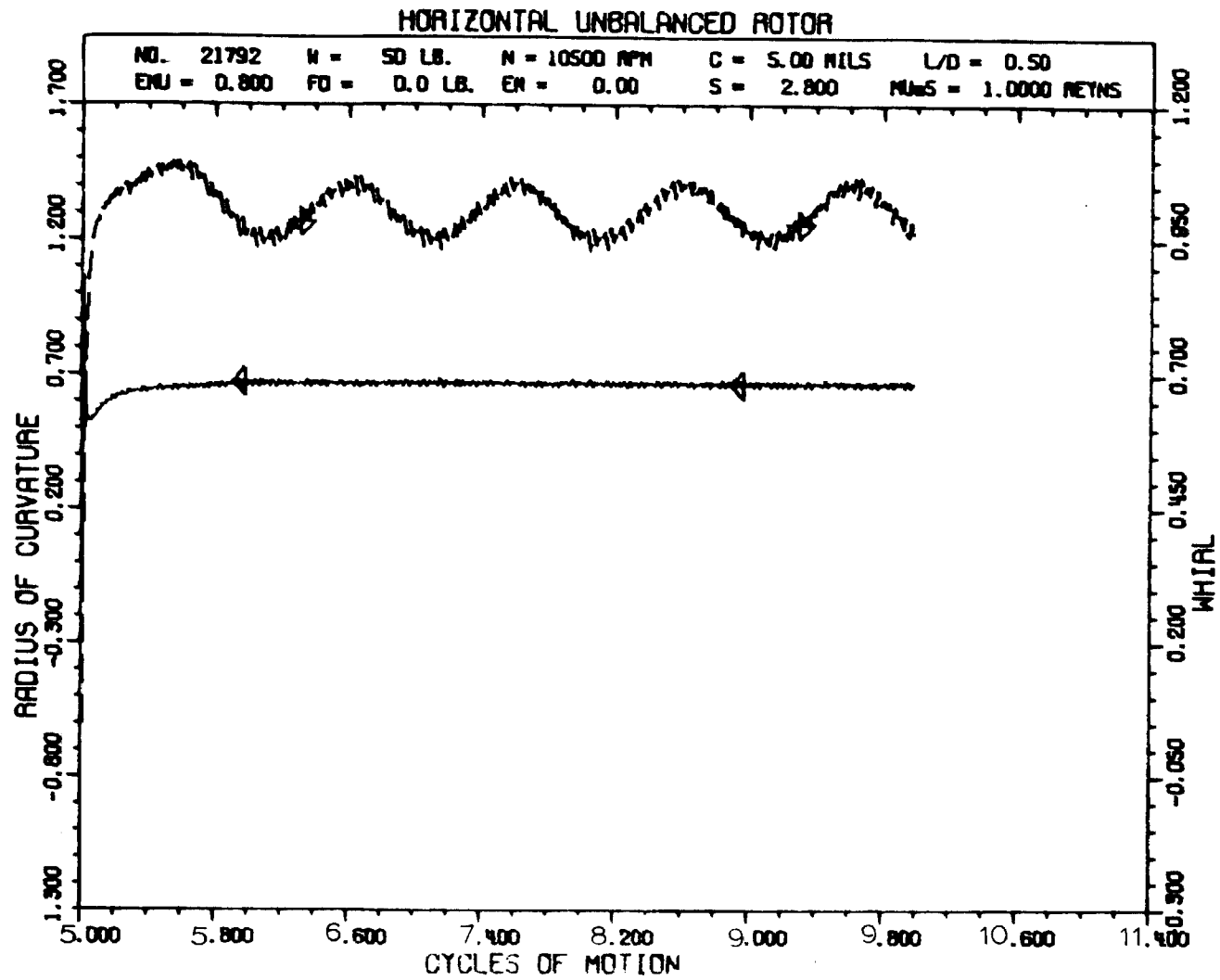
WT = 1.00  
W = 50 LB.  
MUS = 1.000 REYNS  
FMAX = 1044.5 LB. AND  
OCCURS AT 5.77 CYCLE  
WS = 3.96  
ES = 0.139  
FU = 625.79 LB.  
FURATIO = 12.52  
ESU = 0.620



6.51 Journal Orbit of an Unbalanced Horizontal Rotor above the Stability Threshold for Cycles 5 - 10 Showing Synchronous Limit Cycle (N = 10,500)



6.52 Transmissibility and Shaft X-Y Motion vs Cycles of Motion  
 for Cycles 5 - 10 (N = 10,500)



6.53 Radius of Curvature and Whirl vs Cycles of Motion for Cycles  
5 - 10 Illustrating Small Numerical Instability ( $N = 10,500$ )

An increase of EMU to a value of 0.8 produces the "synchronous" limit cycle of Figure 6.47. Figures 6.48, 6.49, and 6.50 are the transmissibility, whirl and radius, and phase angle plots for this case.

Note the cyclic nature of the forces on the bearing as indicated by the TR plot and the fact that the whirl is oscillating about the value of 1.0 while the timing marks on the orbit plot are coming on top of each other and make it appear that the orbit is absolute synchronous while it is not.

With an increase of speed to 10,500 rpm, the limit cycle grows accordingly as shown in Figure 6.51 and the synchronous forcing function predominates the resultant orbit motion. The plot of TR in Figure 6.52 resulted from the improved Euler solution and is the correct result for the case presented in CHAPTER V as Figure 5.9. The radius and whirl plot for this case is included as Figure 6.53 and concludes the series of figures being presented which are related to unbalance loading along.

The cases presented have shown that unbalance in a horizontal rotor will increase the forces being transmitted to the bearings and therefore should be reduced to the smallest value possible. No advantage, as was found for the vertical journal, can be had from unbalance in a horizontal rotor.

#### 6.5 Motion of a Journal Bearing Experiencing Cyclic External Loading

A journal bearing in actual use must support the journal and rotor system and in addition it must be able to maintain its stability and load-carrying capacity under any type of external loading that

might occur. For example, the main bearings of an internal combustion engine experience severe cyclic loading functions through the connecting rods. Journal bearings must be able to support shock loading, plane cyclic loading, rotating loads other than unbalance, or any other type loading that a particular application might involve.

The following sample cases were chosen to illustrate the ability of the method of solution to produce the resulting journal orbits.

Figure 6.54 indicates the orbit of a 200 pound vertical journal with a clearance of 3.76 mils operating at 3600 rpm and experiencing a -200 pound load that is rotating backwards at  $1/2$  the journal angular frequency. The resulting "three-bladed propeller" is the resultant motion of a forward synchronous component plus a nonsynchronous component rotating backward at one-half the angular velocity of the synchronous component.

By applying the formula given by Hull (25)\* there should have been approximately two outer loops. The difference is, of course, that the unbalance forcing function has altered the effect of the external rotating load and results in the three outer loops of Figure 6.54. This type of motion has actually been observed experimentally with two-pole electric motors supported in plane journal bearings<sup>(42)</sup>.

The same conditions for a horizontal bearing is shown in Figure 6.55 with the corresponding whirl and curvature plot presented in Figure 6.56.

---

\*See CHAPTER II, p. 10 for equation given by Hull.

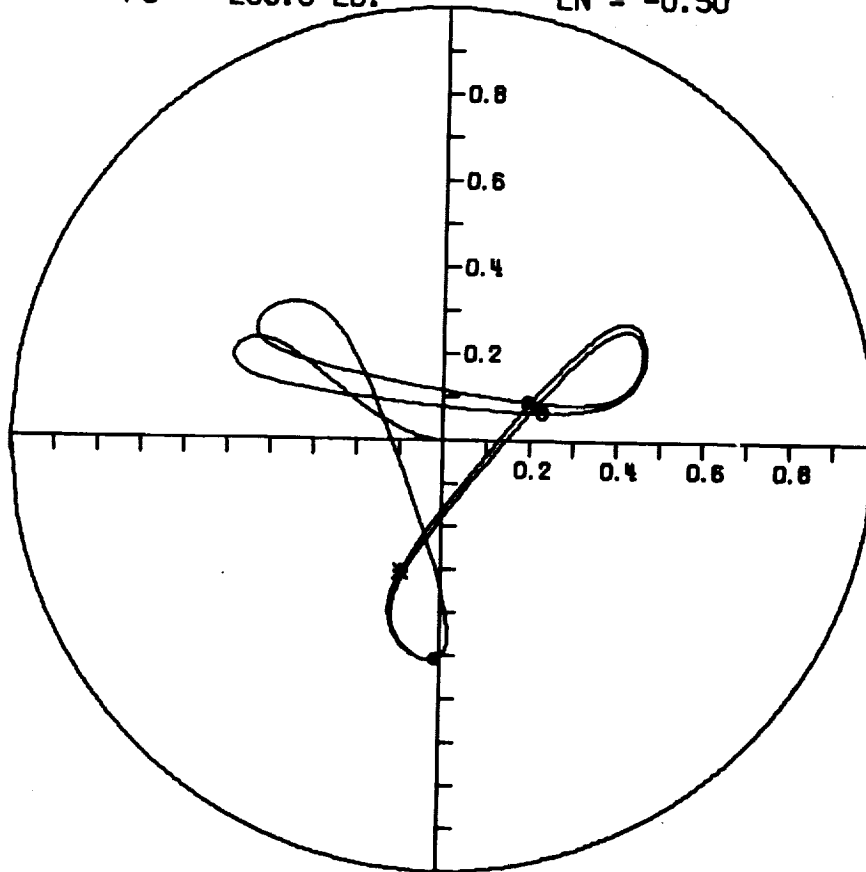
# UNBALANCED ROTOR

NO. 82783

N = 3600 RPM

R = 1.00 IN.  
 L = 1.00 IN.  
 C = 3.76 MILS  
 TRSMAX = 2.13  
 S = 0.424  
 SS = 0.106  
 EMU = 0.27  
 SU = 1.154  
 TRDMAX = 5.79  
 FO = -200.0 LB.

W = 200 LB.  
 MU<sub>5</sub> = 1.000 REYNS  
 FMAX = 425.9 LB. AND  
 OCCURS AT 1.72 CYCLE  
 WS = 1.18  
 ES = 0.500  
 FU = 73.57 LB.  
 FURATIO = 0.37  
 ESU = 0.289  
 EN = -0.50



EULER'S METHOD W-60 H = 0.10  
VERTICAL ROTOR

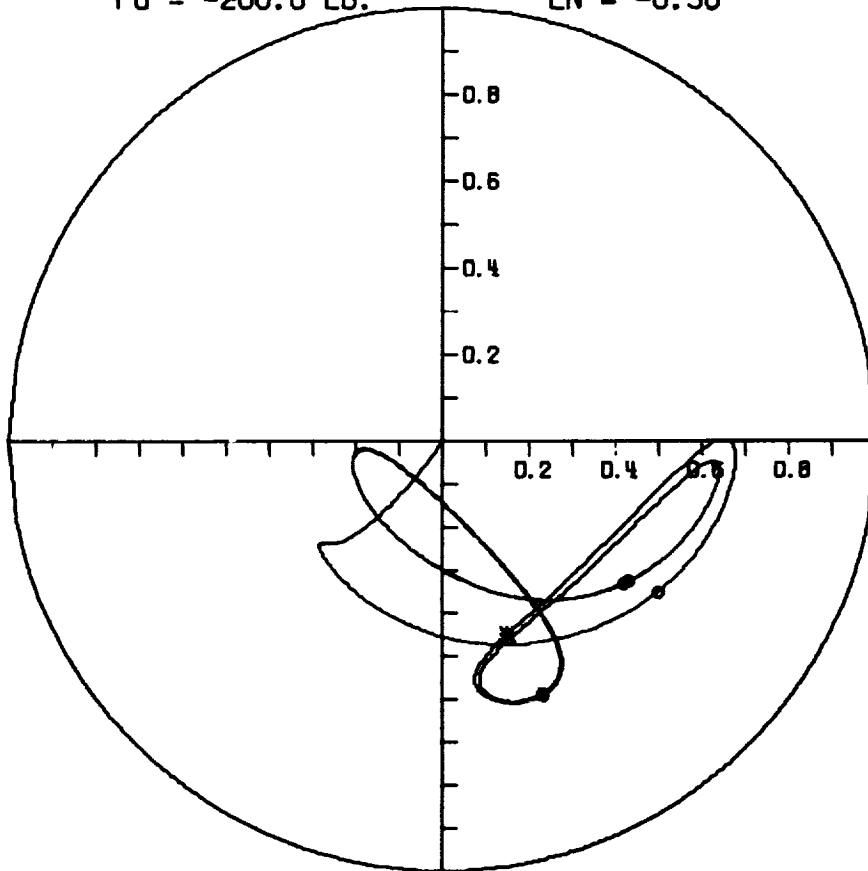
6.54 Journal Orbit of an Unbalanced Vertical Rotor Having a Backward Half-Frequency Rotating Load for 5 Cycles (N = 3600, W = 200, C = 0.00376, L/D = 1/2, FO = -200, EN = -0.5, EMU = 0.27)

# UNBALANCED ROTOR

NO. 82381

N = 3600 RPM

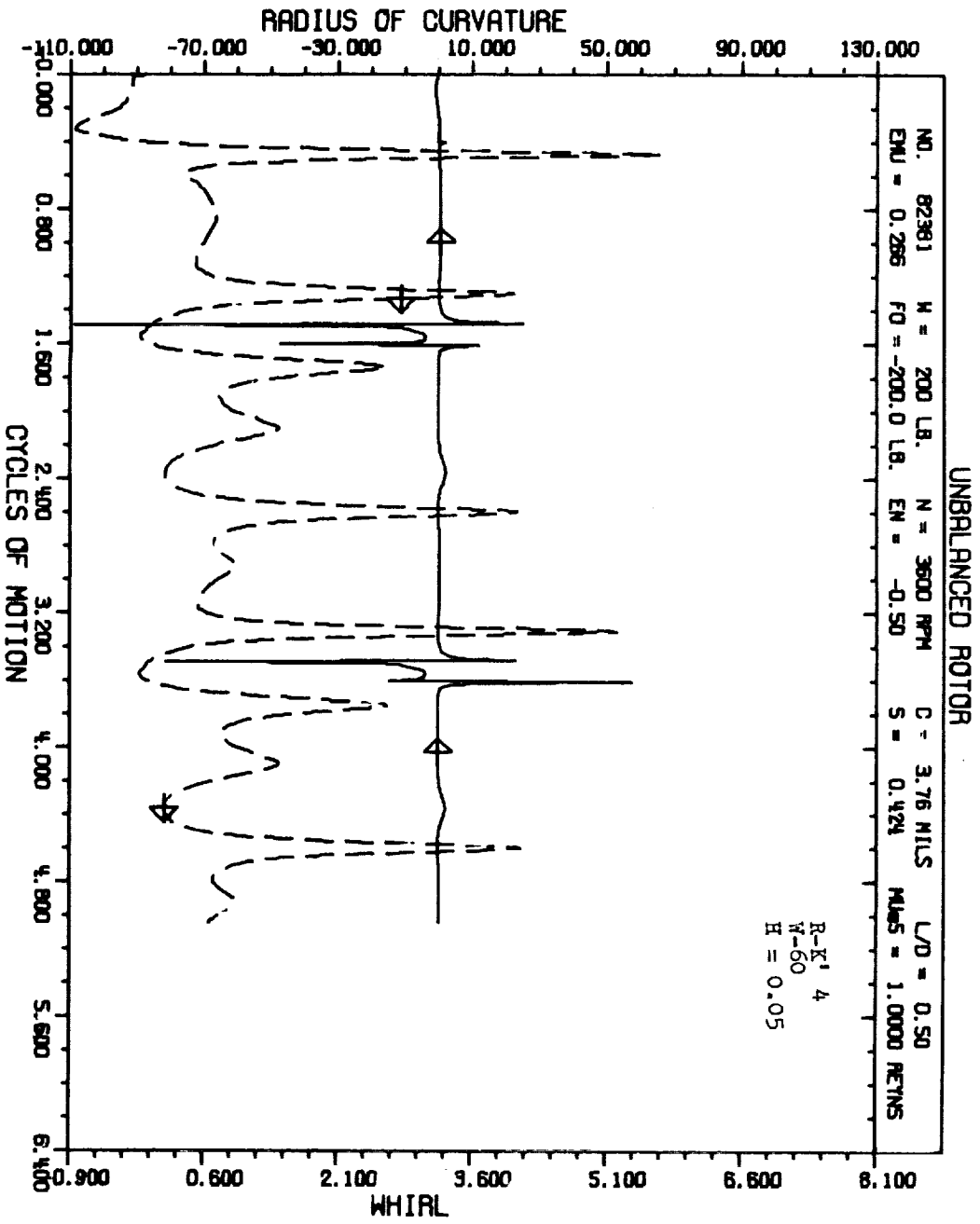
R = 1.00 IN.	W = 200 LB.
L = 1.00 IN.	MU <sub>5</sub> = 1.000 REYNS
C = 3.76 MILS	FMAX = 567.2 LB. AND
TASMAX = 2.84	OCCURS AT 1.63 CYCLE
S = 0.424	WS = 1.18
SS = 0.106	ES = 0.500
EMU = 0.27	FU = 73.57 LB.
SU = 1.154	FURATIO = 0.37
TADMAX = 7.71	ESU = 0.289
FO = -200.0 LB.	EN = -0.50



R-K' 4    W-60    H = 0.05

5 pt. rule

6.55 Journal Orbit of an Unbalanced Horizontal Rotor Having a Backward Half-Frequency Rotating Load for 5 Cycles  
 (N = 3600, W = 200, C = 0.00376, L/D = 1/2, FO = -200, EN = -0.5, EMU = 0.27)



6.56 Radius of Curvature and Whirl vs Cycles of Motion for an Unbalanced Horizontal Rotor (N = 3600)

The next three series of figures are for a 50 pound journal with a clearance of 5 mils experiencing cyclic loading functions. Each case is allowed to run for five cycles of journal rotation, which is 6500 rpm.

The first case, Figure 6.57 has a forward rotating load, rotating at one-half the journal speed. A maximum load of about 500 pounds is developed in the bearing after 3-1/2 cycles as indicated on the plot.

The second case, Figure 6.58, is for a 100 pound backward rotating load ( $EN = -0.5$ ). This case is very similar to that of Figure 6.55 but the synchronous component is not as prevalent so the motion is very close to being backward half-frequency\* whirl. The instantaneous whirl is given in Figure 6.59 and is oscillating about the  $-0.5$  value.

It is obvious that the direction of rotation of the external load has a great effect on the size of the resulting orbit for the given case of the frequency ratio being  $1/2$ . From Equation 3.23, it is obvious that the entire wedge effect of the journal bearing is lost if the precession rate,  $\dot{\phi}$ , is exactly one-half shaft speed. This explains the large limit cycle for the case of the forward rotating load (Figure 6.57) as compared to the relative small orbit for the backward rotating half-frequency load (Figure 6.58).

The next case (Figure 6.60) considered has a vertical (y-coordinate) oscillating load of  $F_{HY} = 100$  pounds and the frequency is one-half the journal angular velocity,  $\omega_j$ . The orbit spirals out in phase with the exciting force and would eventually reach a limit cycle

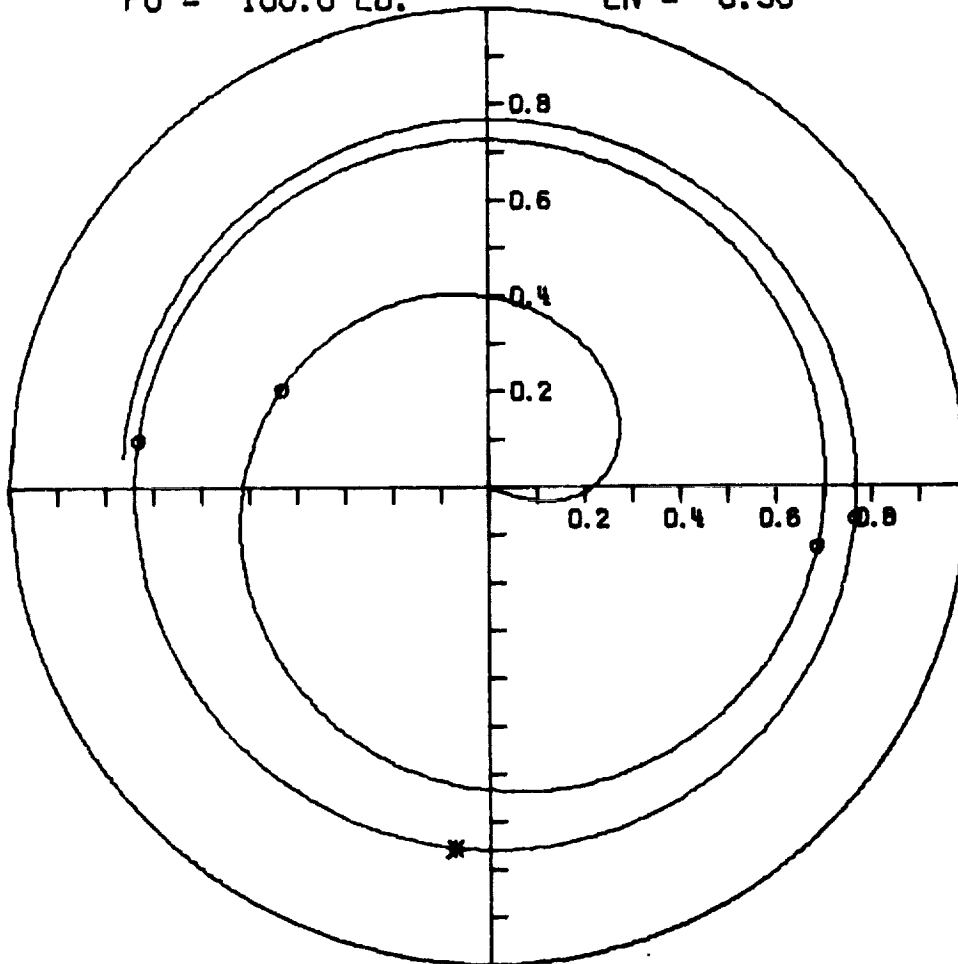
\*This is of course an average or mean value as discussed earlier for horizontal journal bearings.

# HORIZONTAL UNBALANCED ROTOR

NO.123081

N = 6500 RPM  
 A = 1.00 IN.  
 L = 1.00 IN.  
 C = 5.00 MILS  
 TASMAY = 10.00  
 S = 1.733  
 SS = 0.433  
 EMU = 0.001  
 SU = 289.111  
 TRDMAX = 1667.33  
 FO = 100.0 LB.

WT = 1.00  
 W = 50 LB.  
 MU<sub>5</sub> = 1.000 REYNS  
 FMAX = 499.8 LB. AND  
 OCCURS AT 3.50 CYCLE  
 WS = 2.45  
 ES = 0.211  
 FU = 0.30 LB.  
 FURATIO = 0.01  
 ESU = 0.001  
 EN = 0.50



6.57 Journal Orbit of an Unbalanced Horizontal Rotor Having a Forward Half-Frequency Rotating Load for 5 Cycles  
 (N = 6500, W = 50, C = 0.005, L/D = 1/2, EMU = 0.001, FO = 100, EN = -0.5)

# HORIZONTAL UNBALANCED ROTOR

NO. 123082

N = 6500 RPM

A = 1.00 IN.

L = 1.00 IN.

C = 5.00 MILS

TASMAX = 3.44

S = 1.733

SS = 0.433

EMU = 0.001

SU = 289.111

TADMAX = 573.56

FO = 100.0 LB.

WT = 1.00

W = 50 LB.

MU<sub>S</sub> = 1.000 REYNS

FMAX = 171.9 LB. AND

OCCURS AT 0.32 CYCLE

WS = 2.45

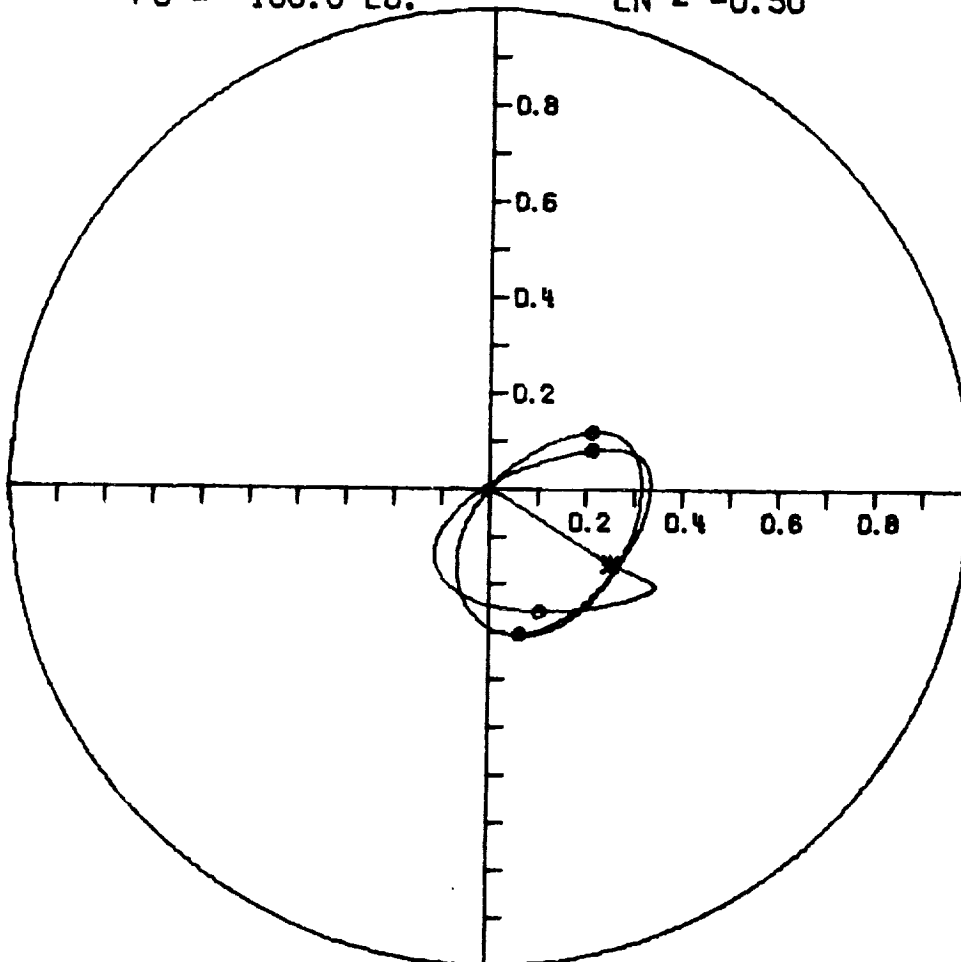
ES = 0.211

FU = 0.30 LB.

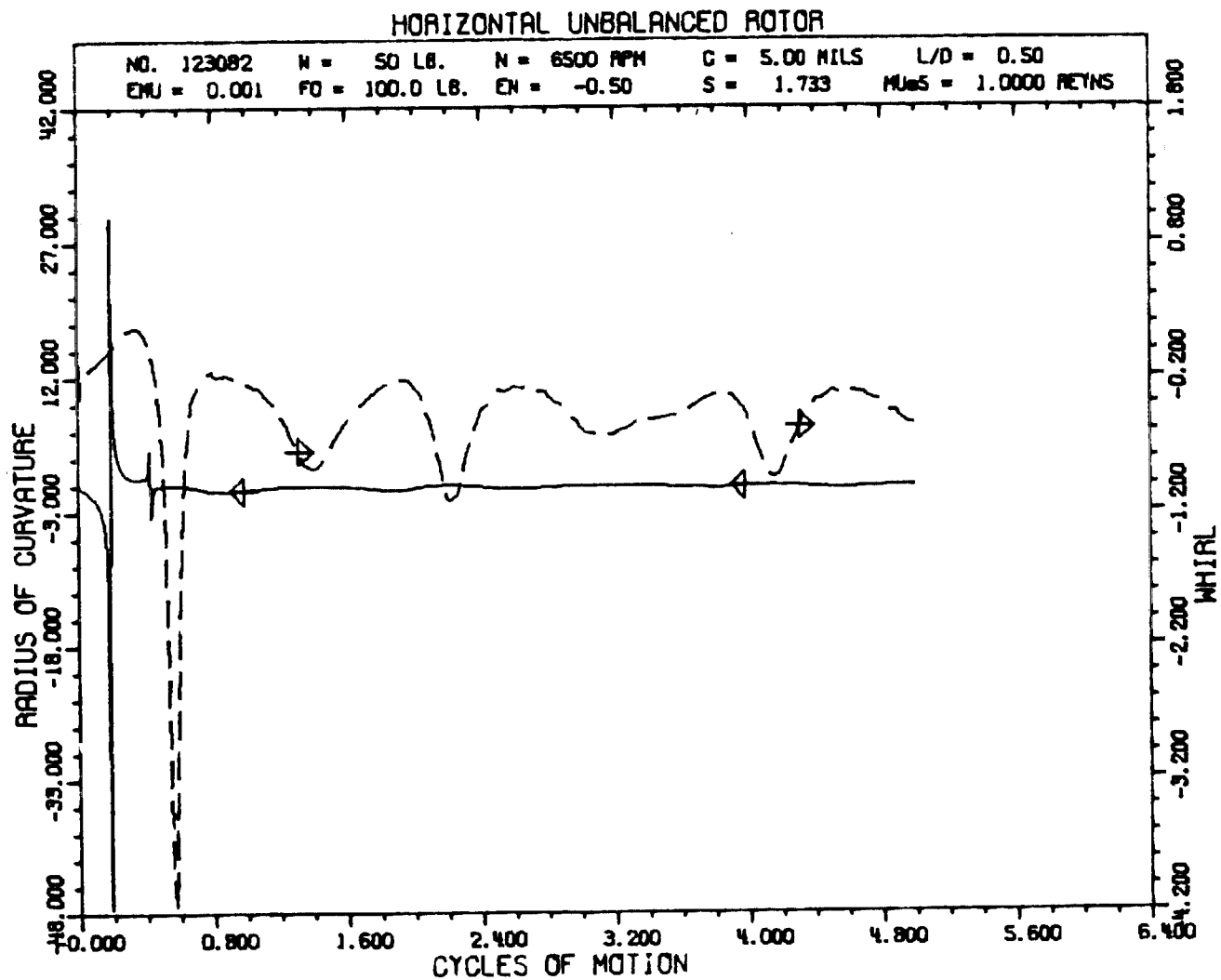
FURATIO = 0.01

ESU = 0.001

EN = -0.50



6.58 Journal Orbit of an Unbalanced Horizontal Rotor Having a Backward Half-Frequency Rotating Load for 5 Cycles (N = 6500, W = 50, C = 0.005, L/D = 1/2, EMU = 0.001, FO = 100, EN = -0.5)



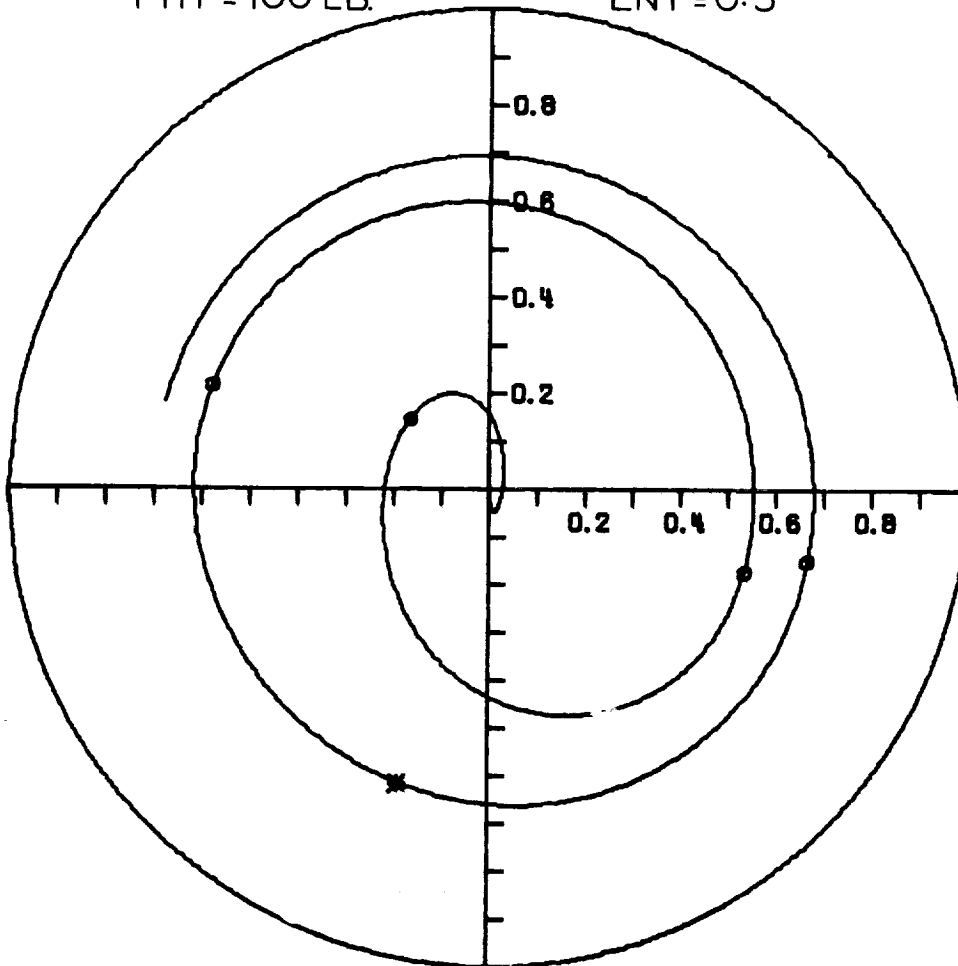
6.59 Radius of Curvature and Whirl vs Cycles of Motion  
(FO = 100, EN = 0.5)

# HORIZONTAL UNBALANCED ROTOR

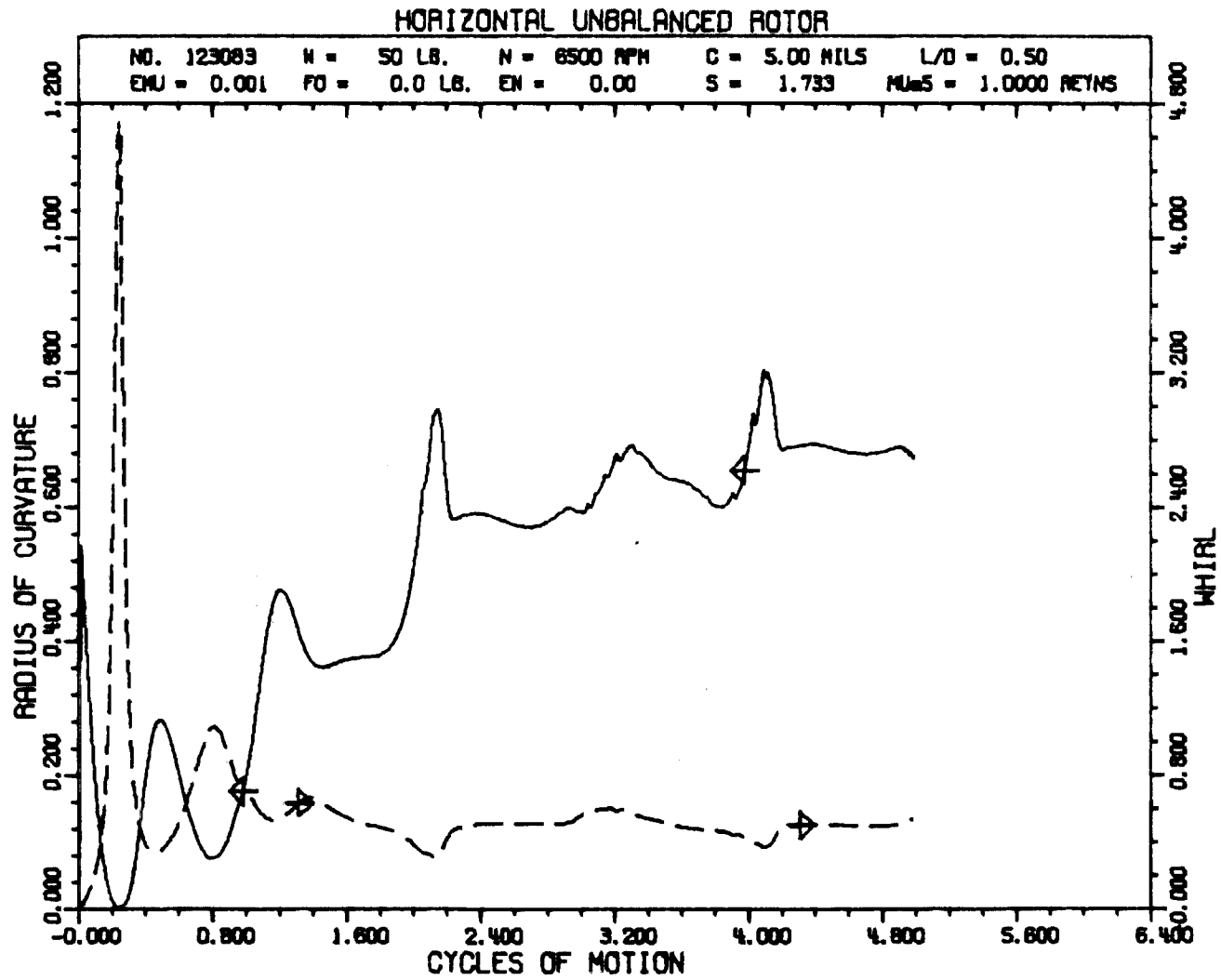
NO. 123083

N = 6500 RPM  
R = 1.00 IN.  
L = 1.00 IN.  
C = 5.00 MILS  
TRSMAX = 4.13  
S = 1.733  
SS = 0.433  
EMU = 0.001  
SU = 289.111  
TADMAX = 688.45  
FHY = 100 LB.

WT = 1.00  
W = 50 LB.  
MUS = 1.000 REYNS  
FMAX = 206.4 LB. AND  
OCCURS AT 3.43 CYCLE  
WS = 2.45  
ES = 0.211  
FU = 0.30 LB.  
FURATIO = 0.01  
ESU = 0.001  
ENY = 0.5



6.60 Journal Orbit of an Unbalanced Horizontal Rotor Having Unidirectional Harmonic Loading for 5 Cycles (N = 6500, W = 50, C = 0.005, L/D = 1/2, EMU = 0.001, FHY = 100, ENY = 0.5)



6.61 Radius of Curvature and Whirl vs Cycles of Motion  
(FHY = 100, ENY = 0.5)

and continue the whipping motion. Figure 6.61 indicates a mean value of 0.5 for the whirl under these conditions.

It would be impossible to include examples of all variations of the loading functions possible with the present program makeup, not to mention the capability of reading force values from data cards into the program for each increment of dimensionless time,  $T$ .

The purpose of this section, as stated earlier, was to give an indication of the possibilities that a program of this type has for practical use in the design of journal bearing for arbitrary loading. The average cost per case on the Burroughs B5500 has been approximately ten dollars, including plotting costs. Two and one-half minutes processor time and one and three-fourths minutes I/O time have been required per case on the Burroughs machine. The automatic plotting feature of the program makes the data reduction the easiest part of the job, instead of the hardest.

CHAPTER VII  
SUMMARY OF BASIC ASSUMPTIONS AND RESULTS;  
SUGGESTIONS FOR EXTENDING THE ANALYSIS

7.1 Discussion of Assumptions

The derivation of Reynolds' equation in CHAPTER III was based on the following standard assumptions:

1. The flow is laminar everywhere in the fluid.
2. The shear stress is related to the shear rate by the viscosity of the fluid (Newtonian fluid) which is constant across the film.
3. Body forces are neglected (i.e. weight of fluid in the film is small in comparison to the other forces acting there).
4. The inertia forces are neglected due to the modified Reynolds number being much less than unity,  $\frac{\rho UL}{\mu} \left[ \frac{h}{L} \right]^2 \ll 1$
5. The pressure across the film is constant.
6. The density of the fluid is a constant.

Reynolds' equation for the plane slider bearing was then modified for the journal bearing configuration in rotating coordinates by considering the linear combinations of the effects of rotation, radial motion, and precession. Reynolds' equation was derived for the journal bearing in fixed x-y coordinates by expressing unit vectors and reducing the tangential velocities to the fixed coordinate set. In so doing the small angle assumption was used to express sine and tangents as their radian value. The journal bearing equation was then reduced to the short bearing equation by neglecting the radial flow

due to pressure gradients, this required the restriction that  $L/D$  be less than unity, as verified by Figure 3.4.

The exact nature of this assumption is not readily apparent from looking at the Reynolds' equation. To better understand the meaning of this assumption Equation 3.9 should be examined. Letting  $x = R\theta$ , that equation can be expressed as:

$$u(y) = \frac{1}{2\mu R} \frac{\partial P}{\partial \theta} \times y(y-h) + \frac{h-y}{h} u_1 + \frac{y}{h} u_2 \quad [7.11]$$

It should be apparent that the circumferential fluid flow is not zero just because the expression containing  $\partial P/\partial \theta$  is omitted. The contributions due to the relative motion of the surfaces and the squeeze film effect which result from integrating the continuity equation are not lost by the short bearing assumption.

The equations of motion for the journal were next derived by considering Newton's second law. Gyroscopic effects, angular acceleration or shaft misalignment were not accounted for and therefore the equations of motion reduced to two coupled, second-order nonlinear differential equations. These equations were then solved by numerical methods for the resulting transient journal motion as presented in the previous chapter.

## 7.2 Discussion of Results and Conclusions

This analysis has proven the feasibility of incorporating fixed cartesian coordinates in the study of journal bearings instead of using the standard rotating coordinates. This makes the extension of a rotor dynamics program to include fluid film bearings very simple since,

without doubt, cartesian coordinates are the standard coordinate set used in rotor-shaft analyses and therefore the extension would not require a complicated transformation between coordinate sets.

The modified stability maps presented as Figures 6.14 and 6.15 are of great importance when considering the design of journal bearings that are operating under external loading or those that are used for a particular application where the system axial coordinate might be inclined at an angle to the horizontal. Figure 6.14 indicates clearly that the region of instability increases as the system is tilted from the horizontal and the balanced vertical unloaded journal is unstable for all speeds of operation as indicated by Figure 6.15.

The constant external loading has been shown to stabilize the journal with far less total load than indicated as necessary by the stability map of Badgley (30), (Fig. 4.2). The example given in CHAPTER VI clearly illustrated that a 150 pound external load would stabilize the 50 pound rotor, whereas the stability map of Badgley (30) indicates that the only way to stabilize the system is to increase the equilibrium eccentricity to a value greater than about 0.73, as illustrated by Figure 6.11. The system was shown to be very stable at an eccentricity of 0.395 under the external load, as shown in Figure 6.13 and predicted by Figures 6.14 and 6.15.

The orbits of the unbalanced vertical journal indicate that a certain degree of unbalance is desirable to reduce the magnitude of the journal motion and bearing forces transmitted. The large limit cycle of the balanced vertical journal could excite unwanted modes of shaft vibration in an actual system. It is of interest to note that

the addition of unbalance can greatly reduce the magnitude of the limit cycles encountered with vertical balanced rotors and also keep the forces transmitted to a lower value than that of a perfectly balanced shaft (See Figures 6.17 and 6.33 for example).

The horizontal journal, in all cases tested, did not have the static or dynamic transmissibility below a value of one at any time. Figure 6.50 was the only plot presented of the phase angle between the unbalance and the journal center displacement. Two important conclusions can be obtained from this plot for the unbalanced horizontal rotor. Figure 6.47 shows the resultant synchronous limit cycle of the journal center but the phase angle in Figure 6.50 has a substantial variation in magnitude. Many investigators assume a constant phase angle to reduce the labor involved in obtaining closed-form solutions for less complex rotor simulations. This single plot clearly indicates that this assumption is not valid. One other important aspect of this plot is the fact that the phase angle is oscillating about the approximate value of  $90^\circ$ . Gunter (42) explains that when the phase angle does not or cannot go through a complete  $180^\circ$  inversion, large resultant forces are transmitted to the support system.

Unbalance in a horizontal journal is highly undesirable and should always be reduced to the lowest possible value. The vertical journal, however, requires the proper unbalance level to allow the system to operate at a low amplitude limit cycle. The conclusions regarding the stability of the vertical journal are listed at the end of section 6.4.1. The most desirable design for a vertical journal should have the unbalance level (EMU) just above 0.16 while the speed parameter  $\omega_s$

should be less than 2.5. Under these conditions, the journal should exhibit small synchronous limit cycles and in some instances the dynamic transmissibility will reduce to a value below unity.

The transmissibility plots have shown the cyclic nature of the large resultant forces being transmitted to the bearing due to unbalance of the journal. This could shorten the life of the bearing surface considerably due to fatigue pitting and hence the loss of the load carrying capacity of the bearing. However, as noted previously, the proper unbalance level is necessary in a vertical journal to reduce the journal motion and the forces transmitted to the bearing surface.

The concept of whirl has been derived and the plots of this quantity indicate that a constant value of whirl cannot exist in a horizontal journal (rotor), but can give the orbit the appearance of a constant whirl due to the averaging of the cyclic nature. The vertical balanced journal was the only configuration that gave a constant whirl ratio.

The developed program has shown the ability to predict journal orbits under various types of external cyclic loading functions and leaves no doubt as to the capability of the program to track arbitrary forcing functions. If the forcing function can be approximated by an analytic expression, then the program may be easily modified to incorporate this loading by changing a single card, otherwise a procedure will have to be added to the present program to read data cards containing values of force for each increment of time the solution will track. The later process would present some difficulty but any arbitrary time dependent forcing function could be incorporated

in the program if desired.

With the more advanced methods of data display available to researchers, the time required for the analysis of computer output has been greatly reduced. This fact permits complex systems to be simulated at a reasonable cost and within a minimum amount of time. Numerical methods that were considered impractical several years ago are now being used very effectively due to the speed and accuracy of the modern digital computers. This fact is of great importance to the practicing engineer due to the widespread availability of teletype terminals which provide easy access to large time-sharing computers at a reasonable cost to the user.

### 7.3 Suggestions for Extending the Analysis

The present analysis may be easily extended to include bearings mounted in flexible, damped supports. This extension would require the addition of two more equations of motion to represent the support motion. The analysis by Gunter (7) and experimental investigations of Tondl (43) indicate that bearing stability may be considerably improved by mounting the bearing in a damped, flexible support system.

One feature of the present program that was not considered in this discussion was the retainer stiffness and damping terms. These quantities should considerably increase the stability of the system if their values were properly chosen.

The conclusions presented in section 6.4.1 concerning the effect of unbalance on the vertical rotor could be extended or corrected by a more extensive study. The trend observed in the limited number of cases

presented in CHAPTER VI indicate that the behavior of an unbalanced journal can be predicted.

The present program has recently been modified to include only the squeeze-film effect of the bearing, which has application in regards to oil-filled clearances being designed into ball bearing supports to help reduce the vibration level of the system.

The effect of journal angular acceleration and varying torque loads would provide some very interesting transient journal motions and would increase the understanding of the rotor orbits being observed in experimental test rigs. The behavior of rotors under extremely high acceleration rates is of great concern at present due to the requirements of the space vehicle boosters. A tremendous amount of energy must be developed in only a few seconds to enable the booster to lift the payload from the launch pad. A better understanding of acceleration rates on rotor behavior could further the understanding of and, hopefully, reduce the vibrations that have been encountered by the astronauts during the initial stage of their flights.

Most analyses to date that have been performed on rotor systems have assumed simple supports or linear relations for the bearings. The present equations in the fixed coordinates could easily be included in such an analysis to give a much better prediction as to the actual system behavior.

Finally, for a complete analysis, the bearing should include considerations for misalignment in addition to rotor angular acceleration, torque, gyroscopic effects, and the forces as predicted by Alford (29). This would then be an integral part of an n-bearing

station, multi-mass, flexible rotor system. This solution will indeed be of great interest to everyone in this field of research.

## BIBLIOGRAPHY

1. Pinkus, O., and Sternlicht, B., Theory of Hydrodynamic Lubrication, McGraw-Hill, New York, 1961.
2. Fuller, D. D., Theory and Practice of Lubrication for Engineers, John Wiley and Sons, Inc., New York, 1963.
3. Reynolds, O., "On the Theory of Lubrication and Its Application to Mr. Beauchamp Tower's Experiment, Including an Experimental Determination of the Viscosity of Olive Oil," Phil. Trans. Roy. Soc., London, Vol. 177, Part 1, 1886, pp. 157-234.
4. Newkirk, B. L., "Shaft Whipping," Gen. Elec. Rev., Vol. 27, 1924, p. 169.
5. Harrison, W. J., "The Hydrodynamic Theory of Lubrication with Special Reference to Air as Lubricant," Trans. Cambridge Phil. Soc., Vol. 22, 1913, p. 39.
6. Badgley, R. H., "Turborotor Instability--Dynamic Unbalance, Gyroscopic, and Variable-Speed Effects with Finite-Length, Cavitated, Fluid-Film Bearings," unpublished Ph.D. thesis, Cornell University, 1967, p. 5.
7. Gunter, E. J., "Dynamic Stability of Rotor-Bearing Systems," NASA SP-113, 1966.
8. Newkirk, B. L., and Taylor, H. D., "Shaft Whipping Due to Oil Action in Journal Bearings," Gen. Elec. Rev., Vol. 28, 1925, pp. 985-988.
9. Robertson, D., "Whirling of a Journal in a Sleeve Bearing," Phil. Mag., Series 7, Vol. 15, 1933.
10. Cardullo, S. E., "Some Practical Deductions from the Theory of Lubrication of Short Cylindrical Bearings," Trans. ASME, Vol. 52, Paper No. MSP-52-12, 1930, pp. 143-153.
11. Sommerfeld, A., "Zur hydronamischen Theorie der Schmiermittreibung," Zeitschrift fur Mathematik und Physik, Vol. 50, 1904.
12. Hagg, A. C., "The Influence of Oil Film Journal Bearings on the Stability of Rotating Machines," J. Appl. Mech., Vol. 68, 1946, p. 211.
13. Ocvirk, F. W., "Short-Bearing Approximation for Full Journal Bearings," NACA TN 2808, 1952.

14. Burwell, J. T., "The Calculated Performance of Dynamically Loaded Sleeve Bearings-III," Journal of Applied Mechanics, Vol. 18, Trans. ASME, Vol. 73, 1951.
15. Poritsky, H., "Contribution to the Theory of Oil Whip," Trans. ASME, Aug. 1953, pp. 1153-1161.
16. Hagg, A. C. and Warner, P. C., "Oil Whip of Flexible Rotors," Trans. ASME, Oct. 1953, pp. 1339-1344.
17. DuBois, G. B., and Ocvirk, F. W., "The Short Bearing Approximation for Plain Journal Bearings," Trans. ASME, Vol. 78, 1955, pp. 1173-1178.
18. Kreisle, L. F., "Very Short Journal-Bearing Hydrodynamic Performance Under Condition Approaching Marginal Lubrication," Trans. ASME, Vol. 78, 1955, pp. 955-963.
19. Newkirk, B. L., and Lewis, J. F., "Oil-Film Whirl--An Investigation of Disturbances Due to Oil Films in Journal Bearings," Trans. ASME, Jan. 1956, pp. 21-27.
20. Boeker, G. F., and Sternlicht, B., "Investigation of Translatory Fluid Whirl in Vertical Machines," Trans. ASME, Vol. 78, 1956, pp. 13-20.
21. Hagg, A. C., and Sankey, G. O., "Some Dynamic Properties of Oil-Film Journal Bearings with Reference to the Unbalance Vibration of Rotors," Journal of Applied Mechanics, Trans. ASME, Vol. 78, 1956, pp. 302-306.
22. Newkirk, B. L., "Varieties of Shaft Disturbances Due to Fluid Films in Journal Bearings," Trans. ASME, Vol. 78, 1956, pp. 985-988.
23. Pinkus, O., "Experimental Investigation of Resonant Whip," Trans. ASME, Vol. 78, 1956, pp. 975-983.
24. Orbeck, F., "Theory of Oil Whip for Vertical Rotors Supported by Plain Journal Bearings," Trans. ASME, Oct. 1958, pp. 1497-1502.
25. Hull, E. H., "Oil Whip Resonance," Trans. ASME, Vol. 80, 1958, pp. 1490-1496.
26. Hori, Y., "A Theory of Oil Whip," Journal of Applied Mechanics, Trans. ASME, June 1959.
27. Sternlicht, B., "Stability and Dynamics of Rotors Supported on Fluid-Film Bearings," Paper 62-WA-190, for meeting Nov. 25-30, 1962.
28. Reddi, M. M. and Trumpler, P. R., "Stability of High-Speed Journal Bearings Under Steady Load-1. The Incompressible Film," Journal of Engineering for Industry, Trans. ASME, Vol. 84, 1962.

29. Alford, J. S., "Protecting Turbomachinery From Self-Excited Rotor Whirl," Trans. ASME, Journal of Eng. for Power, Vol. 87, No. 4, Oct. 1965, pp. 333-344.
30. Badgley, R. H., and Booker, J. F., "Turborotor Instability--Effect of Initial Transients on Plane Motion," Paper No. 68-Lub-7, Presented at ASME-ASLE Lubrication Conference, Oct. 8-10, 1968.
31. Tolle, G. C., and Muster, D., "An Analytic Solution for Whirl in a Finite Journal Bearing with a Continuous Lubricating Film," Paper 69-Vibr-55, Presented at ASME Vibrations Conference, March 30-April 2, 1969.
32. Radzimovsky, E. I., Lubrication of Bearings, The Ronald Press Company, New York, 1959.
33. Fuller, D. D., Theory and Practice of Lubrication for Engineers, John Wiley and Sons, Inc., 1963.
34. Conte, S. D., Elementary Numerical Analysis, McGraw-Hill Book Company, Inc., New York, 1965.
35. Crandall, S. H., Engineering Analysis, McGraw-Hill Book Company, Inc., New York, 1956.
36. Scarborough, J. B., Numerical Mathematical Analysis, The John Hopkins Press, Baltimore, 1958.
37. Bisson, E. E., and Anderson, W. J., "Advanced Bearing Technology," NASA SP-38, 1965.
38. Scheid, F., Theory and Problems of Numerical Analysis, Schaum's Outline Series, McGraw-Hill Book Company, Inc., New York, 1968.
39. Pixley, A. F., and Macek, A. G., "Milne Method-Solution of a System of First Order Ordinary Differential Equations," Mathematical Report Series, MRS-129, 1964.
40. Pixley, A. F., and Macek, A. G., "Hamming Method-Solution of a System of First Order Ordinary Differential Equations," Mathematical Report Series, MRS-126, 1964.
41. Pixley, A. F. and Macek, A. G., "Runge-Kutta-Nystrom Starting Procedure for Use with Milne Type Predictor-Correctors in Solving Systems of Ordinary Differential Equations," Mathematical Report Series, MRS-113, 1963.
42. Gunter, E. J., Private communication.
43. Tondl, A., Experimental Investigations of Self-Excited Vibrations of Rotors Due to the Action of Lubricating Oil Film in Journal Bearings, Wear, 5, 1962, pp. 136-147. (The National Research Institute of Heat Engineering, Prague, Czechoslovakia)

APPENDIX A

Listing of the Computer Program to Plot the Pressure Profiles,  
Pressure Surfaces, and the Film Thickness for the Short  
Journal Bearing (with a sample of the line printer output)



```

BEGIN
ROCLEAN CAVITATE,CIRCLE,FILMTHICK ;
INTEGER N1,I,J;
REAL CDY ;
REAL H,H3;
REAL PI2,DEL,KK<,ZB, X,XV,Y,YV,COSKK,SINKK,ANGX,ANGY
REAL YMIN, DY ;
ARRAY HH(0:80) ;
ARRAY CX,CY,PX,PY,HP(0:80) ;
ARRAY COSK,SINK(0:80),P(0:30,0:80),LENGTH(0:30),GRIDX,GRIDY
[0:80,0:80],THETA(0:80) ;
LABEL ACAMD,ALDONE ;
PLOT(0,0,-4) ; PLOT(4,2,-5) ;
ACAMD;
READ (CR,/,N1)[ALLDONE];
READ (CR,/, X,XV,Y,YV);
READ (CK,/,CAVITATE,CIRCLE,FILMTHICK);
CDY ← 0 ;
PI2 ← 8 × ARCTAN(1);
DEL ← PI2/N1 ;
THETA(1) ← 0 ; THETA(N1+3) ← PI2 ;
FOR I ← 0 STEP 1 UNTIL N1 DO
BEGIN
KKK ← DEL × I ;
THETA(I+2) ← KKK ;
COSK(I) ← COS(KKK) ; SINK(I) ← SIN(KKK) ;
END ;
FOR I ← 0 STEP 1 UNTIL N1 DO
BEGIN
COSKK ← COSK(I) ; SINKK ← SINK(I) ;
H ← 1 - X × COSKK - Y × SINKK ;
HH(I+2) ← H/2 ;
H3 ← H×H×H ;
P(0,I+1) ← ((-X×SINKK+Y×COSKK+2×(XV×COSKK+YV×SINKK))/H3)
×3×PI2 ;
IF CAVITATE THEN
IF P(0,I+1) < 0 THEN P(0,I+1) ← 0 ;
IF P(0,I+1) > CDY THEN CDY ← P(0,I+1) ;
END ;
CDY ← CDY/12 ;
WRITE(LP,<
F5.2,M YV =M,F6.3,/,/, X,XV,Y,YV);
WRITE(LP,< 6(E10,3,X1),/,>,FOR I ← 0 STEP 1 UNTIL N1 DO(P(0,I+1)/4)
);
WRITE (LP(PAGE));
IF CIRCLE THEN
BEGIN
PLOT(0,4,-5);
FOR I ← 1 STEP 1 UNTIL 61 DO
BEGIN
CX(I) ← COSK(I-1) × 0.5 ;
CY(I) ← SINK(I-1) × 0.5 ;
END;
LYNE(CX,CY,61,1);
FOR I ← 1 STEP 1 UNTIL 61 DO HP(I) ← P(0,I) /4 ;
SCALE (HP,01,1.5,YMIN,DY,1);

```

```

FOR I + 1 STEP 1 UNTIL 61 DO
  BEGIN
    PXLII + HPLII * COS(KLI-1)+CXLI) ;
    PYLII + HPLII * SIN(KLI-1)+CYLI) ;
  END ;
  LYNE(PX,PY,61,1) ;
  FOR I + 1 STEP 1 UNTIL 61 DO
    BEGIN
      PLOT(CXLI),CYLI),3) ;
      PLOT(PXLI),PYLI),2) ;
    END ;
    PLOT(0,0,3) ;
    PLOT(0,-4,-5) ;
  END ;
  IF FILMTHICK THEN
    BEGIN
      PLOT(0,-1.5,-5) ;
      PLOT(0,1,3) ;
      PLOT(0,0,2) ; PLOT(PI2,0,2) ;
      PLOT(0,0,3) ;
      LYNE(THETA,Hh,63,1) ;
      PLOT(0, 1.5,-5) ;
    END ;
  IF NOT CAVITATE THEN
    SCALE(SCPI0,*J,61,0,CDY,1)
  ELSE
    SCALE(PCIO,*J,N1+1,16,YMIN,DY,1) ;
  IF NOT CAVITATE THEN PLOT(0,2,-5) ;
  NUMBRC(2.50,4.25,0.10,X ,0,2) ;
  NUMBRC(2.50,4.03,0.10,XV,0,3) ;
  NUMBRC(3.50,4.25,0.10,Y ,0,2) ;
  NUMBRC(3.50,4.03,0.10,YV,0,3) ;
  LENGTHI1 + 0 ; LENGTHI23 + 2 ;
  FOR I + 0 STEP 1 UNTIL 20 DO
    BEGIN
      ZB + 0.05 * I ;
      LENGTH I1+2 + ZB * 2 ;
      FOR J + 0 STEP 1 UNTIL N1 DO
        P1I+2,J+2 + ZB*(1-ZB)*P10,J+1) ;
      END ;
      ANGX + COS(PI2/8) ; ANGY + SIN(PI2/8) ;
      N1 + N1 + 3 ;
      FOR I + 1 STEP 1 UNTIL 23 DO
        FOR J + 1 STEP 1 UNTIL N1 DO
          BEGIN
            GRIDXCI,J + THETA(J) + LENGTHI1 * ANGX ;
            GRIDYCI,J + P1I,J + LENGTHI1 * ANGY ;
          END ;
        FOR I + 1 STEP 1 UNTIL 23 DO
          BEGIN
            PLOT(GRIDXCI,1),GRIDYCI,1),3) ;
            PLOT(GRIDXCI,1),GRIDYCI,1),2) ;
            FOR J + 2 STEP 1 UNTIL N1 DO
              PLOT(GRIDXCI,J),GRIDYCI,J),1) ;
            END ;
            PLOT(0,0,3) ;

```

```
FOR I ← 1 STEP 1 UNTIL 63 DO
BEGIN
  PLOT(GRIDX[1,I],GRIDY[1,I],3)
  PLOT(GRIDX[1,I],GRIDY[1,I],2)
FOR J ← 2 STEP 1 UNTIL 23 DO
  PLOT(GRIDX[J,I],GRIDY[J,I],1)
END
PLOT(0,0,3)
IF NOT CAVITATE THEN PLOT(0,-2,-5)
PLOT(15,0,-3)
GO TO ACARDU ;
ALLDONE:
END.
```

X = 0.50 XV = -0.050 Y = -0.70 YV = -0.050

0.000e+00	0.000e+00	0.000e+00	0.000e+00	0.000e+00	0.000e+00
0.000e+00	0.000e+00	0.000e+00	0.000e+00	0.000e+00	0.000e+00
0.000e+00	0.000e+00	0.000e+00	0.000e+00	0.000e+00	0.000e+00
0.000e+00	0.000e+00	0.000e+00	0.000e+00	6.604e-02	1.460e-01
2.318e-01	3.266e-01	4.343e-01	5.600e-01	7.097e-01	8.017e-01
1.117e+00	1.401e+00	1.763e+00	2.233e+00	2.853e+00	3.683e+00
4.811e+00	6.371e+00	8.561e+00	1.169e+01	1.624e+01	2.296e+01
3.301e+01	4.817e+01	7.100e+01	1.047e+02	1.519e+02	2.100e+02
2.624e+02	2.705e+02	1.896e+02	2.619e+01	0.000e+00	0.000e+00
0.000e+00	0.000e+00	0.000e+00	0.000e+00	0.000e+00	0.000e+00
0.000e+00					

APPENDIX B

The Short Journal Bearing

Computer Program Listing

(with a sample of the line printer output)

BEGIN  
COMMENT  
COMMENT

PROGRAM AS OF APRIL 4, 1969

THIS PROGRAM GIVES THE TRANSIENT SOLUTION OF A ROTOR -FLUID FILM BEARING SYSTEM. THE HYDRODYNAMIC FORCES IN X AND Y DIRECTIONS ARE CALCULATED IN CARTESIAN CO-ORDINATES.

THE EQUATIONS OF MOTION ARE REDUCED TO 4-FIRST ORDER DIFFERENTIAL EQUATIONS AND THEN THEY ARE SOLVED FOR TRANSIENT SOLUTION BY INTEGRATING FORWARD IN TIME BY 6TH ORDER RUNGE-KUTTA METHOD AS A STARTER AND THEN EXTENDED BY ADAMS-BASHFORTH-MOULTON PREDICTOR CORRECTOR METHOD IF GOEULER IS FALSE OR BY A MODIFIED EULER METHOD IF GOEULER IS TRUE.

AN OPTION FOR KEEPING ONLY EVERY KSF CALCULATION IS INCLUDED AS AN OPTION ON CARD 11 .

THE INPUT OF THE PROGRAM IS AS FOLLOWS:

CARD 1.

1. TMAX = NO. OF CYCLES OF ROTOR MOTION
2. H=(RADIAN), STEP INCREMENT.
3. N=NO. OF FIRST ORDER D.E. TO BE SOLVED.

CARD 2.

1. OMEGA = SPEED OF ROTOR (REV/MIN)
2. INCOMEGA = INCREMENT OF ROTOR SPEED (RPM)
3. NUINC = NO. OF INCREMENTS THIS SET OF DATA
4. COMEGA = SPEED OF JOURNAL + BEARING (RPM)

CARD 3.

1. EMU=DIMENSIONLESS UNBALANCE .
2. F0=MAGNITUDE OF APPLIED FORCE IN LBS.
3. EN = NUMBER REPRESENTING THE FRACTION OF THE ANGULAR FREQUENCY OF THE ROTOR OF THE APPLIED FORCE
4. FUCX = CONSTANT FORCE IN THE X-DIR.
5. FUCY = CONSTANT FORCE IN THE Y-DIR.
6. FHX = HARMONIC FORCE IN X-DIR.
7. ENX = FRACTION OF ROTOR ANG. FREQ OF FHX
8. FHY = HARMONIC FORCE IN Y-DIR.
9. ENY = FRACTION OF ROTOR ANG. FREQ OF FHY

CARD 4.

1. CL=CLEARANCE BETWEEN JOURNAL AND BEARING (INCH).
2. R=RADIUS OF THE JOURNAL (INCH).
3. L=LENGTH OF THE BEARING (INCH).
4. W=WEIGHT OF THE ROTOR (LBS).
5. MU=VISCOSITY OF THE LUBRICANT (REYNS).
6. HORIZ = BOOLEAN = TRUE FOR HORIZONTAL ROTOR AND FALSE FOR VERTICAL ROTORS

CARD 5.

1. KRX = RETAINER SPRING RATE IN X-DIR.
2. DNX = RETAINER DAMPING FACTOR IN X-DIR.
3. KRY = RETAINER SPRING RATE IN Y-DIR.
4. DRY = RETAINER DAMPING FACTOR IN Y-DIR.

CARD 6.

1. INITIAL TIME.
2. INITIAL X-DISPLACEMENT.
3. INITIAL X-VELOCITY.
4. INITIAL Y-DISPLACEMENT.
5. INITIAL Y-VELOCITY.

CARD 7.

1. N1 = INTEGER TO BE USED IN WEDDLES RULE INTEG. CIT

```

                MUST BE A MULTIPLE OF SIX(6) )
2. RELAX = RELAXATION FACTOR ≤ 1
CARD 8. - PLOTTER CONTROL , 0 = NO PLOT, 1 = PLOT
CARD 9.
    1. PLOT1 = TRUE FOR ORBIT PLOT
    2. PLOT2 = TRUE FOR TRS PLOT
    3. PLOT3 = TRUE FOR WHIRL PLOT
    4. PLOT4 = TRUE FOR PHASE PLOT
        NOTE: ALL VARIABLES ON CARD 9 ARE BOOLEAN
CARD 10. CASE NUMBER - MONTH-DAY-YEAR-NUMBER , WDY,CND
CARD 11.
    KSF = SKIP FACTOR FOR SMALL STEP INCREMENT
        KSF = 2 TMAX x 6.28 / ( H x 900 ) -----
CARD 12.
    1. RK6LIM = NO. OF TIMES RK6 STARTER IS TO BE USED (24)
    2. GUEULER = BOOLEAN CONTROL. IF TRUE THEN THE SOLUTION
        IS EXTENDED BY THE EULER METHOD, ELSE BY ADAMS .

```

SAMPLE DATA

```

5 IMAX(CYCLES),0.10 H , 4 N,
400 OMEGA SPEED, 0 SPEED INC., 0 NO. OF INC., 400 COMEGA ,
0 EMU , 0 FN , 0 EN,-45000 FOCY,0 FUCY,-40000 FHX,1 ENX,17500 FHY, 3 ENY ,
0.0112 (L,9.7597 K,4.125 L,1000 W,1.48-6 MU ,1 HDRIZ ,
0 KRX,0 DKX ,0 KRY ,0 DRY ,
0 T ,-.65 X ,0 UX ,0 Y ,0 DY ,
50 N1 , 0.50 RELAX ,
    1 PLOT ,
    1 ORBIT ,1 TRS PLOT ,1 WHIRL ,1 PHASE ,
228091 CASE NO. , 22869 WDY , 1 CND ,
2 KSF ,
4 RK6LIM , 1 GUEULER ,

```

---REPEAT THE SERIES FOR EACH CASE ---

```

FORMAT DUT1('EQUIL. POS. = ',F7.4,X10,'FMAX =',F11.4,/,
MS =',F11.4,X17,'TRSMAX =',F11.4,/,
MSS =',F11.4,X16,'MFOCX =',F11.4,/,
MWS =',F11.4,X16,'MFOCY =',F11.4,/,
MPHKG =',F11.4,/.
X31,'MFHX =',F11.4,X2,'MAND ENK =',F6.2,/,
X31,'MFHY =',F11.4,X2,'MAND ENY =',F6.2,/)
FORMAT OUT2 ('EQUIL. POS.(UNBALANCE) =',F 7.4,/,
        MSU =',F11.4,/,
        MFU =',F11.4,/,
MFKRATIO =',F11.4,/,,'TRDMAX =',F11.4,/)
REAL PRX,PRY,T2X,T2Y
REAL EMAX,ET,HMIN,TEMAX,HANGLE
REAL AWT
REAL FOCY,FOCY,<5,K6
REAL SINKK,COSKK
REAL KB,ALFD,ASS,YVIN1,DY1,E,PEC,PES,MDY,CND,T
REAL CONST1
REAL NMXH
REAL
XMIN,YMIN,UX,DY,EMU,EN,K1,K2,K3, W, G,M,COMEGA,OMEGA,R,L,MU,FO,CL,
TMAX,H,PI,FX,FY)

```

```

REAL K4, N0 ;
REAL HX12, ACX,ACY ;
REAL FIR,INCH,ANSI,SSU,DL2 ;
REAL INCOMEGA,K7,K8,K9,K10,K11,K12,FHX,FHY,ENX,ENY,
KRX, DRX,KRY,DKY,JOUKANG ;
REAL FX1,FY1 ;
REAL EE,EF,ANS ;
REAL PI2,DEL ;
REAL KKK ;
REAL TRSMAX, TRDMAX ;
REAL S,SS,SU,FU,FURATIO,FRRG,FMAX,WS ;
REAL RELAX,IMAXI ;
REAL H024 ;
INTEGER NF,NS,NP ;
INTEGER KSF,KC ;
INTEGER NM ;
INTEGER K ;
INTEGER CIRPT ; REAL NUMB ;
INTEGER CASENU ;
INTEGER NUINC ;
INTEGER Q ;
INTEGER J1,J2,J3,J4,J5,J6,J7 ;
INTEGER INCUFAR ;
INTEGER VV,CS,N1,I,J,NA,N ;
INTEGER RKOLIM, NUMERINSTAB ;
INTEGER II ;
BOOLEAN FAIL ;
BOOLEAN GUEULER, NUMSTAB ;
BOOLEAN HORIZ,PLOT1,PL0T2,PLUT3,PL0T4 ;
BOOLEAN BLW ;
BOOLEAN ISCALF ;
  ALPHA ARRAY ALPHA1,ALPHA2[0:2] ;
  ALPHA ARRAY ALP1,ALP2,ALP3,ALP4,ALP5,ALP6,ALP7,ALP8,ALP9,ALP10,
ALP11,ALP12,ALP13,ALP14,ALP15,ALP16,ALP17,ALP18,ALP19,ALP20,
ALP21,ALP22,ALP23,ALP24[0:3] ;
  ALPHA ARRAY ALP25,ALP31,ALP32,ALP33[0:2],ALP26,ALP27,ALP28,ALP29,
ALP30[0:5] ;
  ALPHA ARRAY ALP34,ALP35[0:3] ;
  ALPHA ARRAY ALP36,ALP37[0:5] ;
  ALPHA ARRAY ALP40,ALP41,ALP42,ALP43[0:4] ;
  ALPHA ARRAY ALP44[0:1] ;
  ALPHA ARRAY ALP45,ALP46,ALP47,ALP48[0:1],ALP49[0:3] ;
  ALPHA ARRAY ALP50,ALP51[0:2] ;
  ARRAY RKDX,RKTEMPY,RKK1,RKK2,RKK3,RKK4,RKK5,RKK6[0:5] ;
  REAL ARRAY A,B,C[0:4],Y[0:4],
P,PX,PY[0:400] ;
  REAL ARRAY AY[0:12,0:950] ;
  ARRAY RKAY [0:2,0:4] ;
  ARRAY CX,CY[0:300] ;
  ARRAY SINK,CUSK[0:400] ;
  ARRAY TX,TY[0:3,0:8] ;
  LABEL MONGEMORE,SKIPI ;
  LABEL UNCEMURE,SKIP ;
  LABEL SPEEDLOO ;
  LABEL ALLDUNE,ACARD ;

```

```

4 THE FOLLOWING PROCEDURE ALLOWS EVERY KSF TERM CALCULATED TO BE
4 IN THE FINAL VALUES RETAINED FOR PRINTING .
PROCEDURE SWITCHGD (CONT1); BOOLEAN CONTI ;
BEGIN
  INTEGER F,JJ,L,MS ;
  IF CONTI THEN
    K ← K-5 ;
    P ← KK + KSF ;
    IF KK ≤ 0 THEN KK ← 0 ;
    FOR JJ ← P STEP KSF UNTIL K DO
      BEGIN
        KK ← KK + 1 ;
        FOR LL ← 0 STEP 1 UNTIL 10 DO
          AY(LL, KK) ← AY(L, JJ) ;
        END ;
      IF CONTI THEN
        BEGIN
          K ← K + 5 ; MS ← K - 4 ;
          FOR JJ ← MS STEP 1 UNTIL K DO
            BEGIN
              KK ← KK + 1 ;
              FOR LL ← 0 STEP 1 UNTIL 10 DO
                AY(LL, KK) ← AY(L, JJ) ;
              END ;
            END ;
          K ← KK ; IF CONTI THEN KK ← KK - 5 ;
        END OF SWITCHGD ;

```

```

REAL PROCEDURE ANGLE(PN, PD) ;
COMMENT THIS REAL PROCEDURE CALCULATES THE ANGLE IN RADIAN WHEN THE
OPPOSITE SIDE AND RASE OF THE TRIANGLE IS KNOWN. PN IS THE NUMERATOR
AND PD IS THE DENOMINATOR;
VALUE PN , PD ; REAL PN, PU ;
BEGIN
  REAL B , PI ;
  LABEL L1 , L2 , L3 , L4 ;
  PI ← 3.14159 ;
  IF PN > 0 AND PD = 0 THEN GO TO L1 ;
  IF PN < 0 AND PU = 0 THEN GO TO L2 ;
  IF PN = 0 AND PD = 0 THEN GO TO L3 ;
  R ← ARCTAN(ABS(PN/PD)) ;
  IF PN < 0 AND PD > 0 THEN B ← 2 × PI - B ;
  IF PN > 0 AND PD < 0 THEN B ← PI - B ;
  IF PN < 0 AND PU < 0 THEN B ← PI + B ;
  GO TO L4 ;
L1: B ← PI/2 ;
GO TO L4 ;
L2: B ← 3 × PI / 2 ;
GO TO L4 ;
L3: B ← 0 ;
L4: ANGLE ← B ;
END OF PROCEDURE ;
PROCEDURE TELLTIME(Q) ;
FILE Q ;
BEGIN OWN INTEGER PR1, IO1, EL1, TOG ; INTEGER PR2, IO2, EL2, P, I, E ;

```

```

LIST L((P*90+I*45)/3600,P DIV 60,P MOD 60,I DIV 60,I MOD 60,
      E DIV 60,E MOD 60);
FORMAT F(I,J)(/),*THE COST OF THIS RUN WAS $*,F6.2,10(/),
*PROCESSOR TIME =*,I3,* MINUTES AND *,I2,* SECONDS*,5(/),
M/D TIME =*,I3,* MINUTES AND *,I2,* SECONDS*,5(/),
*ELAPSED TIME =*,I3,* MINUTES AND *,I2,* SECONDS*);
IF TOG#-69 THEN
  BEGIN   TOG#-69; EL1+TIME(1); PRI+TIME(2); IO1+TIME(3)   END
        ELSE
  BEGIN EL2+TIME(1); PR2+TIME(2); IO2+TIME(3); P+((PR2-PRI)/60;
        I+(IO2-IO1)/60; E+(EL2-EL1)/60; WRITE(Q,F,L);   END;
END OF THE TELLTIME PROCEDURE;

PROCEDURE RKSTARTS (K,NF,X1,H,Y,F,DX,TEMPY,K1,K2,K3,K4,K5,K6);
  VALUE K,NF,HJ,REAL X1,HJ,INTEGER K,NF,JAR
  RAY Y(0,0)JARRAY DX,TEMPY,K1,K2,K3,K4,K5,K6(0);
  PROCEDURE FJBEGIN INTEGER I,J,REAL X;
    FOR I+0STEP IUNTIL(NF-1)DO BEGIN X+H*X1+X1JF(X,YI,+J,DX)JF
    NR J+1STEP IUNTIL K DO BEGIN K1(IJ)+DX(IJ)XHJTEMPY(IJ)+K1(IJ)/3.0+YI,JJEND;
    F(H/3.0+X,TEMPY,DX)JFOR J+1STEP IUNTIL K DO BEGIN K2(IJ)+DX(IJ)XHJTEMPY(IJ)
    +(K2(IJ)*6.0+K1(IJ)*4.0)/25.0+YI,JJEND;F((H*2.0)/5.0+X,TEMPY,DX)JFOR J+1S
    TEP IUNTIL K DO BEGIN K3(IJ)+DX(IJ)XHJTEMPY(IJ)+(K3(IJ)*15.0-K2(IJ)*12.0+K1(IJ
    ))/4.0+YI,JJEND;F(H+X,TEMPY,DX)JFOR J+1STEP IUNTIL K DO BEGIN K4(IJ)+DX(I
    J)XHJTEMPY(IJ)+(K4(IJ)*8.0-K3(IJ)*5.0+K2(IJ)*90.0+K1(IJ)*6.0)/81.0+YI,JJEND
    JF((H*2.0)/3.0+X,TEMPY,DX)JFOR J+1STEP IUNTIL K DO BEGIN K5(IJ)+DX(IJ)XHJT
    EMPY(IJ)+(K4(IJ)*8.0+K3(IJ)*10.0+K2(IJ)*36.0+K1(IJ)*6.0)/75.0+YI,JJEND;F((H*
    4.0)/5.0+X,TEMPY,DX)JFOR J+1STEP IUNTIL K DO BEGIN K6(IJ)+DX(IJ)XHJYI+1,J
    J+(K1(IJ)*23.0+K3(IJ)*125.0-K5(IJ)*81.0+K6(IJ)*125.0)/192.0+YI,JJEND END EN
    D;

* * THE FOLLOWING PROCEDURE IS THE PLOTTER CALL THAT GIVES GRID FOR
* * THE TR-X-Y MOTION AND THE WHIRL-RADIUS PLOTS
* * IF THE BOOLEAN B00 IS TRUE THEN THE RIGHT Y-AXIS IS LABELED
* * PROCEDURE SBGRID(AL1,NY,AL2,NX,AL3,NT,AL4,N4,B00);
* *   VALUE NY,NX,NT,N4; REAL NY,NX,NT,N4;
* *   ALPHA ARRAY AL1,AL2,AL3,AL4(0); BOOLEAN B00;
* *   BEGIN
* *     REAL XOT;
* *     NX + -NX;
* *     N4 + -N4;
* *     AXIS(0,0,AL1,NY,-6,90,YMIN,DY);
* *     AXIS(0,0,AL2,NX,-8,0,XMIN,DX);
* *     IF B00 THEN
* *       AXIS (8,0,AL4,N4,-6,90,YMIN1,DY1)
* *     ELSE
* *       AXIS (8,0,AL4,N4,-6,90,0,DY);
* *       AXIS (8,6,AL2,0,-8,180,0,DX);
* *       PLOT(0,6,2)J PLOT(0,6,5,1)J PLOT(8,6,5,1)J PLOT(8,6,1)
* *       PLOT(.4,6,05,3)J
* *       SYMBOL(.4,6,3,0,1,ALP2,0,3)J NUMBER(.723,6,3,0,1,MDY,0,0)J
* *       NUMBER (.82,6,3,0,1,CND,0,0)J
* *       SYMBOL(0.4,6,1,0,1,ALP16,0,5)J NUMBER(.571,6,1,0,1,EMU,0,3)J
* *       SYMBOL(1.685,6,3,0,1,ALP10,0,13)J NUMBER(1.91,6,3,0,1,W,0,0)J
* *       SYMBOL (1.685,6,1,0,1,ALP22,0,17)J NUMBER(1.91,6,1,0,1,FO,0,1)J
* *       SYMBOL(3.15,6,3,0,1,ALP3,0,14)J NUMBER(3.40,6,3,0,1,OMEGA,0,0)J
* *       SYMBOL(3.15,6,1,0,1,ALP23,0,4)J NUMBER(3.4,6,1,0,1,EN,0,2)J

```

```

SYMBOL(4.70,6.3,0.1,ALP6,0,14); NUMBER(4.7,6.3,0.1,CL,0,2);
SYMBOL(4.7,6.1,0.1,ALP8,0,3); NUMBER(4.8,6.1,0.1,S,0,3);
SYMBOL(6.3,6.3,0.1,ALP25,0,5); NUMBER(6.47,5.3,0.1,L/(2*R),0,2);
SYMBOL(6.05,6.1,0.1,ALP11,0,20); NUMBER(6.31,6.1,0.1,MU,0,4);
XOT + 4 = NT*0.06 ;
SYMBOL (XOT,6.55,0.14,AL3,0,NT);
END OF SBGRID ;

```

```

% THE FOLLOWING PROCEDURE CALCULATES THE SHORT BEARING FORCE
% BY THE USE OF WEDDLES RULE INTEGRATION
PROCEDURE FORCE (X,Y,VX,VY,N);
VALUE X,Y,VX,VY,N;
REAL X,Y,VX,VY;
INTEGER N;
BEGIN
REAL H3,FX,FY;
REAL HII ;
INTEGER I,J;
KB + 0 ;
IF X # 0 OR Y # 0 THEN
KB + (X*VY-Y*VX)/(X*X+Y*Y);
FOR I+0 STEP 1 UNTIL N DO
BEGIN
COSKK + COSK[I] ; SINKK + SINK[I] ;
HII + 1 = X * COSKK - Y * SINKK ;
H3 + HII * HII * HII ;
P[I] + (-X*SINKK + Y*COSKK + 2*ALFD * ( VX*COSKK+VY*SINKK))/H3 ;
IF P[I]<0 THEN P[I]+0;
PX[I] + P[I] * COSKK ;
PY[I] + P[I] * SINKK ;
END;
FX+0;
FY+0;
I + N / 6 ;
FOR J + 1 STEP 1 UNTIL I DO
BEGIN
J7 + J*6 ; J6 + J7 - 1 ; J5 + J7-2; J4 + J7-3 ;
J3 + J7-4; J2 + J7-5; J1 + J7-6;
FX + ( PX[J1]+ 5*PX[J2]+ PX[J3]+ 6*PX[J4]+ PX[J5]+
5*PX[J6]+ PX[J7]) + FX ;
FY + ( PY[J1]+ 5*PY[J2]+ PY[J3]+ 6*PY[J4]+ PY[J5]+
5*PY[J6]+ PY[J7]) + FY ;
END;
KKK + DEL * 0.3 ;
FX + FX * KKK ;
FY + FY * KKK ;
FXX+=-FX; FYY+=-FY;
END OF FORCE;

```

```

% THE FOLLOWING PROCEDURE IS THE FUNCTION CALCULATOR FOR THE
% 6TH ORDER RUNGE-KUTTA INTEGRATION PROCEDURE.
PROCEDURE FRK(X,Y,DX); VALUE X;
REAL X; ARRAY Y[0],DX[0] ;
BEGIN
FORCE (Y[ 1],Y[ 3],Y[ 2],Y[ 4],N1) ;
IF K = 2 THEN

```

```

BEGIN
  FXXL + FXX ; FYYL + FYY ;
  END ELSE BEGIN
  FXX + FXXL + FXX*RELAX + FXXL * (1-RELAX) ;
  FYY + FYYL + FYY * RELAX + FYYL * (1-RELAX) ;
  END ;
  DX[1] + Y[2] ;
  DX[2]+EMU*COS( X )+ K1*COS(EN* X )+K2*FXX + K5
  -(K9*Y[1] + K11 * Y[2]) + K7 * SIN(EN* X ) ;
  DX[3] + Y[4] ;
  DX[4]+ EMU * SIN( X )+K1*SIN(EN* X ) +K2*FYY=K3 + K6
  -(K10 * Y[3] + K12 * Y[4]) + K8 * SIN(EN* X ) ;
  END OF FRK ;

% THE FOLLOWING PROCEDURE CALCULATES THE FUNCTIONS NEEDED IN
% ADAMS-BASHFORTH-MOULTON INTEGRATION METHOD
PROCEDURE FUNCTION ( K); VALUE K; INTEGER K;
BEGIN
  FORCE (Y[ 1],Y[ 3],Y[ 2],Y[ 4],N1) ;
  IF K = 2 THEN
  BEGIN
  FXXL + FXX ; FYYL + FYY ;
  END ELSE BEGIN
  FXX + FXXL + FXX*RELAX + FXXL * (1-RELAX) ;
  FYY + FYYL + FYY * RELAX + FYYL * (1-RELAX) ;
  END ;
  F[2]+EMU*COS(Y[ 0])+ K1*COS(EN*Y[ 0])+K2*FXX + K5
  -(K9*Y[1] + K11 * Y[2]) + K7 * SIN(EN* Y[0]);
  AY[11,K-1] + F[2] ;
  F[4]+ EMU * SIN(Y[ 0])+K1*SIN(EN*Y[ 0]) +K2*FYY=K3 + K6
  -(K10 * Y[3] + K12 * Y[4]) + K8 * SIN(EN* Y[0]);
  AY[12,K-1] + F[4] ;
END OF FUNCTION;
% THE FOLLOWING PROCEDURE IS THE ADAMS-BASHFORTH-MOULTON
% INTEGRATION PROCESS
PROCEDURE TIMESTEP (TMAX, H, N, AY, NA);
VALUE TMAX,H,N;
REAL TMAX,H; INTEGER N, NA ;
REAL ARRAY AY[0,0] ;
BEGIN
  INTEGER I,J ; LABEL REPEAT , SMASH;
  FOR I + 0 STEP 1 UNTIL 4 DO
  AY[I,1]+Y[ I];
  K+2;
REPEAT:
  BEGIN
  REAL PP;INTEGER I,J;
  REAL VELO2 ;
  FUNCTION ( K);
  JOURANG + Y[0] ;
  JOURANG + JOURANG - PI2 * ENTIER (JOURANG / PI2 ) ;
  AY[10,K-1] + (JOURANG-ANGLE(Y[3],Y[1])) * CONST1 ;
  K + K-1 ;
  IF AY[10,K] > 180 THEN AY[10,K] + AY[10,K] = 360
  ELSE
  IF AY[10,K] ≤ -180 THEN AY[10,K] + AY[10,K] + 360 ;

```

```

IF AY[10,K] < -180 THEN AY[10,K] ← -180      ELSE
IF AY[10,K] > 180 THEN AY[10,K] ← 180 ;
K ← K + 1 ;
  AY[0,K] ← Y[0] + Y[0] + H ;
  AY[5,K-1] ← K4 × SQRT (FXX*2 + FYY*2) ;
  AY[6,K-1] ← AY[5,K-1] / W ;
  IF AY[5,K-1] > FMAX THEN
BEGIN
  FMAX ← AY[5,K-1] ;
  IF KK ≤ 0 THEN
  NM ← ENTIER((K-2)/KSF) + 1
  ELSE
  NM ← ENTIER((K-1)/KSF) + KK ;
  NMXH ← AY[0,K-1] ;
END ;
  IF K < 4 THEN
BEGIN
  VELO2 ← AY[2,K-1]*2 + AY[4,K-1]*2 ; IF ABS(VELO2) < 10-20 THEN
  AY[8,K-1] ← 0 ELSE AY[8,K-1] ← (F[4] × AY[2,K-1]-F[2] × AY[4,K-1])/
  VELO2 ;
  IF ABS(AY[8,K-1]) > 10-20 THEN AY[7,K-1] ← SQRT(VELO2)/AY[8,K-1] ;
END
  ELSE
  IF K > 5 THEN
BEGIN
  IF AY[5,K-1] ≠ 0 THEN
  IF ABS((AY[5,K-1] - AY[5,K-2])/AY[5,K-1]) > 0.33 THEN
BEGIN
  NUMERINSTAB ← NJMERINSTAB + 1 ;
  IF NUMERINSTAB ≥ 00 THEN
  NUMSTAB ← TRUE ;
END ;
  ACX ← HX12 × (AY[2,K-5] + 8 × (AY[2,K-2] - AY[2,K-4]) - AY[2,K-1]) ;
  ACY ← HX12 × (AY[4,K-5] + 8 × (AY[4,K-2] - AY[4,K-4]) - AY[4,K-1]) ;
  K ← K-3 ;
  VELO2 ← AY[2,K] × AY[2,K] + AY[4,K] × AY[4,K] ;
  IF ABS (VELO2) < 10-20 THEN AY[8,K] ← 0 ELSE
  AY[8,K] ← (ACX × AY[2,K] - ACY × AY[4,K])/ VELO2 ;
  IF ABS (AY[8,K]) > 10-20 THEN AY[7,K] ← SQRT(VELO2) / AY[8,K] ;
  K ← K+3 ;
END ;
  AY[9,K-1] ← KB ;
END ;
  IF K > RK6LIM THEN
BEGIN
  IF GOEULER THEN
BEGIN
  FOR I ← 2 STEP 2 UNTIL 4 DO
BEGIN
  AY[I,K] ← Y[I] + AY[I,K-1] + H × F[I] ;
  AY[I-1,K] ← Y[I-1] + AY[I-1,K-1] + H × AY[I,K] ;
END ;
END
  ELSE

```

```

BEGIN
FOR I ← 2,4 DO
  BEGIN
    I1 ← I/2 + 10 ]
    AY[I,K1] ← Y[I1]+AY[I,K-1]+(H024)×(55×AY[I,K-1]-59×AY[I,K-2]
      +37×AY[I,K-3]-9×AY[I,K-4]) ]
    AY[I-1,K]+Y[I-1]+AY[I-1,K-1]+(H024)×(9×AY[I,K]+19×AY[I,K-1]
      -5×AY[I,K-2] + AY[I,K-3]) ]
  END ]
FUNCTION (K+1) ]
FOR I ← 2,4 DO
  BEGIN
    I1 ← I/2+10 ]
    AY[I,K] ← Y[I1]+ AY[I,K] × (1-RELAX) + RELAX × ( AY[I,K-1] + H024 ×
      (9×AY[I,K] + 19×AY[I,K-1] - 5×AY[I,K-2] + AY[I,K-3] ) ) ]
  END ]
FOR I ← 1,3 DO
  BEGIN
    AY[I,K] ← AY[I,K-1] + H024 × (55×AY[I+1,K-1] - 59×AY[I+1,K-2] +
      37×AY[I+1,K-3] - 9×AY[I+1,K-4] ) ]
    AY[I,K] ← Y[I] + AY[I,K] × (1-RELAX) + RELAX × (AY[I,K-1] +
      H024 × (9×AY[I+1,K] + 19×AY[I+1,K-1] - 5×AY[I+1,K-2] + AY[I+1,K-3))) ]
  END ]
END ]
ELSE
END
BEGIN
  Y[0] ← Y[0] - H ]
  FOR I ← 1 STEP 1 UNTIL 4 DO
    RKAY[0,I] ← Y[I] ]
    RKSTARTS (4,1,Y[0],H,RKAY,FRK,RKDX,RKTEMPY,RKK1,RKK2,RKK3,RKK4,
      RKK5,RKK6) ]
    Y[0] ← Y[0] + H ]
    FOR I ← 1 STEP 1 UNTIL 4 DO
      AY[I,K] ← Y[I] + RKAY[I,I] ]
    END ]
    ET ← SORT(AY[I,K]*2 + AY[3,K]*2 ) ]
    IF ET > EMAX THEN BEGIN
      EMAX ← ET ] HMIN ← CL×(1-EMAX)×1000.0 ]
      TMAX ← AY[0,K]/6.28 ] HANGLE ← ANGLE(AY[3,K],AY[1,K])×CONST1 ]
    END ]
    IF ET > 0.99 THEN
  BEGIN
    Y[1] ← AY[1,K] + AY[1,K]×0.99/ET ]
    Y[3] ← AY[3,K] + AY[3,K]×0.99/ET ]
    IF K > 40 THEN BEGIN
      FAIL←TRUE] GO TO SMASH]
    END]
  END]
  IF K > 900 THEN SWITCHGO (TRUE) ]
  IF KK ≥ (895 - <SF) THEN GO TO SMASH ]
  K←K+1]
  IF Y[0] < TMAX THEN GO TO REPEAT ]
SMASH:
  K←K-1]
  IF KSF ≠ 1 THEN

```

```

SWITCHGD (FALSE) ;
IF FAIL THEN NA ← K-1 ELSE NA ← K ;
Y[0] ← AY[0,NA] ;
Y[1] ← AY[1,NA] ;
Y[2] ← AY[2,NA] ;
Y[3] ← AY[3,NA] ;
Y[4] ← AY[4,NA] ;
END UF TIMESTEP ;
TELLIME(LP) ;

```

```

VV ← 1 ;
DATA CARDS ARE NOW READ IN
ACARD ;
READ (CR,/,TMAX, H, N) (ALLDONE) ;
READ (CR,/,OMEGA,INC,OMEGA,NOINC, OMEGA ) ;
READ(CR,/,EMU,FJ,FN, FOCX,FOCY,FHX,FHY,ENX,FHY,ENY);
READ(CR,/,CL,R,W,MU,HORIZ);
READ (CH,/,KHX,DRX,KRY,DRY);
  READ(CR,/,FUR I←0 STEP 1 UNTIL 4 DO [Y[ I ]]);
  READ(CR,/,NI,REAX ) ;
  READ (CR,/,CS);
  READ (CR,/,PLOT1,PLOT2,PLOT3,PLOT4);
  READ (CR,/,CASEND, WDY,CND ) ;
  READ (CR,/,KSF) ;
  READ (CR,/,KK6LIM,GOEULER);

```

```

G←32.2×12;
H024 ← H/24 ; JD ← 1/10 × TMAX / H ;
HX12 ← 1 / (12 × H) ;
PI2←δ×ARCTAN(1);
TMAX ← TMAX × PI2 ; TMAXI ← TMAX;
CONST1 ← 360 / 212 ;
PI ← PI2 / 2 ;
DEL ← PI2 / N1 ;
FOR I ← 0 STEP 1 UNTIL N1 DO
  BEGIN
    KKK ← DEL × I ;
    COSK[1] ← COS(KKK) ; SINK[1] ← SIN(KKK) ;
  END;
  INCSUFAR ← 0 ;
  SPEDLOOP ;
  NUMSTAB ← FALSE ;
  NUMERINSTAB ← 0 ;
  KK ← 1 - KSF ;
  XMIN ← YMIN ← -1 ; DX ← DY ← 0.33333333 ;
  FAIL ← FALSE ;
  ALFD ← OMEGA / OMEGA ;
  OMEGA←OMEGA×(2×PI)/ 60 ;
  OMEGA←OMEGA×(2×PI)/ 60 ;
  M←W/G;
  KKK ← M × CL × OMEGA × OMEGA ;
  K1 ← FO / KKK ;
  K2 ← CMU × R × L×L×COMEGA)/(2×KKK×CL×CL);
  IF NOT HORIZ THEN FOCY ← FOCY + W ;

```

```

K3 ← W/KKK ;
K4 ← K2 × KKK ;
K5 ← FOCX / KKK ;    K6 ← FOCY / KKK ;
K7 ← FHX/KKK ;      K8 ← FHY/KKK ;
KKK ← KKK / CL ;
K9 ← KRX/KKK ;      K10 ← KRY/KKK ;
KKK ← KKK / OMEGA ;
K11 ← DRX/KKK ;     K12 ← DRY/KKK ;

```

COMMENT

```

S = SOMMERFELD NUMBER = MU(NJ-RPS)×(LDR*2)/(WWT×W×C*2)
SS = SHORT BEARING SOMMERFELD NUMBER = S × (L/D)*2
SU = SOMMERFELD NUMBER BASED ON THE ROTATING UNBALANCE LOAD
    WHERE FU = M×C×EMU×(OMEGA-RAD/SEC)*2

```

```

WWT = LOAD RATIO = SQRT((MG-FOCY)*2+FOCX*2)/MG
P = PROJECTED L/D = (WWT/(L×D)) × W
WS = DYNAMIC SPEED PARAMETER = (NJ-RPS)×SQRT(MC/(WWT×W))×2PI
TRS = STATIC TRANSMISSIBILITY = S(L/R)*2 × F(DIM. BEARING FORCE)
TRD = DYNAMIC TRANSMISSIBILITY = G/(C×OMEGA*2)SS/EMU×F(DIM.)
END OF COMMENT ;

```

```

WWT ← SQRT((W-FOCY)*2+FOCX*2)/W ;
IF WWT = 0 THEN BEGIN
S ← MU × OMEGA × L×R×R×R / ( CL×CL×W×PI ) ;
WS ← OMEGA × SQRT(CL/G) ;
END ELSE BEGIN
S ← MU × OMEGA × L×R×R×R / ( CL×CL×W×PI×WWT ) ;
WS ← OMEGA × SQRT (M×CL/(WWT×W)) ;
END ;
SS ← S×(L/(2×R))*2 ;
PBRG ← (WWT/ (L×2×R)) × W ;
FMAX ← 0 ;
EMAX ← 0 ;

```

\* ITERATIVE PROCESS TO FIND EQUIL. ECCEN. FOLLOWS

```

ANSI ← FIR + INCR + 0.1 ;
DL2 ← (2×R/L)*2 ;
MONCEMORE :
EE ← ANSI × ANSI ; EE2 ← 1-EE ;
SSU ← DL2 × EE2 × EE2 / (PI × ANSI × SQRT (PI×PI×EE2 + 16×EE) ) ;
IF SSU < S THEN
IF ABS((SSU-S))/S < 0.01 THEN
BEGIN
ASS ← ANSI ; GO TO SKIPIT ;
END
ELSE
BEGIN
ANSI ← ANSI + INCR ;
INCR ← INCR / 2 ;
END ;
ANSI ← ANSI + INCR ;
GO TO MONCEMORE ;
SKIPIT :

```

```

IF EMU ≠ 0 THEN

```

```

BEGIN
FU ← M×CL×EMU×Ω×Ω×2 }
FURATIO ← FU / M }
SU ← M×S/FU }

ANSI ← FIR + INCR ← 0.1 }
DL2 ← (2×R/L)*2 }
UNCEMORE }
EE ← ANSI × ANSI } EE2 ← 1-EE }
SSU ← DL2 × EE2 × EE2 / (PI × ANSI × SQRT (PI×PI×EE2 + 16×EF) ) }
IF SSU < SU THEN
IF ABS((SSU-SU))/SU < 0.01 THEN
BEGIN
ANS ← ANSI } GO TO SKIP }
END
ELSE
BEGIN
ANSI ← ANSI - INCR }
INCR ← INCR / 2 }
END }
ANSI ← ANSI + INCR }
GO TO UNCEMORE }
SKIP }
END }

* END OF ITERATIVE PROCESS FOR EQUIL. POS.
*
* THE FOLLOWING PROCEDURE CALL CALCULATES ALL OF THE VALUES FOR
* TIME STEPS UP TO TMAX
* TIMESTEP (IMAX, H, V, AY,NA);

IF NOT HORIZ THEN FOCY ← FOCY - W }
TRSMAX ← FMAX / W }
IF EMU ≠ 0 THEN TROMAX ← FMAX / FU }
COMEGA ← COMEGA × 60 / PI2 } OMEGA ← OMEGA × 60 / PI2 }
WRITE (LP,PAGEJ);
WRITE (LP,<X10,38(“”),X2,“CASE “,I10,X2,38(“”),/ >,CASENO);
IF HURIZ THEN
WRITE (LP,<X46,“HORIZONTAL ROTOR SYSTEM”>)
ELSE
WRITE (LP,<X47,“VERTICAL ROTUR SYSTEM”>);
WRITE (LP,<X48, “FLUID FILM BEARING”>);
WRITE (LP,<X6,“+ =”,F6.4,“ RAD.”,X9,“TMAX =”,F8.3,“ RAD.”,X10,
“ΩMEGA =”,F9.2,“ RPM”,X10, “COMEGA =”,F9.2,“ RPM”>);
X6,“EMU =”,F6.3,“ DIM.”,X8,“FO =”,F8.3,“ LB.”,X13,“MCL =”,E9.2,
“ IN.”,X13,“K =”, F6.2,“ IN.”>;
X6,“L =”,F6.2,“ IN.”, X11,“W =”,F8.2,“ LB.”,X14,“MU =”,E9.2,
“ REYNS”,X9,“FU =”,E11.4,X1,“AND EN =”, F7.3,
//>, H,TMAX,ΩMEGA,COMEGA,EMU,FO,CL,R,L,M,MU,FO,EN);
WRITE (LP,<X6,“RELAXATION FACTOR =”,F6.3,X10,“GDEULER =”,L6,X10,
MRK6LIM = “, 15,>, RELAX,GDEULER, RK6LIM);
WRITE (LP,<X6,“WT =”,F6.2>, WWT);
WRITE (LP,<X6, “N1 =”, 14, />,N1) }
WRITE (LP,<“MAX. ECCENTRICITY =”,F6.4,“ AT “,F6.3,“ CYCLES “,X15,
“HMIN =”,F7.3,“ MILS AT “,F6.1,“ DEGREES CC FROM X AXIS”>;
EMAX,TEMAX,HMIN,HANGLE) }
WRITE (LP,UT1,ASS,FMAX,S,TRSMAX,SS,FOCX,WS,FOCY,

```

```

PRK6,FHX,FIX,FHY,FNY)J
IF EMU # 0 THEN
WRITE (LF,OUTP,ANS,SU,FU,FUKATIO,TRDMAX JJ
WRITE (LP,<RETAINER SPECS ARE:,,X10,,KRX =,E11.4,X2,,MLP/IN,,
X10,,DRX =,L11.4,X2,,LR=SEC/IN,,//,X10,,KRY =,E11.4,X2,,LB/IN,,
X10,,DRY =,L11.4,X2,,LR=SEC/IN,,//>,KRX,DRX,KRY,DRY)J
WRITE (LP,<X4,,TIME,,X 5,,X-DIR,,X6,,X-VEL,,X7,,Y-DTR,,
X7,,Y-VEL,,X7,,FORCE,,X6,,IRS ,,X9,,RADIUS,,X3,,PHT,,X4,,
PH-IF,,X3,,BETA,,//>)J
IF NUMSTAR THEN
WRITE (LF,<X10,,***** NUMERICAL INSTABILITY *****>,
/X10,,I6,, "USCILLATIONS IN ",I7,, " STEPS",//>,NUMERINSTAR,NAKKSI)J
WRITE (LP,<FY.4,X1,4(E11.4,X1),F12.2,X1,2(F12.4,X1),2(F7.3),X2,14>,
FOR I # 1 STEP 1 UNTIL NA DO I
FOR J # 0 STEP 1 UNTIL 10 DOI AY(J,I)J)J
IF FAIL THEN WRITE (LP,<*****FAILURE*****>)J
  THE REMAINDER OF THE PROGRAM PLUTS THE FOLLOWING DATA
  1 - JOURNAL ORBIT PATH
  2 - TRANSMISSIBILITY AND X-Y MOTION UN THE SAME GRID
  3 - THE WHIRL AND RADIUS OF CURVATURE OF THE PATH
  4 - PHASE ANGLE OF DISP. RELATIVE TO UNBALNCE
  **** NUMBER OF BLOCKS PER SET OF DATA =(NDINC + 1)* SUM OF CAHD 9
  IF CS # 0 THEN
  BEGIN
  REAL WXYZ J
  NA # NA - 1 J
  IF VV # 1 THEN BEGIN
  FILL ALP1[*] WITH MBALANC,,MED ROT,,MOR " J
  FILL ALP2[*] WITH MND. "J
  FILL ALP3[*] WITH "V = "J,RPM,,M "J
  FILL ALP4[*] WITH "R = "J,IN,,M. " J
  FILL ALP5[*] WITH "L = "J,IN,,M. " J
  FILL ALP6[*] WITH "C = "J,MT,,MLS "J
  FILL ALP7[*] WITH "TRSMAX,, " = "J
  FILL ALP8[*] WITH "S = "J
  FILL ALP9[*] WITH "SS = "J,LB,,M. "J
  FILL ALP10[*] WITH "M = "J,MUE5 =,,M "J,REYM,,MNS "J
  FILL ALP11[*] WITH "MUE5 =,,M "J, "J, "J, "J
  FILL ALP12[*] WITH "FMAX =,,M "J, "J, "J, "J
  FILL ALP13[*] WITH "OCCURS,, " AT "J, "J, "J, "J, "J
  FILL ALP14[*] WITH "MS = "J
  FILL ALP15[*] WITH "MES = "J
  FILL ALP16[*] WITH "EMU = "J
  FILL ALP17[*] WITH "SU = "J
  FILL ALP18[*] WITH "TROMAX,, " = "J, "J, "J, "J, "J
  FILL ALP19[*] WITH "FU = "J, "J, "J, "J, "J
  FILL ALP20[*] WITH "FURATI,, "D = "J, "J, "J, "J, "J
  FILL ALP21[*] WITH "FSU = "J
  FILL ALP22[*] WITH "FD = "J, "J, "J, "J, "J
  FILL ALP23[*] WITH "MEN = "J
  FILL ALP24[*] WITH "UNBALAN,, "NCD RM,, "UTOR "J
  FILL ALP25[*] WITH "L/D = "J
  FILL ALP26[*] WITH "TRANSM,, "ISSIRI,, "LITY, " , "TR = F,, " / W (DI,,
  "M) " J
  FILL ALP27[*] WITH "CYCLES,, " OF MOV,, "TION " J

```

```

FILL ALP2AL*) WITH MSHAFT *,X,Y,MUM,PIIDN *,*(DIM,*)
FILL ALP29L*) WITH MINSTAN*,TANEDUM,*,S WHIR*,*L * )
FILL ALP30L*) WITH MRADIUS*,* OF CUM,*,KVAVTUR*,*E * )
FILL ALF31L*) WITH MAMOTIM,*,*ON * )
FILL ALP32L*) WITH MY-MOTI*,*,*ON * )
FILL ALP33L*) WITH MHIRL *,* )
FILL ALH34L*) WITH MPHASE *,*,*ANGLE *,*,* BETAM*)
FILL ALP40L*) WITH MHORIZOM,*,*NTAL B*,*,*BALANCE*,*,*D ROTOM,*,*R * )
FILL ALF41L*) WITH MVERTICOM,*,*AL BAL,*,*,*ANCED *,*,*RCTOR * )
FILL ALF42L*) WITH MHORIZOM,*,*NTAL UM,*,*,*NBALAN*,*,*,*CED ROM,*,*TOR * )
FILL ALP43L*) WITH MVERTICOM,*,*AL UNB*,*,*BALANCE*,*,*D ROTOM,*,*R * )
FILL ALP44L*) WITH *MT = * * )

*
* THE X-Y COORDINATES OF A 3 INCH RADIUS CIRCLE IS CALCULATED
* FOR THE FLUTTER PROCEDURE THAT WILL PLOT OUT THE JOURNAL PATH
K ← 0 )
FOR T ← -3 STEP 0.05 UNTIL 0.001 DD
BEGIN
K ← K + 1 )
CX[K] ← T + 3 ) CY[K] ← SQRT(ABS(9-T**2)) + 3 )
END )
J4 ← K-1 )
FOR N ← 1 STEP 1 UNTIL J4 DD
BEGIN
J5 ← K+N ) J6 ← K-N )
CX[J5] ← 6-CX[J6] )
CY[J5] ← CY[J6] )
END )
K ← K + J4 )
J4 ← K-1 )
FOR N ← 1 STEP 1 UNTIL J4 DD
BEGIN
J5 ← K+N ) J6 ← K-N )
CX[J5] ← CX[J6] )
CY[J5] ← 6-CY[J6] )
END )
CIRP1 ← 2*xK-1 )
PLOT (2,0,-4) ) PLOT (2,0,-5) )
VV ← VV + 1 )
END )
SCALES (AVL3,*,*),NA,YMIN,UY,CS) )
SCALES (AVL1,*,*),NA,XMIN,UX,CS) )

LYNE (CX,CY,CIRP1,1) )
PLOT (0,3,3) ) PLOT(6,3,2) ) PLOT(3,6,3) ) PLOT(3,0,2) )
FOR T ← 0 STEP 0.30 UNTIL 6.001 DD
BEGIN
PLOT(3,T,3) ) PLOT (3.1,T,2) )
END )
FOR T ← 0 STEP 0.30 UNTIL 6.001 DD
BEGIN
PLOT (T,3,3) ) PLOT (T,2.90,2) )
END )
FOR NUMB ← 0.8 STEP -0.2 UNTIL 0.15 DD

```

```

NUMBER (3+ 3*NUMB=.52,2.75,0.1 ,NUMB,0,1);
FOR NUMB + 0.2 STEP 0.2 UNTIL 0.801 DO
NUMBER (2.72,3+ 3*NUMB=0.05 , 0.1 ,NUMB,0,1);

SYMBOL (AY[1,1], AY[3,1], .49, ALPHA1 , 0,-13);
SYMBOL (AY[1,NM],AY[3,NM],0.1,ALP1,0,-15);
CS + 6.28 /(H*KSF) ;
FOR I + CS STEP CS UNTIL NA DO
SYMBOL (AY[1,I], AY[3,I], .07, ALPHA1 , 0, -5);
IF FAIL THEN
SYMBOL (AY[1,NA], AY[3,NA],0.14,ALPHA1,0,-12);
LYNE (AY[1,*], AY[3,*], NA, 1);
IF EMU = 0 THEN
BEGIN
IF HORIZ THEN
SYMBOL (0.94,9.25,0.21,ALP40,0,25)
ELSE
SYMBOL (1.12,9.25,0.21,ALP41,0,23);
END
ELSE
IF HORIZ THEN
SYMBOL (0.76,9.25,0.21,ALP42,0,27)
ELSE
SYMBOL (0.94,9.25,0.21,ALP43,0,25);

MU + MU * 10000 ;
CL + CL * 1000 ;

SYMBOL(5.60,8.9,.1,ALP2,0,3); NUMRER(5.76,8.9,.1 ,MDY ,0,0);
NUMBER (5.85,8.9,.1 ,CND,0,0);
SYMBOL(0.75,8.50,.14,ALP3,0,13); NUMBER(1.11,8.50,.14,OMEGA,0,0);
SYMBOL(0.75,8.25,.14,ALP4,0,13); NUMBER(0.75,8.25,.14,R,0,2);
SYMBOL(0.75,8.00,.14,ALP5,0,13); NUMBER(0.75,8.00,.14,L,0,2);
SYMBOL(0.75,7.75,.14,ALP6,0,14); NUMBER(0.75,7.75,.14,CL,0,2);
SYMBOL(0.75,7.50,.14,ALP7,0,8); NUMBER(1.35,7.50,.14,TRSMAX,0,2);
SYMBOL(0.75,7.25,.14,ALP8,0,3); NUMBER(0.87,7.25,.14,S,0,3);
SYMBOL(0.75,7.0,.14,ALP9,0,4); NUMBER(1.0,7.0,.14,SS,0,3);
SYMBOL(3.75,8.50,.14,ALP44,0,6); NUMBER(3.87,8.50,.14,WWT,0,2);
SYMBOL(3.75,8.25,.14,ALP10,0,13); NUMBER(4.11,8.25,.14,W,0,0);
SYMBOL(3.75,8.00,.14,ALP11,0,20); NUMBER(4.11,8.00,.14,MU,0,3);
SYMBOL(3.75,7.75,.14,ALP12,0,22); NUMBER(4.5,7.75,.14,FMAX,0,1);
SYMBOL(3.90,7.50,.14,ALP13,0,22); NUMBER(4.74,7.50,.14,NMXH/6.28,
0,2);
SYMBOL(3.75,7.25,.14,ALP14,0,4); NUMBER(3.75,7.25,.14,WS,0,2);
SYMBOL(3.75,7.0,.14,ALP15,0,4); NUMRER(3.75,7.0,.14,ASS,0,3);
IF EMU ≠ 0 THEN
BEGIN
SYMBOL(.75,6.75,.14,ALP16,0,5); NUMBER(1.6,6.75,.14,EMU,0,2);
SYMBOL(.75,6.50,.14,ALP17,0,4); NUMRER(1.6,6.5,.14,SU,0,3);
SYMBOL(.75,6.25,.14,ALP18,0,8); NUMRER(1.59,6.25,.14,TRDMAX,0,2);
SYMBOL(3.75,6.75,.14,ALP19,0,16); NUMBER(4.11,6.75,.14,FU,0,2);
SYMBOL(3.75,6.50,.14,ALP20,0,9); NUMBER(4.59,6.50,.14,FURATIO,0,2);
SYMBOL(3.75,6.25,.14,ALP21,0,5); NUMBER(4.11,6.25,.14,ANS,0,3);
IF FU ≠ 0 THEN BEGIN
SYMBOL(.75,6.00,.14,ALP22,0,15); NUMBER(1.11,6.00,.14,FO,0,1);

```

```

SYMBOL(3.75,6.00),.14,ALP23,0,4)} NUMBER(3.87,6.00,.14,EN,0,2)}
END} ELSE
IF FO # 0 THEN
BEGIN
SYMBOL(.75,6.75,.14,ALP22,0,15)} NUMBER(1.11,6.75,.14,FO,0,1)}
SYMBOL(3.75,6.75,.14,ALP23,0,4)} NUMBER(3.87,6.75,.14,EN,0,2)}
END }

FOR I + 1 STEP 1 UNTIL NA DO AY[0,I]+AY[0,I]/PI2} NA + NA + 1 }
AY[C,NA] + ENTIER(AY[0,I])}
SCALE (AY[0,*J],NA,8,XMIN,DX,1)} NA + NA- 1 }
IF PLOT2 THEN BEGIN
PLOT(12,0,-3)}
IF TRSMAX < 1.5 THEN DY + 0.25 ELSE
IF TRSMAX < 3 THEN DY + 0.50 ELSE
IF TRSMAX < 6 THEN DY + 1.00 ELSE
IF TRSMAX < 12 THEN DY + 2.00 ELSE
IF TRSMAX < 24 THEN DY + 4.0 ELSE
IF TRSMAX < 48 THEN DY + 8 ELSE
BEGIN
DY + 16 }
FOR I + 1 STEP 1 UNTIL NA DO
IF AY[6,I] > 96 THEN AY[6,I] + 96 }
END}
YMIN + 0 }
SCALES (AY[6,*J],NA ,YMIN,DY,1)}
YMIN1 + -1 } DY1 + 0.333333 }

IF EMU = 0 THEN BEGIN
IF HORIZ THEN
SRGRID (ALP26,32,ALP27,16,ALP40,25,ALP28,24,TRUE)
ELSE
SRGRID (ALP26,32,ALP27,16,ALP41,23,ALP28,24,TRUE) }
END
ELSE
IF HORIZ THEN
SRGRID (ALP26,32,ALP27,16,ALP42,27,ALP28,24,TRUE)
ELSE
SRGRID (ALP26,32,ALP27,16,ALP43,25,ALP28,24,TRUE) }
LYNE (AY[0,*J],AY[6,*J],NA ,1)}
NAMELINE (AY[0,*J],AY[1,*J],NA,1,ALP31,8,TRUE)}
NAMELINE (AY[0,*J],AY[3,*J],NA,1,ALP32,8,TRUE)}
FOR J + 1,4 DO
BEGIN
KKK + ENTIER (NA x J / 5 )}
SYMBOL (AY[0,KK],AY[6,KK]),21,ALP1, 90,-10)}
KKK + KKK + ENTIER (NA x 1 / 15 ) }
SYMBOL (AY[0,KK],AY[1,KK]),21,ALP1,-90,-10)}
KKK + KKK + ENTIER (NA x 1 / 15 ) }
SYMBOL (AY[0,KK],AY[3,KK]),21,ALP1,-90,-10)}
END}

END}
IF PLOT3 THEN BEGIN
PLOT(12,0,-3)}

```

```

AY[7,NA ] + 0 ; AY[7,NA-1] + 1.20 ;
AY[8,NA ] + 0 ; AY[8,NA-1] + 1.20 ;
SCALE (AY[7,*],NA,6,YMIN ,DY ,1) ;
SCALE (AY[8,*],NA,6,YMIN1,DY1,1) ;
NA + NA = 2 ;

IF EMU = 0 THEN BEGIN
IF HORIZ THEN
SBGRID (ALP30,19,ALP27,16,ALP40,25,ALP33,5,TRUE)
ELSE
SBGRID (ALP30,19,ALP27,16,ALP41,23,ALP33,5,TRUE) ;
END
ELSE
IF HORIZ THEN
SBGRID (ALP30,19,ALP27,16,ALP42,27,ALP33,5,TRUE)
ELSE
SBGRID (ALP30,19,ALP27,16,ALP43,25,ALP33,5,TRUE) ;
LYNE (AY[0,*],AY[7,*],NA,1) ;
DASHLINE (AY[0,*],AY[8,*],NA,1) ;
FOR J + 1,4 DO
BEGIN
KKK + ENTIER (NA * J / 5 ) ;
SYMBOL (AY[0,KKK],AY[7,KKK],.21,ALP1, 90,-10) ;
KKK + KKK + ENTIER (NA * 1 / 15 ) ;
SYMBOL (AY[0,KKK],AY[8,KKK],.21,ALP1,-90,-10) ;
END ;

NA + NA+2 ;
END ;
IF PLOT4 THEN
BEGIN
PLOT(12,0,-3) ;
YMIN + -180 ; JY + 60 ;
SCALES (AY[10,*],NA,YMIN,DY,1) ;

IF EMU = 0 THEN BEGIN
IF HORIZ THEN
SBGRID(ALP34,18,ALP27,16,ALP40,25,ALP34,18,FALSE)
ELSE
SBGRID(ALP34,18,ALP27,16,ALP41,23,ALP34,18,FALSE) ;
END
ELSE
IF HORIZ THEN
SBGRID(ALP34,18,ALP27,16,ALP42,27,ALP34,18,FALSE)
ELSE
SBGRID(ALP34,18,ALP27,16,ALP43,25,ALP34,18,FALSE) ;
LYNE (AY[0,*],AY[10,*],NA,1) ;

END ;
IF FAIL THEN
PLOT(12,0,-5) ;
IF FAIL THEN FOR I + 1 STEP 1 UNTIL (1+4*(NOINC=INCSOFAR)) DO
PLOT(0,0,-3) ELSE PLOT(12,0,-3) ;

```

```

CL ← CL × U.C01 ; MU ← MU × 0.00001 ;
CS ← 1 ;
END;
IF FAIL THEN INCSOFAR ← NOINC ;
INCSOFAR ← INCSOFAR + 1 ; IF INCSOFAR > NOINC THEN GO TO ACARD
ELSE OMEGA ← OMEGA + INCOMEGA ;
CUMEGA ← CUMEGA + INCOMEGA ;
TMAX ← TMAX + TMAXI ;
KKK ← (OMEGA-INCOMEGA)/OMEGA ;
Y[2] ← Y[2] × KKK ; Y[4] ← Y[4] × KKK ;
GO TO SPEFULOPP ;
ALLUNE ;
WRITE (LP[PAGE]) ;
TELLTIME(LP) ;

```

END.

\*\*\*\*\* CASE 5291 \*\*\*\*\*

VERTICAL ROTOR SYSTEM  
FLUID FILM BEARING

H = 0.0500 RAD.      TMAX = 31.416 RAD.      OMEGA = 4000.00 RPM      COMEGA = 4000.00 RPM  
EMU = 0.010 DIM.      FO = 0.000 LB.      CL = 5.00E-03 IN.      R = 1.00 IN.  
L = 1.00 IN.      W = 50.00 LB.      MU = 1.00E-05 REYNS      FO = 0.0000E+00 AND EN = 0.000

RELAXATION FACTOR = 1.000      GOEULER = TRUE      RK6LIM = 4

WT = 0.00  
N1 = 60

MAX. ECCENTRICITY = 0.0872 AT 5.008 CYCLES      HMIN = 4.564 MILS AT 192.7 DEGREES CC FROM X AXIS

EQUIL. POS. = 0.3063      FMAX = 2.4839  
S = 1.0667      TRSMAX = 0.0497  
SS = 0.2667      FOCX = 0.0000  
WS = 1.5068      FOCY = 0.0000  
PBRG = 0.0000  
FHX = 0.0000 AND ENX = 0.00  
FHY = 0.0000 AND ENY = 0.00

EQUIL. POS.(UNBALANCE) = 0.0087  
SU = 46.9806  
FU = 1.1352  
FURATIO = 0.0227  
TRDMAX = 2.1880

RETAINER SPECS ARE:  
KRX = 0.0000E+00 LB/IN      DRX = 0.0000E+00 LB-SEC/IN  
KRY = 0.0000E+00 LB/IN      DRY = 0.0000E+00 LB-SEC/IN

TIME	X-UTR.	X-VEL.	Y-DIR.	Y-VEL.	FORCE	TRS	RADIUS	PHI	PHIB	RETA
0.0000	0.0000E+00	0.0000E+00	0.0000E+00	0.0000E+00	0.00	0.0000	0.0000	0.000	0.000	0
0.0500	1.2028E-05	4.7190E-04	2.0529E-07	1.2256E-05	0.12	0.0025	0.0009	0.539	0.349	2
0.1000	4.6309E-05	8.9092E-04	1.6176E-06	4.8032E-05	0.23	0.0047	0.0015	0.598	0.365	4
0.1500	1.0031E-04	1.2615E-03	5.3752E-06	1.0581E-04	0.33	0.0067	0.0024	0.519	0.380	6
0.2000	1.8078E-04	1.6093E-03	1.4079E-05	1.7408E-04	0.43	0.0085	0.0031	0.526	0.268	7
0.2500	2.7638E-04	1.9119E-03	2.7264E-05	2.6370E-04	0.51	0.0102	0.0031	0.625	0.269	9
0.3000	3.8503E-04	2.1730E-03	4.5906E-05	3.7284E-04	0.58	0.0116	0.0032	0.687	0.291	10
0.3500	5.0482E-04	2.3959E-03	7.0890E-05	4.9967E-04	0.64	0.0129	0.0033	0.739	0.317	12
0.4000	6.3349E-04	2.5834E-03	1.0301E-04	6.4242E-04	0.70	0.0140	0.0034	0.785	0.342	14
0.4500	7.7089E-04	2.7380E-03	1.4298E-04	7.9933E-04	0.75	0.0150	0.0034	0.827	0.366	15
0.5000	9.1398E-04	2.8619E-03	1.9141E-04	9.6873E-04	0.79	0.0158	0.0035	0.866	0.387	17
0.5500	1.0618E-03	2.9570E-03	2.4886E-04	1.1490E-03	0.83	0.0166	0.0035	0.902	0.407	18
0.6000	1.2131E-03	3.0251E-03	3.1578E-04	1.3384E-03	0.86	0.0172	0.0035	0.936	0.425	20
0.6500	1.3665E-03	3.0676E-03	3.9257E-04	1.5356E-03	0.89	0.0178	0.0035	0.967	0.442	21
0.7000	1.5208E-03	3.0859E-03	4.7952E-04	1.7390E-03	0.92	0.0183	0.0036	0.995	0.458	23
0.7500	1.6748E-03	3.0813E-03	5.7688E-04	1.9472E-03	0.94	0.0188	0.0036	1.021	0.473	24
0.8000	1.8276E-03	3.0547E-03	6.8482E-04	2.1588E-03	0.96	0.0191	0.0036	1.044	0.487	25
0.8500	1.9779E-03	3.0073E-03	8.0344E-04	2.3724E-03	0.97	0.0195	0.0036	1.064	0.499	27
0.9000	2.1249E-03	2.9400E-03	9.3278E-04	2.5868E-03	0.99	0.0198	0.0036	1.082	0.511	28
0.9500	2.2676E-03	2.8536E-03	1.0728E-03	2.8007E-03	1.00	0.0200	0.0036	1.097	0.523	29
1.0000	2.4050E-03	2.7489E-03	1.2235E-03	3.0130E-03	1.01	0.0202	0.0037	1.109	0.533	30
1.0500	2.5364E-03	2.6268E-03	1.3846E-03	3.2248E-03	1.02	0.0204	0.0037	1.118	0.543	32
1.1000	2.6608E-03	2.4880E-03	1.5560E-03	3.4280E-03	1.03	0.0206	0.0038	1.125	0.553	33
1.1500	2.7714E-03	2.3331E-03	1.7374E-03	3.6286E-03	1.04	0.0207	0.0038	1.130	0.561	34
1.2000	2.8856E-03	2.1631E-03	1.9286E-03	3.8232E-03	1.04	0.0209	0.0039	1.132	0.570	35
1.2500	2.9845E-03	1.9784E-03	2.1291E-03	4.0110E-03	1.05	0.0210	0.0039	1.133	0.577	36
1.3000	3.0735E-03	1.7799E-03	2.3387E-03	4.1909E-03	1.05	0.0211	0.0040	1.131	0.584	37
1.3500	3.1519E-03	1.5683E-03	2.5568E-03	4.3621E-03	1.06	0.0212	0.0041	1.128	0.591	38
1.4000	3.2191E-03	1.3442E-03	2.7830E-03	4.5238E-03	1.06	0.0213	0.0042	1.124	0.598	39
1.4500	3.2746E-03	1.1085E-03	3.0167E-03	4.6752E-03	1.07	0.0213	0.0043	1.118	0.604	40
1.5000	3.3176E-03	8.6170E-04	3.2575E-03	4.8156E-03	1.07	0.0214	0.0044	1.111	0.609	41
1.5500	3.3479E-03	6.0468E-04	3.5047E-03	4.9443E-03	1.07	0.0215	0.0045	1.104	0.614	42
1.6000	3.3648E-03	3.3815E-04	3.7578E-03	5.0607E-03	1.08	0.0215	0.0046	1.095	0.619	44
1.6500	3.3679E-03	6.2883E-05	4.0160E-03	5.1641E-03	1.08	0.0216	0.0048	1.086	0.624	45
1.7000	3.3569E-03	-2.2036E-04	4.2787E-03	5.2540E-03	1.08	0.0217	0.0049	1.077	0.628	46
1.7500	3.3314E-03	-5.1079E-04	4.5452E-03	5.3299E-03	1.09	0.0217	0.0050	1.068	0.632	47
1.8000	3.2910E-03	-8.0762E-04	4.8147E-03	5.3914E-03	1.09	0.0218	0.0052	1.058	0.636	47

